DSPACE

https://dspace.org/

Evaluation of the feasibility of beneficiating sewage sludge from municipal wastewater treatment works

Mudzanani, Khuthadzo Ednah

2022

https://hdl.handle.net/10539/34934

Downloaded from a DSpace repository. https://dspace.org/



Evaluation of the feasibility of beneficiating sewage sludge from municipal wastewater treatment works

by

Khuthadzo Edna Mudzanani

(389767)

A thesis submitted to the Faculty of Engineering and the Built Environment, University of the Witwatersrand, Johannesburg, in fulfillment of the requirements for the degree of Doctor of Philosophy in Engineering

Supervisor: Prof. M.O. Daramola

Co-Supervisor: Prof S.E. Iyuke

Co-Supervisor: Dr. R Mbhele

September 2022

DECLARATION

I declare that this dissertation is my unaided work. It is being submitted for the degree of Doctor of Philosophy in Chemical Engineering to the University of the Witwatersrand, Johannesburg, South Africa. It has not been submitted before for any degree or examination to any other University.


_____ signed on the 08th day of February, 2022

Signed at University of the Witwatersrand, Johannesburg, South Africa

ABSTRACT

The study aims to enhance biogas production using the Anaerobic Digestion (AD) from the municipal wastewater sludge and evaluate the feasibility of the value-added products from the by-products of the biogas production. The main objectives are to first understand the physicochemical & microbiological characteristics of the digester feed, optimize the digestion process, evaluate the enhancement by co-digestion with different industrial bio-wastes, and conduct a model-based simulation to predict the performance of the AD process and synthesis of (Sludge-based Activated Carbon) SAC. Most research efforts have focused primarily on the use of co-substrate to boost biogas production and few studies have explored anaerobic co-digestion of specific organic wastes as co-substrates to optimize biogas production; however, none have conducted a comparative study of various co-substrates or bio-wastes. The knowledge gap that was identified is the lack of understanding of the interactive mechanism between the primary substrate and co-substrates in the digestion system. By use of the simulation model, this study provides insights into the physicochemical analysis of the parameters that catalyze and those that can inhibit anaerobic digestion. Literature reports frequently on the synthesis of the adsorption materials from the bio-wastes and a few explore synthesis from the digestate such as SAC. Further research reported the feasibility to synthesize SAC from waste sludge at a low cost of the modification process, highly efficient, and with low installation, operations, and maintenance costs.

The physicochemical and microbiological characterization was performed on the wastewater treatment works (WWTW) sewage sludge, from the City of Tshwane (CoT) and Joburg Water (JW) using the standard procedure for examination of water and wastewater. The study examined the anaerobic co-digestion of sewage sludge and six organic waste materials as possible co-substrates for enhancement using the bio-methane potential technique, the semi-continuous, and the pilot plant trials. The simulation was carried out using MATLAB Simulink, and additional equations and simulations were added to the standard model to develop tools to investigate the feasibility of co-digesting sewage sludge with biowaste. The synthesis technique to modify waste sludge into SAC involved physical and chemical activation to increase surface area and enhance the porous structure. Prior to the batch studies; the textual, physical, and composition of the material were evaluated using SEM, TGA, FTIR, and EDX. The performance test was carried out by the removal of Cr(VI) & Cd(II) heavy metals, from wastewater.

The results presented show that WWTW sewage sludge contains a high potential methane production, 28.6 & 27.8 g CH_4/kg feed in COT2 PS and JW1 NW sewage sludge, respectively. However, a well-balanced high COD with C/N ratio and VS concentration in the ranges of 10-100 g/kg feed, C/N of 17–36, and VS 80–98% TS is recommended. The microbiology data showed that the high-throughput sequencing analysis showed clear differences in microbial communities available in the sewage sludge along with the AD inhibiting microbes. The microbial analysis

indicated that *Proteobacteria* is the most abundant phylum, followed by the *Bacteroidetes, Firmicutes*, and *Actinobacteria.* The archaea community of hydrogenotrophic methanogen genus enrichment includes methanogens such as *Methanobacterium, thermoautotrophicum, Methanosarcina barkeri*, and *Methanobacterium wolfei*. Thus both sewage sludge from COT and JW WWTP can be a suitable substrate for efficient anaerobic digestion. Co-substrates such as molasses, food waste, animal manure, and fresh produce waste performed well at co-digestion maximum ratios. Soft drink waste and sewage sludge co-digestions had a maximum co-digestions ratio of 25%. Furthermore, except for manure, co-digestion of all other solid co-substrates resulted in additional VS and COD residuals in digested sludge. In contrast, the majority of liquid co-substrates tested here demonstrated a significant synergistic effect, increasing the removals of TS, VS, and COD during anaerobic digestion. Thus, anaerobic co-digestion might be considered a cost-effective solution that could contribute to the energy self-efficiency of WWTWs and sustainable waste management. A significant reduction in the biogas yield; from 10.23 to 2.02 NL/day was also observed in the semi-continuous setup when the OLR reached the level of 2.90 gVS/L.day. The simulation results report that the optimal mixture and parameter dependence were two aspects to be investigated. The best combination of two separate input variables identified was for S_{IN}, $S_{IC,}$ and q, based on the trial and error observation this propagates during a simulation. One noticeable peak each was discovered in both S_{IC} and S_{IN} , stages 1 and 2. Even though the flow rate shows a poor fitment to the particle swarm optimization, the increase of gas production is noticed until the maximum of 161 m3/day is noticed at stage 20. This corresponds to the operating conditions that were mentioned previously.

The SEM results showed that SAC material has a rougher surface with spheres of various dimensions indicating a well-developed porous structure compared to what was reported previously in the literature. TGA results showed a remarkable weight loss of ~30.64% and ~64% observed for raw sludge and SAC material, respectively. The activation led to an increase of oxygen-containing functional groups (C-OH, O-H, and C=O) which might increase the adsorption capacity of the material. The elements present in the sample based on EDX analyses were mainly P, Na, K, Fe, and Ca. All these characteristics contributed to a high adsorption capacity of metal ions such as Cr(VI), Cd(II), dyes, and other impurities on SAC. The material performance was carried out by adsorption of Cr(VI) and removal adsorption efficiency was reported. Batch adsorption studies reported that the highest Cr(VI) removal efficiency was achieved with the SAC by 99.99 %, whereas 60,50 & 40,71 % removal efficiency was achieved from CGAC & raw sludge, respectively. The maximum or equilibrium removal (99.99 %) of Cr (VI) and Cd (II) was achieved by 0.8 and 1.4 g SAC dosage, respectively. This behavior is due to the fact that at increased sorbent dosage, there are more available active adsorption sites for the adsorbate to adhere to, hence, a high percentage removal. The adsorption capacity at equilibrium (qe) was found to increase from 8.91 to 312.50 mg/g with an increase in the initial dye concentrations from 50 to 500 mg/L.

Dedication

This thesis is dedicated to my son, Lefa Hope who gave me the strength to do more even when things were difficult.

I would also like to dedicate this to my mother, Mrs. Joyce Mudzanani who had to endure so much during the preparation of this thesis.

Acknowledgments

"*The secret of getting ahead is getting started today*". The author would like to acknowledge the following organizations and people for their contribution and help:

- First and foremost, I am extremely grateful to my supervisor, Prof Michael O. Daramola, whose contribution throughout my entire PhD proved invaluable. I am appreciative of his unwavering support and patience during my studies. He could've given up on me so many times, but he never loses hope in me. His vast expertise and depth of knowledge have encouraged me in my academic studies and everyday life. I am also grateful for his assistance during the preparation and assessment of all papers, including this thesis. The attendance of the EUBCE conferences in 2019 and 2021 would not have been accomplished without him.
- Council for Scientific and Industrial Research (CSIR) for funding the project and hosting me under a studentship programme. I extend a huge "thank you" to my colleagues and friends at CSIR i.e., Lindani Mdlalose, Nomvuyo Nomadolo, Vongani, Vusani, and Katekani. And also, amongst others, I would like to thank Mavhungu, John, Sarah, Tshidi, Thuli, and Bongi for being such an inspiration and encouragement.
- The University of the Witwatersrand, Johannesburg (School of Chemical and Metallurgical Engineering), The laboratory assistance team; Bruce, Motlatsi, Jeanette & Dr Wumi Sadare, for laboratory setup and analysis assistance. My gratitude also goes to the SEERU research unit for allowing me to showcase my work in technical presentation meetings.
- The University of Johannesburg, Department of Chemical Engineering. Process, Energy, and Environmental Technology Station (PEETS) Doornfontein for allowing me to use their instruments and facility.
- To the most valuable mentors;
    - Dr V Masindi for the guidance, reviewing my work, and beneficial feedback.
    - Dr Samson Masebinu for the BMP setup and being an inspiration
- The author would like to thank all the WWTPs for providing samples of anaerobic digesters used in this study and all the co-substrates providers.
- Substrate's collection team, research assistant/driver
- My family for support, prayers & perseverance; (Lugisani Mudau, Maggie Machumela), my mother & the entire "*Mudzanani Playground*" team members.
- Mr W. Monyethabeng, without whom this thesis would not have been finished at all. Thank you for all the support, for the courage to take difficult decisions, for late nights companionship & coffee during the write-up, and a whole lot of motivation.
- To the almighty God, THANK YOU

Publications and Presentations

The following publications and conference presentations emanated from this study. Kindly note that this thesis is a careful compilation of these publications and presentations.

Publications

Mudzanani K, Van Heerden E. Mbhele R N. Daramola M O., 2021. Enhancement of biogas production via co-digestion of wastewater treatment sewage sludge and brewery spent grain. *Sustainability* **2021**, 13, 8225. https://doi.org/10.3390/su13158225

Mudzanani K, Van Heerden E. Mbhele R N. Daramola M O., 2021. Towards Developing an Optimum Anaerobic Co-Digestion from Wastewater Sewage Sludge as Biogas Production Enhancement Technique: Physicochemical Characteristics & Microbial Community of Methanogens of the Feedstock. 8th European Biomass Conference and Exhibition (EUBCE 2021), Online 25-27 April 2021

Mudzanani K, Iyuke S E., Daramola M,O,. 2022 Co-Digestion of Wastewater Treatment Sewage Sludge with Various Biowastes for Enhancement of Biogas Production. Materials Today Proceedings, Volume 65, Part 3, Pages 2172-2183. https://doi.org/10.1016/j.matpr.2022.05.539

Mudzanani, K., Iyuke, S.E., and Daramola, M.O. 2022. Application of the Modified ADM1 Model to the Anaerobic Co-Digestion of Sewage Sludge for Methane Production. International Journal of Environmental and Technology. (submitted)

Mudzanani K, Iyuke S.E., Daramola M O., 2022. Strategic Removal of Cr(VI) and Cd(II) containing from Aqueous Solutions Using a Sludge-based Activated Carbon adsorbent. Chemical and Biochemical Engineering Quarterly. (submitted)

Conferences

Mudzanani K, Mbhele R N. Daramola M O., 2018. Microbial Community Composition and Physico-chemical characteristics of the Methane Production Feedstock via CSIR two-staged Anaerobic Digestion. 4th National Conference on Global Climate Change, GCC 2018, Polokwane, Limpopo. 3-6th December.

Mudzanani K, Daramola M O., 2018. Towards testing the viability of the CSIR two-staged Anaerobic Digester implementation in low-income municipalities. Out-Of-The Box 2018 Human Settlements Conference. CSIR, Pretoria, South Africa. 24-25 October 2018

Mudzanani, K., Ejekwu, O. and Daramola, M.O. 2019. Dissolution kinetics of corncob in lithium perchlorate solvent system. 27th European Biomass Conference and Exhibition (EUBCE 2019), Lisbon, Portugal, 27-30 May 2019

Mudzanani K, Iyuke S E., Daramola M O, (2021) Co-Digestion of Wastewater Treatment Sewage Sludge with Various Biowastes for Enhancement of Biogas Production. International Conference on Engineering for a Sustainable World (ICESW 2021) 29-30 November 2021

Table of Contents

CHAPTER 1: INTRODUCTION

1.1. Introduction 1
1.2. Background of the Study 1
1.3. Problem Statement 4
1.4. Research questions 5
1.5. Research Objectives and Aims 6
1.5.1. Aim 6
1.5.2. Objectives 6
1.6. Contribution to knowledge 7
1.7. Thesis layout 7
References 9

CHAPTER 2: LITERATURE REVIEW

2.1. Advances in Biogas Production Technologies 11
2.2. Feasibility of biogas production in South Africa 13
2.3. Feedstocks for Biogas production, waste materials 15
2.3.1. Organic Industrial wastes 15
2.3.2. Sewage Sludge 15
2.4. Energy from Biogas 18
2.5. Anaerobic Digestion: Biogas Production Process 20
2.6. The reaction pathway of Anaerobic Digestion 22
2.6.1. Hydrolysis 22
2.6.2. Acidogenesis or fermentation phase 24
2.6.3. Acetogenesis 25
2.6.4. Methanogenesis 25
2.7. Anaerobic Digestion Process Challenges 26
2.8. Key Parameters affecting anaerobic digestion 29
2.8.1. Ammonia 30
2.8.2. Sulfates 31
2.8.3. Alkali and Alkaline Earth Metals 32
2.8.4. Volatile Fatty Acids (VFA) 33
2.8.5. Composition of the feed or substrate 34

2.8.5.1. Physico-chemical characteristics 34
2.8.5.2. Microbial community 34
2.8.5.3. Substrate Solid Content 35
2.8.6. Number of Process Stages and Process Phases 36
2.8.7. pH 36
2.8.8. VFA to TA Ratio 37
2.8.9. Temperature 38
2.8.10. Hydraulic Retention Time 39
2.8.11. Organic Loading Rate 40
2.8.12. C/N ratio 41
2.8.13. Bioreactor configuration 42
2.8.14. Agitation 42
2.8.15. Type of Substrate and Source 43
2.8.16. Pre-treatment 44
2.8.17. Use of Additives 44
2.9. Anaerobic Co-digestion 44
2.9.1. Mechanism of Co-digestion 45
2.9.2. Carbohydrate's co-substrates 46
2.9.3. Protein co-substrates 47
2.9.4. Lipids co-substrate 48
2.9.5. Other Co-substrates 49
2.9.6. The approach of selecting suitable co-substrate 49
2.9.6.1. Composition of the co-substrate 49
2.10. Microbial Community in anaerobic digestion 55
2.10.1. Microbial Community in Stages of Anaerobic Degradation 56
2.11. Feasibility of Synthesizing Activated Carbon from sludge 57
2.11.1. Activated Carbon Production Techniques 58
2.11.2. Carbonization 59
2.11.3. Activation 59
2.11.3.1. Physical Activation 59
2.11.3.2. Chemical Activation 60
2.12. SAC as an adsorbent material 60
2.12.1. Removal of Heavy Metals By Adsorption 60
2.13. Quality Improvement of Digestated material 61
2.14. Adsorption Mechanisms of the activated carbon 62
2.15. Factors Influencing the Adsorption Efficacy 65
2.15.1. Pore Size and the Morphological Structure 66

2.15.2. Surface Chemistry of the material 67
2.15.3. Hydrophobicity Interaction 68
2.15.4. Temperature: Production and Operational 68
2.15.5. Elemental Composition 69
2.15.6. Adsorbent Dosage and Contact Time 70
2.15.7. Surface Charge 70
2.16. Modified Biochar for Wastewater Remediation 70
2.16.1. The Modification of Biochar 70
2.16.2. Adsorbate Interactions with the modified biochar 73
2.16.2.1. Sorption 73
2.16.2.2. Ion Exchange 74
2.16.2.3. Precipitation 74
2.17. Chapter Summary 75
References 77

CHAPTER 3: MATERIAL AND METHODS

3.1. Sample, Study Area, and Sampling Method 92
3.1.1. Base Substrate and Sampling 92
3.1.2. Chemicals 92
3.1.3. Organic co-substrates Sources 92
3.2. Preparation of substrates 93
3.3. Proximate and Ultimate Analysis of Organic Waste 94
3.4. Inoculum 94
3.5. Theoretical Biogas Potential 95
3.6. Surface Characterization techniques 96
3.6.1. Fourier Transform Infrared (FTIR) 96
3.6.2. Scanning Electron Microscope (SEM) 96
3.6.3. Thermogravimetric Analysis (TGA) 96
3.6.4. Surface area analysis 97
3.6.5. Ultraviolet-visible spectroscopy (UV-Vis) 97
3.7. Physicochemical Characterization techniques 99
3.8. Microbiological Characterization techniques 100
3.9. Anaerobic Digestion & Co-digestion with Biochemical Methane Potential 103
3.9.1. Batch Experimental Set-up 104
3.10. Anaerobic Digestion: Semi-continuous process 108
3.10.1. Benchtop study 108
3.10.2. Pilot trials 109

3.11. Synthesis of the sewage sludge-based activated carbon 112
3.12. The adsorption performance of the material 113
3.12.1. Batch adsorption study 113
3.12.2. Batch equilibrium studies 114
Reference 115

CHAPTER 4: ANAEROBIC CO-DIGESTION OF SEWAGE SLUDGE WITH DIFFERENT BIOWASTES TO ENHANCE BIOGAS PRODUCTION

4.1. Introduction 119
4.2. Materials and Method 121
Please refer to Section 3.1-3.5 and Section 3.7-3.10 for information on materials and methods 121
4.3. Results and Discussion 122
4.3.1. SEM Imaging 122
4.3.2. Taxonomic Profile of the Microbial Community 123
4.3.3. Microbial Community in Anaerobic Digestion 124
4.3.4. Archaeal community composition. 126
4.4. Anaerobic Co-digestion experiments 127
4.4.1. Physicochemical characteristics of co-substrates 127
4.4.2. Batch studies, Sludge, and Co-substrates 130
4.4.2.1. Co-digestion with high solid content wastes 130
4.4.2.2. Co-digestion with low solid content (liquid) wastes 146
4.4.2.3. Collective results for the batch study 147
4.4.3. Biogas Production: Semi-continuous studies 150
4.4.4. COD Removal Efficiency in AD Bench Studies 151
4.4.5. Pilot plant Trials: CSIR-AD Semi-continuous 152
4.4.6. COD Removal Efficiency in AD Pilot Plant trial 156
4.5. Conclusion 156
References 158

CHAPTER 5: APPLICATION OF THE MODIFIED ADM1 MODEL TO STUDY KINETICS OF THE ANAEROBIC DIGESTION OF SEWAGE SLUDGE FOR METHANE PRODUCTION PROCESS

5.1. Introduction 166
5.2. Material and Methodology 170
5.2.1. Analytical Method 170
5.2.2. Mathematical Model Development 171
5.2.3. Sensitivity analysis 177
5.2.4. Flow chart for code running ADM1 model. 179
5.3. Results and Discussion 180

5.3.1. ADM1 Simulation using Measure Parameters 183
5.3.2. Model calibration and Validation 188
5.4. Conclusion 197
Reference 198

CHAPTER 6: FEASIBILITY STUDY ON SYNTHESIS OF SEWAGE SLUDGE-BASED ACTIVATED CARBON: PROSPECTS OF MUNICIPAL WASTEWATER REMEDIATION

6.1. Introduction 204
6.2. Materials and Methods 205
Please refer to Section 3.6 and Section 3.11-3.12 for information on materials and methods 205
6.3. Results and Discussion 205
6.3.1. SAC Characterization 205
6.3.1.1. The textural properties 205
6.3.1.2. SEM: Morphology Analysis 207
6.3.1.3. TGA: Thermogravimetric Analysis 209
6.3.1.4. FT-IR analysis 210
6.3.1.5. ED-XRF analysis 212
6.3.2. Material Performance: Comparison 213
6.3.2.1. Comparison of SAC against CGAC and raw sludge 213
6.3.3. SAC Performance: Effect of the operation conditions 214
6.3.3.1. Effect of the initial pH 214
6.3.3.2. Effect of SAC dosage 216
6.3.3.3. Effect of initial concentration on adsorption equilibrium 217
6.3.4. Adsorption Isotherm: Effect of Temperature 219
6.3.4.1. Langmuir isotherm 219
6.3.4.2. Freundlich isotherm 220
6.4. Conclusions 221
References 223

CHAPTER 7: CONCLUSIONS & RECOMMENDATIONS

7.1. Introduction 228
7.1.1. Contribution to knowledge 228
7.2. Conclusions 228
7.3. Recommendations for Future Research 232

APPENDICES

A: Initial Data, ADM1 Code 234

List of Figures

Figure 1.1: Current practice of sludge treatment in the municipality WWTP, adapted from (DEA, 2014; Department of Energy, 2019; Water Research Commission, 1997) 3

Figure 2.1: Total primary energy supply, Source: DoE Energy Balances, 2019 13

Figure 2.2: Renewable energy resources mix hydropower, nuclear, wind, solar, and coal energy, source: EGB Engineering, 2018 16

Figure 2.3: Breakdown of sewage sludge disposal options at municipal WWTWs (adapted from DEA, 2018) 22

Figure 2.4: A simplified schematics presentation of the AD stages, Adapted from (Tetteh & Rathilal, 2020) 26

Figure 2.5: Simultaneous hydrolysis reaction. (i) Carbohydrates: Lactose, a polysaccharide, is hydrolyzed to produce galactose and glucose, both monosaccharides. (ii) Lipids: triglycerides are split into three fatty acids and glycerol in the presence of water molecules. (iii) Proteins: peptide bonds are broken to separate amino acids. Adapted from (Rea, 2014) 29

Figure 2.6: Schematic of microbial processes and the stepwise progression of these processes in the anaerobic digestion process for methane production. Source: (Rea, 2014) 31

Figure 2.7: Effect of pH and Temperature on the balance between ammonium ion and ammonia (Emerson, et al. 2015) 38

Figure 2.8: Sulphate-reducing bacteria compete for resources with the CH4 forming microbial community 39

Figure 2.9: Anaerobic bacterial growth rate at different temperature profiles (Rosato (2008)) 45

Figure 2.10: Effect of HRT on specific and daily biogas yield, Source: Masebinu 2018 47

Figure 11: Influence of agitation on degradation of volatile solid, Source (Meegoda et al., 2012) . 50

Figure 2.14: Adsorption mechanism of organic pollutant on biochar surface (Ahmad, et al. 2014) 69

Figure 2.15: IUPAC standard for Pore size classification (Y. Wang et al., 2019) 72

Figure 2.16 Adsorption mechanism on biochar surface in two temperature ranges (Ahmad et al., 2014) 74

Figure 2.17: A Simplified Schematic of Some Acidic Surface Groups on Activated Carbon (Chen et al., 2008) 77

Figure 2.18 Pictorial Definition of adsorption & Ion Exchange Process 79

Figure 3.1: Spectrophotometric analysis method using standard Hach test kits 109

Figure 3.2: Illustration of Sample & PacBio sequence generation procedure, adapted from (PacBio, 2015) 111

Figure 3.3: An Increased biogas production rate compared to reference, B increase of biogas production degree of degradation and C a combination of A and B (Odnell, 2018). 114

Figure 3.4: Automatic Methane Potential Test System II (AMPTS II) (Bioprocess Control Sweden AB) 115

Figure 3.5: The Digester setup in the BMP setup Substrates & inoculum measurements 116

Figure 3.6: Eudiometer setup for estimating biogas from substrates 117

Figure 3.7: The semi-continuous test was conducted for a duration of 150 days 118

Figure 3.8: CSIR Semi-continuous Digester, Ritter gas flowmeter, and Geotech Biogas5000 119

Figure 3.9: Procedure on how to adjust the OLR 121

Figure 3.10: Sludge-based Activated Carbon (SAC) 122

Figure 4.1: A simplified schematic presentation of the anaerobic digestion phases, adapted from (Salihi et al., 2018) 130

Figure 4.2: The biochemical methane potential test using the automatic methane potential test system (AMPTS II). 134

Figure 4.3: SEM micrographs of sewage sludge a) Raw sludge before anaerobic digestion b) Digested sewage sludge. 138

Figure 4.4: The Bacterial community composition classified as phylum, class, order, family and genus; the taxonomic distribution of the microbial community in the sewage sludge sample 139

Figure 4.5: Kingdom Archaeal community composition in classification of class and significant family. 140

Figure 4.6: The microbial metabolic pathway during anaerobic digestion constructed using the most abundant AD species, adapted from [19]. 141

Figure 4.7: Cumulative methane production plotted against time for co-digestion of sewage sludge and biowaste as co-substrates 144

Figure 4.8: Methane cumulative results for co-digestion of sludge with fresh produce and dairy thick waste 146

Figure 4.9: Cumulative methane production for co-digestion with liquid wastes as co-substrates..... 147

Figure 4.10: Methane production of Driefontein WWTW sludge and the co-substrates.....148

Figure 4.11: Methane production of Driefontein WWTW sludge and the co-substrates.....149

Figure 4.12: Semi-continuous biogas production per day 151

Figure 4.13: The COD of the feed and after the BMP study, and the COD removal efficiency 152

Figure 4.14: Pilot plant Trial 1, methane & carbon dioxide concentration and pH profile.....153

Figure 4.15: Pilot plant Trial 2 methane and carbon dioxide concentration and pH profile.....154

Figure 5.1: Anaerobic digestion process, composites degration to inerts and hydrolysis reactants, through a disintergration step. 167

Figure 5.2: Mass balance boundary around CSTR in the anaerobic digestion system, adapted from Batstone et al (2002).....172

Figure 5.3: Flow chart for running the ADM1 model using Matlab/SimulinkTM.....178

Figure 5.4: Model simulation component output, Substrate number output 1-6 180

Figure 5.5: Model simulation component output, Substrate number output 7-12 181

Figure 5.6: Model simulation component output, Substrate number output 13-19.....183

Figure 5.7: Model simulation component output, Substrate number output 20-25.....184

Figure 5.8: Model simulation component output, Substrate number output 20-25.....185

Figure 5.9: Model simulation component output, Substrate number output 26-30.....186

Figure 5.10: Component pH output from model simulation.....186

Figure 5.11: Component output for gas production, pressure and flowrate.....187

Figure 5.12: Sensitivity analysis plot for the simulated ADM1.....188

Figure 5.13: Change sensitivity for $K_{S,IN}$ & $K_{i,nh3}$ as function of in S_{IN} 189

Figure 5.14: Optimal combination of S_{IC} & S_{IN} input variables propagates during a simulation.....191

Figure 5.15: Q_{IN}, and how the resulting gas production changes during the simulation.....192

Figure 6.1: SEM micrographs,(A): Raw sludge,(B): SAC shows spherical carbon particles on the surface of carbonized. 206

Figure 6.2: Thermal decomposition of raw sewage sludge and SAC 207

Figure 6.3: FTIR spectra of CGAC (a) raw sewage (b) and SAC (c) samples. 208

Figure 6.4: EDX spectra or Semi-quantitative XRF analysis of the raw sludge SAC and raw sludge samples 210

Figure 6.5: Adsorption of Cr(VI) by the sewage sludge-based activated carbon with time 211

Figure 6.6: Effect of initial pH on adsorption of Cr (VI) and Cd (II) 213

Figure 6.7: Effect of adsorbent dosage on adsorption of Cr (VI), Cd (II. Conditions: pH=10 for Cd (II); pH=2.0 for Cr (VI); 250 mg/L adsorbate concentration; 24 hrs. contact time 214

Figure 6.8: The adsorption uptake versus adsorption time at various initial concentrations at 30°C on sludge-based activated carbon. 215

Figure 6.9: The Langmuir linear plots of Ce/Qe versus Ce 217

Figure 6.10: Linearized Freundlich isotherm for adsorption 218

List of Tables

Table 2.1: Key research gaps/challenges 13
Table 2.2: Total waste distribution data in South Africa (tons) (Department of Environmental Affairs, 2018). 14
Table 2.3: Characteristics of municipal sewage sludge. Source: (Rulkens, 2008) 17
Table 2.4: The Advantages and Disadvantages of Anaerobic Digestion, Environmental, Economic & Energy Aspects 19
Table 2.5: VFA/TA ratio, their impact, and recommended response actions, Masebinu, 2018) 37
Table 2.6: Potential co-substrate identified for anaerobic co-digestion of sewage sludge 51
Table 2.7: Summary of Microbial Community in Stages of Anaerobic Degradation, adapted from (Wirth et al., 2012) 57
Table 2.8: Functional Groups on Activated Carbon Surfaces & the corresponding Assignments (Shen et al., 2008) 72
Table 4.1: The physicochemical characteristics (pH, TS, VS & COD) of raw COT and JW sewage sludge (COT1,2 & JW 1,2) 142
Table 4.2: The physicochemical characteristics (TOC, C/N, TA & TKN) 143
Table 4.3: Inhibitory factor analysis 145
Table 4.4: Characterization of the Inoculum 151
Table 4.5: Composition of raw sludge and co-substates 153
Table 4.6: Composition of the blends (on 1:3 ratio) sewage sludge & co-substrates for co-digestion experiments. 154
Table 4.7: Removal of COD, TS & VS in co-digestion of sewage sludge with high solid content wastes. 146
Table 4.8: Removal of COD, TS & VS in co-digestion of sewage sludge with dairy thick waste. 151
Table 5.1: Measured parameters as inputs for ADM1 170
Table 5.2: Inhibition factors and equations summarized 175
Table 6..1: Characteristics of porous structure of the raw sludge and SAC. 204
Table 6.2: Summary of Langmuir Isotherm model constants and R2 values obtained from the linear plot 215
Table 6.3: Summary of Freundlich Isotherm model constants and R2 values obtained from the linear plot 216

List of Abbreviations

ACD	Anaerobic Co-digestion
AD	Anaerobic digestion
AMPTS	Automatic methane potential test system
ANOVA	Analysis of variance
BET	Brunauer-Emmet-Teller
BMP	Biochemical Methane Potential
BMP	Biochemical methane potential
BSG	Brewery Spent grain
C/N	Carbon to nitrogen ratio
CAPEX	Capital expenditure
CAPEX	Capital expenditure
Cd	Cadmium
CH_4	Methane
CHP	Combined heat and power
Co	Cobalt
CO_2	Carbon dioxide / Carbon (iv) oxide
COD	Chemical Oxygen Demand
COD	Content of oxygen demand
CoT	City of Tshwane
Cr(VI)	Hexavalent Chromiun
DIET	Direct interspecies electron transfer
DW	Dairy Waste
EDX	Energy dispersive X-ray
Fe	Iron
FOG	Fat, oil and grease
FPW	Fresh Produce Waste (Fruit and vegetable)
H & hr	hour
H_2	Hydrogen
H_2S	Hydrogen sulphide
HRT	Hydraulic Retention Time
HRT	Hydraulic retention time
ISR	Inoculum to substrate ratio

KOH	Potassium Hydroxide
LCFA	Long-Chain Fatty Acids, 12 or more carbon atoms
m^3	Cubic meter
MSW	Municipal solid waste
N and N_2	Nitrogen
NaOH	Sodium Hydroxide
NH_3	Ammonia
Ni	Nickel
NL	Normal Litre
NW	Northern Works
O and O_2	Oxygen
OFMSW	Organic fraction of municipal solid waste
OLR	Organic loading rate
OLR	Organic Loading Rate, expressed as g VS/L day
OPEX	Operating expenditure
pH	Power of hydrogen
RPM	Revolution per minute
S/N	Signal-to-noise ratio
SDGs	Sustainable development goals
SEM	Scanning Electron Microscopy
ST	Coke drainage waste
TA	Total Alkalinity
TA	Total alkalinity
TGA	Thermogravimetric analysis
TS	Total Solids
USAB	Up-flow sludge anaerobic blanket
VFA	Volatile Fatty Acids, less than 12 carbon atoms
VFA/TA	The ratio of volatile fatty acid to total alkalinity
VS	Volatile Solids
WAS	Waste Activated Sludge
WWTP	Waste Water Treatment Plant
yr	Year
Zn	Zinc
ΔG^o sw	Gibbs free energy of Reaction

CHAPTER 1

INTRODUCTION

1.1. Introduction

Renewable energy such as biogas and the recycling of industrial biowaste helps combat global warming, climate change, air pollution, and ocean acidity. It also helps us reduce our carbon footprints, protects the environment, and is an energy system that's fit for the 21st century (Masindi, Chatzisymeon, et al., 2018; Masindi, Madzivire, et al., 2018). The first biogas production via the AD process is dated back to 1859, however until recently that scientists and researchers start to focus on the concept due to energy shortages (Gerardi, 2003). The purpose of this study is to optimize the digestion process, evaluate the enhancement by co-digestion with of different industrial bio-wastes, and conduct a model-based simulation to predict the performance of the AD process and synthesis of (Sludge-based Activated Carbon) SAC, the value-added product using the AD by-products. This chapter will provide an introduction to the study by first discussing the background and context, followed by the research problem, the research aims, objectives and questions, the significance, and finally, the limitations.

1.2. Background of the Study

According to the 2015 Department of Water and Sanitation (DWS) report, the sustainable disposal or treatment of solid sludge in an environmentally acceptable manner is a major problem faced by most municipalities' wastewater treatment plants (WWTP) in South Africa (Herselman & Moodley, 2009; WRC, 1997). According to the Department of Environmental Affairs (DEA) report, there are more than 841 WWTPs, and fewer than 60 discharge clean water to the environment (Department of Environmental Affairs, 2014). The current regulatory legislation that governs the handling, disposal, management, and re-use of sludge is controlled by the Department of Water Affairs (DWA) in terms of the National Water Act (Act 36 of 1998) and the Environment Conservation Act (Act 73 of 1989). The act aims "To provide for fundamental reform of the law relating to water resources; to repeal certain laws; and to provide for matters connected therewith" (Government of South Africa, 1998). Despite this policy, roughly 67% of South African

sewage water systems do not abide by these regulatory requirements (Government of South Africa, 1998). As a developing country, SA urban areas have rapid progress in urbanization and industrialization which results in a high population and thus a continuous increase in the production of sewage sludge. Hence if not attended to, the volume of generated sewage sludge is expected to double by 2030 (Nahman et al., 2009). Furthermore, as a mandate of frameworks, RSA urges industries to use affordable sources of energy to improve living conditions and reduce environmental impact.

Raw sludge has a potential threat to the environment if released without processing. Figure 1.1 shows the current practices applied for sewage sludge management, as indicated most of these practices are detrimental to the environment (Judex et al., 2012). However, the sludge contains a significant amount of organic compounds that can be converted to biogas (CH_4 and CO_2) via the anaerobic digestion (AD) process (Bachmann, 2015; Ewings, 2018). The biogas generated can either be used for vehicle fuelling, cooking, heating, and power generation (Gerardi, 2003). Based on the analysis conducted on behalf of WRC in 2018, 30 MW annually could be saved by municipalities if this process is optimized properly (Musvoto et al., 2018). South Africa was one of the first countries in the world to utilize digesters as part of sludge management in WWTP, with the first municipal digesters built as far back as 1940 (Bachmann, 2015). And yet the problem of sewage sludge management and discharge of unsafe water persist. This is because most digesters at WWTP were not built to capture and use the biogas produced, but rather to assist in sludge management only. Thus, the technology was overlooked in such a way that the process was not optimized, maintained, or operated to its full functionality (Musvoto et al., 2018).

South Africa has approximately 50 major municipalities; these municipalities have wastewater treatment plants large enough to operate an effective biogas plant which in turn could save about 30 MW of electricity (Department of Energy, 2019; Musvoto et al., 2018). A practical example is the Northern Works Wastewater Treatment plant owned by Johannesburg Water treats about 430 million litres of sewage a day (Deacon & Louw, 2013). There are more than 200 biogas digesters scattered across South Africa and yet the use of biogas is not growing as fast as it is supposed to be in the country irrespective of its benefits such as reducing energy-related problems such as pollution and energy shortage (Pecharaply et al., 2007)

Sludge has a potential threat to the environment. Figure 1.1 shows the current practices applied or sewage sludge management, as indicated most of these practices are detrimental to the environment.

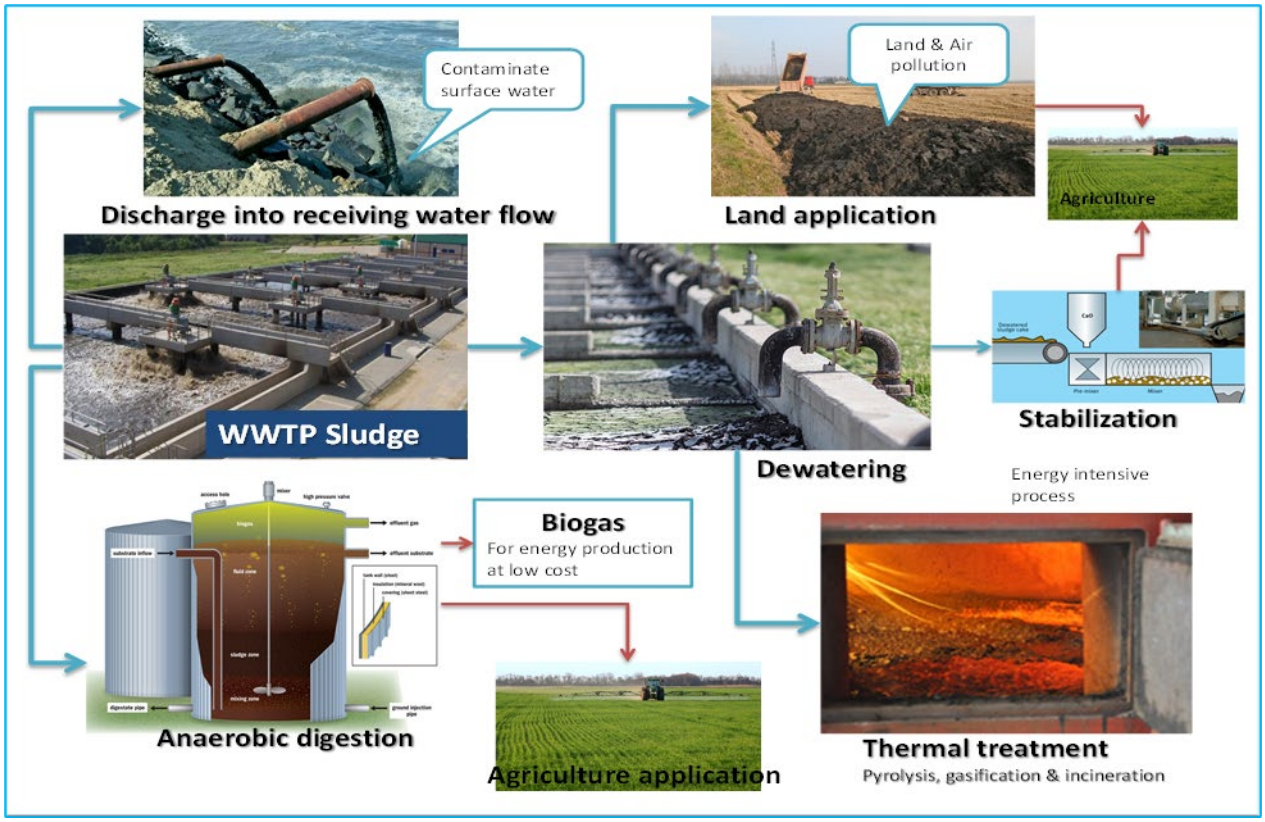


Figure 1.1: Current practice of sludge treatment in the municipality WWTP, adapted from (Department of Environmental Affairs, 2014; Department of Energy, 2019; Water Research Commission, 1997)

Anaerobic digestion & agricultural application posed to be a better option as opposed to disposal via sea discharge or landfill, dewatering, and thermal treatment such as incineration, pyrolysis and gasification (WRC, 1997). Since the beneficial use of sludge is the most encouraging technique by the DWA, research and technology innovation should be the main focus to ensure sustainable waste management. The use of sludge to ensure zero waste will be highly beneficial (Oladejo et al., 2019). The country is still experiencing serious energy constraints thus industries are urged to make the transition to more diverse energy sources such as renewable energy (Musvoto et al., 2018). The CSIR has been doing renewable energy research for more than a decade now, including the production of biogas which can be converted to electricity. It was then identified that sewage waste, agricultural and farming wastes can be utilized as feed to generate the industries' off-grid electricity (Musvoto et al., 2018). This will be the best alternative to a

'cleaner' and more sustainable feed supply as compared to coal use, additionally saving electricity costs.

For research purposes, The Council for Scientific and Industrial Research, Built Environment (CSIR-BE) has designed a semi-automated Anaerobic Digester (AD) that is operational and is utilized to serve as a research platform to test the production of biogas with a potential to generate electricity. The current challenge with this AD is the efficiency, and low biogas production which is due to the feed composition, and operating parameters such as temperature, pH, stirring, and feeding conditions. As a result of insufficient methane, the Combined Heat & Power (CHP) engine does not run. To keep the digester running, external energy is required which defeats the purpose of the self-sustaining AD process (Herselman & Moodley, 2009). Literature reports that it is possible to achieve further optimization of the process (Anukam et al., 2019). So far 61% methane biogas has been recorded, however, this can be improved to ensure the highest possible yield, estimated to be 80% CH_4 of biogas per feed material, i.e., sewage sludge from the municipal WWTW (Deacon & Louw, 2013)This is among other biogas-producing industries which are facing low biogas generation.

The main purpose of this research study is to enhance the AD process via co-digestion to increase biogas production and beneficiate the digested material. The AD co-digestion technique will then be utilized in an attempt to solve the challenge. Hence additives, co-substrates, and the pre-treatment process will be evaluated to see if biogas production yield can be increased. The polished or improved AD model of the anaerobic digestion plant will be carried out as added task. To ensure complete beneficiation of sewage sludge from the municipality, the evaluation of the routes that can be applied to make digested material and wastewater produced applicable in other processes was carried out.

1.3. Problem Statement

As mentioned previously the major challenge with AD is the low efficiency of biomethane production which can be improved by anaerobic co-digestion of sludge with various biowastes from different industries. Most research efforts have primarily focused on the use of co-substrates to boost biogas production, and few studies have investigated anaerobic co-digestion of specific organic wastes as co-substrates to optimize biogas production; however, no comparative study of various co-substrates or

bio-wastes has been conducted (Almomani & Bhosale, 2020)The identified knowledge gap is a lack of understanding of the interactive mechanism in the digestion system between the primary substrate and co-substrates (Sosnowski et al., 2003)The simulation model specifically the ADM1 can be improved to provide insights into the physicochemical analysis of the parameters that catalyze and those that can inhibit anaerobic digestion (Mendes et al., 2015)

The other challenge is not achieving "zero-waste" production during the AD process. Digestate, the dry by-product that is normally dumped on the drying beds poses a further environmental risk (Pecharaply et al., 2007)The most recent application as fertilizers in the agriculture sector, however, there are challenges related to properties thus failing to be South African Bureau of Standards (SABS) approved (Mitchell et al., 2014). Literature frequently reports on the synthesis of adsorption materials from bio-wastes, and a few investigate synthesis from digestate, such as SAC. Due to the chemical and physical structure of the sludge material, appropriate techniques can be applied to synthesize SAC from waste sludge at a low cost of the modification process, highly efficient, and with low installation, operations, and maintenance costs (Bian et al., 2018).

1.4. Research questions

Through the course of this research, an attempt will be made to answer the following questions:

1.4.1. What are the physicochemical & microbiological characteristics of the primary substrates and the co-substrates, the feed material for biogas production?

1.4.2. Can the current applied AD process be optimized further by manipulating major operating conditions, i.e. pH, temperature, and the feed composition?

1.4.3. Which combination or mix design of sludge and co-substrates can significantly enhance biogas production, and increase the quality and quantity of biomethane that is sufficient for a self-sustaining AD process?

1.4.4. Can the Anaerobic Digestion Model 1 (ADM1) be improved to provide specific insights into the physicochemical analysis of the parameters that catalyze and those that can inhibit the anaerobic digestion process, and thus compare the simulation with experimental results?

1.4.5. What methods can be applied to produce value-added products from the digestate, the by-products from the anaerobic digestion to achieve a zero-waste AD process?

1.5. Research Objectives and Aims

1.5.1. Aim

The overall aim of this study is to increase biomethane production via anaerobic co-digestion of municipal wastewater sludge and various biowastes. Further, evaluate the feasibility of the value-added products from the by-products of biogas production.

1.5.2. Objectives

To achieve the proposed aim of this study, the specific objectives pursued are;

1. To assess the physicochemical & microbiological characteristics of the primary substrates, sewage sludge, and the co-substrates, industrial biowastes.

2. To conduct laboratory batch studies on the effect of major operating parameters i.e. pH, temperature, and the feed composition, optimize the process, and thus implement on the pilot scale.

3. To evaluate the anaerobic co-digestion to increase biomethane production by co-digesting sludge as primary substrates and different industrial biowastes as co-substrates in BMP and semi-continuous processes.

4. Application of the modified ADM1 model to study the physicochemical, and biochemical kinetics of the anaerobic digestion of sewage sludge for biomethane production.

5. To evaluate the performance of Sludge-based Activated Carbon (SAC) derived from the digested material and thus explore its application in wastewater treatment.

1.6. Contribution to knowledge

This research provides information about the use of South African municipal wastewater treatment effluents in anaerobic biogas production and new knowledge which addresses the research gaps in the study is listed below.

1.6.1. Detailed physicochemical & microbiological characteristics of the sludge as primary substrates, specifically for CoT and JW and the co-substrates which industrial wastes that get dumped with being analyzed.

1.6.2. Introduction of the new and novel BMP technique which was developed in our lab for this specific research.

1.6.3. A comparative study of sludge co-digestion with various co-substrates or bio-wastes, The manuscript has been published on ScienceDirect.

1.6.4. The use of MATLAB Simulink for simulation of the modified ADM1 for a specific substrate and co-substrates blend, comparison with experimental results.

1.6.5. Waste beneficiation by synthesizing Sludge-based Activated Carbon (SAC) derived from the digested material and thus exploring its application in wastewater treatment.

To provide quick access to the information documented in this thesis, the results of this study have been communicated to the scientific community through peer-reviewed journal articles and contributions to conferences (see Appendix B for copies of these contributions)

1.7. Thesis layout

Chapter 2

This chapter provides an outlook on the energy sector in South Africa and evaluates the various energy production methods that are used in the country. It highlights the drawbacks of energy derived from fossil fuels. It examines the country's efforts toward the intensification of clean and sustainable energy like the anaerobic digestion process. Furthermore, the chapter will clarify the potential of municipal sewage sludge waste as feedstocks for anaerobic digestion for biogas production in South Africa and the rest of the world.

Chapter 3

The chapter will describe the material that was used in the study as well as the approach used to obtain the research's goals & objectives. The source, sampling, and characterization of organic waste were primarily covered. The batch BMP test and semi-continuous digesting methodology for the AD process. The procedure for modifying and synthesizing the Sludge-based activated carbon material is also described, as is the material performance test.

Chapter 4

The primary findings of this study were presented, and their significance was addressed. This chapter has provided and examined the results of characterization of sewage sludge and organic waste, as well as theoretical and BMP. The possible impact of co-substrates on sewage sludge AD, as well as ideal circumstances for its application, were also investigated. Two manuscripts are published in *"EUBCE conference proceedings"* and the *"Sustainability"* journal is included, See Appendix B.

Chapter 5

This chapter presents the developed methods for evaluating the co-digestion model based on Anaerobic Digestion Model No. 1 (ADM1).

Chapter 6

This chapter presents the results of the investigation of the effect of adsorption of metal ions (Cr (VI) and Cd^{2+}) and dyes. The Adsorption studies, kinetics & Isotherms of heavy metal & dyes using sludge-based activated carbon. The findings from this work have been compiled in a manuscript that is currently under review in the "Chemical & Biochemical Engineering Quarterly" (see Appendix B).

Chapter 7

This chapter presents the study's conclusions and recommendations. The purpose of this study was summarized. A conclusion based on results that addressed the research questions was offered. Furthermore, future work recommendations and limits in this study were documented.

References

Almomani, F., & Bhosale, R. R. (2020). Enhancing the production of biogas through anaerobic co-digestion of agricultural waste and chemical pre-treatments. Chemosphere, 255. https://doi.org/10.1016/j.chemosphere.2020.126805

Anukam, A., Mohammadi, A., Naqvi, M., & Granström, K. (2019). A review of the chemistry of anaerobic digestion: Methods of accelerating and optimizing process efficiency. Processes, 7(8), 1–19. https://doi.org/10.3390/PR7080504

Bachmann, N. (2015). Sustainable biogas production in municipal wastewater treatment plants. In IEA Bioenergy.

Bian, Y., Yuan, Q., Zhu, G., Ren, B., Hursthouse, A., & Zhang, P. (2018). Recycling of waste sludge: Preparation and application of sludge-based activated carbon. International Journal of Polymer Science, 2018. https://doi.org/10.1155/2018/8320609

Deacon, S., & Louw, P. (2013). The installation of CHP at Johannesburg Northern waste treatment works. 11. http://carbonn.org/uploads/tx_carbonndata/BIOGAS PAPER REV4.pdf

Department of Energy. (2019). The South African Energy Sector Report 2019. In Department of Energy. http://www.energy.gov.za

Department of Environmental Affairs. (2014). National Guideline for the Discharge of Effluent From Land-based Sources into the Coastal Environment.

Ewings, S. (2018). Build a biogas plant. http://www.build-a-biogas-plant.com/biogas-downloads/

Gerardi, M. H. (2003). The Microbiology of Anaerobic Digesters. https://doi.org/10.1002/0471468967

Goverment of South Africa. (1998). National Water Act 3 of 1998. Government Gazette, 36. https://doi.org/10.1163/9789004272224_029

Herselman, J. (Golder A. A., & Moodley, P. (Zitholele C. (2009). Guidelines for the Utilisation and Disposal of Wastewater Sludge: Volume 4 Requirements for the beneficial use of sludge at high loading rates (Vol. 4, Issue June).

Judex, J. W., Gaiffi, M., & Burgbacher, C. H. (2012). Gasification of dried sewage sludge: Status of the demonstration and the pilot plant. Waste Management, 32(4), 719–723.

Masindi, V., Chatzisymeon, E., Kortidis, I., & Foteinis, S. (2018). Assessing the sustainability of acid mine drainage (AMD) treatment in South Africa. Science of the Total Environment. https://doi.org/10.1016/j.scitotenv.2018.04.108

Masindi, V., Madzivire, G., & Tekere, M. (2018). Reclamation of water and the synthesis of gypsum and limestone from acid mine drainage treatment process using a combination of pre-treated magnesite nanosheets, lime, and CO2bubbling. Water Resources and Industry. https://doi.org/10.1016/j.wri.2018.07.001

Mendes, C., Esquerre, K., & Matos Queiroz, L. (2015). Application of Anaerobic Digestion Model No. 1 for simulating anaerobic mesophilic sludge digestion. Waste Management, 35(1), 89–95. https://doi.org/10.1016/j.wasman.2014.10.013

Mitchell, S. A., de Wit, M. P., Blignaut, J. N., & Crookes, D. (2014). Waste Water Treatment Plants : The Financing Mechanisms Associated with Achieving Green Drop Rating (Issue 2085). http://www.wrc.org.za/wp-content/uploads/mdocs/2085-1-14.pdf

Musvoto, E., Ngwenya, N., Mangashena, H., & Mackintosh, A. (2018). Energy Recovery From Wastewater Sludge - A Review of Appropriate Emerging and Established Technologies for the South African Industry: Vol. TT 752/18.

Nahman, A., Wise, R., & de Lange, W. (2009). Environmental and resource economics in South Africa: Status quo and lessons for developing countries. South African Journal of Science, 105(October), 350–355.

Oladejo, J., Shi, K., Luo, X., Yang, G., & Wu, T. (2019). A review of sludge-to-energy recovery methods. Energies, 12(1), 1–38. https://doi.org/10.3390/en12010060

Pecharaply, A., Parkpian, P., Annachhatre, A. P., & Jugsujinda, A. (2007). Influence of anaerobic co-digestion of sewage and brewery sludges on biogas production and sludge quality. Journal of Environmental Science and Health - Part A Toxic/Hazardous Substances and Environmental Engineering, 42(7), 911–923. https://doi.org/10.1080/10934520701369818

Sosnowski, P., Wieczorek, A., & Ledakowicz, S. (2003). Anaerobic co-digestion of sewage sludge and organic fraction of municipal solid wastes. Advances in Environmental Research, 7(3), 609–616. https://doi.org/10.1016/S1093-0191(02)00049-7

WRC. (1997). Permissible Utilisation and Disposal of Sewage Sludge Edition 1 (Issue August, p. 83). Water Research Commission.

CHAPTER 2

LITERATURE REVIEW

This chapter offers a breakdown of the energy market in South Africa. It explores the different energy supplies that are used in the country and addresses the problems caused by energy extracted from fossil fuels. It explores the country's efforts to strengthen clean and sustainable energy resources, such as the production of biogas via anaerobic digestion (AD). In addition, the technical aspects are clarified. Furthermore, it explains the technical barriers faced by the AD process and concludes by proposing different strategies that could be used to accelerate its large-scale production from biowaste feedstocks.

2.1. Advances in Biogas Production Technologies

Various countries have actively promoted a massive global biogas market in recent decades. Furthermore, advanced biogas production technologies have been endorsed by local or international supportive rules, such as research, design, and development of financial funds, subsidization, and guaranteed electricity purchase contracts, to compete with outdated energy suppliers. Over the last few decades, methane has been used as important fossil fuel and converted to generate power, transportation, and heating. Currently, organic waste resources account for the majority of methane consumption and utilization, but bio-methane production from waste recovery approaches has increased significantly. Over the last nine years, its production capacity has increased by 4%. (from 2010 to 2018). Currently, approximately 3.5 megatonnes of oil equivalent (Mtoe) of biomethane is produced globally, with a potential for biomethane production of over 700 Mtoe.

The various applications of biogas technology provide a multi-purpose solution for generating energy for the industrial or social sectors. These applications of biogas are shown in Figure 2.1. Biogas is mainly consumed for combined heat and power (CHP) for electricity generation, hydrogen production units, and advanced energy systems such as fuel cells (Ref). The main advantage of on-site electricity generation is that it eliminates

transportation losses and increases reliability due to independence from a centralized grid that is primarily powered by traditional fossil fuels (Ref). It also generates additional economic profit by meeting the required in-house power demand and selling the excess electricity.

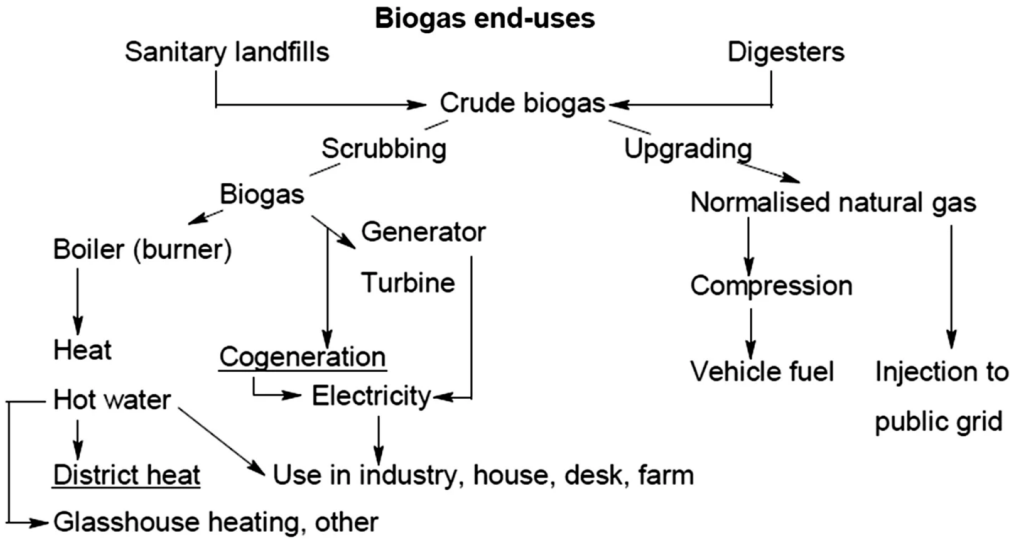


Figure 2.1: Applications and utilization of biogas

Several studies in recent years have shown a decline in the use of a single substrate (or mono-digestion) for AD since it is associated with low methane yield due to operational issues and process instability (Kumar and Samadder, 2020; Serrano et al., 2021). As a result, critical reviews thoroughly examined the application of several useful technologies to improve AD and energy recovery (Atelge et al., 2020; Nguyen et al., 2021). Furthermore, in recent years, this technology has evolved to simultaneous digestion of two or more substrates as organic wastes with other industrial biowastes, in anaerobic co-digestion (Astals et al., 2014). This is a feasible option to overcome the drawbacks of mono-digestion and to improve plant's economic feasibility. Anaerobic co-digestion is the combined treatment of several wastes with complementary characteristics (Astals et al., 2014). However, the key challenges with anaerobic co-digestion are; the pretreatment requirements, understanding of the physicochemical composition of the feed, the complexity of the microbial dynamics, and the modeling data being unavailable (Ref). Indeed, more research is required to address some of the drawbacks associated with the enhancement of biomethane via anaerobic co-digestion. Thus, the key research challenges to be addressed are listed in Table 2.1.

Table 2.1: Key research gaps/challenges

Challenges	Proposed Solution
Low biomethane yield due to anaerobic mono-digestion	Application of the anaerobic co-digestion
Lack of physicochemical data and a microbial consortium of the substrate and the co-substates	Conduct a physicochemical and microbiological analysis on all substrates to understand the synergy, compatibility, and nutrient balance.
Some co-substrates may require pretreatment	Conduct thorough research on the alternatives
The combination of substrates results in the complexity of chemical reactions and the microbial dynamics	Simulation to model and study the physicochemical, and biochemical kinetics of the co-digestion
The policy related to targeting zero-waste production	Waste beneficiation by synthesizing Sludge-based Activated Carbon (SAC) derived from the digested material

2.2. Feasibility of biogas production in South Africa

South Africa has a high degree of urbanization and industrialization that highlights major cities are witnessing increased population growth. As a consequence, the production of biowaste materials has sporadically increased (Herselman & Moodley, 2009). Deposits were highlighted as the potential cause of birth defects and respiratory diseases such as asthma. The Ministry of Health has also expressed concerns about the illegal disposal since it entices illness from flies, mosquitoes, and rats to sites in which sites are located (Department of Health, 2018).

Disposal of organic wastes on disposal sites occurs gradually and thus can take years to come to completion. AD effects on landfills can persist for up to 20-40 years, posing considerable environmental concerns (GreenCape, 2020). The costs of recycling these effluents are prohibitively expensive in recent years, often reaching millions of Rands. Existing waste disposal processes, do not comply with these rules, necessitating the development of new and innovative biowaste management approaches (APWC, 2020).

The concept of "waste-to-energy" has been gaining traction among various stakeholders in South Africa. Anaerobic digestion employs a wide range of biowaste effluents that are

plentiful but pose a disposal challenge. This approach significantly solves the issues associated with the disposal of waste and it is more environmentally friendly than landfills, incineration, or discharge (Stafford et al., 2019).

South Africa has seen a dramatic rise in waste production over the past years. A total of 7.80 million tons of waste was generated by the municipal sector for South Africa in 2018 as shown in Table 2.2. The agricultural sector produced 2.95 million tons and 12.1 million tons of waste were created by the industrial sector From these data it is clear that there is a considerable increase in waste volume in South Africa (Department of Environmental Affairs, 2018). Consequently, in 1997, 42,3 million tons were produced by organic municipal waste, an increase of which 69 million in 2014. Biowaste production increased by 63.1 percent during this time. Data from the Ministry of Environment also showed that waste volume is increasing every year in South Africa by about 11 million tons (Department of Environmental Affairs, 2018).

Table 2.2: Total waste distribution data in South Africa (tons) (Department of Environmental Affairs, 2018).

Waste Type	**Tonne in 2017**	**% waste**
Municipal Waste	4 821 430	3,55
Commercial and industrial waste	3 550 505	2,62
organic waste	30 499 455	22,47
Agricultural	2 954 461	2,18
Construction and demolition waste	4 482 992	3,30
Fly ash and dust	31 420 488	23,15
Paper	2 211 225	1,63
Plastic	1 113 362	0,82
Glass	2 492 636	1,84
Metals	4 035 929	2,97
Tires	238 000	0,18
Bottom ash	5 385 968	3,97
Slag	5 000 150	3,68
Mineral	335 000	0,25
Electronic	66 321	0,05
Sewage sludge	657 963	0,48
Miscellaneous	327 250	0,24
Other	36 161 137	26,64
Subtotal	135754272	1

Several studies have evaluated the ability of various organic sources for biogas production. The use of food products, for example, is a highly preferred substrate because of their nutritional composition and high moisture content (Elbeshbishy & Nakhla, 2012; Rabii et al., 2019). Using biowaste effluents for processing would greatly improve the process economics since these feedstocks are readily available, considered waste materials, and have high methane efficiency. The use of methanogenic bacteria is well known in the literature, especially in microbial bioprocesses (Q. Wang et al., 2016a; Xu et al., 2018).

2.3. Feedstocks for Biogas production, waste materials

2.3.1. Organic Industrial wastes

Effluent streams from sweets, cheese, cereals manufacturers, sugar refineries, breweries, paper mills, and liquor manufacturers are examples of industrial waste. These industries generate a significant amount of wastewater, which consists of sugars and starches. As a result, this promotes the production of biogas by acidogenic bacteria i.e. Clostridium and Bacillus species which produces methane through a series of metabolic reactions. (Gonzalez-Fernandez et al., 2018). The use of wastewaters for anaerobic digestion for biogas production provides a forum for the generation of renewable energy while eliminating pollutants from water. Furthermore, using wastewater to produce energy is beneficial because it wouldn't pollute the environment and provides energy recovery simultaneously (Dong et al., 2009).

2.3.2. Sewage Sludge

The wastewater treatment process produces sewage sludge as a by-product. Sewage sludges generated by wastewater treatment plants continue to cause environmental issues due to their volume and method of reuse. When the population grows, so does the amount of sewage sludge. “Figure 2.2 shows conventional disposal practices in South Africa, such as incineration, landfill, and application to agricultural property, are inefficient and have significant limitations. As a result, turning this waste material into a resource that can improve environmental protection is a more sustainable and cost-effective solution. The primary components of sewage sludge are water and organic matter (6.5% to 48%).” (Dowdy et al., 1976).

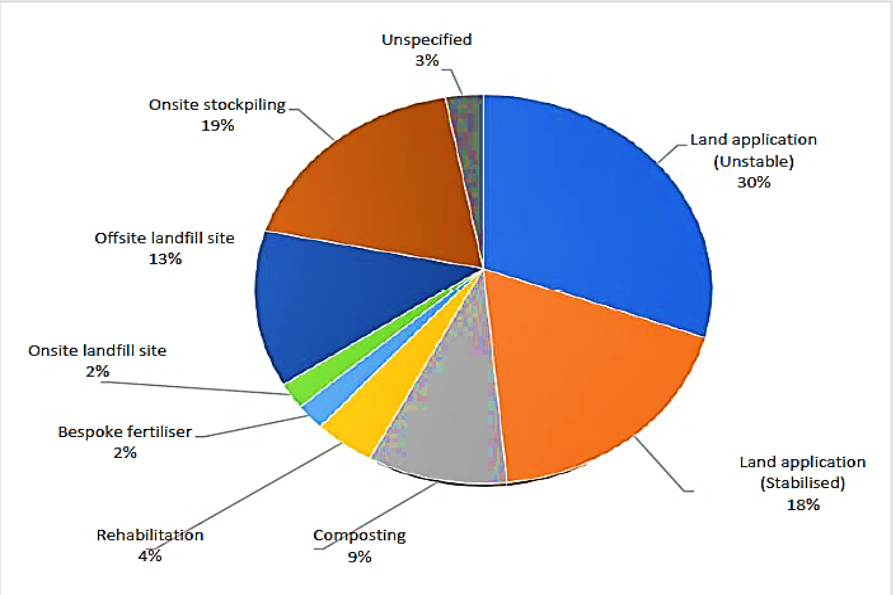


Figure 2.2: "Breakdown of sewage sludge disposal options in SA's municipal WWTWs (adapted from DEA, 2018) "

"Sewage sludge includes both agriculturally valuable compounds (such as organic matter, nitrogen, phosphorus, and potassium, as well as, to a lesser degree, calcium, sulfur, and magnesium) and contaminants, which typically include heavy metals, organic pollutants, and pathogens. This can both be advantageous and also hinders the rate of biogas production. Sludge characteristics are determined by the original pollution load of the treated water, as well as the technical characteristics of the wastewater and sludge treatments performed. (Nielfa, Cano, Pérez, et al., 2015).

"Toxins found in sewage sludge include inorganic and organic pesticides, surfactants, hormones, pharmaceuticals, nanoparticles, and many others (S. Chen et al., 2021). Furthermore, the presence of several pathogenic living organisms, such as bacteria, viruses, and protozoa, as well as other parasitic helminths, can endanger the health of humans, animals, and plants." Adequate sludge treatment will significantly reduce the number of pathogenic and parasitic organisms in sludge before application to soil, reducing potential health risks (Omar, 2017). The characteristics of different types of sewage sludge are depicted in Table 2.3.

Table 2.3: Characteristics of municipal sewage sludge. Source: (Rulkens, 2008)

Parameter	Type of sludge		
	Untreated primary sludge	Digested primary sludge	Secondary sludge
Total dry solids [TS], (%)	2.0–8.0	6.0–12.0	0.8–1.2
Volatile solids (% of TS)	60–80	30–60	59–88
Grease and fats (% of TS)	7–35	n/a	5–12
Protein (%TS)	20–30	15–20	32–41
Cellulose (% of TS)	8.0–15.0	8.0–15.0	7–9.7
Phosphorus (% of TS)	0.8–2.8	1.5–4.0	2.8–11.0
Nitrogen (%of TS)	1.5–4	1.6–6.0	2.4–5.0
Potassium (% of TS)	0–1	0–3.0	0.5–0.7
pH	5.0–8.0	6.5–7.5	6.5–8.0

Among other organic waste, sewage sludge has been successfully digested anaerobically. Anaerobic digestion has a number of environmental advantages, including the generation of a green energy carrier, the likelihood of nutrient recycling, and the elimination of waste volumes. There is a long history of treating sewage sludge anaerobically at wastewater treatment plants to generate bioenergy, but the process has not been optimized for biogas production (Koch et al., 2019).

However, anaerobic digestion of sewage sludge as the sole substrate has some drawbacks, such as low organic conversion efficiency, the problem of odour, long retention time, and low methane yield; during high-solid anaerobic digestion of dewatered sludge, the high ammonia content becomes an inhibitory factor (Chen et al., 2008). The quality of the supernatant from treated sludge thickening and dewatering is another disadvantage of using sewage sludge anaerobic digestion. It contains suspended solids, dissolved and particulate organic materials, ammonia nitrogen, some phosphorus, and other compounds in high concentrations (Chen et al., 2008). This return flow increases the loads on the wastewater treatment system's solids, oxygen demand, and nutrients, but it can be treated separately depending on the operational conditions (Chen et al., 2008).

2.4. Energy from Biogas

The biogas released to the headspace of the AD reactor is mainly composed of CH_4 of 50-70%, 30-50% of CO_2, the remaining is H_2O as steam, H_2S, and trace compounds such as NH_3, siloxanes, H_2, N_2, and O_2. Because of the composition of biogas, a frequent valorization method for biogas collected straight from the digester is open flame burning, which produces heat and electricity via an internal combustion engine. At this point, the only things that need to be removed from biogas are H_2S, trace chemicals, and condensate. Biogas combustion raises many environmental concerns, both global and local. According to recent studies, the creation of H_2, synthetic natural gas, and biomethane are viable alternatives to biogas combustion. Specific biomethane content and energy density must be assured for these high-end products.

Along with biogas, a biosolids by-product known as digestate is generated, which has the potential to be beneficial in agricultural applications. As demonstrated by the AD products, AD technology provides energy, environmental, waste management, and socioeconomic benefits. The disadvantages of the anaerobic digestion process are presented as well in Table 2.4.

Table 2.4: The Advantages and Disadvantages of Anaerobic Digestion, Environmental, Economic & Energy Aspects

	Advantages	Disadvantages
Environmental related	• Reduction of greenhouse gas emissions by capturing methane gas & fossil fuel substitute • Effective removal of pathogens & toxic material when operated at an optimal temperature • Contributes to climate change mitigation • Reduces odour below unprocessed waste odour levels.	• CH_4 can easily be released into the environment if not properly monitored • Can cause an odour nuisance, if not operated or maintained efficiently • Accumulation of the toxic in the digester
Economic related	• Recovery of secondary raw materials, economic returns on organic fertilizer sale • Efficient resource recovery, economic returns on energy sales • Reduction in operational cost for collecting waste • Possible reduction of energy costs via onsite power production • Creates local job opportunities and increases local tax revenue	• Requires a high level of investment in installation and operating costs • Post-treatment process is necessary before any discharge
Energy aspects	• Net production when biogas is used. • Conservation of nonrenewable energy sources • The flexibility of use as heat, power, transport, or natural gas grid integration	• AD takes longer to start up the process due to hydrolysis and the slow growth rate of methanogens, which requires energy • Requires the large energy inputs to fuel and operate the equipment used

2.5. Anaerobic Digestion: Biogas Production Process

Biogas production is broadly considered one of the biggest and most effective approaches to the depletion of natural resources, energy shortage, and the challenges of environmental contamination (Guo et al., 2015). The concept of anaerobic digestion is to treat organic waste products as feedstock to generate biogas and digested material that can be used as compost (Gonzalez-Fernandez et al., 2015). AD is technical terminology for when organic material is broken down by microorganisms in an oxygen-free environment. Commonly, the produced biogas is composed of 60-80 % CH_4, 20-40 % carbon dioxide, and traces of other gases such as H_2S, ammonia, and hydrogen (Nghiem et al., 2017a). Because it is high in organic and inorganic plant nutrients, the digested material has the potential to replace inorganic fertilizers. The presence of potentially toxic metals and pathogens in this feedstock, on the other hand, frequently limits such applications (Y. Liu et al., 2020). However, the digested material can be used to synthesize a valuable material such as granulated activated carbon. Activated carbon is a carbonaceous residue formed when biomass is thermally converted in an oxygen-depleted environment (Cuetos et al., 2017).

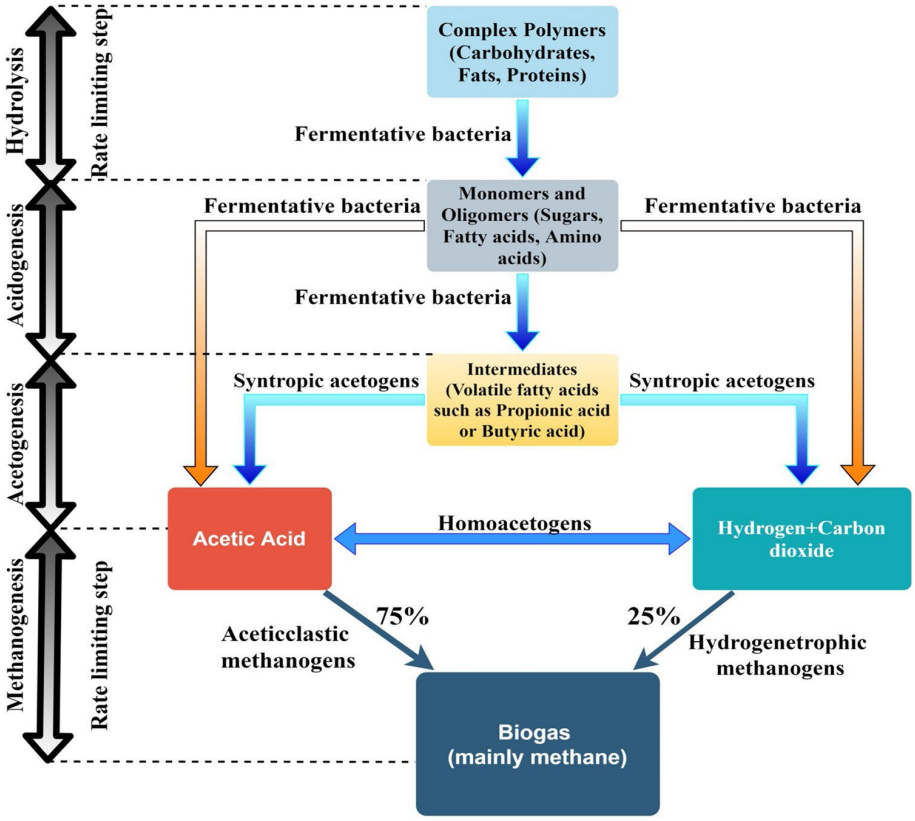


Figure 2.3: A simplified schematics presentation of the AD stages, Adapted from (Tetteh & Rathilal, 2020).

Biogas is produced through the sequential metabolism of an organic substrate by mutually dependent anaerobic microorganisms. "This metabolic route is made up of four major steps, as indicated in Figure 2.3: hydrolysis, acidogenesis, acetogenesis, and methanogenesis. The initial step in the biogas production process is hydrolysis, in which the complex organic polymer is broken down into simple soluble components by the fermentative bacteria. The hydrolysis reaction breaks down polymers of carbohydrates, protein, and lipids into their monomers of sugar, amino acids, and long-chain fatty acids." "For high cellulose substrates, the hydrolysis stage is regarded as the most critical and limiting stage in an AD process, whereas for low cellulose substrates, the methanogenesis stage is the limiting stage. Following hydrolysis, subsequent stages of the AD process can only digest hydrolyzed substrate." During the acidogenesis stage, acidogenic bacteria ferment the hydrolyzed soluble substrates into VFAs, producing a minor amount of CO_2, H_2, and acetic acid (Bajpai, 2017; Morales-Polo et al., 2018; Mudzanani et al., 2019a).

$$CH_3COOH \rightarrow CH_4 + CO_2 \qquad (Acetoclastic\ methanogenesis) \qquad (2.1)$$

In the acetogenesis step, these intermediate products are subsequently oxidized to acetate and H_2 by homoacetogenic and obligatory H_2 producing bacteria, respectively (Matheri et al., 2016). " In the preliminary step of methanogenesis, acetolactic and hydrogenotrophic methanogens convert acetate and H_2 into CH_4. As seen in Equation 2.1, acetolactic methanogen generates CH_4 solely from acetic acid, whereas hydrogenotrophic methanogen generates CH_4 from both H_2 and CO_2. "Each stage's microorganisms have varied responses and sensitivities to operational and environmental circumstances (Masebinu, 2018). The best way to run an AD process is to have a balanced population at each phase that is interrelated and interdependent. For an AD process to be stable, the conversion and utilization of substrate throughout each phase of the process must be accomplished (Bachmann, 2015).

$$CO_2 + 4H_2 \rightarrow CH_4 + 2H_2O \qquad (Hydrogenotrophic\ methanogenesis) \qquad (2.2)$$

As illustrated in Singh et al., (2017), biogas is generated when the bubble in a substrate slurry is formed once the four reaction steps have been successfully executed. It is only then that the bubble will be released after the internal pressure equals or exceeds the external pressure exerted on it. "The static pressure of the slurry at the bubble depth

from the surface of the slurry, the pressure in the reactor's headspace, and any other external force all act against the biogas bubble. Biogas is released into the reactor headspace when the partial pressure of the biogas bubble surpasses the total pressure acting against it"(Singh, 2017).

When bubbles begin with a radius of zero, the roughness available at the micro level of the gas bubble aids in gas nucleation and provides the requirement of infinite pressure, such as the roughness of the digester wall and possibly specks of solid particles around the bubble. Agitation also aids in lowering the static pressure of the slurry acting on the biogas bubble. As a result, for AD processes with intermittent agitation, there is frequently an increase in biogas flow rate when the agitation is initiated. The biogas released into the reactor's headspace can be collected and stored for cleaning or direct use." (Babaee et al., 2013; Hamawand & Baillie, 2015).

2.6. The reaction pathway of Anaerobic Digestion

The reaction pathway of AD is governed by the biological breakdown of organic matter under anaerobic conditions. "The airtight chamber develops sludge at its bottom and with the lack of oxygen in the chamber, a chemical reaction takes place that creates methane-rich biogas (Hamawand & Baillie, 2015). The anaerobic digestion process can convert about 40 ~ 80% of the organic solids to methane (CH_4), which is a highly valuable hydrocarbon that can be combusted or oxidized with oxygen to release energy. It is this characteristic that makes biogas produced from AD a good feed for electricity production via the use of Combined Heat Power (CHP) engine (Deacon & Louw, 2013).

As indicated in Figure 2.3, the four key processes in the AD process are hydrolysis, acidogenesis, acetogenesis, and methanogenesis, which require the ongoing breakdown of the original material into smaller units by specific groups of microorganisms involved in each step." These organisms degrade the by-products of earlier processes systematically.

2.6.1. Hydrolysis

This is an extracellular process that occurs on the bacterial cell's exterior in the surrounding liquid, where enzymes from microorganisms such as cellulase, protease, amylase, and lipase break down organic materials or long chain molecules into smaller molecules. Different specialized bacteria create these enzymes, which catalyze the breakdown process (Lindmark et al., 2014; J. Zhang et al., 2017). Decomposition or

breaking down of long chains of complex carbohydrates, proteins, and lipids into smaller molecules. Extracellular enzymes, for example, "must first liquefy the feed particulate material in the form of cellulose, hemicellulose, lignin, and pectin before acidogenic bacteria may consume it. According to Charalambous, (2015) when substrates are in the form of particles, hydrolysis becomes the rate-limiting step. Figure 2.4 depicts examples of hydrolysis reactions.

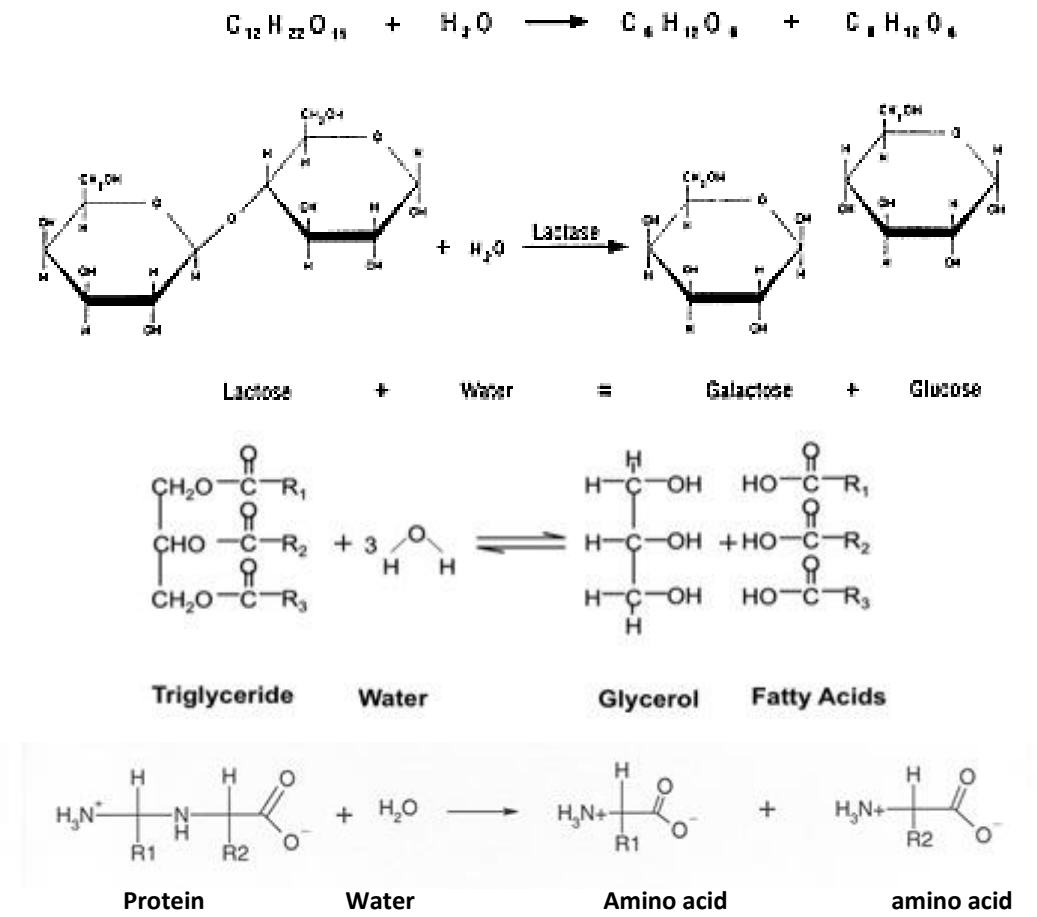


Figure 2.4: Simultaneous hydrolysis reaction. (i) Carbohydrates: Lactose, a polysaccharide, is hydrolyzed to produce galactose and glucose, both monosaccharides. (ii) Lipids: triglycerides are split into three fatty acids and glycerol in the presence of water molecules. (iii) Proteins: peptide bonds are broken to separate amino acids. Adapted from (Rea, 2014)

Because digester feedstock can be made up of a variety of components and materials, there are numerous versions of hydrolysis; carbohydrates, lipids, and proteins are all broken down into smaller molecules by this initial step of anaerobic digestion. " Polysaccharides (complex sugars) are broken down into monosaccharides in the case of a carbohydrate. Figure 2.4 shows the breakdown of lactose into monosaccharides such as galactose and glucose. In the presence of water molecules, typical lipids such as

triglycerides are broken down into three fatty acids and glycerol. In the case of proteins, peptide bonds are broken to separate amino acids (Bergland et al., 2015).

Certain complicated compounds cannot always be hydrolyzed in anaerobic circumstances. Lignin is an example of such a case. Under anaerobic conditions, lignin, an important complex polymer that forms an integral element of plant secondary cell walls, cannot be destroyed at all, but proteins, simple sugars, and starch hydrolyze reasonably rapidly. The relatively simple hydrolysis of cellulose and hemicellulose is carried out by specialized bacteria (Campanaro et al., 2016).

2.6.2. Acidogenesis or fermentation phase

The hydrolysis products are transformed into methanogenic substrates as a result of the work done by acidogenic or fermentative bacteria (Rea, 2014). "Simple sugars, amino acids, and fatty acids break down into acetate, carbon dioxide, and hydrogen (70%) as well as volatile fatty acids (VFA) and alcohols (30%) (Rea, 2014). Because of the diversity of the existing bacterial community, fermentation of simple substrates may result in the creation of a variety of products. Equations 2.3, 2.4, and 2.5, for example, depict the conversion of glucose to acetate, ethanol, and propionate. respectively, adapted from:

$$C_6H_{12}O_6 + 2H_2O \rightarrow 2CH_3COOH + 2CO_2 + 4H_2 \quad (2.3)$$

$$C_6H_{12}O_6 \rightarrow 2CH_3CH_2OH + 2CO_2 \quad (2.4)$$

$$C_6H_{12}O_6 + 2H_2 \rightarrow 2CH_3CH_2COOH + 2H_2O \quad (2.5)$$

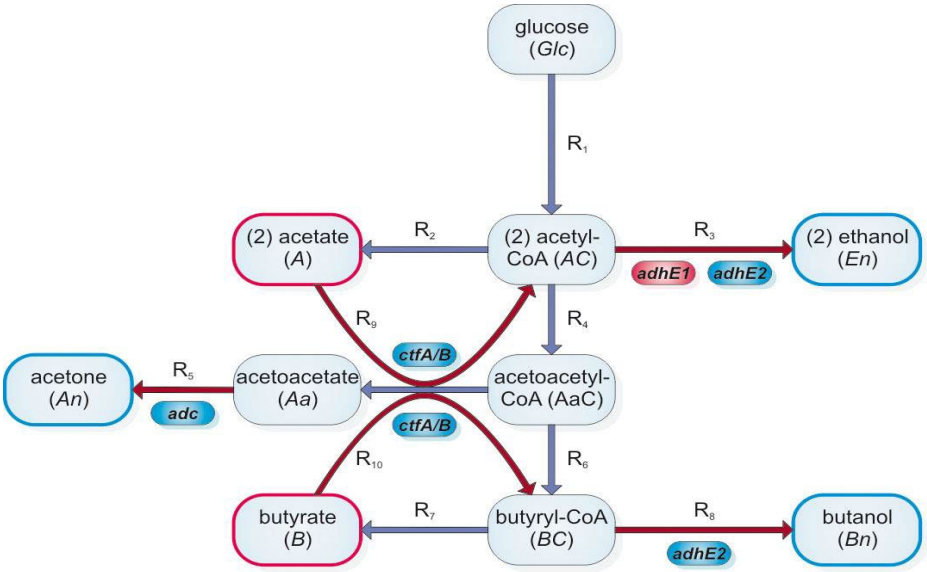


Figure 2.5: Schematic of microbial processes and the stepwise progression of these processes in the anaerobic digestion process for methane production. Source: (Rea, 2014)

Acidogenic bacteria convert hydrolysis products into volatile fatty acids. Some hydrogen, carbon dioxide, and acetic acid are also created, allowing the acetogenesis stage to be skipped. Acidogenesis is depicted in Figure 2.5 as the process by which bacteria generate acetate and butyrate (volatile fatty acids) from glucose (Sikora et al., 2017). Within an equilibrated environment, around 30% of the organic matter is converted to short-chain fatty acids or alcohols, while the majority of the organic matter is transformed into easily available substrates for methanogenic bacteria (acetate, hydrogen, and carbon dioxide). As by-products of amino acid fermentation, ammonia and hydrogen sulfide may be produced as AD inhibitors (Lindmark et al., 2014).

2.6.3. Acetogenesis

Certain fermentation products are transformed to acetate and hydrogen by obligatory hydrogen-generating bacteria during the acetogenesis process (Pan et al., 2019). These fermentation products include alcohols, aromatic fatty acids, and VFAs with more than two carbon atoms (C. Liu et al., 2016a). Simple organic acids, carbon dioxide, and hydrogen are formed by acetogenic or acid-producing bacteria during the transformation of the products produced during the acidogenic phase.

The main acids produced are propionic acid (CH_3CH_2COOH), acetic acid (CH_3COOH), ethanol (C_2H_5OH), and butyric acid ($CH_3CH_2CH_2COOH$) while the products of volatile fatty acids and alcohol are acetate, carbon dioxide, and hydrogen gas created by hydrogen-producing acetogenic bacteria. Acetate is created by homoacetogenic bacteria from carbon dioxide and hydrogen gas, whereas the majority of acetate is produced by hydrogen-producing acetogenic bacteria (Al Mamun & Torii, 2015) .

2.6.4. Methanogenesis

An anaerobic digestion system requires the presence of a diversity of methane-forming bacteria (methanogens) for methanogenesis to be successful, as there are no one methane-forming bacterial species that can degrade all available substrates (X. Liu et al., 2014).Methanogenic bacteria include *Methanobacillus, Methanobacterium, Methanosarcina,* and *Methanococcus*. Acetate is the source of an estimated 70% of the methane created throughout the process of methanogenesis. The remaining 30% of methane is produced due to the reduction of carbon dioxide by hydrogen and other electron donors. Methanogenesis is classified into two categories based on the substrates used by the methanogens (Babel, 2014; Siddique & Wahid, 2018a). There are two main types of methanogenesis which are:

1. Hydrogenotrophic methanogenesis, in which hydrogen and carbon dioxide are transformed into methane via the following mechanism, Equation 2.6:

$$CO_2 + 4H_2 \rightarrow CH_4 + 2H_2O \quad (2.6)$$

2. Aceticlastic or autotrophic methanogenesis, in which methane is produced from the conversion of acetate by the following reaction, Equation 2.7:

$$CH_3COOH \rightarrow CH_4 + CO_2 \quad (2.7)$$

The methanogenesis process is influenced by several operating parameters, including feedstock composition, feeding rate, temperature, and pH. Methane production may be inhibited or stopped as a result of digester overloading, temperature changes, or even massive influxes of oxygen. As previously stated, hydrolysis may be the rate-limiting step when substrates are in particulate form; however, for Fruits and Vegetable Waste (FVW), which are cellulose-poor substrates, Cecchi et al.,2006 and Mata-Alvarez et al., 2003 suggests that the rate-limiting step is methanogenesis because these wastes tend to acidify to VFA, which inhibits methanogenesis.

Aerobic microorganisms transform complicated insoluble organic compounds into simple versions that are soluble and can be ingested by the microorganisms during hydrolysis. Polysaccharides are broken down into monosaccharides, heavy molecules such as lipids to short-chain fatty acids, proteins to soluble substances i.e. nucleic acids, and amino acids to pyrimidines and purines. "Acidogenesis occurs when acid-forming anaerobic digestion microbes transform low-molecular-weight hydrolysis components to lower molecular weight intermediate compounds of volatile fatty acids and alcohol. These acids and alcohols are degraded to acetic acid, hydrogen gas, and CO_2 in the subsequent step, acetogenesis. The last phase is the methane formation step, methanogenesis. The anaerobic methanogens convert the acetic acids into methane & CO_2. The second group of methanogen uses hydrogen gas as an electron donor and CO_2 as an electron acceptor and thus reduces carbon dioxide by hydrogen to form methane (Guo et al., 2015; Hafner & Rennuit, 2016; Sikora, Detman, Chojnacka, & Błaszczyk, 2017).

2.7. Anaerobic Digestion Process Challenges

Though it is an established wastewater treatment technology for organic waste management, the AD process nevertheless suffers from three major drawbacks. "Instabilities caused by highly degradable organic substrates have an impact on process

efficiencies and product quality assurance; adaptability of the suitable substrate due to failure to digest highly recalcitrant lignocellulosic biomass requiring pre-treatment; and effluent and emissions management (volume of digestate and the extent of degradability of the substrate which controls digestate emission levels) (Gaballah et al., 2020; Paritosh et al., 2018).

The substrate used in the AD method, among other parameters, has a strong influence on product stability and quality assurance. Substrate-induced instabilities are caused by differences in the bioavailability of methanogenic and acidogenic microorganisms. This imbalance causes slow syntrophic metabolism of fermentative intermediates such as VFAs alcohol and propionate. At a high organic loading rate, these intermediates are easily stimulated (OLR). The methanogenic process of AD is inhibited by excessive accumulation of these intermediates, which results in a drop in pH, increased VFAs, and NH_3 concentrations (Ahn et al., 2006a; Martínez et al., 2016a). The combination of these factors of low pH, and accumulation of VFA and NH_3, often leads to a possible failure of the AD process. This substrate-related instability cannot be completely removed from the AD process; rather an approach towards reducing their impact is needed (Oliveira et al., 2018; Wirth et al., 2012). Mizuki, et al. (2016) pointed out that the inhibitory compounds embedded in the microbial cell of the substrate or the intermediate inhibitor produced after a chemical reaction in the digester cause instability in AD. These intermediate compounds are needed for an AD process to progress towards the formation of CH_4, according to Tetteh & Rathilal, (2020) and Madsen, et al. (2017); however, their rate of development must be regulated. The stability of an AD process cannot be assured if they are not regulated (Tufaner & Avşar, 2016).

Under anaerobic conditions, cellulose, hemicellulose, and lignin, as well as their extractives, are candidates for the AD phase. Since they form a protective layer over cellulose and are biologically refractory, lignin and hemicellulose, in particular, restrict the hydrolysis efficiency of cellulase enzymes. Under AD conditions, lignin becomes immune to degradation due to its small" surface area, intermolecular bonds, and cellulose fiber crystallinity (Dasgupta & Chandel, 2020). If pre-treatment is not performed before use, restrained hydrolysis decreases the overall efficiency of an AD operation (Ramdani et al., 2015).

Aside from substrate-induced instability and the lignocellulosic biomass's limits, the high-value biogas application strategy necessitates comprehensive post-treatment. The efficiency of the first law of thermodynamics for biogas-fuelled combined heat and power (CHP) engines ranges from 57.5 to 80% (Tsai, 2012). However, only about 35-42 percent of the energy content of biogas is converted into electricity during the combustion phase, while the rest is converted into heat (Franks et al., 2013). Apart from the fraction of thermal energy needed for heating the digester, which has no economic value, the rest is lost.

The presence of CO_2 in biogas, which is a non-combustible gas, contributes to the inefficiency of using biogas in CHP. The calorific value of biogas is reduced when CO_2 is present, as is the real energy density. In addition, as compared to natural gas, it slows down the flame speed and reduces the level of flammability(Werther & Ogada, 1999). Furthermore, transporting CO_2-concentrated biogas is more costly. These issues affect biogas's long-term viability; as a result, upgrading biogas to biomethane, which has properties similar to natural gas, is a viable option. The spatial and temporal decoupling of biogas output from biogas upgrading is attracting global interest.

Cleaning biogas is needed before it can be used in simple applications in specialized equipment and machinery. CH_4 enrichment by CO_2 removal is needed "to achieve natural gas efficiency, i.e. biomethane suitable for vehicle fuel (CH_4 content >96%, heating value of about 37 MJ/Nm^3) (L. Zhang et al., 2020). Biogas upgrading is the term used to describe the combined cleaning and enrichment operation. In comparison with electricity production via CHP engines, biomethane generation may recover around 80% of the energy content of the biogas with minimal heat loss (Deacon & Louw, 2013).

Chemical and physical absorption, membrane isolation, pressure swing adsorption, and cryogenic cooling are examples of traditional biogas upgrading technologies (L. Zhang et al., 2020). These systems are resource intensive and have been thoroughly scrutinized (Angelidaki et al., 2018). These innovations also add \$0.15-0.4/Nm^3 of biogas to the overall operating cost of a biogas plant. For biogas upgrading, absorption and adsorption have been commonly used. Because of its large specific surface area and pore structure, activated carbon has been widely used for adsorption, allowing for a high CO_2 adsorption rate (Okeola et al., 2012).

However, high pressure and high-temperature pre-processing of activated materials are frequently needed for efficient CO_2 selectivity (De Mes et al., 2003). Large quantities of raw materials, such as water during evaporation, impact both the capital and operational costs of a biogas plant when high pressure is not used (Okeola et al., 2012). "The digestate quality assurance process, which deals with the preservation of soil nutrients and their availability in the soil during the application, is another challenge in the AD process. Another problem in digestate quality control is the residual impact of digestate application on the soil and the ecosystem (Negreanu-Pirjol et al., 2012).

Because of the high water content of the digested material, it is common practice in large-scale plants to separate the liquid and solid fractions of the digestate to make storage and transportation easier. The digestate's nutritional value has been stated to be reduced as a result of this separation procedure (Pfeifer & Obernberger, 2007). Furthermore, using the digestate from an unstable AD process runs counter to the principle of environmental protection, as there is a risk of CH_4 emissions into the atmosphere due to incomplete substrate degradation, soil nutrient depletion, and leaching (Wambugu et al., 2019).

To minimize the effect of substrate-related inhibition on digestate efficiency, several methods have been used, including air stripping, chemical precipitation, and steam distillation. Aside from ensuring the consistency of the digestate, another problem with AD is the digestate volume control. The digestate from AD accounts for about 80% of the total waste processed. As a result, without comprehensive posttreatment processes such as thermal drying and pellet forming, AD does not substantially reduce waste volume (Rajesh Banu et al., 2016).

2.8. Key Parameters affecting anaerobic digestion

The production rate of biogas depends upon the type of sludge and also the operating conditions of the digester. This includes temperature, pH, mixing, retention time, and the composition of the feedstock. The sludge composition parameters can be categorized in physical and chemical properties, physicochemical and microbiological characteristics (Kaparaju, Buendia, Ellegaard, & Angelidakia, 2008; Kim, Oh, Chun, & Kim, 2006; Liu, Wang, Hu, & Song, 2014). In which significant physical parameters are total & volatile solid content, alkalinity, and Volatile Fatty Acid. The chemical characteristics are C: N ratio, COD, and heavy metals content.

If the metabolic intermediates generated by a substrate reaction under anaerobic conditions are inhibitory to a certain population of the microbial community within the digester, the balance of the microbial population within the digester can be altered. This type of substrate-induced inhibition has been identified as the primary source of process instability in AD (Astals et al., 2014). Ammonia, sulfide, alkali, and alkaline-earth metals, as well as organic acids, are major inhibitors that produce or encourage the release of other metabolites. These inhibitors are required in trace amounts to improve the biodegradability of the substrate. However, due to the varying amounts of the complexes, as well as the antagonism, acclimation, and synergism of their interaction, the proportion released by the substrate could vary substantially and hinder the AD processes. When inhibition occurs, the rate of biogas production decreases, as does the overall efficiency of the AD process. A number of inhibitors have been recorded, as well as their permitted amounts in a digester (Y. Chen et al., 2008; Milledge et al., 2019). Chen et al. (2018) provided a comprehensive evaluation of these inhibitors. However, a quick assessment is provided in the following subsections to clarify their impact on the AD process.

2.8.1. Ammonia

The biological breakdown of nitrogen-rich organic materials, such as protein, results in the formation of NH_3. The Buswell Equation, as described by Symons and Buswell, can theoretically be used to determine the amount of NH_3 that can be created from a substrate (Morales-Polo et al., 2019). The free NH_3 and ammonium (NH_4^+) compound forms of inorganic ammonia-nitrogen contribute significantly to the instability of the AD process depending on temperature and pH. As the pH rises, so does the free NH_3; however, at lower pH, NH_4^+ is the predominant form, as illustrated in Figure 2.6 (Y. Chen et al., 2008). Equation 2.8 gives the conversion of NH_4^+ to NH_3. Because the inhibitory effect of NH_3 is greater than that of the NH_4^+ ion, the intended temperature and pH of AD processes must take into account the qualities of the substrate to be employed (Milledge et al., 2019).

$$NH_3 = NH_4 \times 10pH / (\exp [6344 \times (273 + T) -1]) + 10pH \text{ [g/l]} \quad (2.8)$$

The methanogenic phase is the least tolerant of the four stages encountered during the decomposition of organic waste, and it is also impacted by inhibitors (Webster et al., 2016). For process stability, it was proposed that the overall NH_4^+/L concentration be

kept below 3000 mg/L. Other studies, however, have obtained process stability that is greater than the required value. Furthermore, the total NH_4^+ inhibitory range is 1000-6000 mg/L, but the free NH_3 inhibitory range is 50-100 mg/L. As a result, the concentration recorded "during optimal plant performance should be noted; any variation from this indicates a process disruption (Cornet, 2017). Factors affecting the permitted limits of NH_3 are likewise subject to management to reduce their concentrations. These variables include pH, operating temperature, co-digestion, the requirement to modify the C/N ratio, the presence of other ions, "microbial acclimatization, and the use of additives (Dioha et al., 2013).

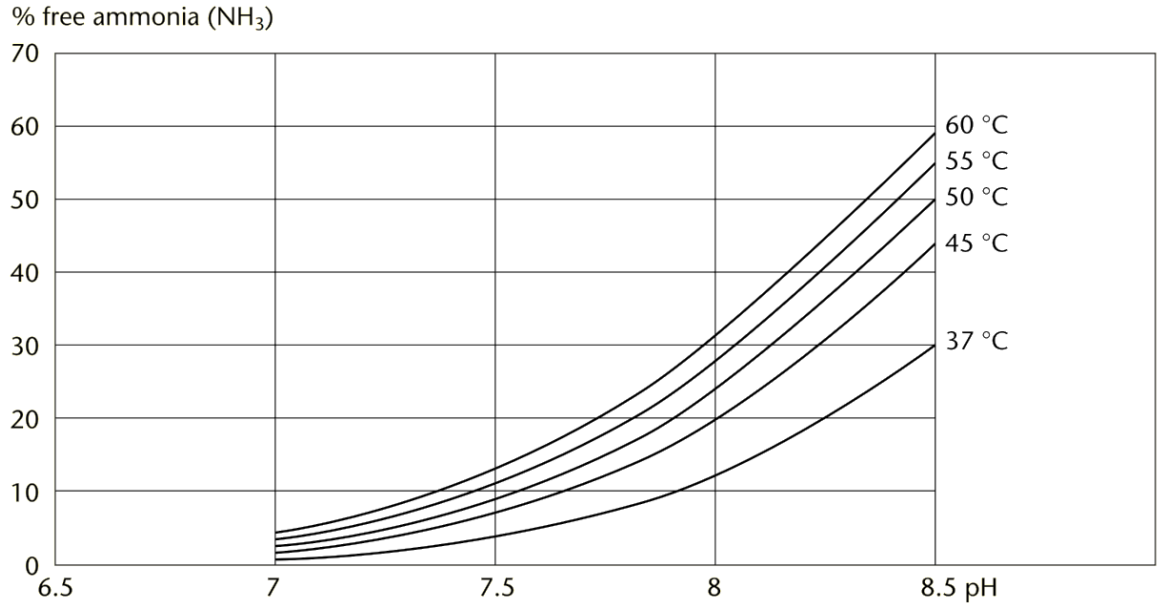


Figure 2.6: The influence of temperature and pH on the balance of ammonium ion and ammonia (Emerson, et al. 2015)

2.8.2. Sulfates

Sulphates are frequent components in the AD wastewater treatment process, and they are converted to sulfides by sulfate-reducing bacteria." Lactate is turned into acetic acid by the sulfate-reducing bacteria, which is then transformed into CO_2 and HCO_3^-. As illustrated in Figure 2.7, the sulfate-reducing bacteria compete for resources, both organic and inorganic, with the CH_4-forming microbial community; and they are then poisonous chemicals to diverse microbes, encouraging the synthesis of CH_4 (Cornet, 2017). Uncontrolled sulfate reduction is undesirable in AD because it may increase the concentration of H_2S in the biogas produced (Cornet, 2017).

When sulfate concentrations in an AD exceed 3-5 g/L, the methanogenesis stage of biogas production is inhibited (Ait Ahsaine et al., 2017; Amha et al., 2018). "In anaerobic digestion, lower concentrations of sulfates converted to sulfides can precipitate hazardous heavy metals. The use of an anaerobic filtration system, biological pre-treatment, co-digestion, pH control, and additive concentration regulation are some of the methods for minimizing sulfate levels in an AD process (Amha et al., 2018; Cornet, 2017). In the anaerobic digester, several microorganisms compete for the same substrate and electron acceptor. Methane-producing bacteria produce methane, while sulfate-reducing bacteria make acids and alcohols. By sulfate reduction and sulfide hydrogen (H_2S), sulfate (SO_4^{2-}) is utilized to make hydrogen (Gerardi, 2003; Shah et al., 2014).

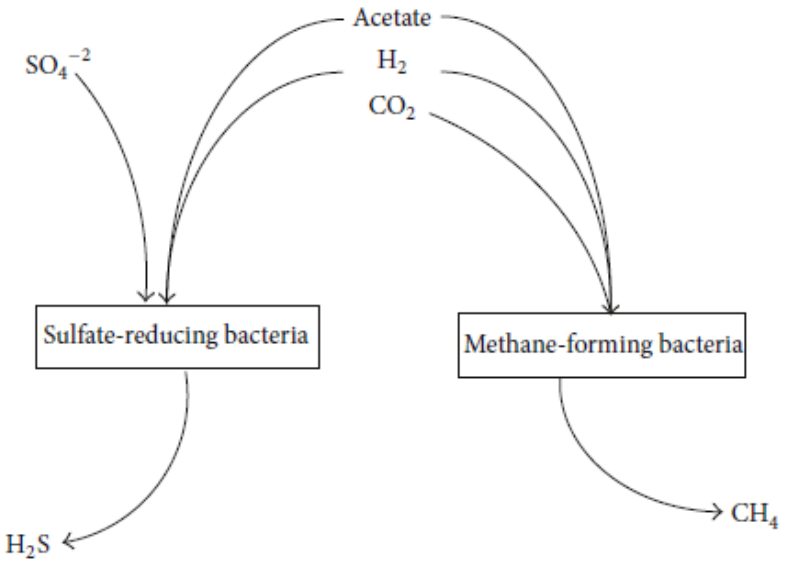


Figure 2.7: Sulphate-reducing bacteria compete for resources with the CH_4-forming microbial community (Gerardi, 2003).

2.8.3. Alkali and Alkaline Earth Metals

Alkali metals, such as Na, K, and Li, are soft metals with low melting points that belong to the group of metals having a valency of 1. To become stable, they can readily give up one electron. Alkali metals are positively charged due to the loss of an electron, and can easily form ionic bonds. They generate alkaline hydroxide when they react with water, raising the pH of the aqueous medium. They are present in the substrate that is injected into digesters, and they become accessible throughout the degradation process or when the pH is adjusted chemically. At trace-element levels, they are required for microbial

development; however, at high quantities, they become toxic to the AD process, and bacterial cell dehydration is conceivable, due to osmotic pressure (Rafiee et al., 2019).

Non-metallic compounds, such as Mg and Ca, that are insoluble in water and resistant to heating are referred to as alkaline earth metals. They're also needed in trace amounts. The solution becomes basic when an alkaline earth metal, such as Ca, interacts with water at ambient temperature. Excessively high pH promotes the build-up of NH_3 in AD patients. Fe, Co, Cu, Zn, Cd, and Ni are other heavy metals that can be detected in substantial amounts in urban sewage and sludge. Heavy metal ions are not bioavailable and can build up to dangerous quantities overtime levels (Kalemba & Barbusiński, 2017). At toxic levels, however, they inhibit enzymes that promote fast substrate breakdown. Apart from inhibition, the presence of heavy metals prevents the digestate from being used as an organic fertilizer because of the potential for harm to human health. Constant monitoring of the feed source and composition entering the digester, pH management, dilution of the substrate, and co-digestion are all techniques to reduce the concentration of heavy alkali and alkaline earth metals in-situ AD. According to Marchioretto et al (2007), several approaches have been used to lower heavy metal concentration in the digested slurry, including oxidation, reduction, solubilization, and increasing pH (Pilarska et al., 2018).

2.8.4. Volatile Fatty Acids (VFA)

Any organic acid (carboxylic acid) with fewer than six carbon atoms is classified as a VFA i.e., acetic acid ($C_2H_4O_2$), formic acid (CH_2O_2), butyric acid ($C_4H_8O_2$), propionic acid ($C_3H_6O_2$), and valeric acid ($C_5H_{10}O_2$). Acetic acid, which is the preferred fuel for acetoclastic archaea, propionic acid, and butyric acid are the most relevant for the AD process (Palacios-Ruiz et al., 2008). VFAs, like other inhibitors, degrade to acetic acid, which serves as a substrate for other activities that aid in the formation of CH_4 in AD. The excess build-up, on the other hand, slows down the progression of AD. "The main effect of VFA accumulation is a drop in pH, which inhibits methanogen activity (Ltzhft et al., 2014; Palacios-Ruiz et al., 2008). When highly degradable substrates are fed at a high OLR, VFAs accumulate. Because each phase of the AD process is interconnected, extra acids are created if the hydrolysis phase is faster than the others.

The amount of acetic acid that can be converted to CH_4 is reduced due to the slowdown of the methanogenic process and the slower conversion rate. Due to the constant

accumulation of acetic acid, high acid levels in the digester might build up, and the pH decreases below the digester's healthy limits. Co-digestion, pH management, acetate enrichment, and OLR reduction are all methods for lowering VFA build-up (Martínez et al., 2016a; Wambugu et al., 2019). Because substrate-induced inhibitors cannot be completely removed from an AD process, the bioavailability of these inhibitors is limited using a combination of technological approaches and changes in operating circumstances. A review of existing techniques is offered, along with recommendations for appropriate operating ranges to help reduce the impact of substrate-induced inhibitors.

2.8.5. Composition of the feed or substrate

Several investigations have found that the substrate causes destabilization during the digestion of OFMSW. Different ways of managing AD instability have been explored. The sub-sections that follow provide a comprehensive overview of different approaches.

2.8.5.1. Physico-chemical characteristics

Besides the efficiency of the system, the methane potential of sludge can be correlated to the concentration of Chemical Oxygen Demand (COD) content. COD describes the amount of oxygen needed to completely oxidize the sludge under aerobic conditions by measuring the oxygen equivalent of the organic matter content. However, in anaerobic digestion oxygen is not consumed, thus no reduction of COD occurs. As a result, COD is removed by converting organic compounds to methane, carbon dioxide, hydrogen, and negligible amounts of other gases (Reungsang, Pattra, & Sittijunda, 2012).

The unbalanced nutrients are regarded as an important factor limiting anaerobic digestion of organic wastes. For effective anaerobic digestion carbon to nitrogen ratio should be maintained between 20 & 30. Lower C: N ratio is likely to result in ammonia accumulation in the digester which inhibits micro-organism activities. Higher C: N ratio result in low-quality gas production. Different types of material are mixed to maintain the optimum C: N ratio of the feedstock (Dioha, Ikeme, Nafi, Soba, & Mbs, 2013).

2.8.5.2. Microbial community

The microbial communities present in anaerobic digestion substrates' are extremely diverse, and they play an important role in excess sludge treatment, determining sludge reduction performance and methane production efficiency. Because microorganisms have varying adaptabilities, several investigations revealed that the dominant microbial population and metabolic pathway always changed along with changing fermentation

circumstances (Gerardi, 2003). A better understanding of the microbiology of anaerobic digesters and process modifications have permitted the use of anaerobic digesters for diluting wastewater and a large variety of industrial wastes. Therefore, it is valuable to find the changes in microbial community structure in response to the microbiologic reaction pathway during the digestion of sewage sludge (Manyi-Loh et al., 2013).

2.8.5.3. Substrate Solid Content

For maximum yield, the total solid (TS) content of the substrate serves as a guideline for the AD technology division, whether wet digestion or dry digestion is used. The TS provides recommendations for selecting appropriate mechanical components for transportation and mix homogeneity. Although there is no official definition for when a substrate should be utilized in wet or dry digestion, the usual rule-of-thumb is that the AD process with a TS level of 15% can be considered wet AD, and it can be considered dry when the TS content reaches 30% by mass of substrate (Hilkiah Igoni et al., 2008). In addition to dry AD, the OLR recommends that it be at least 3.5 kgVS/(m^3.day) (C. Liu et al., 2016b).

The TS limit for wet digestion is set to allow for easy substrate pumping into the digester; however, where the substrate particles are finely dispersed with a high proportion of dissolved solids, the substrate can be pumped at up to 20% TS (X. Liu et al., 2014). The stability and yield of the AD process have been reported to be affected by TS concentration. Bouallagui, et al. (2005) discovered that a substrate with a TS concentration of 6% of the substrate's wet weight favours process stability at the expense of high biogas output. Also, Alkanok, et al. (2010) digested FVW with a 5% TS concentration and found that the volatile solid (VS) degradation was high. When the mixing is not efficient enough in a wet digestion process, high TS can result in a dead zone within the digester apart from the energy required to agitate the substrate.

Wet digestion enables for constant and continuous biogas production while also reducing the movement of heavy equipment conveying the substrate. To achieve continuous and stable biogas production, numerous batch reactors are built and operated in parallel with a temporal offset difference between the reactors in dry digestion. Because mixing the substrate is difficult in dry digestion, compressed biogas is recycled and pumped into the digester from the bottom, while percolate is sprayed from the top (Ait Ahsaine et al., 2017).

2.8.6. Number of Process Stages and Process Phases

The separation of substrate degradation phases and the use of numerous stages have been used to improve the stability of the AD process. Multiple-stage digestion supports several forms of oxidation and reduction processes, as well as pH optimum and acidogenic and methanogen development rates, to boost process stability (Hamawand & Baillie, 2015). The biogas production process, as described in Section 2.10, consists of four major stages. However, these can be divided into two major categories: hydrolysis and acidogenesis (acid formation) and acetogenesis and methanogenesis (CH_4 forming phase). Both the acid and CH_4 generating phases occur concurrently in a single tank in the single-phase AD process. The two-phase process, on the other hand, refers to the separation of both processes into two tanks.

The number of phases is determined by the layout of the facility. A three-stage single-phase AD system consists of an open holding tank, a digester, and digestate storage; however, if the holding tank is sealed and runs at a similar temperature as the main digester but for a shorter retention time, it is referred to as a three-stage two-phase AD system (Q. Wang et al., 2016a). The advantages of multiple steps and phases include hydrolyzing the substrate, lowering intermediate inhibitor concentrations, and buffering OLR in the first stage. The methanogens may easily digest the hydrolyzed and homogenized substrate in the next stage. For optimal substrate degradation, many AD facilities treating OFMSW use a two-phase process with a faster degradation rate, shorter hydraulic retention time (HRT), and increased process stability. In terms of total investment cost, the single stage is cost-effective. The biogas yield, on the other hand, necessitates a compromise between the four stages' operational conditions. As a result, a low biogas output is more likely, or a larger HRT is required. To improve the stability of AD and the biogas yield in single stage AD, the digestate is often recycled (Prabhudessai et al., 2013).

2.8.7. pH

The addition of alkaline chemicals to change the pH to levels between 6.8 and 7.5, so neutralizing the acidification process, is a traditional strategy for addressing the instability induced by fast acidification (Cossu et al., 2016). A $pH \leq 7$ indicates a steady accumulation of VFA, but a $pH > 8$ indicates growing NH_3 concentration. Increases in pH often enhance free NH_3 inhibition by moving the NH_3^-/NH_4^+ equilibrium in the digester towards NH_3 production (Awe et al., 2017). A pH of 4-7 is achievable during the acid-

forming stage of AD. In contrast, constant pH monitoring is required for the CH_4 forming step to regulate the feeding rate, because restoration of the AD process at a critical pH range is time-consuming, and this might have severe financial consequences (Xu et al., 2018). While it is critical to keep an eye on pH, it can be deceiving at high levels of total alkalinity (TA). The accumulation of VFA at high TA levels is difficult to detect only by measuring the pH value. As a result, the ratio of VFA to TA is frequently studied in order to determine the digester's divergence from stability.

2.8.8. VFA to TA Ratio

In a digester, the VFA to TA ratio is an important substrate evolution monitoring measure. "The VFA/TA parameter is the ratio of the volatile fatty (organic) acid measured in equivalent mg of acetic acid per litre (mg CO_3COOH/L) to the TA (inorganic) parameter, which measures the digestate's alkaline buffer capacity in equivalent mg$CaCO_3$/L (Palacios-Ruiz et al., 2008). The VFA/TA ratio, according to Bensmann et al. (2011), gives a faster response to changes in digester stability than the pH, especially in a well-buffered system, and it is usually considered a better indication than the pH alone. On the limits of the VFA/TA ratio for biogas plants, many conclusions have been published. Wolf (2012) proposed that a plant's VFA/TA be examined during its peak performance time and that such an AD plant be benchmarked against the optimal value that must not be surpassed. The expected values for the various ratios of VFA/TA, their impact, and recommended interventions are presented in Table 2.5 (Masebinu, 2018).

Table 2.5: VFA/TA ratio, their impact, and recommended response actions, Masebinu, 2018)

VFA/TA ratios	Inference	Response Measure
>0.6	Highly excessive substrate input	Stop adding substrate
0.5-0.6	Excessive substrate input	Add less substrate
0.4-0.5	Plant is heavily loaded	Monitor plant closely
0.3-0.4	Biogas production is at maximum	Keep substrate input constant
0.2-0.3	Substrate input is too low	Slowly increase the substrate
<0.2	Substrate input far too low	Rapidly increase substrate

The potential VFA to TA ratio values, impacts, and actions are shown in Table 4. When the VFA to TA dimensions is greater than 0.6, the substrate has a very high VFA/TA ratio input. Stop adding more substrate is the inference response. When the VFA/TA ratio is between 0.5 and 0.6, excessive substrate intake is inferred, and the inference response is

to use less substrate. At 0.4-0.5, the plant is heavily laden. When the VFA/TA ratio reaches 0.3-0.4, biogas production is at its highest; keep an eye on the plant and maintain a consistent substrate input. The VFA/TA ratio of 0.2-0.3 indicates that the substrate input is insufficient; therefore, the operator should progressively increase the substrate. When the VFA/TA is less than 0.2, the substrate input is too low, and the operator must quickly expand the substrate (Masebinu, 2018).

2.8.9. Temperature

The viability of the microbial community that aids biogas production depends on maintaining a constant operating temperature. The AD process might be substantially hampered by a sudden fluctuation or operating outside of the desired range. As indicated in Figure 2.8, three temperature working ranges have been documented (Satimanont et al., 2012). The psychrophilic ranges from 25 to 40 ℃, whereas the mesophilic ranges from 35 to 40 ℃, and the thermophilic ranges from 40 to 60 ℃. The rate of deterioration is quite slow at lower temperatures. Although the rate of breakdown is quick and the biogas yield rate is best at high temperatures, the bacteria are extremely sensitive to temperature fluctuations within this range. As a result, in addition to the significant energy consumption and accompanying cost, such a process necessitates extensive process monitoring. The mesophilic temperature range is frequently used for these two reasons.

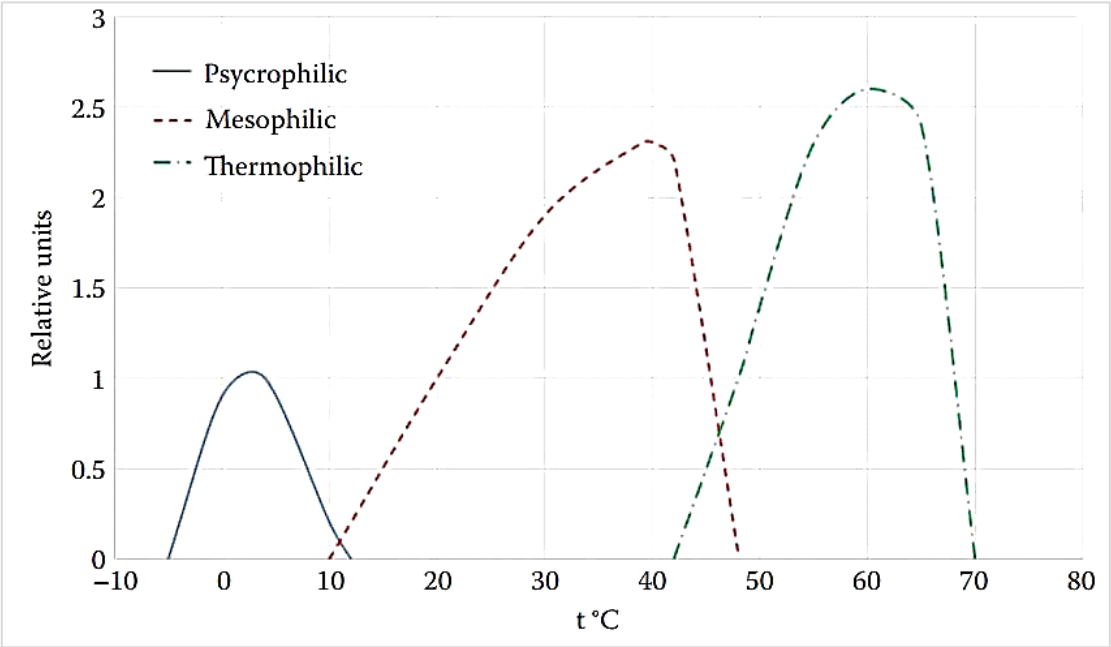


Figure 2.8: The efficiency of anaerobic bacterial growth at various temperature profiles (Rosato., 2008).

2.8.10. Hydraulic Retention Time

Hydraulic Retention Time (HRT) is regarded as an important control parameter affecting continuous biogas production processes (Zhang et al., 2006). HRT needs to be regulated during biohydrogen fermentation processes in order to inhibit biogas-consuming bacteria (Lin and Lay, 2004). The choice of HRT in biogas production is dependent upon the type of substrate used. However, short HRTs are ideal for biogas processes, because they suppress the methanogenic bacteria that require relatively longer times to grow as compared to acidogenic bacteria (Liu et al., 2008). For example, methanogens are known to have slow specific growth rates of 0.0167-0.02 h^{-1} whereas acidogens are reported to have a relatively higher specific growth rate of 0.172 h^{-1} (Khanna and Das, 2013). Kim et al. (2004) reported that short HRTs below 72 hours increase biogas efficiency. Several studies on biogas processes have indicated that the pH and HRT are joint parameters (Lee et al., 2010; Liu et al., 2008; Shin and Youn, 2005); since it has been shown that short HRTs result in low pH. In addition, both of these parameters have been viewed as effective in the inhibition of biogas-consuming bacteria (Oh et al., 2004). HRT controls microbial growth and hence this process parameter must be greater than the maximum growth rate of bacteria to prevent biomass washout (Hallenbeck and Ghosh, 2009).

Maximizing biogas yield is critical for a stable process, and this can only be done above a particular HRT, which varies based on the substrate being treated. The HRT shows how long a substrate is retained in a digester, which influences the degree of degradation that can be achieved. Bouallagui et al. (2009) found that HRT of less than 12 days had a deleterious impact on the stability of the AD process in FVWs. According to Di Maria and Barratta (2015), a digester with a 25-day HRT produced 10.34% more specific CH4 than one with a 14-day HRT. According to Aboudi et al. (2014), extending the HRT by lowering the substrate flow rate can help the AD process recover faster in a stressed digester. The specific and daily biogas yields can be depicted based on the microstructure, substrate flow rate, and digester volume, as shown in Figures 2.9A, total gas production, and Figure 2.9B, daily gas production (Tufaner & Avşar, 2016). Figure 2.9 A and B further indicate that the laboratory result and full-scale plant operation are not identical. As a result, despite probable retention guidelines derived from the BMP test, this variance must be taken into account in order to achieve a biogas production of about 80% from the substrate.

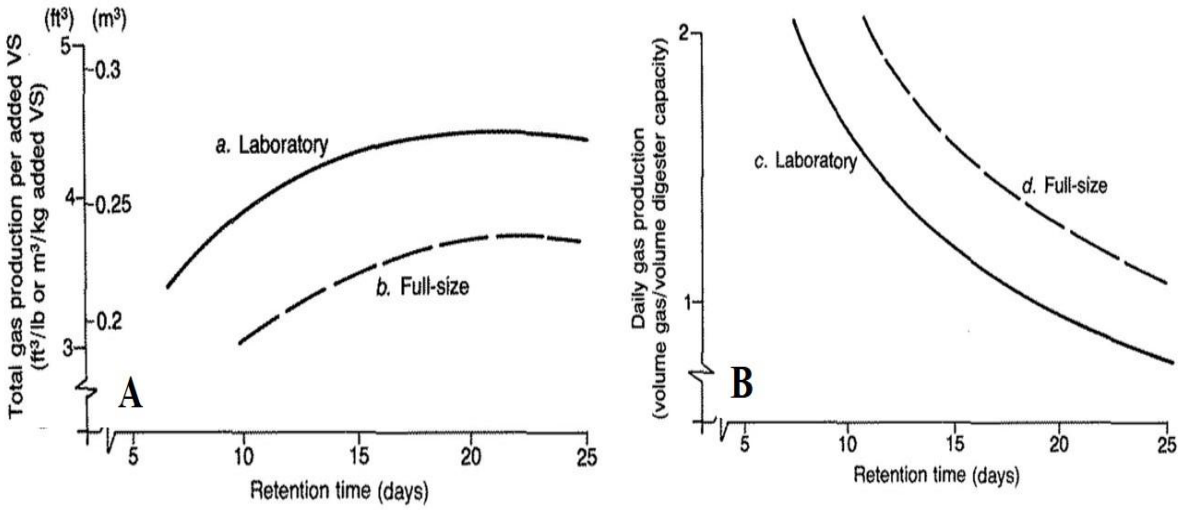


Figure 2.9: Effect of HRT on specific and daily biogas yield, (Masebinu, 2018)

2.8.11. Organic Loading Rate

The organic Loading rate (OLR) is a measure of the biological conversion capacity of the anaerobic digestion process (Morimoto et al., 2004). The OLR affects various fermentation conditions, such as the production of VFAs, COD removal efficiency, pH, as well as variations in the composition of the active biomass, with consequent modifications of the associated metabolic pathways (De Gionnis et al., 2013). However, OLR is also affected by various parameters such as the type of substrates, temperature, and source of inoculum used. Several authors investigated the effect of OLR on biohydrogen production. For example, Shin and Youn (2005) observed that increasing OLR up to 8 g VS/L/d while maintaining a long HRT of 5 days enhanced the production of biohydrogen. Hong and Haiyun (2010) maximized the production of biohydrogen when the OLR was increased from 4 to 8g VSS/L/d at a long HRT of 8.92 days from food waste. A maximum biohydrogen production rate of 5.4 L H_2/d was reported at OLR of 29 g COD /L d and 110 g TVS/ L d, respectively by Tawfik and El-Qelish (2012) and Zahedi et al. (2012).

The OLR of the digester is an option to examine to establish a compromise between the level of stability and the high yield rate. The OLR is a measurement of how much degradable material is fed into the digester. It has been reported that a low OLR results in good process stability. This method enables the monitoring of changes in digester stability, as well as the prompt implementation of appropriate corrective actions in the event of an anomaly. The ideal OLR for FVW and OFMSW is usually between 2-3 kgVS/m^2 (m^3.day). Although a greater OLR is preferable, because AD is a biological

process, a high OLR can result in catalyzed intermediate inhibitor synthesis (Milledge et al., 2019). Rosato (2008) recommended that the OLR be kept at 2 kgVS/(m^3.day) to ensure that the AD process runs smoothly. Although optimal OLR has been reported to be between 2-3 kgVS/(m^3.day), Aboudi, et al. (2006) found that for the co-digestion of sugar beet with pig manure, greater OLR values of 11.2 kgVS/(m^3.day) are achievable.

According to the literature, an exceptionally high OLR generates an imbalance and changes the microbial population. Due to the long adaption process, this mismatch affects methanogenic conversion efficiency, resulting in low CH_4 content in biogas (Kuscu & Sponza, 2007). As a result, it is possible to conclude that OLRs are substrate specific and that each system must be explored separately. It has been claimed that online real-time monitoring can help manage any changes in the process condition under high OLR in a very diverse AD system. Real-time monitoring is superior to delayed feedback, which is commonly used in commercial operations due to cost considerations (Dareioti & Kornaros, 2014).

2.8.12. C/N ratio

To achieve consistent regulation of the AD process, a balanced ratio of macronutrients and micronutrients is required. The C/N ratio is a representation of the quantity of nutrition in the feedstock. As a result, this ratio has an impact on the process's performance and stability (Dioha et al., 2013). In general, the best C/N ratios for increased biogas generation are between 20 and 30:1. During the co-digesting of chicken manure with wheat straw, an optimal range of 25-30:1 has been reported (Lu et al., 2017b). A significant C/N ratio variation from 25-30:1, indicates excessive carbon and insufficient nitrogen, causing inefficient metabolism, leading to inefficient substrate conversion and thus low biogas output. Low C/N ratio, i.e., excessive nitrogen and low carbon, causes NH_3 accumulation and pH values that are above the ideal range for methanogens. Co-digestion can help to balance the C/N ratio. The effect of the C/N ratio on the lowering of NH_3 concentration was examined by Zeshan et al. (2004). At a C/N ratio of 32:1, the NH_3 content in the digestate of the AD process was lowered by 30%, resulting in between 50 and 73% greater energy for the system. This implies that increasing the C/N ratio to its optimal range will enhance carbon concentration while reducing the amount of NH_4^+ produced by high protein concentrated feed. Furthermore, N, S, and P are important, and the C: N: P: S ratio of the substrate in the digester should be 600:15:5:3 for overall system optimality.

2.8.13. Bioreactor configuration

Different bioreactor configurations have been used in biogas production studies. The size of these bioreactors varies from small-scale (100-500 mL) to semi-pilot scale (2-10 L) or pilot-scale (>20 L) and are operated under batch, semi-continuous or continuous conditions (Saka and Kumar, 2010; Show et al., 2011). In an industrial-scale process; continuous digestion processes are recommended for evaluation of various aspects such as monitoring the digestion conditions, production and yield, and practical engineering aspects (Ismail et al., 2009). Examples of bioreactor configurations used in biogas production include:

1. Continuous stirred tank reactors (CSTRs)
2. Up-flow anaerobic sludge blanket reactors (UASBRs)
3. Anaerobic fluidized bed reactors (AFBRs)
4. Anaerobic sequencing batch reactors (ASBRs)
5. Membrane reactors (MRs)

Amongst these reactors, CSTRs are widely used in the AD processes (Gomez et al., 2006; Kim et al., 2011; Nandi and Sengupta, 1998) because they offer effective homogenous mixing patterns. Furthermore, CSTRs ensure good substrate-microbe contact as well (Show et al., 2011). The reactors could reach steady-state and exhibit high efficiency and stable performance when the operational conditions are optimized (Show et al., 2011). The setback for the application of CSTRs in continuous biogas production is biomass washout. Therefore, to ensure stable biogas production processes, the use of reactor systems with immobilized cells, such as anaerobic fluidized bed reactors (AFBRs) and upflow anaerobic sludge blanket reactors (UASBRs), has been proposed (Singh and Wahid, 2014). Immobilized reactors offer many advantages such as higher biomass density, improved operation stability, easier separation of solids and liquids, and reduced risk of contamination (Abreu et al., 2012; Hung et al., 2007; Singh and Wahid, 2014; Temudo et al., 2007; Yasin et al., 2011).

2.8.14. Agitation

Another technique to boost biogas generation is to use agitation. Agitation helps to homogenize the substrate within the digester, maintain a consistent temperature, promote microorganism access to the substrate, and break down restraining barriers to

liberate biogas. Because of the enhanced access to bacteria, agitation accelerates the quick breakdown of volatile solids (VS), as illustrated in Figure 2.10 (Meegoda et al., 2012). Agitation also prevents heavy material from settling at the bottom of the digester, which can restrict the digester's working volume. The effect of agitation on the decomposition of volatile solids is depicted in Figure 2.10.

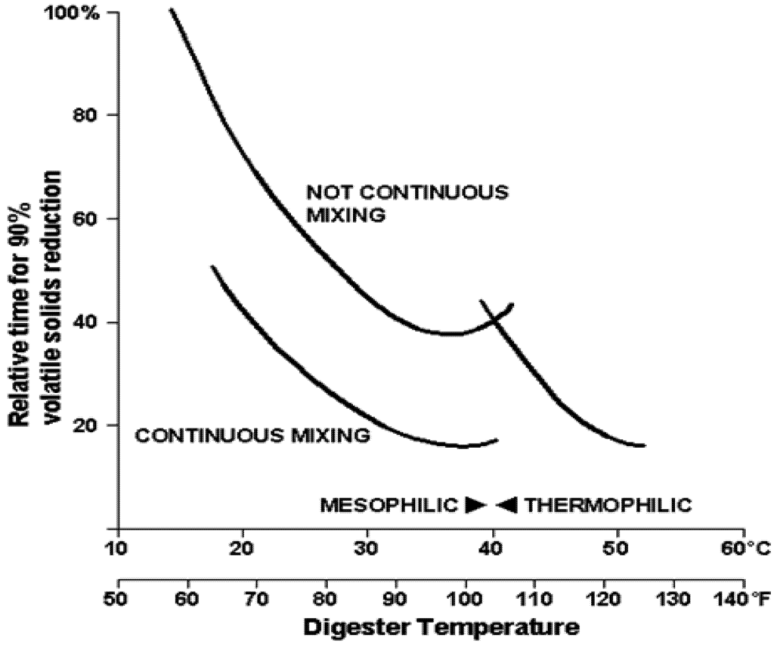


Figure 2.10: The effect of agitation on the degradation process of VS, volatile solids, Source (Meegoda et al., 2012)

2.8.15. Type of Substrate and Source

There are several different types of substrates for AD. Various portions of a substrate species will provide distinct outcomes and induce different intermediary inhibitors (Lindmark, n.d.). According to the literature, there are roughly 342 substrates with distinct biomethane yields when different parts of the substrate are examined. According to the report, the specific biomethane yield varies between 345 and 419 NmL CH_4/kgVS for cellulose, and between 81 and 409 NmL CH_4/kgVS for banana stems and peels respectively. Gunaseelan (2009) looked at fruit and vegetable substrates and discovered that the specific biomethane potential for fruits was 180-730 NmL CH_4/kgVS and for veggies was 190-400 NmL CH_4/kgVS. The author concluded that there was significant variance among fruit kinds, as various parts of the same variety had considerably varied findings. It's crucial to look into the parts of the substrate that make up the bulk of the waste to be processed to see if the low biogas yield is due to inhibition (Bong et al., 2018).

2.8.16. Pre-treatment

Pre-treatment of the substrate is frequently used to lower the action of inhibitors when exposed to anaerobic conditions to improve the process stability of an AD process. Pre-treatment is used to make the substrate more digestible and limit the number of intermediate inhibitors that may arise. Physical, chemical, or biological procedures could be used for pre-treatment (Morales-Polo et al., 2018). To break the lignin structure of biomass, physical pretreatment requires mixing, grinding, and steam explosion. Chemical pre-treatment often includes acid and alkaline chemicals (Peng et al., 2014). Biological pre-treatment methods that use a consortium of bacteria and enzymes are also utilized (Lebiocka et al., 2018).

2.8.17. Use of Additives

Additives are used in the digester to improve substrate biodegradation, promote stability by lowering inhibitory chemical concentrations, and encourage microbial activity (Ahring et al., 1995). The addition of microbial inoculum for bioaugmentation of hydrolytic or methanogenic activity is an example of biological additives (Lebiocka et al., 2018). Inorganic additives, such as macronutrients (P, N, and S) and micronutrients (Fe, Ni, Mo, Co, W, and Se), are also possible (Siddique & Wahid, 2018a; Ugwu & Enweremadu, 2020). The ideal concentrations of these additions have been reported to be 200 mg calcium per litre, 100-200 mg sodium per litre, and 400 mg potassium per litre (Siddique & Wahid, 2018a). 2500-4000 mg Ca/L, >400 mg Mg/L, 3500-5500 mg Na/L, and >5800 mg K/L are some of the inhibitory values (Ahn et al., 2006b). Some of these inorganics can be found in incineration ashes, which explains why they are sometimes employed as an additive (Wannapokin et al., 2017), In addition, conductive substances with a high capacity for biomass immobilization, such as iron, have been used to stabilize the AD process. (Cuetos et al., 2017).

2.9. Anaerobic Co-digestion

Anaerobic Co-digestion (ACD) is a method for obtaining an ideal substrate mix with attributes that satisfy some of the required requirements for successful digestion while also increasing the AD process' buffering capacity (Al bkoor Alrawashdeh et al., 2017). It also stimulates the diversity of the microbial community, rendering the AD process towards biogas production efficiently (Nielfa, Cano, & Pérez, 2015). The ratio of different forms of trash within the substrate mix affects the microbial population in a digester as well as the biogas production (Pecharaply et al., 2007). When comparing mono-digestion

with co-digestion of food waste with FVWs at a ratio of 1:3, Pavi et al. (2007) found greater biogas outputs and process stability. The ideal mix ratio of aloe vera waste to dairy manure was reported to be 3:1 by Huang et al (2016). According to Li et al. (2007), a 1:1 ratio of rice husk to pig dung is optimal. Molinuevo-Salces, et al. (2018) found that a 1:1 mix ratio for AD of vegetable waste with pig manure was optimum.

In addition, Yang et al. (2017) discovered that raising the co-substrate fraction by 5% during codigestion enhanced CH_4 production by 22.4%. Codigestion increased the CH_4 output rate by 18-48 percent, according to Carvanato et al. (2019) and Koch et al. (2020). When maize silage was co-digested with chicken and cattle dung, Ozturk (2007) saw a 120% increase in CH_4 output. In an AD process, Ozturk et al (2007) found that codigestion reduced NH_3 toxicity. Due to the wide range of substrate characteristics, it may be concluded that there are no apparent ideal levels for co-digestion. Co-digestion, on the other hand, that enhances the C/N ratio to around 30 is ideal.

Anaerobic Co-digestion refers to the digestion of multiple biodegradable substrates in an AD system (Y. Hu et al., 2018a). However, the digestion of a biodegradable mixture of feedstock containing a base substrate that an AD system was built to handle limits the success of co-digestion. The fundamental aim is to increase biogas production in an AD plant by incorporating a substrate that produces significantly more biogas per cubic centimeter than the baseline substrate (Al bkoor Alrawashdeh et al., 2017). The composition of substrates might change significantly between anaerobic digesters, posing varied challenges based on the feed characteristics combined with the system parameters chosen. The addition of an organic substance will raise the reactor volume, however, this challenge can prevail over some reduction of inhibiting pathways, which can be complemented by better COD removal efficiencies (Nghiem et al., 2017a).

2.9.1. Mechanism of Co-digestion

The key mechanism for codigestion is the balance of various parameters in the co-substrate combination, including macro and micronutrients, carbon to nitrogen (C: N) ratio, pH, inhibitors or toxic chemicals, OLR, the biodegradability of organic matter, and solids content (Rabii et al., 2019). These parameters are among the principal drivers of the microbial community structure. When the parameters are balanced, anaerobic co-digestion can increase CH_4 production by 50–200% or even higher, depending on the operating conditions and the co-substrates used (Álvarez et al., 2010). Anaerobic co-

digestion between sewage sludge and the organic fraction of the municipal solid waste has been the most reported co-digestion mixture. It was then noticed that there is a fast accumulation of VFAs which led to digester breakdown and instabilities (Maunonen-eskelinen et al., 2013). As a result, between 2010 and 2013 the publications dealing with fats, oils and greases and algae as sludge co-substrate increased. The interest increased because both co-substrates, sewage sludge, and FOG can be obtained at the same wastewater treatment plant (Sugumar et al., 2016; Yang et al., 2015).

In ACD, the knowledge of the chemical composition and other characteristics of the co-substrate is an important tool in the accurate development of the anaerobic digestion process (Elbeshbishy & Nakhla, 2012). It is therefore essential to understand the main components of the substrate that drives AD such that it can be easier to classify them. In the microbial context of anaerobic digestion, the principal components of substrates are carbohydrates, lipids, and protein (Nielfa, Cano, Pérez, et al., 2015). These components have to be efficient and balanced to obtain successful degradation steps in order of hydrolysis, acidogenesis, acetogenesis, and then methanogenesis (refer to Figure 2.3). Carbohydrates are hydrolyzed to sugars, which are then degraded to volatile fatty acids (VFAs), prior to further conversion to acetate, carbon dioxide & hydrogen. The lipids are hydrolyzed into long fatty acids and glycerol, these long fatty acids are converted into VFAs which are broken down into acetate and H_2/CO_2. Proteins are hydrolyzed and degraded by proteolytic enzymes into peptides and individual amino acids. The peptides and amino acids are then acidified into VFAs, hydrogen, ammonium, and reduced to sulfur. The VFAs are further converted by acetogens into acetate and H_2/CO_2 by the methanogens (Elbeshbishy & Nakhla, 2012; Ramdani et al., 2015).

Though not exact, the co-substrates in this study have been categorized as carbohydrates, protein, and lipids-rich co-substrates. In summary, lipids-rich co-substrates exhibit an increased biogas potential and are considered to be a promising feed for ACD. On the other hand, carbohydrate-rich and protein-rich substrates are also feasible as they are good producers of volatile fatty acids and protein-rich substrates demonstrate a good buffering capacity owing to the production of ammonia.

2.9.2. Carbohydrate's co-substrates

Material concentrated in carbohydrates is among some of the promising substrates for methane production. They pose a lower risk of AD process disturbance, however, the

carbohydrates rich material requires time for degradation to complete (Katahira et al., 2013; Kim & Kim, 2018). Lignocellulosic materials, animal by-products & some industrial wastes are the most common carbohydrate-rich material that can be considered co-substrates. Lignocellulosic biomass is plant-based materials such as fruit, grains, vegetables, and root crops, typically rich in different polysaccharides. Polysaccharides are chains of sugars linked in linear chains or branched chains that are recalcitrant and hence cannot be easily biodegradable (Martínez et al., 2016b; Ragauskas et al., 2014). As a result, lignocellulosic substrates are widely available but not easily applied in biogas production due to their poor anaerobic degradation. Literature reports that lignocellulosic materials can be coupled with the growth of hydrolytic bacteria and this factor can increase the overall degradation rate (Nielfa, Cano, & Fdz-Polanco, 2015; Nielfa, Cano, & Pérez, 2015).

Though, there are biodegradable carbohydrate-rich co-substrates they typically contain high concentration sugar monomers that might cause a fast accumulation of volatile fatty acids (Nielfa, Cano, Pérez, et al., 2015). Brewery spent grain is one of the biodegradable carbohydrate-rich materials. (Binder & Raines, 2010) reported that when coupled with sewage sludge they complement each and increase methane production. Co-digestion of municipal sewage sludge and brewery spent grain reported a methane increase of 66 % when fed at 95:5 on a volatile solids basis (Álvarez et al., 2010). See Table 2.6 for the list of other co-substrates categorized under carbohydrates rich material.

2.9.3. Protein co-substrates

Protein and fat-rich substrates have high energy content and consequently a high methane potential, but they can occasionally induce process disruptions due to the production of inhibitory chemicals or foaming. Waste from animal raising (slaughterhouse, dairy, animal manure, aquaculture sludge), ethanol fermentation (distiller's waste), food industry, and households are all protein-rich feedstock for biogas production. Proteins are made up of long chains of amino acids that are connected by peptide (or amide) bonds, and there are 20 distinct amino acids of varying lengths. Protein breakdown efficiency is determined by the structure and solubility of these molecules. The presence of at least one amine group is a characteristic shared by all amino acids ($-NH_2$). As a result, ammonia is produced during protein degradation, and its inhibitory effects have been documented. Nevertheless, the incorporation of plant

material (carbohydrate material) with a high carbon content balances the feedstock's carbon to nitrogen (C/N) ratio, minimizing the likelihood of ammonia inhibition (Álvarez et al., 2010; Elbeshbishy & Nakhla, 2012; Rabii et al., 2019).

Animal manures are the most commonly reported co-substrate for sewage sludge co-digestion because they produce intriguing biogas outputs. Animal manures provide a buffering capacity as well as a diverse spectrum of nutrients (Magdalena et al., 2017; Stravalaci, 2017). Because of the balancing of numerous parameters in the co-substrate combination, the beneficial synergy effects frequently found in co-digestion have presented the potential for increased methane outputs. The environmental benefits of using a protein substrate in biogas plants are far greater than those of any other substrate due to the combined effect of producing methane as a non-fossil fuel and reducing methane emissions to the atmosphere from unwanted anaerobic degradation during storage and application on the fields (Møller et al., 2014; Nielfa, Cano, Pérez, et al., 2015). See Table 2.6 for the list of co-substrates categorized under protein-rich material.

2.9.4. Lipids co-substrate

High lipid content substrate is considered as a suitable source for anaerobic treatment and a potential energy source since lipids have a significant methane yield when compared to other organic compounds such as carbohydrates and proteins (Y. Hu et al., 2018b; Kuang, 2003). Despite their considerable methane potential, lipids and lipid-rich wastes are rarely employed as the only substrate in AD. This is because they have developed operational issues such as clogging, foaming, and biomass flotation (Nielfa, Cano, & Pérez, 2015; Rabii et al., 2019). Materials with a high-fat content include slaughterhouse waste, some food waste, and grease-separation sludge. Fat molecules are hydrolyzed to long-chain fatty acids (LCFA) and glycerol, depending on their length (saturated or unsaturated). In AD, lipids are generally rapidly degraded, whereas LCFA conversion can be a rate-limiting process (Awe et al., 2017; Francioso et al., 2010).

Several studies reported the higher methane yields in co-digestion of lipids material i.e., FOG combined with municipal sewage sludge compared with sludge mono-digestion. This is expected due to the high biodegradability and high energy content of lipids waste (Y. Hu et al., 2018b). In the co-digestion of FOG and sewage sludge, it is reported that the maximum methane yield can be achieved at a grease content of 46% on a VS

basis (O'Connor, 2012). It was also reported that co-digestion of lipid-rich wastes demonstrated better stability under thermophilic conditions than the mesophilic condition which increases the cost of heating the digester. Otherwise, if not heated it requires a specific reactor such as the siphon-driven self-agitated anaerobic reactor (Kuang, 2003; Tsai, 2012). See Table 2.6 for the list of co-substrates categorized under lipids-rich material.

2.9.5. Other Co-substrates

Besides the carbohydrates, protein, and lipids co-substrates, other co-substrates can be co-digested with municipal sewage sludge to enhance biogas production. These co-substrates are indicated in Table 2.6. The emerging studies focus on utilizing nanoparticles as additives to feed bacteria that break down natural substances in anaerobic digestion. Nanoparticles are naturally unstable, however, they can be designed to provide ions in a controlled approach, to achieve maximum enhancement of biogas production (Faisal et al., 2018). To do this, nanoparticles are dissolved and fed into the anaerobic digester to nurture microbial organisms responsible for the degradation of organic material. As a result, biogas production can be increased up to 200%, thereby increasing methane generation. Methane production can be enhanced by a Nano iron oxide (Fe_3O_4 NPs). In Faisal et al, (2019) nanoparticles were added into a WAS anaerobic digester at pH 7.0 & mesophilic conditions for 60 days. There was an increase of 234% in methane production and 180% in biogas production.

2.9.6. The approach of selecting suitable co-substrate

To facts to look at before selecting a suitable source, co-substrate are distance, cost, sustainability & availability. The co-substrate must preferably be waste that is available at no cost. The proximity of the co-substrate supplier to the Treatment Works plant is among the selection criteria. The amounts of organic waste generated at particular sites must be sufficient. The source of the co-substrate must be sustainable in terms of the waste production per year and the sustainability of the source needs to be considered to ensure continuous availability of the co-substrate.

2.9.6.1. Composition of the co-substrate

In AD, the amount of biogas produced is dependent on factors such as digesting temperature & pH, organic loading rate (OLR), hydraulic retention time (HRT), solid retention time (SRT), digester shape, and type. These factors are operational variables

that can be controlled to increase biogas production from any given substrate. However, the composition of what is fed into the digester determines the limited amount of biogas that can be produced from that particular substrate. Hence, if the operators are confident that the operational variables are at optimum, the enhancement of feed composition is an alternative measure when one is considering optimizing the biogas production further. Therefore, understanding the characteristics of the feed and ways to manipulate it is a crucial step to increasing biogas generation. The feed composition is described by the number of parameters such as chemical oxygen demand (COD), total solids (TS), volatile solids (VS), total organic carbon (TOC), total Kjeldahl nitrogen (TKN), ammonium nitrogen (NH_3-N), alkalinity, volatile fatty acid (VFA), orthophosphates (PO_4^{2-}) and total phosphorus (TP).

VFA, COD, TS, and VS quantify the organic matter available for biodegradation and ash content contained in the feedstock. The COD determines the limit of biogas that can be produced from a given substrate. The co-substrate must have COD greater than the COD value of wastewater treatment plant sludge; the literature suggests a COD value in the range of 8.1 to 21.3 g/L. Furthermore, the TS & VS value of the co-substrate must be high, the ratio VS/TS must be close to 99% (Hilkiah Igoni et al., 2008; Pecharaply et al., 2007). In addition to that, it can be advantageous if the co-substrate has to favor synergisms, can dilute harmful compounds, optimize methane production and not disrupt digestate quality (Al bkoor Alrawashdeh et al., 2017). The high content of moisture and organic content classify the material among the most suitable co-substrates for AD.

TKN and TOC determine the Carbon-to-Nitrogen (C/N) ratio, which describes the nutritional balance of the feed. The other critical variables involved in methane production are the concentrations of proteins, lipids, and carbohydrates. In some instances, variations in concentrations of lipids and carbohydrates increase the production of methane by more than 500 % (Álvarez et al., 2010; Rulkens, 2008)." The co-substrate must not produce excessive oxygen and must maintain a pH between 6.8 & 7.8. Additionally, it must have sufficient nutrients (N & P) and be advantageous if it contains trace metals such as Fe, Co, and Ni.

Table 2.6: Potential co-substrate identified for anaerobic co-digestion of sewage sludge

Categories	Sub-categories	Substrates	Possible CH4 Enhancement (theory)	Sources	Identified source	Location	Highlights/ or Effects	Reference
Carbohydrates-rich Co-substrates	Raw Plant Material	Agricultural (Rice, Corn…	72% increase	Grain & Forage Crop Farms	Afgri, AgriSA	Centurion	Increase digester volume	(Saha, 2003)
		Grains, maize, beans, beets	54-60 % increase	Grain & Forage Crop Farms	Afgri, AgriSA	Centurion	Increase digester volume	(Jackowski et al., 2019)
		Ley crops	54-60 % increase	Grain & Forage Crop Farms	Afgri, AgriSA	Centurion	Increase digester volume	(De Mes et al., 2003)
		Fibre & Cardboard Waste	54-60 % increase	Wood processing ind.	SAWPA	Isando, JHB	Increase digester volume	(Sjostrom, 1993)
		Energy Crops (wheat, miscanthus	80% increase	Agri Farms	Afgri, AgriSA	Centurion	Increase digester volume	(Rabii et al., 2019)
		Processed Plants (Woods, Grass)	25 % increase	Pulp & Paper Ind	SAPPI, Mondi, Typek	Mpumalanga	Increase digester volume	(Rabii et al., 2019)
	Industrial Organic Waste	Fermentation Residues	178 % increase	Vinification plants	Danone, SAB	Bryanston	May contain inhibitory chemicals	(Al bkoor Alrawashdeh et al., 2017)
		Pretreated plants	200% increase	Wood processing ind.	SAWPA	Isando, JHB	May contain inhibitory chemicals	(Ayeni et al., 2013)
		Ice cream Waste	2-40 % increase	Ice cream production waste	Ice cream waste Co.	Randburg, JHB	Causes foaming	(Lu et al., 2017a)
		Sawdust (wet)	0.04 -12 % increase	Wood processing ind.	SAWPA	Isando, JHB	Good for dewatering process	(Lu et al., 2017a)
		Sugar Cane Molasses	27-57 % increase	Sugar producing ind	Tongaat, Hullets	Germiston, Illovo	Requires mixing	(Kalemba & Barbusiński, 2017)
		Bakery /Confectionary Waste	12-44% increase	Bakery	Sasko, Albany	Aeroton	Increase Digester volume	(Pilarska et al., 2018)

		Coffee & Tea grounds	11-20% increase	Coffee & Tea production	Unilever	Bryanston	Unknown	(Neves et al., 2006)
		Coke waste Syrup	-	Carbonated soft drink ind	Cocacola	Nigel or Pretoria	Unknown	
		Brewery Spent grains	66-150% increase	Breweries	SAB,	Rosslyn. Pretoria	Available at a cost	(Jackowski et al., 2019)
	Algae	Micro algae	23-27 % increase	Cyanobacteria Ponds	-	-	Unknown	(Olsson, 2018; Siddique & Wahid, 2018b)
	Cellulose	Micro Crystalline Cellulose	12-30% increase	Cotton industries	SACTMA	Bruma, JHB	Expensive to get	(Suárez et al., 2014)
	Mixed Fresh Produce	Fruits & Veg wastes	38.7-82 % increase	Fresh Produce Markets	JHB Fresh Produce	City Deep Market	Requires milling	(Brahim et al., 2019)
Protein-rich Co-substrates	Manure	Horse excreta	11-23% increase	Horses Husbandry	Race Course	Turfontein	Available in small quantities	(Lu et al., 2017a)
		Cow dungs	12-74 % increase	Beef Farms	Beef Co, Karan Beef	Pretoria	Digester accumulation	(Møller et al., 2014)
		Poultry Manure	5-10 % increase	Chicken Farms	Astral Poultry	Olifantsfon tein	Digester accumulation	(Babaee et al., 2013)
		Pig manure	7-40 % increase	Piggery	N & N Abattoir	Nigel	Digester accumulation	(Lu et al., 2017a)
		Goat excreta	0.1-75% increase	Goat Farms	N & N Abattoir	Nigel	Digester accumulation	(De Mes et al., 2003)
	Abattoir wastes	Blood & water waste	80% increase	Abattoir	Beef Co	Pretoria	High protein may inhibit production	(Cuetos et al., 2017)
		Stomach content /Offal	4.2-60% increase	Abattoir	Beef Co	Pretoria	High protein may inhibit production	(De Mes et al., 2003; Lu et al., 2017a)
		Slaughterhouse waste	100-162% increase	Abattoir	Beef Co	Pretoria	High protein may inhibit production	(Rabii et al., 2019)
	Other Industrial Waste	Industrial Liquid waste	60-82 % increase	Milk, yoghurt or whey producing industries	Clover	Rooderpo ort	Formation of froth & foam	(Charalambous, 2015)
		Dairy wastes (milk,	60-82 %		Clover	Rooderpo	Formation of froth & foam	(Sakeus, 2016)

		butter, cheese)	increase			ort		
		Food Waste	11% to 180%.	Restaurants, Malls or Mass Market			Denitrification effect	(Nghiem et al., 2017b)
Lipids-rich Co-substrates	Waste oil	Sunflower, Palm, Olive, Coconut	0.04-31 % increase	Restaurants & oil industries	Wilmar food Service	Randfontein	Thermophilic temp & mixing	(O'Connor, 2012)
	Refinery waste	Petrol, diesel & coke waste	7.4 %- 142 % increase	Refineries	Natref	Sasolburg	Thermophilic temp & mixing	(Q. Wang et al., 2016b)
	Fats	Butcher's fat	20-96.7 % increase	Fats producing industries	Beef Co	Pretoria	Lipids accumulation at high conc.	(Martínez et al., 2016b)
	Glycerine	Glycerol	28-60% increase	Refineries	Unilever	Bryanston	Thermophilic temp & mixing	(Rabii et al., 2019)
	Grease	Grease	20-96.7 % increase	Refineries	Unilever	Bryanston	High lipids content may cause accumulation	(Sandriaty et al., 2018)
Municipal Organic Waste	Landfill leachates	Landfill leachates	-	Landfills	Pikitup landfill	Rooderport	Not easily accessable	(Siddique & Wahid, 2018b)
	Organic Fraction (OFMSW)	Organic Fraction (OFMSW)	22-87% increase	Municipal collections sites	Pikitup	Rooderport	Requires milling	(Nielfa, Cano, & Fdz-Polanco, 2015)
Emerging Co-substrates	Nanoparticles	Mg, Ca, Co	50 - 75 % increase	Purchase	Manufacturing Industries		Expensive	(Faisal et al., 2018)
		Aluminium	35.7 % reduction	Coffee Capsules waste	Nespresso		Requires crushing	(Faisal et al., 2018)
		Nickel	90-150 % increase	Purchase	Manufacturing Industries		Expensive	(Faisal et al., 2018)
		Carbon based nanomaterials	40 % increase	Purchase	Manufacturing Industries		Expensive	(Faisal et al., 2018)
		Iron (Fe), ZVI	100-200 % increase	Iron & Steel industries	Arcelor Mittal	Vereenigin g	Expensive	(Faisal et al., 2018)
	Metal Oxides	ZnO	0% increase	Purchase	Manufacturing Industries		Expensive	(Faisal et al., 2018)
		Iron oxide (Fe (II), Fe(III))	100- 200 % increase	Iron & Steel industries	Arcelor Mittal	Vereenigin g	Expensive	(Faisal et al., 2018)

Composite mixture	Balancing of substrates composition	Lipids - Se & Tungsten Food Waste	80-100% increase 11-180% increase	Purchase Restaurants, Malls or Mass Market	Manufacturing Industries Mall	Expensive	(Nielfa, Cano, & Pérez, 2015) (Morales-Polo et al., 2018)
CH_4 producing Element/Compound	Hydrogen	H_2	12-40% increase	Purchase	Manufacturing Industries	Expensive	(Wambugu et al., 2019)
	Acetic acid	CH_3COOH	50-60 % increase	Purchase	Manufacturing Industries	Expensive	(Q. Wang et al., 2016a)
	Carbon Oxide	CO2	0-10% reduction	Purchase	Manufacturing Industries	Expensive	(Dioha et al., 2013)
Conductive Materials	Biochar	Biochar	40 % increase	Purchase	Manufacturing Industries	Expensive	(González et al., 2018)
	Graphite	Graphite	40% increase	Purchase	Manufacturing Industries	Expensive	(González et al., 2018)
	Activated Carbon	Activated Carbon	40 % increase	Purchase	Manufacturing Industries	Expensive	(González et al., 2018)

2.10. Microbial Community in anaerobic digestion

Diverse microorganisms used as pure cultures are used in the anaerobic digestion bioprocess. Many studies documented in the literature used mixed cultures. Mixed culture biogas production is more advantageous than pure culture biogas production for the following reasons: (i) minimal sterility is needed, (ii) high microbial diversity increases conversion efficiency, (iii) microbial synergism exists, (iv) continuous bioprocesses are favoured, and (v) diverse substrates are used. These organisms are removed from a range of environments, such as soils, compost and sewage sludge (Bahram et al., 2019; Gerardi, 2003; Joyce et al., 2018).

Proteobacteria members are dominant and active anaerobic digesters species, according to microbial community identification of various biogas generating activated systems. They are spore-shaped gram-positive and rod-shaped, compulsory facultative anaerobes. They also use a range of substrates that are very interesting for the development of biogas processes (Madigan et al., 1997; Wang et al., 2008). It is reported that the proportion of bacteria in total after pre-treatment is over 60% (Pan et al., 2008). The heat resistance of spores is probably due to this (Fang et al., 2006; Wang et al., 2008). Many studies of biogas production processes have used Clostridium species, including includes C. butyricum (Yokoi et al., 2002), *C. beijerinckii KCTC 1785* (Kim et al., 2008), *C. bifermentans* (Wang et al., 2003), and *C. tyrobutyricum ATCC 25755* (Liu et al., 2006). Lin et al. (2007) studied the effect of four clostridial strains *C. acetobutylicum M121, C. tyrobutyricum FYa102, C. butyricum ATCC19398,* and *C. beijerinckii L9,* respectively and obtained a high yield of biomethane.

Bacteroides, Nitrospirae, Firmicutes and *Actinobacteria* phylum have also been found to be useful in the processing of biogas. These organisms are facultative anaerobes that are Gram negative and rod-shaped. In comparison to Clostridium species, they contain low levels of methane. Manyi-Loh (2013) used *Actinobacteria* to boost biomethane production and achieve a maximum yield. Bacillus species are also reported as facultative anaerobes. Pseudomonas sp., Actinomyces sp., Streptococcus sp., Klebsiella sp., and Escherichia coli are among the bacteria that produce biogas. Due to the decreased diversity of the biomass in pure cultures, metabolic pathways are easily identified. Moreover, studies employing pure cultures can reveal important information regarding conditions that promote high methane yield and production rate (Elsharnouby et al., 2013). Nonetheless, using pure cultures has its own limitations such as strict sterilization

procedures and the selectivity of substrates (Hawkes et al., 2002). Microbial conversion of acetogenesis products by biomethane-producing *Methanobacterium* species is associated with two metabolic pathways as shown previously. The first pathway is called hydrogenotrophic methanogenesis where hydrogen and carbon dioxide are converted into methane and acetotrophic methanogenesis where methane is formed from the conversion of acetate (Campanaro et al., 2016; Doloman et al., 2017; Guo et al., 2015; Rui et al., 2015).

2.10.1. Microbial Community in Stages of Anaerobic Degradation

Ferdeş et al., (2020) reported that bacteria belonging to the community of relative anaerobes, such as *Enterobacterium* and *Streptococcus* are responsible for the hydrolysis. Joycen et al., (2018) reported the microbial activities which caused acidification are *Bacteroidetes* dominating at 37°C and *Firmicutes* dominating at 55°C in bioreactor leachates. *Clostridia* and *Bacteroidales* were found to be more abundant in thermophilic and mesophilic environments in biogas plants that used energy crops as a feedstock (Venkiteshwaran et al., 2015). The phylogenetic class *Clostridia*, on the other hand, has been suggested as a marker for biogas plants that operate at mesophilic temperatures (Joycen et al., 2018). *Clostridiales* were also found during the anaerobic conversion of office paper to methane at 55°C, which resulted in a rapid drop in pH from 7.8 to 5.8 due to hydrolytic and acidogenic microbial activity (Wirth et al., 2012).

During acidogenesis stage, the facultative anaerobes use oxygen that is accidentally introduced into the process, creating favourable conditions for the development of the obligatory anaerobes of the following genera: *Bacillus, Pseudomonas, Clostridium, Micrococcus,* or *Flavobacterium* (Krzysztof Ziemiński, 2012). During acetogenesis stage, the acid-phase products are converted to acetates and hydrogen by the acetate bacteria i.e., the genera of *Syntrophomonas* and *Syntrophobacter* (Jeihanipour et al., 2011; Sanz & Köchling, 2007). The acid-phase products can be used by methanogenic bacteria to produce biomethane.

For many reasons, methanogens are an important group of microorganisms and their ability to process organic matter to methane is the most significant. A large majority of CH_4 in the methane digestion process is a result from acetic acid conversions by heterotrophic methane bacteria and only few bacteria can produce methane from acetic acid. The CO_2 reduction by autotrophic methane bacteria is the result of only 30% of

methane produced in this procedure. *Methanobacterium, methanobrevibacter and methanosaeta* are the most common methanomicrobials (De Vrieze et al., 2012; Frąc et al., 2017). "The summary of possible owing to the cooperation of four different groups of microorganisms and are presented in Table 2.7.

Table 2.7: Summary of Microbial Community in Stages of Anaerobic Degradation, adapted from (Wirth et al., 2012)

Reaction type	Potential Microorganisms	Main Product
Hydrolysis	*Enterobacterium, Streptococcus, Clostridia and Bacteroidales*	CO_2
Acidogenesis	*Bacillus, Pseudomonas, Clostridium, Micrococcus,* or *Flavobacterium*	H_2
Acetogenesis	*Syntrophomonas* and *Syntrophobacter*	CH_3COOH
Methanogenesis	*Methanobacterium, methanobrevibacter and methanosaeta*	CH_4

2.11. Feasibility of Synthesizing Activated Carbon from sludge

Anaerobic digestion, as previously mentioned, is a well-established organic waste management technology that produces biogas and digestate as end products. The nutrients in organic matter are conserved and mineralized to more soluble and biologically available forms during anaerobic digestion, resulting in a more predictable biofertilizer. The crops benefit from the presence of these essential plant nutrients when treated effluents are recycled back to productive agricultural lands at sufficient rates. Other nutrient recovery technologies can be used to reduce the nutrient content of the digested wastewater if cropland is not usable (Koch et al., 2019; Nghiem et al., 2017a).

Biogas can be generated mainly from animal dung, food & kitchen waste, industrial organic waste, or any type of wet organic waste. The activity of methanogenic microbes in anaerobic digesters (biogas plants) breaks down complex organic molecules in multiple steps, resulting in biogas and bio-fertilizer as the end product. There is a significant difference between using organic waste directly in the soil and after composting it in a biogas plant. The nutrients in raw organic waste are complex, making it difficult for soil microbes to act on it and convert it into crop/plant absorption form. However, in the case of composted organic fertilizer from the biogas plant, it is already

broken into the simplest form so that the plant readily uses it without any further conversion (Cavinato, 2011; Rulkens, 2008).

Moisture material, organic carbon, potassium, nitrogen, phosphorus, and other elements are present in biogas slurry (composted organic fertilizer) in percentages, of 40.21, 11.77, 0.33, 0.71, and 0.43 with a C:N ratio of 17:1 on average. The C:N ratio of organic waste without composting would be in the range of 20:1. Bio-fertilizer from a biogas plant has the following advantages over non-composted agricultural waste used directly on crops or plants: Reduced length, decreased odour, decreased pathogens, and weed seeds, and decreased spontaneous emissions of CH_4, NH_3, and N_2O into the atmosphere. Thermal decomposition of carbonaceous material is normally accompanied by activation with steam or carbon dioxide at a high temperature to create activated carbon. The process involves two steps: carbonization and activation (Lucian & Fiori, 2017).

2.11.1. Activated Carbon Production Techniques

Activated carbon, also known as biochar, is a carbonaceous residue derived from the thermal conversion of biomass in an oxygen-depleted environment. It can be generated using processes such as pyrolysis, gasification, hydrothermal carbonization, and torrefaction- all of which do not require any sort of activation. Biochar's surface area is less effective than activated carbon due to the lack of activation; however, biochar is less expensive to produce (González et al., 2018).

The key components of biomass are cellulose, hemicellulose, and lignin, with minor quantities of pectin, protein, extractives, and ash. Depending on the type of biomass, the quality of these components varies. On a dry basis, cellulose, hemicellulose, and lignin typically make up 40-60, 20-40, and 10-25 percent of biomass content, respectively. "The structural building blocks of biomass (cellulose, hemicellulose, and lignin) go through a series of reactions during thermal decomposition, including dehydration, cross-linking, depolymerization, fragmentation, rearrangement, condensation, and carbonization at various temperatures (Mudzanani et al., 2019b; Paritosh et al., 2018). Biochar, condensable liquid (bio-oil), and non-condensable gases (syngas) are all formed as a result of these processes. The desired product and its application are determined by the biomass used and the devolatilization temperature. The thermal conditions are the maximum pyrolytic temperature, heating rate, strain, and residence time, while the

biomass characteristics are elemental composition, pellet size, and mineral content in the ash (Pavlík et al., 2016).

From sludge materials, hydrothermal carbonization creates hydrochar, while gasification favours the formation of gaseous-phase products. Auto- and allo-thermal reactors are two types of thermal reactors used in pyrolysis. The heat of the reaction is given by the partial oxidation of the biomass in the auto-thermal reactor. This partial oxidation generates enough heat to catalyze the endothermic reaction. The reactor is known as allo-thermal when the heat of reaction comes from an external source such as natural gas and another biomass. The properties of pyrolytic products and their yields which differ for the same biomass due to differences in heat source (Jackowski et al., 2019).

2.11.2. Carbonization

Carbonization is the process of heating carbonaceous material to high temperatures, typically between 500 and 800°C, in an inert atmosphere (Smith et al., 2009). Most non-carbon elements, such as oxygen, hydrogen, nitrogen, and sulphur, are removed during carbonization, leaving a fixed carbon mass with a rudimentary pore structure. Aromatic sheets are formed by the remaining carbon atoms, which are randomly cross-linked., which is identical to that of graphite. The internal carbon mass (or tar) from the decomposition, which has formed a less porous structure, may be filled or blocked in the free interstices between the sheets (Okeola et al., 2012).

2.11.3. Activation

The activation process clears the char between the aromatic sheets by removing the tarry products produced during carbonization, as well as enhancing the formation of a structure with a large number of pores of different shapes and sizes (Bansal and Goyal, 2005). The activation process removes disorganized carbon and exposes aromatic sheets to activation agents, resulting in the formation of a microporous structure. Physical and chemical activation are the two forms of activation.

2.11.3.1. Physical Activation

Physical activation is a two-step process i.e., the activation with oxidant gases, such as CO_2, steam, or oxygen, followed by carbonization, which allows for selective oxidation of atoms through controlled gasification (Bansal et al., 1988). The method is normally carried out at temperatures ranging from 800 to 1100 degrees Celsius. The removal of a significant amount of internal carbon mass allows for the creation of the porous structure within the activated carbon (Hsu & Teng., 2000). The activation process begins

with carbon disorganization through thermal decomposition, followed by a 10% burn-off, which results in the opening of the blocked pores. The aromatic ring then starts to burn, resulting in active sites and larger pores (Bansal et al., 1988).

2.11.3.2. Chemical Activation

Chemical activation is a one-step process in which the carbonization and activation steps are carried out concurrently by carbonizing the carbonaceous material that has previously been impregnated with chemical activating reagents (Smith et al., 2009; Bansal et al., 1988). Chemical activation is typically carried out at temperatures ranging from 400 to 800 °C. In the activated carbon manufacturing industry, phosphoric acid (H_3PO_4) is commonly used as an activating agent. In addition, zinc chloride ($ZnCl_2$), sulphuric acid (H_2SO_4), sodium hydroxide (NaOH), potassium hydroxide (KOH), and various chloride salts of magnesium, calcium, ferric, and aluminum are used. These chemicals are dehydrating agents, but they dehydrate at varying rates depending on the precursor content. For example, instead of hydrocarbons, $ZnCl_2$ can release hydrogen and oxygen gas inside the material by forming water molecules. As a result, keeping more carbons in the carbonaceous material increases the percentage yield of activated carbon. In addition to suppressing tar formation, $ZnCl_2$ produces a carbon skeleton and creates a porous structure (Caturla et al., 1991).

2.12. SAC as an adsorbent material

The sludge-based Activated Carbon (SAC) is an environmentally friendly adsorbent with strong adsorption efficiency, a wide variety of raw material sources, stable chemical properties, and the ability to be reused and recovered multiple times. It also has good thermal stability and has been confirmed as being safe to use at this time. The possibility of trace metal leaching during the application of SACs to wastewater is a major concern. As a result, it's crucial to figure out if SAC can contaminate wastewater by leaching its inorganic elements. Chen et al. (2002) investigated the heavy metal leaching problem of SACs in a report. The amount of Cr, Cd, Cu, Zn, Pb, and Ni released was measured, and the amounts of the leached metals were found to be within the acceptable ranges for most industrial effluent treatment applications, with the exception of Zn.

2.12.1. Removal of Heavy Metals By Adsorption

Physical adsorption is defined as the adhesion of a chemical species onto the surface of particles (Zha et al., 2018). Adsorption has several disadvantages, including the high cost

of the adsorbent, hard separation of the adsorbent from dye, disposal issues, and low surface area (De Filippis et al., 2013). Many researchers have focused on a solution for the adsorption disadvantages and the development of low-cost and highly efficient adsorbents to treat dyes (Mu & Wang, 2016). This study introduces the use of low-cost adsorbent SAC which is derived from the waste and synthesized in an environmentally friendly manner. Based on the activation process and the modification the study will analyze its physical and chemical stability, properties, and performance in the removal of heavy metals.

This study aims to focus on the removal of heavy metals by adsorption, specifically chromium (Cr) and cadmium (Cd) because the in-house analyst identified them as the most difficult heavy metals to remove in the JW municipal since that is the research study's focus area. Drinking water pollution is a growing source of contention in modern society. Heavy metals are metallic elements with toxic properties and a relatively high density, specific gravity, or atomic weight (Setshedi, 2014). In general, humans are more likely to be exposed to heavy metals through water consumption, and thus toxic metal bioaccumulation occurs in the human body (Setshedi, 2014).

As compared to trivalent chromium (Cr^{3+}), hexavalent chromium (Cr^{6+}) is more toxic, and this form results from industrial pollution (Vivek Narayanan & Ganesan, 2009). Excessive consumption of this form may cause skin irritation, digestive problems, and lung cancer. According to WHO, the maximum allowed concentration of Chromium in water is 0.05mg/L (Setshedi et al., 2013). Cadmium (Cd), on the other hand, is a naturally occurring element in the earth's crust. Acute exposure to significantly higher cadmium levels can cause diarrhoea, vomiting, fever, lung damage, and muscle pain (Nordberg, 2004). While some diseases, such as kidney disease and bone damage, reproductive problems, and possibly cancer, are caused by chronic cadmium exposure (De Filippis et al., 2013)

2.13. Quality Improvement of Digestated material

As previously mentioned, one of the difficulties with AD is ensuring the consistency of the digestate. When AD is running at maximum efficiency, it produces digestate with organic soil enhancement properties, and micronutrients that increase soil agronomic quality, and serves as a renewable source of depleting elemental phosphorus. Incomplete digestion of organic matter, whether due to the AD's instability or a short HRT, results in

digestate containing CH_4 and NH_3 that are quickly released into the atmosphere, thereby contradicting the AD's sustainability requirements. Furthermore, because of the incomplete digestion, the digestate is exposed to aerobic conditions, resulting in a sluggish microbial phase in the soil.

Digestate has been used as an agricultural fertilizer without being mixed with biochar. Biochar, on the other hand, has been shown to improve digestate properties through its cation exchange potential, which aids plant affinity for micro- and macronutrients as well as the soil's water-holding capacity (Cuetos et al., 2017). Biochar-enhanced digestate improves soil fertility, reduces nutrient leaching, and allows for carbon capture and storage. Since biochar can be applied directly to the soil, it can be used as an adsorbent in-situ AD without needing regeneration, preserving soil nutrients (S. Chen et al., 2002).

This lowers the expense of treating the adsorbent after it has been saturated with impurities. Organic material that is often spread on fields without digestion may be mixed with biochar in certain cases to boost the properties for soil application (Zhao et al., 2019). Biochar's efficacy in degrading VFAs and odour management for compost was compared to a control sample by Awasthi, et al. (2009). Biochar was used by Kizito et al. (2019) to reduce the concentration of NH_4-N in a digestate from an AD phase. Kizito et al. 2008 investigated the ability of biochar generated by slow pyrolysis to recover phosphate from liquid swine digestate and found it to be successful.

Shen, et al. (2002) found that the digestate from a biochar-amended digester had higher total Ca, Fe, Mg, and K levels than the digestate from a control digester. The dose of biochar had a direct relationship with the rise in nutrient concentration in the digestate. Biochar, according to (Frąc et al., 2017) will help with nutrient retention and minimize nutrient leaching after land application of digestate derived from a biochar-amended crop.

2.14. Adsorption Mechanisms of the activated carbon

In addition to moisture and ash, activated carbon contains fixed carbon, labile carbon, and other volatile compounds (Meyer-Kohlstock et al., 2016). Because of the co-existing carbonized and non-carbonized fractions, which have different sorption mechanisms, the biochar surface is heterogeneous. Sorption is described as an increase in the density of a solid sorbent's interfacial layer due to molecular exchange with a fluid called sorbate moving across the solid sorbent (Jung et al., 2019). According to Wang et al., (2018),

depending on the intermolecular forces that characterize the sorbate-immobile phase interaction, three sorption routes are possible, which are chemisorption, physisorption, and ion-exchange techniques. Chemisorption is less common in environmental systems because of the tight covalent bonds, which favour orbital mixing. The physisorption path, which is more common in environmental systems, can be divided into adsorption and absorption depending on how the sorbate interacts with the solid (Agrafioti et al., 2013).

The interaction of a molecule at the interface between a fluid and the surface of a solid whose atomic/molecular lattice cannot be penetrated by the sorbate molecule is referred to as adsorption. According to (Ambaye et al., 2020) adsorption can take three different forms i.e., the physical path, in which the adsorbate settles on the adsorbent's surface; the surface precipitation route, in which adsorbate layers form on the adsorbent; and the pore filling route, in which the adsorbate condenses into the adsorbent's pores. The adsorption process phenomena are facilitated by either hydrogen bonding, electrostatic attraction, ion exchange, or hydrophobic effect. The sorption of organic and inorganic adsorbates onto biochar is one of the mechanisms for removing them as shown in Figure 2.11. Adsorption of metals on biochar occurs primarily by precipitation, ion exchange, and electrostatic attraction onto the adsorbent's surface, while van der Waals forces, hydrogen bonding, and hydrophobic interactions are the adsorption mechanisms for organic molecules. The affinity of organic molecules and their adsorption on the surface of biochar is favoured by functional groups (hydroxyl, carboxyl, carbonyl, amine). The electron donor/acceptor adsorption process is based on the unequal distribution of electrons between the organic compound and the adsorbent (biochar) functional groups.

It's worth noting that the interaction between organic compounds with nitro- and chloro-substituent groups and the adsorbent are greatly reduced at this stage. As a result of the strong electron acceptor existence of the substituent group in the compound, the electrostatic interaction between the organic compound and the biochar increases (Mu'azu et al. 2017). Because of interactions over the hydrophobic sites shown in Figure 2.11, the degree of solubility of an organic pollutant influences the rate of adsorption on biochar. If the pollutant has a hydrophobic functional group, it can be bound to hydrophobic biochar in this way. The overall micropore and mesopore volumes affect the sorption of organic contaminants onto biochar by pore-filling (Said et al., 2014). Alkaline biochar surfaces can also precipitate water-soluble pollutants. Biochar

decreased the mobility of Pb, a heavy metal, in an aqueous solution, according to (Ahmad et al., 2014), due to the precipitation of insoluble Pb-phosphate.

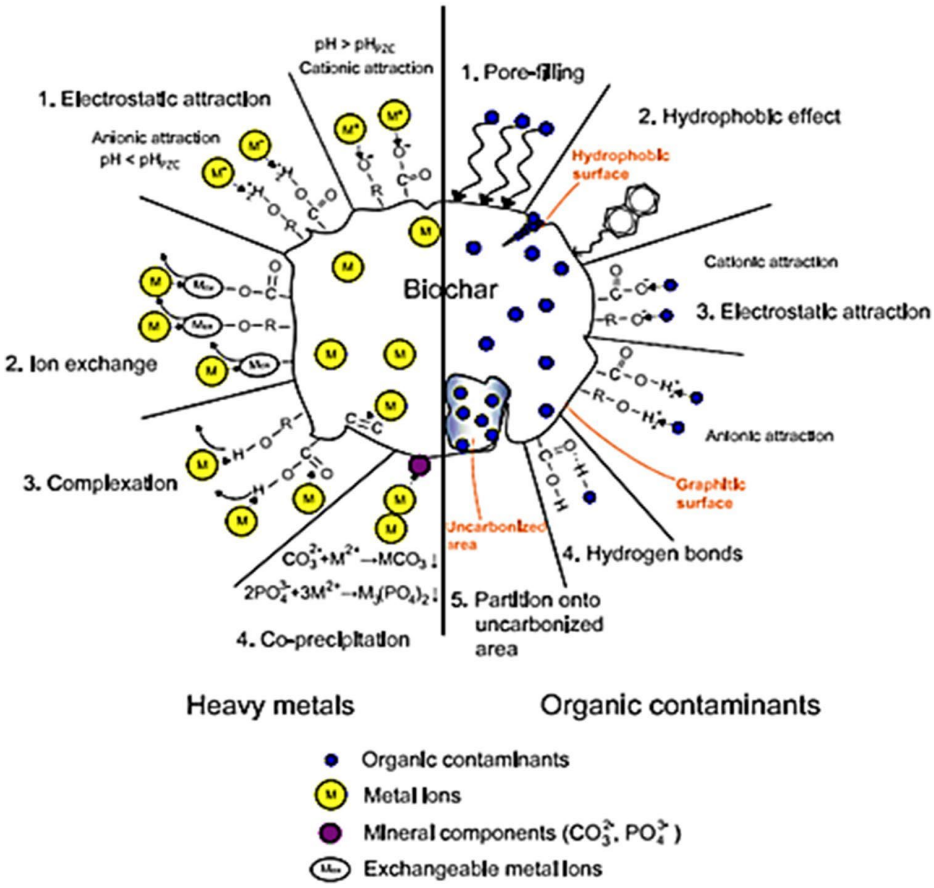


Figure 2.11: Adsorption mechanism of organic pollutant on biochar surface (Ahmad, et al. 2014).

Owing to the high penetration of the pollutant on the biochar surface, the adsorption potential of biochar generally increases as the ionic radius of the pollutant decreases (Ambaye et al., 2020). As a result, when considering adsorption on biochar surface, the atomic or ionic size of contaminants is a consideration to consider. Another possible adsorption mechanism is electrostatic activity between the biochar surface and organic pollutants, as shown in Figure 2.11. Metal exchange with alkali metals such as K+ and Na+, which are present on the biochar surface, may promote electrostatic attraction (Ahmad et al., 2014). "

Because of the dissociation of oxygen-containing functional groups, biochar surfaces are typically negatively charged, which may aid in the electrostatic attraction of positively

charged organic compounds (S. H. Hu & Hu, 2014). The loss of oxygen- and hydrogen-containing functional groups causes the biochar to become less polar and more aromatic as the pyrolytic temperature rises above 450 °C. This affects the biochar's adsorption potential for polar aqueous organic pollutants (Zhao et al., 2019). The electrostatic repulsion between negatively charged organic compounds on biochar was discovered to facilitate H-bonding and thus adsorption. With reduced H-bonding between water and the oxygen-functional group, hydrophobic sites become more attractive to the non-polar contaminant (Rio et al., 2005).

There are three stages to the adsorption process, which are; continuous adsorption, known as the transition zone; no adsorption, known as the clean zone; and equilibrium, known as the exhausted zone (Al Mamun & Torii, 2015). The first stage occurs when an adsorbate comes into contact with the adsorbent for the first time. Due to mass transfer based on the ion-concentration gradient, this is characterized by a high absorption rate. Following this, the adsorption rate slows as the sorption sites fill up, showing the end of physical adsorption in the second regime (Martínez et al., 2016a).

Finally, the interaction between the adsorbent and the adsorbate happens at a much slower rate, with a gradual rise that corresponds to chemisorption and diffusion until all active sites are completely saturated. As the adsorbent becomes completely saturated with the adsorbate, a breakthrough point occurs, followed by equilibrium (Kutty et al., 2019). This occurs when the inflow concentration is nearly equal to the outflow concentration, implying that no further adsorption occurs over the adsorbent's interfacial layers. The time it takes to achieve saturation varies depending on the dosage rate, the adsorbate concentration, and the adsorbent's affinity for the adsorbate. Depending on the use and exposure, a saturated adsorbent will usually be regenerated. This offers a cost benefit over other methods of impurity removal (Masebinu, 2018).

2.15. Factors Influencing the Adsorption Efficacy

Several factors affect the efficiency of biochar during adsorption, Hence Masebinu, (2018) divided them into two categories: adsorbent material and adsorbate characteristics. Biochar's properties, such as morphological structure and reactivity, are determined by its physisorption isotherm characteristics, which are influenced by the pyrolytic condition (Ambaye et al., 2020).

2.15.1. Pore Size and the Morphological Structure

When a gaseous sorbate is transferred over a solid sorbent's interfacial layer, the density of the interfacial layer increases. The accessible amount of micropores, rather than the internal surface area of the adsorbent, governs and limits the absorption of an adsorbate by an adsorbent. Figure 2.12 shows how the pores on the biochar are classified by the width of their openings. The micropores are responsible for biochar's surface area and high adsorptive potential, the mesopores for liquid-solid adsorption processes, and the macropores for aeration, hydrology, root movement, and bulk soil structure (Y. Wang et al., 2019).

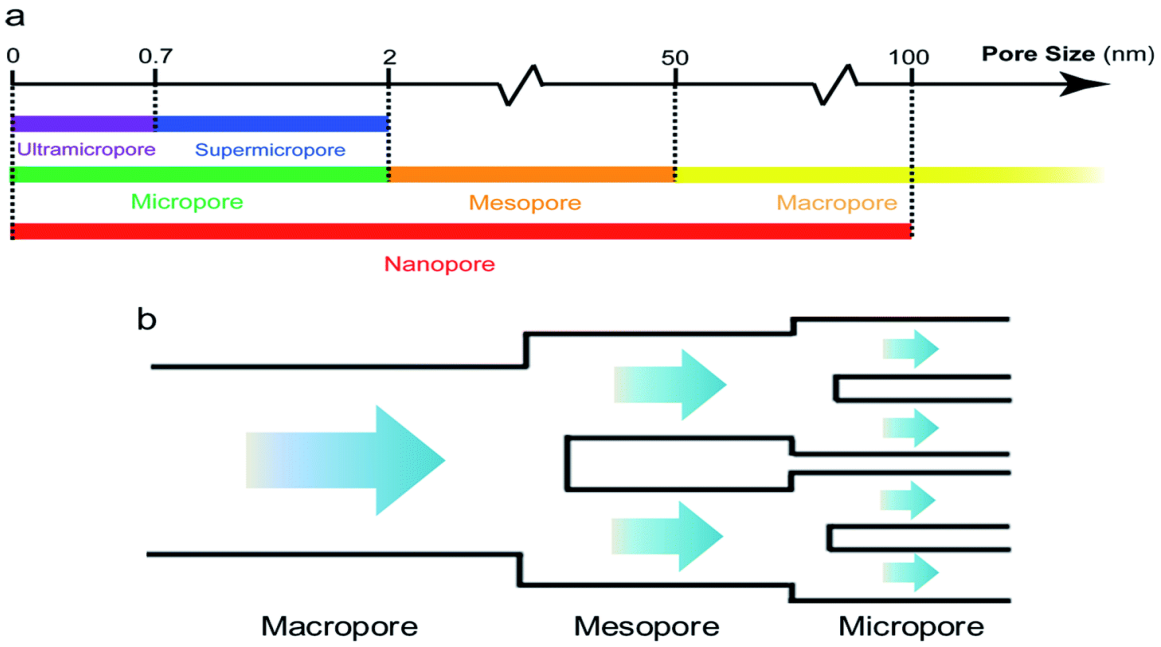


Figure 2.12: IUPAC standard for Pore size classification (Y. Wang et al., 2019)

According to Ahmad et al., (2014) biochar formed at high temperatures has a high proportion of micropores, ranging from 50 to 78 percent of total pores. Bousba & Meniai, (2013) reports that a large adsorbate can cause steric restriction of sorption capability at micropore sites. As a result, the size of the adsorbate affects the biochar sorption rate. When smaller particle sizes are used, the mass transfer constraint at sorption sites can be reduced, according to (Boumediene et al., 2018). This strengthens the adsorbate's van der Waal force of penetration into the adsorbent. The adsorbate's molecular diameter can influence its adsorption rate in part. An adsorbent with a pore size between 3.5-3.7 Å will adsorb CO_2 with a molecular diameter of 3.4 Å but it will reject CH_4 of 3.8 Å (Masebinu, 2018). Increasing pressure at standard temperature also favours increased adsorption for smaller-sized pores.

2.15.2. Surface Chemistry of the material

The surface chemistry of biochar has a significant influence on its ability to adsorb a specific chemical compound (Rio et al., 2005). The adsorption rate of biochar is determined by the types and levels of surface-functional groups. The pyrolytic temperature range and chemical composition of the biomass used as feedstock determine the distribution of surface-functional groups (Mu'azu et al., 2017). In a Fourier transform infrared spectroscopy, the wide band of 3337 cm^{-1} suggested heavy H_2 bonding in the biomass used as feedstock, stretching vibration attributed to water, (Ahmadi et al., 2013). The reported strong H_2 bonding was decreased as the pyrolytic temperature increases.

Furthermore, (Wen et al., 2019) reported that the O-H, C=O, C=C, $-CH_2$, and $-CH_3$ functional groups in biochar were altered due to pyrolytic conditions, which promotes biochar hydrophobic interactions. The amount of N- and S- functional groups in biochar derived from sewage sludge and poultry waste is higher than in woody biomass materials. The surface chemistry of biochar is described by these dominant functional groups, which can be altered when exposed to an aqueous solution. The changes are due to the interaction of the functional groups with water and the pH of the solution (Agrafioti et al., 2013). As a result, pH influences the sorption phase of biochar by manipulating the metal ion speciation.

Phenolic and carboxylic groups release protons and gain a negative charge as pH rises, while simple functional groups, such as amine, take up a proton and gain a positive charge as pH falls (Pöykiö et al., 2019). This means that an adsorbent's adsorption behaviour is also affected by the medium's pH. Due to the reduction of electrostatic forces between the adsorbent and the adsorbate ions, changes in the pH of the medium may have a substantial effect on the capacity of the biochar to adsorb certain compounds (Rio et al., 2005). Kizito et al. (2009) demonstrated the effect of changes in the pH of an aqueous medium on biochar adsorption capability. When the pH of the digestate was between 4 and 8, the adsorption of NH_4^+ from the digestate of an anaerobic digester treating pig manure over biochar was higher (Rio et al., 2005). When the pH of the digestate was 4 >pH> 8, however, the adsorption efficiency was decreased.

2.15.3. Hydrophobicity Interaction

Biochar's hydrophobicity plays an important role in the adsorption of insoluble adsorbate (Ahmad et al., 2014). The O- and N-containing functional groups define the degree of hydrophobicity, and this indicates the dominant polar group. The biochar becomes more hydrophobic as the number of O and N-containing functional groups in the biochar decreases. Water-adsorbing adsorbents are known as hydrophilic adsorbents. Because of competition with adsorbate and the filling of available sites with water, they are less successful (Wei et al., 2019). The lack of O-containing functional groups on the biochar surface prevents water penetration through H-bonding. Adsorbates that are non-polar and have poor solubility in aqueous solutions are more likely to be adsorbed in the pores of biochar. Since CO_2 is a non-polar compound, it can be adsorbed into biochar's sorption sites and retained in the required pore sizes (Ferrasse et al., 2015).

2.15.4. Temperature: Production and Operational

The maximum pyrolytic temperature has a big impact on biochar properties and yield, as well as environmental applications (González et al., 2018). The loss of volatiles is determined by temperature, which also affects the structure of biochar. Due to higher porosity and fixed carbon, raising the pyrolytic temperature increases the adsorption potential of the biochar (Ambaye et al., 2020). The affinity of biochar for organic and inorganic compounds is partly determined by the temperature at which it is produced. Because of the increased surface area and micropore distribution, the higher the pyrolytic temperature, the better the biochar is for adsorption of organic pollutants (Oladejo et al., 2019), because of the improved surface area, the increased distribution of micropores and the higher level of hydrophobicity.

However, at temperatures over 450 °C, the capacity to adsorb organic pollutants would be harmed due to the loss of oxygen- and hydrogen-containing functional classes. Biochar made at temperatures below 450°C, as shown in Figure 2.13, is ideal for the adsorption of both inorganic and polar organic pollutants. Electrostatic attraction, precipitation, and O-containing functional groups all help to speed up the sorption rate in low-temperature biochar (Kumar et al., 2009).

Biochar's sorption efficiency is influenced by the temperature of the medium in which it is used. Ambaye et al., (2020) found that raising the experimental temperature for NH_4^+-N adsorption from 15 to 45 °C improves the adsorption efficiency. They believed that the

adsorption process was endothermic, meaning that the temperature should be raised above 30 °C to a maximum of 45 °C in reality. L. Zhang et al., (2020) investigated biochar adsorption efficiency for in-situ biogas upgrading under mesophilic and thermophilic conditions. They found that high CO_2 adsorption resulted in higher CH_4 concentrations in biogas and faster degradation rate for thermophilic conditions when compared to the mesophilic yield.

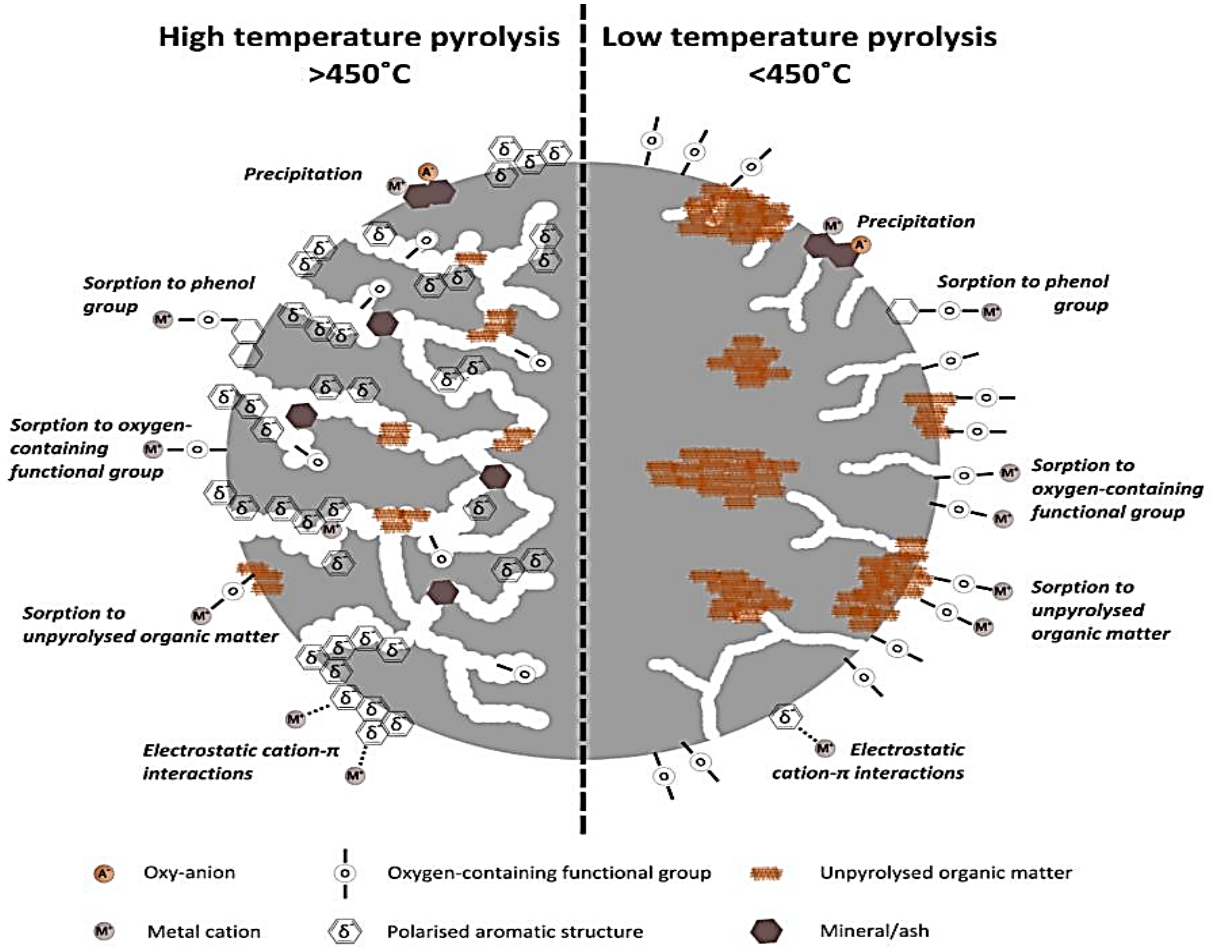


Figure 2.13: Adsorption mechanism on biochar surface in two temperature ranges (Ahmad et al., 2014)

2.15.5. Elemental Composition

When determining the aromaticity and polarity of biochar, the molar ratio of elements is critical (Sosnowski et al., 2003) Low O/C and H/C ratios mean that there is a lot of O_2 and H_2 lost during pyrolysis, resulting in biochar with a lot of fixed carbon (Kumar et al., 2009). Low oxygen levels in biochar indicate that oxygenated functional groups have been removed, rendering the biochar alkaline. The loss of O_2 results in a high O/C ratio, which suggests high hydrophobicity and the dominant polar group. Since H_2 is mainly

correlated with organic matter in biomass, the H/C molar ratio reflects the degree of carbonization (Kumar et al., 2009).

To differentiate biochar from biomass that has not been, or has been only slightly thermochemically changed, the International Biochar Initiative (IBI) recommends a maximum value of 0.7 for the molar H/C ratio (Wang et al., 2009). "The alkali and alkaline earth metals present in biochar are determined by the ash elemental composition (Jeng et al., 2019). Alkali and alkaline earth metals are important in the second stage of the volatile cracking reaction, which increases the biochar's potential porosity (Kumar et al., 2009). In an aqueous medium, carbonates in ash foster liming effects and increase the alkalinity contribution of biochar.

2.15.6. Adsorbent Dosage and Contact Time

The adsorbent dose determines the sorbent-sorbate equilibrium of an adsorption system. The concentration of monovalent and divalent cations increases as the dose is increased. Increased adsorption efficiency of biochar with different dosages has been attributed to an increase in the number of sorption sites, while a decrease when the dosage rate is too high is partly due to overlapping layers of adsorption sites that shield the pores. The efficiency of adsorption has also been stated to increase with the contact time until saturation is reached (Setshedi et al., 2013).

2.15.7. Surface Charge

The magnitude of the electrical potential difference between the inner and outer surfaces of the various aggregates states of a material is measured by surface charge. It can be used to investigate phenomena like particle repulsion and attraction. The conversion of organic waste to CH_4 has been accelerated and stabilized using conductive carbon-based materials. This property has also been mentioned in relation to biochar and its function in increasing its adsorption efficiency.

2.16. Modified Biochar for Wastewater Remediation

2.16.1. The Modification of Biochar

While a wide BET surface area is a significant factor for activated carbon with a high pollutant uptake potential, the pollutants will not be eliminated if the activated carbon's internal and external surfaces do not have tolerance for the targeted contaminants (Smith et al., 2009). As a result, the activated carbons' surface chemistry may be more important than their porosity (specific surface area). Activated carbons are non-polar

adsorbents in general. They prefer to adsorb organic chemicals over polar inorganic organisms. Organic compound sorption mechanisms are typically a balance of hydrogen-bonding forces in solution and Van der Waals forces between activated carbon and organic compounds. Surface modification of activated carbon is needed to improve the polarity of the activated carbon in order to adsorb inorganic compounds, which in this study are primarily heavy metals.

Carbon-oxygen, carbon-hydrogen, carbon-nitrogen, carbon-sulphur, and carbon-halogen surface groups are integrated into the primary adsorbing surface or the edges of activated carbon (Bansal and Goyal, 2005). Carbon-oxygen surface groups are the most important compounds that influence the wettability, polarity, and acidity of activated carbon. There are three kinds of surface areas of carbon-oxygen, acids, bases, and neutrals, and different post activation treatments such as oxidation or ammonization will increase or decrease the concentration of each group (Shen et al., 2008).

At temperatures of up to 400°C, carbons react with oxygen, air, carbon dioxide, or steam, or with aqueous oxidants such as nitric acid, sulfuric acid, or phosphoric acid at room temperature to form acidic surface classes. Low-temperature oxidations tend to produce strong acidic groups like carboxylic, while high-temperature oxidations may produce weak acid groups like phenol (Shafeeyan et al., 2010). Acidic surface groups boost the carbon surface's hydrophilic properties and polarity; some typical acidic groups are shown in Figure 2.14 Chen et al. (2003) reacted activated carbon with 1 M citric acid to modify it.

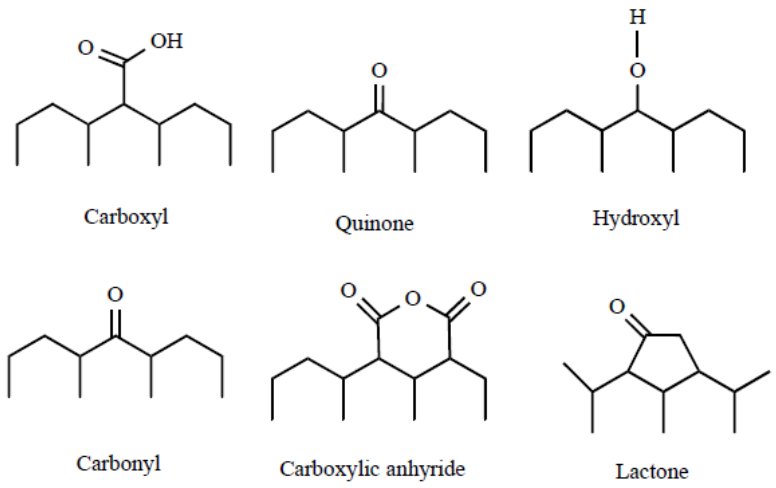
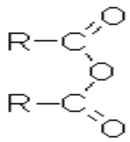
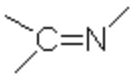
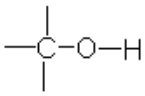
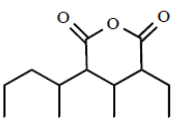
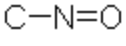
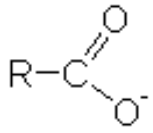


Figure 2.14: A Simplified Schematic of Some Acidic Surface Groups on Activated Carbon (Chen et al., 2008).

The neutral surface groups are primarily oxygen groups produced by oxygen chemisorption at ethylene type unsaturated sites on the carbon surface (Bansal and Goyal, 2005). Based on the allocated wavenumbers from the Fourier transform infrared spectroscopy (FTIR) study, Table 2.8 summarizes the major functional groups of activated carbon.

Table 2.8: Functional Groups on Activated Carbon Surfaces & the corresponding Assignments (Shen et al., 2008)

Functional Groups	**Assignment Regions (cm^{-1})**	**Functional Groups**	**Assignment Regions (cm^{-1})**
C-O in ethers	1000 - 1300	C=N	1480-1660
			
Alcohols	1049-1276, 3200-3640	Cyclic amides	646,1461-1546, 1685
-C-OH (stretching)	1000-1220	C-N	1190
			
O-H	1160-1200, 2500-3620	C=C=N	2070-2040
Carboxylic acid	1120-1200, 1665-1760, 2500-3300	N-O-	1300-1000
Carboxylic anhydride	980-1300, 1740-1880		1500-1600
			
Lactones			1160-1370, 675-1790

Carboxyl (R-COO-)		1560 - 1650
C-H (stretching)		2600-3000

2.16.2. Adsorbate Interactions with the modified biochar

Since the primary goal of this research is to look at aqueous inorganic contaminants, especially heavy metals, it's important to understand how heavy metals interact with SBACs. To extract heavy metals from aqueous solutions, three main mechanisms are used: sorption, ion exchange, and precipitation. The pH of the solution has a significant impact on the efficacy of these mechanisms.

2.16.2.1. Sorption

Sorption is the process by which a foreign species adheres to a solid's surface as shown in Figure 2.16. Physical and chemical sorption are the two forms of sorption based on the various forces involved in the sorption method. Van der Waals, ion-dipole, and hydrogen bonding are the forces involved in physical sorption; these processes are normally reversible. Chemical sorption uses stronger forces in ionic or covalent bonds, making it an irreversible operation (Gong, 2013). Batch adsorption methods are often used in the laboratory or to treat small volumes of polluted effluents. A universal phenomenon is the transition of substances from a mobile phase (liquid or gaseous) to a solid phase. Sorption equilibria provide basic physiochemical data for assessing the sorption process's applicability as a unit activity.

2.16.2.2. Ion Exchange

Ion exchange, which is one of the common sorption mechanisms involving physical sorption, refers to the reversible stoichiometric process of the exchange of ions between two different phases in contact; it occurs more commonly between the solid and liquid phases (see Figure 2.15). The exchange reaction between two ions can be expressed as (Gong, 2013). :

$$\text{Solid} - (M_1^{n+})m + nM_2^{m+} \Leftrightarrow \text{Solid} - (M_2^{m+})n + mM_1^{n+} \quad (2.9)$$

This expression demonstrates that the metal ions in the solution are exchanged with the ions in the solids (or activated carbons) for an equivalent quantity of cations.

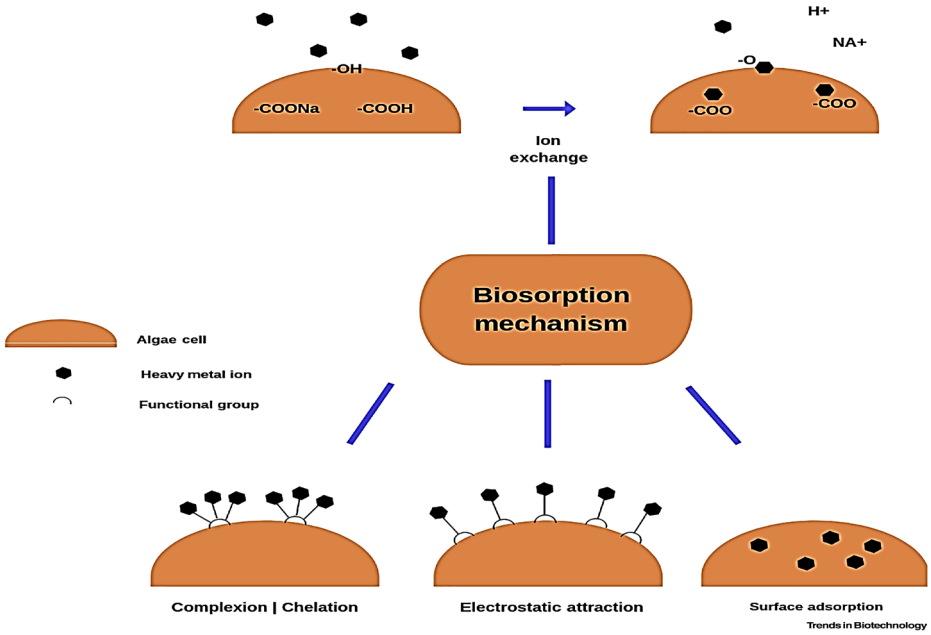


Figure 2.15: Pictorial definition of adsorption & Ion Exchange Process, (Gong, 2013).

2.16.2.3. Precipitation

Precipitation is controlled by the solubility of the elements in a solution. Most heavy metals such as Cr(VI), Al(III), Cu(II), Zn(II), Cd(II), Pb(II), and Fe(II), are expected to precipitate as hydroxides due to the hydrolysis reaction in the solution which is expressed as:

$$H - OH + M^{n+} \leftrightarrow H - O - M^{(n-1)+} + H^{+} \qquad (2.10)$$

According to this reaction, the pH (concentration of H+) dominates the direction of the reaction, which indicates that metal precipitation is sensitive to the pH of the solution.

2.17. Chapter Summary

From the literature, it can be understood that anaerobic digestion is a technology used to treat organic waste products under oxygen-free conditions to generate biogas, in which the digested material can be used for fertilization. Biogas that is produced from anaerobic digestion is mainly composed of CH_4, CO_2, H_2, and a trace of H_2S. The production rate of biogas depends upon the type of sludge and also the operating conditions of the digester. This includes temperature, pH, mixing, retention time, and the

composition of the feedstock. As such these parameters require monitoring and control to ensure improvement in the gas yield & quality.

The complexities of the AD method were illustrated in the literature review, and traditional approaches for dealing with some of these challenges were addressed. Several studies in recent years have shown a decline in the use of a single substrate (or mono-digestion) for AD since it is associated with low methane yield due to operational issues and process instability. As a result, critical reviews thoroughly examined the application of several useful technologies to improve AD and energy recovery. Furthermore, in recent years, this technology has evolved to simultaneous digestion of two or more substrates as organic wastes with other industrial biowastes, in anaerobic co-digestion (Al bkoor Alrawashdeh et al., 2017). This is a feasible option to overcome the drawbacks of mono-digestion and to improve plant's economic feasibility.

The key challenges with anaerobic co-digestion are; the pretreatment requirements, understanding of the physicochemical composition of the feed, the complexity of the microbial dynamics, and the modeling data being unavailable (Regueiro et al., 2014; Sanz & Köchling, 2007). Indeed, more research is required to address some of the drawbacks associated with the enhancement of biomethane via anaerobic co-digestion.

Biochar's potential role in mitigating these problems was also addressed. Many synthesis variables influence biochar adsorption performance. The biochar processing conditions, the ionic strength of the interacting contaminants, and the concentration of the target contaminants are among the synthesis variables.

The interaction of these variables on biochar sorption efficiency in an AD operation, as well as the best combination of them, is unknown. It is critical to gain a better understanding of the impact of these synthesis variables on achieving simultaneous process performance, stability, and AD product quality assurance. The essential properties and mechanisms of biochar that have been established to promote its application to AD were discussed in this section. The reason why the AD had no impact or was counter-productive was addressed. The negative effect of biochar on AD can be due to a lack of understanding of the appropriate range of desired biochar properties when all synthesis variables are taken into account. Awareness of the appropriate range of properties and synthesis variables will help enhance pyrolytic conditions for controlling and reproducing selectively engineered biochar properties for in-situ AD applications.

Typically, commercial-grade granular activated carbon has been applied to AD without regard for the effect on digestate content for agronomic applications or the financial consequences. Biochar's application in AD has largely been based on batch thermophilic operating conditions in the literature, with only a few researches published for mesophilic operating conditions. AD promotes the quick leaching of biochar alkali metals at higher temperatures, as well as rapid digestion.

Given the popularity of the mesophilic AD method, which accounts for 57% of all installed AD, biochar application in mesophilic conditions should have been thoroughly investigated. When studies of mesophilic biochar-added digestion have been attempted, they have only been done at the batch stage. Batch BMP studies of biochar-amended substrates performed under laboratory optimal conditions are insufficient to generalize biochar use in mesophilic semi-continuous AD processes. Furthermore, since the batch process is difficult to scale up to a full-scale plant continuously, the high output of biochar recorded in the literature may be affected.

As a result, the literature lacks a long-term study of biochar application to AD under conditions close to those found in a full-scale plant, and the true efficiency of biochar for a full-scale plant is unknown. This claim was backed up by the literature, which proposed a long-term experiment to determine the effect of biochar on semi-continuous AD. This is yet another known void in the literature that this thesis study is attempting to fill.

Adsorption has several disadvantages, including the high cost of the adsorbent, hard separation of the adsorbent from dye, disposal issues, and low surface area. This study introduces the use of low-cost adsorbent SAC which is derived from the waste and synthesized in an environmentally friendly manner. Based on the activation process and the modification the study will analyze its physical and chemical stability, properties, and performance in the removal of heavy metals. This study aims to focus on the removal of heavy metals by adsorption, specifically chromium (Cr) and cadmium (Cd) because the in-house analyst identified them as the most difficult heavy metals to remove in the JW municipal wastewater which is the research study's focus area. In general, humans are more likely to be exposed to heavy metals through water consumption, and thus toxic metal bioaccumulation occurs in the human body.

Since the primary goal of this research is to look at aqueous inorganic contaminants, especially heavy metals, it's important to understand how heavy metals interact with

SBACs. To extract heavy metals from aqueous solutions, three main mechanisms are used: sorption, ion exchange, and precipitation. The pH of the solution has a significant impact on the efficacy of these mechanisms.

References

Agrafioti, E., Bouras, G., Dimitrios, K., & Diamadopoulos, E. (2013). Biochar production by sewage sludge pyrolysis. Journal of Analytical and Applied Pyrolysis, 101(0165–2370), 72–78.

Ahmad, M., Rajapaksha, A. U., Lim, J. E., Zhang, M., Bolan, N., Mohan, D., Vithanage, M., Lee, S. S., & Ok, Y. S. (2014). Biochar as a sorbent for contaminant management in soil and water: A review. In Chemosphere (Vol. 99, pp. 19–33). Elsevier Ltd. https://doi.org/10.1016/j.chemosphere.2013.10.071

Ahmadi, M., Bayati, N., Babaei, A. A., & Teymouri, P. (2013). Sludge Characterization of an Industrial Wastewater Treatment Plant, Iran. Iranian Journal Of Health Sciences, 1(2), 10–18. https://doi.org/10.18869/acadpub.jhs.1.2.10

Ahn, J. H., Do, T. H., Kim, S. D., & Hwang, S. (2006a). The effect of calcium on the anaerobic digestion treating swine wastewater. Biochemical Engineering Journal, 30(1), 33–38. https://doi.org/10.1016/j.bej.2006.01.014

Ahn, J. H., Do, T. H., Kim, S. D., & Hwang, S. (2006b). The effect of calcium on the anaerobic digestion treating swine wastewater. Biochemical Engineering Journal. https://doi.org/10.1016/j.bej.2006.01.014

Ahring, B. K., Sandberg, M., & Angelidaki, I. (1995). Volatile fatty acids as indicators of process imbalance in anaerobic digestors. Applied Microbiology and Biotechnology, 43(3), 559–565. https://doi.org/10.1007/BF00218466

Ait Ahsaine, H., Zbair, M., & El Haouti, R. (2017). Mesoporous treated sewage sludge as outstanding low-cost adsorbent for cadmium removal. Desalination and Water Treatment, 85, 330–338. https://doi.org/10.5004/dwt.2017.21310

Al bkoor Alrawashdeh, K., Pugliese, A., Slopiecka, K., Pistolesi, V., Massoli, S., Bartocci, P., Bidini, G., & Fantozzi, F. (2017). Codigestion of Untreated and Treated Sewage Sludge with the Organic Fraction of Municipal Solid Wastes. Fermentation, 3(3), 35. https://doi.org/10.3390/fermentation3030035

Al Mamun, M. R., & Torii, S. (2015). Enhancement of production and upgradation of biogas using different techniques- a review. International Journal of Earth Sciences and Engineering, 8(2), 877–892.

Álvarez, J. A., Otero, L., & Lema, J. . (2010). A methodology for optimising feed composition for anaerobic co-digestion of agro-industrial wastes. Bioresource Technology, 101(4), 1154–1158.

Ambaye, T. G., Vaccari, M., van Hullebusch, E. D., Amrane, A., & Rtimi, S. (2020). Mechanisms and adsorption capacities of biochar for the removal of organic and inorganic pollutants from industrial wastewater. International Journal of Environmental Science and Technology.

https://doi.org/10.1007/s13762-020-03060-w

Amha, Y. M., Anwar, M. Z., Brower, A., Jacobsen, C. S., Stadler, L. B., Webster, T. M., & Smith, A. L. (2018). Inhibition of anaerobic digestion processes: Applications of molecular tools. Bioresource Technology, 247(September 2017), 999–1014. https://doi.org/10.1016/j.biortech.2017.08.210

Angelidaki, I., Treu, L., Tsapekos, P., Luo, G., Campanaro, S., Wenzel, H., & Kougias, P. G. (2018). Biogas upgrading and utilization: Current status and perspectives. Biotechnology Advances, 36(2), 452–466. https://doi.org/10.1016/j.biotechadv.2018.01.011

APWC. (2020). Waste classification report The Commonwealth Litter Programme, South Africa (Issue March 2020).

Astals, S., Batstone, D. J., Mata-Alvarez, J., & Jensen, P. D. (2014). Identification of synergistic impacts during anaerobic co-digestion of organic wastes. Bioresource Technology, 169, 421–427. https://doi.org/10.1016/j.biortech.2014.07.024

Awe, O., Lu, J., Wu, S., Zhao, Y., Nzihou, A., Lyczko, N., & Doan, P. (2017). Effect of oil content on biogas production and performance stability of anaerobic digestion of food waste (pp. 1–11).

Ayeni, A. O., Hymore, F. K., Mudliar, S. N., Deshmukh, S. C., Satpute, D. B., Omoleye, J. A., & Pandey, R. A. (2013). Hydrogen peroxide and lime based oxidative pretreatment of wood waste to enhance enzymatic hydrolysis for a biorefinery: Process parameters optimization using response surface methodology. Fuel, 106, 187–194. https://doi.org/10.1016/j.fuel.2012.12.078

Babaee, A., Shayegan, J., & Roshani, A. (2013). Anaerobic slurry co-digestion of poultry manure and straw: effect of organic loading and temperature. Journal of Environmental Health Science and Engineering. https://doi.org/10.1186/2052-336X-11-15

Babel, S. (2014). Anaerobic co-digestion of sewage and brewery sludge for biogas production and land application Archive of SID Anaerobic co-digestion of sewage and brewery sludge for biogas production and land application. 1. https://doi.org/10.1007/BF03326067

Bachmann, N. (2015). Sustainable biogas production in municipal wastewater treatment plants. In IEA Bioenergy.

Bahram, M., Anslan, S., Hildebrand, F., Bork, P., & Tedersoo, L. (2019). Newly designed 16S rRNA metabarcoding primers amplify diverse and novel archaeal taxa from the environment. Environmental Microbiology Reports, 11(4), 487–494. https://doi.org/10.1111/1758-2229.12684

Bajpai, P. (2017). Anaerobic Technology in Pulp and Paper Industry. 7–13. https://doi.org/10.1007/978-981-10-4130-3

Bergland, W. H., Dinamarca, C., & Bakke, R. (2015). Temperature Effects in Anaerobic Digestion Modeling. August 2016, 261–269. https://doi.org/10.3384/ecp15119261

Binder, J. B., & Raines, R. T. (2010). Fermentable sugars by chemical hydrolysis of biomass. Proceedings of the National Academy of Sciences of the United States of America, 107(10), 4516–4521.

https://doi.org/10.1073/pnas.0912073107

Bong, C. P. C., Lim, L. Y., Lee, C. T., Klemeš, J. J., Ho, C. S., & Ho, W. S. (2018). The characterisation and treatment of food waste for improvement of biogas production during anaerobic digestion – A review. Journal of Cleaner Production, 172. https://doi.org/10.1016/j.jclepro.2017.10.199

Boumediene, M., Benaïssa, H., George, B., Molina, S., & Merlin, A. (2018). Effects of pH and ionic strength on methylene blue removal from synthetic aqueous solutions by sorption onto orange peel and desorption study. J. Mater. Environ. Sci, 9(6), 1700–1711. https://doi.org/10.26872/jmes.2018.9.6.190

Bousba, S., & Meniai, A. H. (2013). Adsorption of 2-chlorophenol onto sewage sludge based adsorbent: Equilibrium and kinetic study. Chemical Engineering Transactions, 35(January), 859–864. https://doi.org/10.3303/CET1335143

Brahim, A., Villen-Guzman, M., Gomez-Lahoz, C., & Rodriguez-Maroto, Jose M Garcia-Herruzo, Francisco Vereda-Alonso, C. (2019). Anaerobic co-digestion of mixed sewage sludge and fruits and vegetable wholesale market waste: Composition and seasonality effect. Journal of Water Process Engineering, 31(100848).

Campanaro, S., Treu, L., Kougias, P. G., De Francisci, D., Valle, G., & Angelidaki, I. (2016). Metagenomic analysis and functional characterization of the biogas microbiome using high throughput shotgun sequencing and a novel binning strategy. Biotechnology for Biofuels, 9(1), 1–17. https://doi.org/10.1186/s13068-016-0441-1

Cavinato, C. (2011). Anaerobic Digestion Fundamentals I (Issue August, pp. 1–47). University of Jyvaskyla. http://www.biogas-info.co.uk/

Charalambous, P. (2015). Anaerobic digestion of Dairy Wastewater. 455, 15.

Chen, S., Gao, J., & Dong, B. (2021). Bottlenecks of anaerobic degradation of proteins in sewage sludge and the potential targeted enhancing strategies. Science of the Total Environment, 759. https://doi.org/10.1016/j.scitotenv.2020.143573

Chen, Y., Cheng, J. J., & Creamer, K. S. (2008). Inhibition of anaerobic digestion process: A review. Bioresource Technology, 99(10), 4044–4064. https://doi.org/10.1016/j.biortech.2007.01.057

Cornet, C. (2017). Inhibiting factors in the anaerobic digestion process for biogas production.

Cossu, R., Morello, L., Raga, R., & Cerminara, G. (2016). Biogas production enhancement using semi-aerobic pre-aeration in a hybrid bioreactor landfill. Waste Management, 55, 83–92. https://doi.org/10.1016/j.wasman.2015.10.025

Cuetos, M. J., Martinez, E. J., Moreno, R., Gonzalez, R., Otero, M., & Gomez, X. (2017). Enhancing anaerobic digestion of poultry blood using activated carbon Enhancing anaerobic digestion of poultry blood. Journal of Advanced Research, 8(3), 297–307. https://doi.org/10.1016/j.jare.2016.12.004

Dareioti, M. A., & Kornaros, M. (2014). Effect of hydraulic retention time (HRT) on the anaerobic co-

digestion of agro-industrial wastes in a two-stage CSTR system. Bioresource Technology, 167, 407–415. https://doi.org/10.1016/j.biortech.2014.06.045

De Filippis, P., Di Palma, L., Petrucci, E., Scarsella, M., & Verdone, N. (2013). Production and characterization of adsorbent materials from sewage sludge by pyrolysis. Chemical Engineering Transactions, 32, 205–210. https://doi.org/10.3303/CET1332035

De Mes, T. Z. D., Stams, A. J. M., Reith, J. H., & Zeeman, G. (2003). Methane Production by Anaerobic Digestion of Wastewater and Solid Waste. In Bio-methane & Bio-hydrogen: status and perspectives of biological methane and hydrogen production (Vol. 286, pp. 58–102). Dutch Biological Hydrogen Foundation. https://doi.org/10.1016/j.biortech.2010.08.032

De Vrieze, J., Hennebel, T., Boon, N., & Verstraete, W. (2012). Methanosarcina: The rediscovered methanogen for heavy duty biomethanation. In Bioresource Technology (Vol. 112, pp. 1–9). Elsevier. https://doi.org/10.1016/j.biortech.2012.02.079

Deacon, S., & Louw, P. (2013). The installation of CHP at Johannesburg Northern waste treatment works. 11. http://carbonn.org/uploads/tx_carbonndata/BIOGAS PAPER REV4.pdf

Dioha, I. J., Ikeme, C., Nafi, T., Soba, N. I., & Mbs, Y. (2013). Effect of Carbon To Nitrogen Ratio on Biogas Production. International Research Journal of Natural Sciences, 1(3), 1–10.

Doloman, A., Soboh, Y., Walters, A. J., Sims, R. C., & Miller, C. D. (2017). Qualitative Analysis of Microbial Dynamics during Anaerobic Digestion of Microalgal Biomass in a UASB Reactor. International Journal of Microbiology, 2017. https://doi.org/10.1155/2017/5291283

Elbeshbishy, E., & Nakhla, G. (2012). Bioresource Technology Batch anaerobic co-digestion of proteins and carbohydrates. Bioresource Technology, 116, 170–178. https://doi.org/10.1016/j.biortech.2012.04.052

Faisal, S., Hafeez, F. Y., Zafar, Y., Majeed, S., & Leng, X. (2018). A Review on Nanoparticles as Boon for Biogas Producers — Nano Fuels and Biosensing Monitoring. Applied Sciences, 9(59), 1–19. https://doi.org/10.3390/app9010059

Ferdeș, M., Dincă, M. N., Moiceanu, G., Zabava, B. S., & Paraschiv, G. (2020). Microorganisms and enzymes used in the biological pretreatment of the substrate to enhance biogas production: A review. Sustainability (Switzerland), 12(17). https://doi.org/10.3390/su12177205

Ferrasse, J., Akkache, S., & Roche, N. (2015). Thermochemical Conversion of Sewage Sludge by TGA-FTIR Analysis : Influence of Mineral Matter Added. Drying Technology: An International Journal, 1–9(July), 1–11. https://doi.org/10.1080/07373937.2015.1036283

Frąc, M., Jezierska-Tys, S., Oszust, K., Gryta, A., & Pastor, M. (2017). Assessment of microbiological and biochemical properties of dairy sewage sludge. International Journal of Environmental Science and Technology, 14(4), 679–688. https://doi.org/10.1007/s13762-016-1179-9

Francioso, O., Rodriguez-Estrada, M. T., Montecchio, D., Salomoni, C., Caputo, A., & Palenzona, D. (2010). Chemical characterization of municipal wastewater sludges produced by two-phase anaerobic

digestion for biogas production. Journal of Hazardous Materials, 175(1–3), 740–746. https://doi.org/10.1016/j.jhazmat.2009.10.071

Franks, L., Euston-Brown, M., Ferry, A., & Giljova, S. (2013). Municipal wastewater treatment works - biogas to energy. http://www.cityenergy.org.za/uploads/resource_336.pdf

Gaballah, E. S., Abomohra, A. E.-F., Xu, C., Elsayed, M., Abdelkader, T. K., Lin, J., & Yuan, Q. (2020). Enhancement of biogas production from rape straw using different co-pretreatment techniques and anaerobic co-digestion with cattle manure. Bioresource Technology, 309. https://doi.org/10.1016/j.biortech.2020.123311

Gerardi, M. H. (2003). The Microbiology of Anaerobic Digesters. https://doi.org/10.1002/0471468967

Gong, X. (2013). Modification and utilization of sewage sludge-based activated carbon as metal adsorbents [The University of British Columbia]. http://hdl.handle.net/2429/44964

Gonzalez-Fernandez, C., Barreiro-Vescovo, S., De Godos, I., Fernandez, M., Zouhayr, A., & Ballesteros, M. (2018). Biochemical methane potential of microalgae biomass using different microbial inocula. Biotechnology for Biofuels, 11(1), 1–11. https://doi.org/10.1186/s13068-018-1188-7

Gonzalez-Fernandez, C., Sialve, B., & Molinuevo-Salces, B. (2015). Anaerobic digestion of microalgal biomass: Challenges, opportunities and research needs. In Bioresource Technology (Vol. 198). https://doi.org/10.1016/j.biortech.2015.09.095

González, J., Sánchez, M., & Gómez, X. (2018). Enhancing Anaerobic Digestion: The Effect of Carbon Conductive Materials. C, 4(4), 59. https://doi.org/10.3390/c4040059

GreenCape. (2020). Waste: 2020 Market Intelligence Report.

Guo, J., Peng, Y., Ni, B. J., Han, X., Fan, L., & Yuan, Z. (2015). Dissecting microbial community structure and methane-producing pathways of a full-scale anaerobic reactor digesting activated sludge from wastewater treatment by metagenomic sequencing. Microbial Cell Factories. https://doi.org/10.1186/s12934-015-0218-4

Hamawand, I., & Baillie, C. (2015). Anaerobic digestion and biogas potential: Simulation of lab and industrial-scale processes. Energies, 8(1), 454–474. https://doi.org/10.3390/en8010454

Herselman, J. (Golder A. A., & Moodley, P. (Zitholele C. (2009). Guidelines for the Utilisation and Disposal of Wastewater Sludge: Volume 4 Requirements for the beneficial use of sludge at high loading rates (Vol. 4, Issue June).

Hilkiah Igoni, A., Abowei, M. F. N., Ayotamuno, M. J., & Eze, C. L. (2008). Effect of Total Solids Concentration of Municipal Solid Waste on the Biogas Produced in an Anaerobic Continuous Digester. Agricultural Engineering International, X, 1–11.

Hu, S. H., & Hu, S. C. (2014). Application of magnetically modified sewage sludge ash (SSA) in ionic dye adsorption. Journal of the Air and Waste Management Association, 64(2), 141–149. https://doi.org/10.1080/10962247.2013.842947

Hu, Y., Kobayashi, T., Zhen, G., Shi, C., & Xu, K. (2018a). Effects of lipid concentration on thermophilic anaerobic co-digestion of food waste and grease waste in a siphon-driven self-agitated anaerobic reactor. Biotechnology Reports, 19, e00269. https://doi.org/10.1016/j.btre.2018.e00269

Hu, Y., Kobayashi, T., Zhen, G., Shi, C., & Xu, K. (2018b). Effects of lipid concentration on thermophilic anaerobic co-digestion of food waste and grease waste in a siphon-driven self-agitated anaerobic reactor. Biotechnology Reports, 19, e00269. https://doi.org/10.1016/j.btre.2018.e00269

Jackowski, M., Semba, D., Trusek, A., Wnukowski, M., Niedzwiecki, L., Baranowski, M., & Krochmalny, K. (2019). Hydrothermal Carbonization of Brewery ' s Spent Grains for the Production of Solid Biofuels. 1–11. https://doi.org/10.3390/beverages5010012

Jeihanipour, A., Niklasson, C., & Taherzadeh, M. J. (2011). Enhancement of solubilization rate of cellulose in anaerobic digestion and its drawbacks. Process Biochemistry, 46(7), 1509–1514. https://doi.org/10.1016/j.procbio.2011.04.003

Joyce, A., Ijaz, U. Z., Nzeteu, C., Vaughan, A., Shirran, S. L., Botting, C. H., Quince, C., O'Flaherty, V., & Abram, F. (2018). Linking microbial community structure and function during the acidified anaerobic digestion of grass. Frontiers in Microbiology, 9(MAR), 1–13. https://doi.org/10.3389/fmicb.2018.00540

Jung, K. W., Lee, S. Y., & Lee, Y. J. (2019). Optimized preparation of activated carbon from municipal sewage sludge and application to the adsorption of azo dye from aqueous solutions. Environmental Progress and Sustainable Energy, 38(s1), S267–S276. https://doi.org/10.1002/ep.13008

Kalemba, K., & Barbusiński, K. (2017). Anaerobic co-digestion of sewage sludge and molasses. E3S Web of Conferences, 22, 00075. https://doi.org/10.1051/e3sconf/20172200075

Katahira, R., Sluiter, J. B., Schell, D. J., & Davis, M. F. (2013). Degradation of Carbohydrates during Dilute Sulfuric Acid Pretreatment Can Interfere with Lignin Measurements in Solid Residues. Journal of Agricultural and Food Chemistry, 61(13), 3286–3292. https://doi.org/10.1021/jf303727t

Kim, M.-J., & Kim, S.-H. (2018). Evaluation of the Degradation of Carbohydrate-based Material During Anaerobic Digestion for High-efficiency Biogas Production. Journal of Biosystems Engineering, 43(2), 110–118. https://doi.org/10.5307/JBE.2018.43.2.110

Koch, K., Hafner, S. D., Weinrich, S., & Astals, S. (2019). Identification of Critical Problems in Biochemical Methane Potential (BMP) Tests From Methane Production Curves. Frontiers in Environmental Science, 7(November), 1–8. https://doi.org/10.3389/fenvs.2019.00178

Krzysztof Ziemiński. (2012). Methane fermentation process as anaerobic digestion of biomass: Transformations, stages and microorganisms. African Journal of Biotechnology, 11(18), 4127–4139. https://doi.org/10.5897/ajbx11.054

Kuang, Y. (2003). Enhancing anaerobic digestion of lipids in wastewater by addition of co-substrates. Murdoch University.

Kumar, R., Mago, G., Balan, V., & Wyman, C. E. (2009). Physical and chemical characterizations of corn stover and poplar solids resulting from leading pretreatment technologies. Bioresource Technology, 100(17), 3948–3962. https://doi.org/10.1016/j.biortech.2009.01.075

Kuscu, O. S., & Sponza, D. T. (2007). Effects of hydraulic retention time (HRT) and sludge retention time (SRT) on the treatment of nitrobenzene in AMBR/CSTR reactor systems. Environmental Technology, 28(September), 285–296. https://doi.org/10.1080/09593332808618792

Kutty, S. R. M., Almahbashi, N. M. Y., Nazrin, A. A. M., Malek, M. A., Noor, A., Baloo, L., & Ghaleb, A. A. S. (2019). Adsorption kinetics of colour removal from palm oil mill effluent using wastewater sludge carbon in column studies. Heliyon, 5(10), e02439. https://doi.org/10.1016/j.heliyon.2019.e02439

L??tzh??ft, H. C. H., Boe, K., Fang, C., & Angelidaki, I. (2014). Comparison of VFA titration procedures used for monitoring the biogas process. Water Research, 54(February), 262–272. https://doi.org/10.1016/j.watres.2014.02.001

Lebiocka, M., Montusiewicz, A., & Cydzik-Kwiatkowska, A. (2018). Effect of bioaugmentation on biogas yields and kinetics in anaerobic digestion of sewage sludge. International Journal of Environmental Research and Public Health, 15(8). https://doi.org/10.3390/ijerph15081717

Lindmark, J. (n.d.). The Biogas Optimization Project The BioGasOpt-project. 1–15.

Lindmark, J., Thorin, E., Bel Fdhila, R., & Dahlquist, E. (2014). Effects of mixing on the result of anaerobic digestion: Review. Renewable and Sustainable Energy Reviews, 40, 1030–1047. https://doi.org/10.1016/j.rser.2014.07.182

Liu, C., Li, H., Zhang, Y., Si, D., & Chen, Q. (2016a). Evolution of microbial community along with increasing solid concentration during high-solids anaerobic digestion of sewage sludge. Bioresource Technology, 216, 87–94. https://doi.org/10.1016/j.biortech.2016.05.048

Liu, C., Li, H., Zhang, Y., Si, D., & Chen, Q. (2016b). Evolution of microbial community along with increasing solid concentration during high-solids anaerobic digestion of sewage sludge. Bioresource Technology. https://doi.org/10.1016/j.biortech.2016.05.048

Liu, X., Wang, M., Hu, X., & Song, Y. (2014). Effect of Total Solids Content on the Biogas Production and Phosphorus Release from Excess Sludge. Advanced Materials Research, 1010–1012(August 2014), 1006–1009. https://doi.org/10.4028/www.scientific.net/AMR.1010-1012.1006

Liu, Y., Cheng, H., & He, Y. (2020). Application and mechanism of sludge-based activated carbon for phenol and cyanide removal from bio-treated effluent of coking wastewater. Processes, 8(1). https://doi.org/10.3390/pr8010082

Lu, X., Jin, W., Xue, S., & Wang, X. (2017a). Effects of waste sources on performance of anaerobic co-digestion of complex organic wastes : taking food waste as an example. Scientific Reports, January, 1–9. https://doi.org/10.1038/s41598-017-16068-z

Lu, X., Jin, W., Xue, S., & Wang, X. (2017b). Effects of waste sources on performance of anaerobic co-digestion of complex organic wastes: Taking food waste as an example. Scientific Reports, 7(1), 1–

9. https://doi.org/10.1038/s41598-017-16068-z

Lucian, M., & Fiori, L. (2017). Hydrothermal carbonization of waste biomass: Process design, modeling, energy efficiency and cost analysis. Energies, 10(2). https://doi.org/10.3390/en10020211

Magdalena, J. A., Mahdy, A., Godos, I. De, Unit, B. P., & Unit, B. (2017). Protein : A Key Macromolecule For an Efficient Tested in Biochemical Methane Potential (BMP) Tests. Biotechnological Processes Unit, 84(3), 25–34.

Manyi-Loh, C. E., Mamphweli, S. N., Meyer, E. L., Okoh, A. I., Makaka, G., & Simon, M. (2013). Microbial anaerobic digestion (bio-digesters) as an approach to the decontamination of animal wastes in pollution control and the generation of renewable energy. International Journal of Environmental Research and Public Health, 10(9), 4390–4417. https://doi.org/10.3390/ijerph10094390

Martínez, E. J., Gil, M. V., Fernandez, C., Rosas, J. G., & Gómez, X. (2016a). Anaerobic codigestion of sludge: Addition of butcher's fat waste as a cosubstrate for increasing biogas production. PLoS ONE, 11(4), 1–13. https://doi.org/10.1371/journal.pone.0153139

Martínez, E. J., Gil, M. V, Fernandez, C., Rosas, J. G., & Gómez, X. (2016b). Anaerobic Codigestion of Sludge : Addition of Butcher ' s Fat Waste as a Cosubstrate for Increasing Biogas Production. PLoS ONE, 11(4), 1–13. https://doi.org/10.1371/journal.pone.0153139

Masebinu, S. O. (2018). Anaerobic Digestion Process Stabilisation and in-situ Upgrading of a Biogas System [University of Johanneburg]. www.uj.ac.za

Matheri, A. N., Belaid, M., & Seodigeng, T. (2016). Mathematical Modelling for Biogas Production. University of Johannesburg.

Maunonen-eskelinen, I., Leppänen, T., Pascalev, A., Ambagtsheer, F., Lundin, S., Carroll, J. J., Carroll, J. J., Carroll, J. J., Harfield, S. G., Davy, C., Mcarthur, A., Munn, Z., Brown, A., Brown, N., Guglielmino, L. M., Toffler, A., Botha, J., Coetzee, M. M., Coetzee, M. M., … Thomson, D. (2013). Mosby's Medical Dictionary - E-Book. Indian Journal of Urology : IJU : Journal of the Urological Society of India, 25(2), 1802. https://doi.org/10.4103/0970-1591.56203

Meegoda, J. N., Hsieh, H. N., Rodriguez, P., & Jawidzik, J. (2012). Sustainable community sanitation for a rural hospital in Haiti. Sustainability, 4(12), 3362–3376. https://doi.org/10.3390/su4123362

Meyer-Kohlstock, D., Haupt, T., Heldt, E., Heldt, N., & Kraft, E. (2016). Biochar as additive in biogas-production from bio-waste. Energies, 9(4). https://doi.org/10.3390/en9040247

Milledge, J. J., Nielsen, B. V., & Harvey, P. J. (2019). The inhibition of anaerobic digestion by model phenolic compounds representative of those from Sargassum muticum. Journal of Applied Phycology, 31(1), 779–786. https://doi.org/10.1007/s10811-018-1512-4

Møller, H. B., Moset, V., Brask, M., Weisbjerg, M. R., & Lund, P. (2014). Feces composition and manure derived methane yield from dairy cows: Influence of diet with focus on fat supplement and roughage type. Atmospheric Environment, 94, 36–43.

Morales-Polo, C., Cledera-Castro, M. del M., & Soria, B. Y. M. (2019). Biogas production from vegetable and fruit markets waste-compositional and batch characterizations. Sustainability (Switzerland), 11(23). https://doi.org/10.3390/su11236790

Morales-Polo, C., del Mar Cledera-Castro, M., & Moratilla Soria, B. Y. (2018). Reviewing the Anaerobic Digestion of Food Waste: From Waste Generation and Anaerobic Process to Its Perspectives. Applied Sciences, 8(10), 1804. https://doi.org/10.3390/app8101804

Mu'azu, N. D., Jarrah, N., Zubair, M., & Alagha, O. (2017). Removal of phenolic compounds from water using sewage sludge-based activated carbon adsorption: A review. International Journal of Environmental Research and Public Health, 14(10), 1–34. https://doi.org/10.3390/ijerph14101094

Mu, B., & Wang, A. (2016). Adsorption of dyes onto palygorskite and its composites: A review. Journal of Environmental Chemical Engineering, 4(1), 1274–1294. https://doi.org/10.1016/j.jece.2016.01.036

Mudzanani, K., Ejekwu, O., Ayeni, A. O., & Daramola, M. O. (2019a). Dissolution kinetics of corncob in lithium perchlorate solvent system. European Biomass Conference and Exhibition Proceedings.

Mudzanani, K., Ejekwu, O., Ayeni, A. O., & Daramola, M. O. (2019b). Dissolution kinetics of corncob in lithium perchlorate solvent system. European Biomass Conference and Exhibition Proceedings, 307–311.

Negreanu-Pirjol, B., Negreanu-Pirjol, T., Badea, N., Parachiv, G. M., Gorun, E., Sirbu, R., & Meghea, A. (2012). Physicochemical and microbiological characterisation of municipal sludge from romanian black sea coast wastewater treatment plants. Journal of Environmental Protection and Ecology, 13(4), 2232–2239.

Neves, L., Oliveira, R., & Alves, M. (2006). Anaerobic co-digestion of coffee waste and sewage sludge. In Waste management (New York, N.Y.) (Vol. 26). https://doi.org/10.1016/j.wasman.2004.12.022

Nghiem, L. D., Koch, K., Bolzonella, D., & Drewes, J. E. (2017a). Full scale co-digestion of wastewater sludge and food waste : Bottlenecks and possibilities. Renewable and Sustainable Energy Reviews, 72(November 2016), 354–362. https://doi.org/10.1016/j.rser.2017.01.062

Nghiem, L. D., Koch, K., Bolzonella, D., & Drewes, J. E. (2017b). Full scale co-digestion of wastewater sludge and food waste : Bottlenecks and possibilities. Renewable and Sustainable Energy Reviews, 72(November 2016), 354–362. https://doi.org/10.1016/j.rser.2017.01.062

Nielfa, A., Cano, R., & Fdz-Polanco, M. (2015). Theoretical methane production generated by the co-digestion of organic fraction municipal solid waste and biological sludge. Biotechnology Reports, 5(1), 14–21. https://doi.org/10.1016/j.btre.2014.10.005

Nielfa, A., Cano, R., & Pérez, A. (2015). Co-digestion of municipal sewage sludge and solid waste : Modelling of carbohydrate , lipid and protein content influence. https://doi.org/10.1177/0734242X15572181

Nielfa, A., Cano, R., Pérez, A., & Fdez-Polanco, M. (2015). Co-digestion of municipal sewage sludge and solid waste: Modelling of carbohydrate, lipid and protein content influence. Waste Management &

Research, 33(3), 241–249. https://doi.org/10.1177/0734242X15572181

O'Connor, K. (Spectrum B. (2012). Proof-of-Concept for Co-Digestion of Food Waste , Fats , Oil and Grease , and Wastewater Sludge (Issues 12–22).

Okeola, O. F., Odebunmi, E. O., & Ameen, O. M. (2012). Comparison of sorption capacity and surface area of activated carbon prepared from jatropha curcas fruit pericarp and seed coat. Bulletin of the Chemical Society of Ethiopia, 26(2), 171–180. https://doi.org/10.4314/bcse.v26i2.2

Oladejo, J., Shi, K., Luo, X., Yang, G., & Wu, T. (2019). A review of sludge-to-energy recovery methods. Energies, 12(1), 1–38. https://doi.org/10.3390/en12010060

Oliveira, J. V, Alves, M. M., & Costa, J. C. (2018). Biochemical methane potential of brewery by-products. Clean Technologies and Environmental Policy, 20(2), 435–440. https://doi.org/10.1007/s10098-017-1482-2

Olsson, J. (2018). Co-digestion of microalgae and sewage sludge : A feasibility study for municipal wastewater treatment plants. Mälardalen University, Sweden.

Omar, R. K. (2017). Physicochemical Characterization of Sewage Sludge of Gaza Wastewater Treatment Plant for Agricultural Utilization. 25(2), 72–78.

Palacios-Ruiz, B., Méndez-Acosta, H. O., Alcaraz-González, V., González-Álvarez, V., & Pelayo-Ortiz, C. (2008). Regulation of Volatile Fatty Acids and Total Alkalinity in Anaerobic Digesters. IFAC Proceedings Volumes, 41(2), 13611–13616. https://doi.org/10.3182/20080706-5-kr-1001.02305

Pan, J., Ma, J., Zhai, L., Luo, T., Mei, Z., & Liu, H. (2019). Achievements of biochar application for enhanced anaerobic digestion: A review. Bioresource Technology, 292. https://doi.org/10.1016/j.biortech.2019.122058

Paritosh, K., Yadav, M., Mathur, S., Balan, V., Liao, W., Pareek, N., & Vivekanand, V. (2018). Organic fraction of municipal solid waste: Overview of treatment methodologies to enhance anaerobic biodegradability. Frontiers in Energy Research, 6(August), 1–17. https://doi.org/10.3389/fenrg.2018.00075

Pavlík, Z., Fořt, J., Záleská, M., Pavlíková, M., Trník, A., Medved, I., Keppert, M., Koutsoukos, P. G., & Černý, R. (2016). Energy-efficient thermal treatment of sewage sludge for its application in blended cements. Journal of Cleaner Production. https://doi.org/10.1016/j.jclepro.2015.09.072

Pecharaply, A., Parkpian, P., Annachhatre, A. P., & Jugsujinda, A. (2007). Influence of anaerobic co-digestion of sewage and brewery sludges on biogas production and sludge quality. Journal of Environmental Science and Health - Part A Toxic/Hazardous Substances and Environmental Engineering, 42(7), 911–923. https://doi.org/10.1080/10934520701369818

Peng, L., Bao, M., Wang, Q., Wang, F., & Su, H. (2014). The anaerobic digestion of biologically and physicochemically pretreated oily wastewater. Bioresource Technology, 151, 236–243. https://doi.org/10.1016/j.biortech.2013.10.056

Pfeifer, J., & Obernberger, I. (2007). Technological Evaluation of an Agricultural Biogas CHP Plant as Well as Definition of Guiding Values for the Improved Design and Operation. W15th European Biomass Conference & Exhibition, 7-11 May 2007, Berlin, Germanyater, May, 1864–1868.

Pilarska, A. A., Pilarski, K., Wolna-maruwka, A., & Boniecki, P. (2018). Use of Confectionery Waste in Biogas Production by the Anaerobic Digestion Process. 1–14. https://doi.org/10.3390/molecules24010037

Pöykiö, R., Watkins, G., & Dahl, O. (2019). Characterisation of Municipal Sewage Sludge as a Soil Improver and a Fertilizer Product. Ecological Chemistry and Engineering S, 26(3), 547–557. https://doi.org/10.1515/eces-2019-0040

Prabhudessai, V., Ganguly, A., & Mutnuri, S. (2013). Biochemical Methane Potential of Agro Wastes. Journal of Energy, 2013, 1–7. https://doi.org/10.1155/2013/350731

Rabii, A., Aldin, S., Dahman, Y., & Elbeshbishy, E. (2019). A Review on Anaerobic Co-Digestion with a Focus on the Microbial Populations and the Effect of Multi-Stage Digester Configuration. Energies, 12(1106), 1–25. https://doi.org/10.3390/en12061106

Rafiee, M., Salehi, E., Sharifi, K., Mohammadi, A. H., Rohani, A., & Sabeti, M. (2019). Enhancement of biogas production efficiency using appropriate low-temperature pretreatments of municipal treatment plants' excess sludge. Environmental Progress and Sustainable Energy, 38(3). https://doi.org/10.1002/ep.13072

Ragauskas, A. J., Beckham, G. T., Biddy, M. J., Chandra, R., Chen, F., Davis, M. F., Davison, B. H., Dixon, R. a, Gilna, P., Keller, M., Langan, P., Naskar, A. K., Saddler, J. N., Tschaplinski, T. J., Tuskan, G. a, & Wyman, C. E. (2014). Lignin valorization: improving lignin processing in the biorefinery. Science (New York, N.Y.), 344(6185). https://doi.org/10.1126/science.1246843

Rajesh Banu, J., Ushani, U., Merrylin, J., & Kaliappan, S. (2016). Evaluation of operational parameters for biodegration of bacterially disintegrated sludge. Desalination and Water Treatment, 57(52), 25018–25027. https://doi.org/10.1080/19443994.2016.1150888

Ramdani, N., Hamou, A., Lousdad, A., & Al-Douri., Y. (2015). Physicochemical characterization of sewage sludge and green waste for agricultural utilization N. Environmental Technology, 36(12), 1594–1604. https://doi.org/10.1080/09593330.2014.998716

Rea, J. (2014). Kinetic Modeling and Experimentation of Anaerobic Digestion. In Massachusetts Institute of Technology.

Regueiro, L., Carballa, M., & Lema, J. M. (2014). Outlining microbial community dynamics during temperature drop and subsequent recovery period in anaerobic co-digestion systems. Journal of Biotechnology, 192(Part A), 179–186. https://doi.org/10.1016/j.jbiotec.2014.10.007

Rio, S., Faur-Brasquet, C., Le Coq, L., & Le Cloirec, P. (2005). Structure characterization and adsorption properties of pyrolyzed sewage sludge. Environmental Science and Technology, 39(11), 4249–4257. https://doi.org/10.1021/es0497532

Rui, J., Li, J., Zhang, S., Yan, X., Wang, Y., & Li, X. (2015). The core populations and co - occurrence

patterns of prokaryotic communities in household biogas digesters. Biotechnology for Biofuels, 8(158), 1–15. https://doi.org/10.1186/s13068-015-0339-3

Rulkens, W. (2008). Sewage sludge as a biomass resource for the production of energy: Overview and assessment of the various options. Energy and Fuels. https://doi.org/10.1021/ef700267m

Saha, B. C. (2003). Hemicellulose bioconversion. Journal of Industrial Microbiology and Biotechnology, 30(5), 279–291. https://doi.org/10.1007/s10295-003-0049-x

Said, A., Hakim, M. S., & Rohyami, Y. (2014). The Effect of Contact Time and pH on Methylene Blue Removal by Volcanic Ash. International Conference on Chemical, Biological and Environmental Sciences, May, 12–15. https://doi.org/10.17758/iaast.a0514002

Sakeus, K. (2016). Anaerobic Digestion of Dairy Manure Wastewater, Food and Fruit Waste, A Sustainable Source of Bio-Energy and Waste Management (Issue May). Stellenbosch University.

Sandriaty, R., Priadi, C., Kurnianingsih, S., & Abdillah, A. (2018). Potential of biogas production from anaerobic co-digestion of fat , oil and grease waste and food waste. 02047, 1–5.

Sanz, J. L., & Köchling, T. (2007). Molecular biology techniques used in wastewater treatment: An overview. In Process Biochemistry (Vol. 42, Issue 2, pp. 119–133). Elsevier. https://doi.org/10.1016/j.procbio.2006.10.003

Satimanont, S., Apanee, L., & Sujitra, W. (2012). Effect of Temperature and Time on Dilute Acid Pretreatment of Corn Cobs. International Journal of Chemical, Molecular, Nuclear, Materials and Metallurgical Engineering, 6(4), 316–320. http://waset.org/publications/7851/effect-of-temperature-and-time-on-dilute-acid-pretreatment-of-corn-cobs

Setshedi, K. Z. (2014). Removal of Heavy Metals from Industrial Wastewater Using Polymer-Clay Nanocomposites as Novel Adsorbents (Vol. 153) [TSHWANE UNIVERSITY OF TECHNOLOGY]. https://doi.org/10.1017/CBO9781107415324.004

Setshedi, K. Z., Bhaumik, M., Songwane, S., Onyango, M. S., & Maity, A. (2013). Exfoliated polypyrrole-organically modified montmorillonite clay nanocomposite as a potential adsorbent for Cr(VI) removal. Chemical Engineering Journal, 222(Vi), 186–197. https://doi.org/10.1016/j.cej.2013.02.061

Shah, F. A., Mahmood, Q., Shah, M. M., Pervez, A., & Asad, S. A. (2014). Microbial Ecology of Anaerobic Digesters: The Key Players of Anaerobiosis. The Scientific World Journal, 2014(183752), 21. https://doi.org/10.1155/2017/3852369

Siddique, M. N. I., & Wahid, Z. A. (2018a). Achievements and perspectives of anaerobic co-digestion: A review. In Journal of Cleaner Production (Vol. 194). https://doi.org/10.1016/j.jclepro.2018.05.155

Siddique, M. N. I., & Wahid, Z. B. A. (2018b). Enhanced Methane Yield by Codigestion of Sewage Sludge with Microalgae and Catering Waste Leachate. Water Environment Research, 90(9), 835–839. https://doi.org/10.2175/106143017x15131012153031

Sikora, A., Detman, A., Chojnacka, A., & Błaszczyk, M. K. (2017). Anaerobic Digestion : I . A Common

Process Ensuring Energy and the the Circulation Circulation the of Gaseous Biofuels Production of Gaseous Biofuels. In A. F. Jozala (Ed.), Fermentation Processes (pp. 271–301). InTech, under CC BY 3.0 license. https://doi.org/10.5772/61924

Singh, S. (2017). Optimization of Biogas Production from City of Johannesburg Market Waste by Anaerobic Digestion (Vol. 0002, Issue August). University of Johanneburg.

Sjostrom, K. (1993). Rapid Pyrolysis of Wood with Application to Gasification. Advances in Thermochemical Biomass Conversion, 977–85.

Sosnowski, P., Wieczorek, A., & Ledakowicz, S. (2003). Anaerobic co-digestion of sewage sludge and organic fraction of municipal solid wastes. Advances in Environmental Research, 7(3), 609–616. https://doi.org/10.1016/S1093-0191(02)00049-7

Stafford, W. H. L., Lotter, G. A., von Maltitz, G. P., & Brent, A. C. (2019). Biofuels technology development in Southern Africa. Development Southern Africa, 36(2), 155–174. https://doi.org/10.1080/0376835X.2018.1481732

Stravalaci, M. (2017). Identification And Characterization Of Mediators Of Toxicity Of AB Oligomers By Genome Wide Screening In Caenorhabditis Elegans Identification and Characterization of Mediators of Toxicity of Ab Oligomers by Genome Wide Screening in Caenorhabditis elegans.

Suárez, A. G., Nielsen, K., Köhler, S., Merencio, D. O., & Reyes, I. P. (2014). Enhancement of Anaerobic Digestion of Microcrystalline Cellulose Using Natural Micronutrient Sources. 31(02), 393–401.

Sugumar, S., Shanmuga, P. R., & Dinesh, S. (2016). A Review on Performance Study of Anaerobic Digestion to Enhance the Biogas Production. International Journal of Civil Engineering and Technology, 7(6), 202–206. http://www.iaeme.com/IJCIET/issues.asp?JType=IJCIET&VType=7&IType=6%0A1.

Tetteh, E. K., & Rathilal, S. (2020). Kinetics and nanoparticle catalytic enhancement of biogas production from wastewater using a magnetized biochemical methane potential (Mbmp) system. Catalysts, 10(10), 1–19. https://doi.org/10.3390/catal10101200

Tsai, W. T. (2012). An analysis of the use of biosludge as an energy source and its environmental benefits in Taiwan. Energies, 5(8), 3064–3073. https://doi.org/10.3390/en5083064

Tufaner, F., & Avşar, Y. (2016). Effects of co-substrate on biogas production from cattle manure: a review. International Journal of Environmental Science and Technology, 13(9), 2303–2312. https://doi.org/10.1007/s13762-016-1069-1

Ugwu, S. N., & Enweremadu, C. C. (2020). Enhancement of biogas production process from biomass wastes using iron-based additives: types, impacts, and implications. Energy Sources, Part A: Recovery, Utilization and Environmental Effects, 1–23. https://doi.org/10.1080/15567036.2020.1788675

Venkiteshwaran, K., Bocher, B., Maki, J., & Zitomer, D. (2015). Relating Anaerobic Digestion Microbial Community and Process Function : Supplementary Issue: Water Microbiology. Microbiology Insights, 8s2, MBI.S33593. https://doi.org/10.4137/mbi.s33593

Vivek Narayanan, N., & Ganesan, M. (2009). Use of adsorption using granular activated carbon (GAC) for the enhancement of removal of chromium from synthetic wastewater by electrocoagulation. Journal of Hazardous Materials, 161(1), 575–580. https://doi.org/10.1016/j.jhazmat.2008.03.113

Wambugu, C. W., Rene, E. R., van de Vossenberg, J., Dupont, C., & van Hullebusch, E. D. (2019). Role of Biochar in Anaerobic Digestion Based Biorefinery for Food Waste. Frontiers in Energy Research, 7(March), 1–13. https://doi.org/10.3389/fenrg.2019.00014

Wang, Q., Liang, Y., Zhao, P., Li, Q. X., Guo, S., & Chen, C. (2016a). Potential and optimization of two-phase anaerobic digestion of oil refinery waste activated sludge and microbial community study. Scientific Reports, 6(August), 1–10. https://doi.org/10.1038/srep38245

Wang, Q., Liang, Y., Zhao, P., Li, Q. X., Guo, S., & Chen, C. (2016b). Potential and optimization of two-phase anaerobic digestion of oil refinery waste activated sludge and microbial community study. Scientific Reports, 6(August), 1–10. https://doi.org/10.1038/srep38245

Wang, Y., Zhao, W., Zheng, W., Chen, S., & Zhao, J. (2019). Preparation of N-doped carbon nanosheets from sewage sludge for adsorption studies of cr(VI) from aqueous solution. Nanomaterials, 9(2). https://doi.org/10.3390/nano9020265

Wannapokin, A., Unpaprom, Y., Ramaraj, R., Wannapokin, A., Ramaraj, R., & Unpaprom, Y. (2017). An investigation of biogas production potential from fallen teak leaves (Tectona grandis). Emer Life Sci Res, 3(1), 1–10. https://doi.org/10.7324/ELSR.2017.31110

Webster, T. M., Smith, A. L., Reddy, R. R., Pinto, A. J., Hayes, K. F., & Raskin, L. (2016). Anaerobic microbial community response to methanogenic inhibitors 2-bromoethanesulfonate and propynoic acid. MicrobiologyOpen, 5(4), 537–550. https://doi.org/10.1002/mbo3.349

Wei, L., Qin, K., Ding, J., Xue, M., Yang, C., Jiang, J., & Zhao, Q. (2019). Optimization of the co-digestion of sewage sludge, maize straw and cow manure: microbial responses and effect of fractional organic characteristics. Scientific Reports, 9(1), 1–10. https://doi.org/10.1038/s41598-019-38829-8

Wen, H., Zhang, D., Gu, L., Yu, H., Pan, M., & Huang, Y. (2019). Preparation of sludge-derived activated carbon by fenton activation and the adsorption of Eriochrome Black T. Materials, 16(6). https://doi.org/10.3390/ma12060882

Werther, J., & Ogada, T. (1999). Sewage sludge combustion. Progress in Energy and Combustion Science, 25(1), 55–116. //doi.org/10.1016/S0360-1285(98)00020-3.

Wirth, R., Kovács, E., Maráti, G., Bagi, Z., Rákhely, G., & Kovács, K. L. (2012). Characterization of a biogas-producing microbial community by short-read next generation DNA sequencing. Biotechnology for Biofuels. https://doi.org/10.1186/1754-6834-5-41

Xu, R., Zhang, K., Liu, P., Khan, A., Xiong, J., Tian, F., & Li, X. (2018). A critical review on the interaction of substrate nutrient balance and microbial community structure and function in anaerobic co-digestion. In Bioresource Technology (Vol. 247). https://doi.org/10.1016/j.biortech.2017.09.095

Yang, G., Zhang, P., Zhang, G., Wang, Y., & Yang, A. (2015). Bioresource Technology Degradation

properties of protein and carbohydrate during sludge anaerobic digestion. Bioresource Technology, 192, 126–130. https://doi.org/10.1016/j.biortech.2015.05.076

Zha, Y., Wang, Y., Liu, S., Liu, S., Yang, Y., Jiang, H., Zhang, Y., Qi, L., & Wang, H. (2018). Adsorption characteristics of organics in the effluent of ultra-short SRT wastewater treatment by single-walled, multi-walled, and graphitized multi-walled carbon nanotubes. Scientific Reports, 8(1), 1–12. https://doi.org/10.1038/s41598-018-35374-8

Zhang, J., Loh, K. C., Lee, J., Wang, C. H., Dai, Y., & Wah Tong, Y. (2017). Three-stage anaerobic co-digestion of food waste and horse manure. Scientific Reports, 7(1), 1–10. https://doi.org/10.1038/s41598-017-01408-w

Zhang, L., Kuroki, A., & Tong, Y. W. (2020). A Mini-Review on In situ Biogas Upgrading Technologies via Enhanced Hydrogenotrophic Methanogenesis to Improve the Quality of Biogas From Anaerobic Digesters. Frontiers in Energy Research, 8. https://doi.org/10.3389/fenrg.2020.00069

Zhao, J. J., Shen, X. J., Domene, X., Alcañiz, J. M., Liao, X., & Palet, C. (2019). Comparison of biochars derived from different types of feedstock and their potential for heavy metal removal in multiple-metal solutions. Scientific Reports, 9(1), 1–12. https://doi.org/10.1038/s41598-019-46234-4

CHAPTER 3

APPROACH & METHODOLOGY

This chapter gives insight into the materials and methods used in this research study. This includes information about material characterization and analytical techniques. The anaerobic digestion of sewage sludge mono-digestion & the co-substrates in both batch studies & semi-continuous processes are included in this chapter. Moreover, overall adsorption experimental procedures, batch, and fixed-bed column sorption are presented.

3.1. Sample, Study Area, and Sampling Method

3.1.1. Base Substrate and Sampling

The sewage sludge was collected on an Adhoc basis, within 6 months from four different municipal WWTWs in Gauteng Province, South Africa, Johannesburg Water (JW), and City of Tshwane (CoT) area as a case study. The sample points selected were primary sludge (PS) & waste activated sludge (WAS) sampling points. This was selected because these points are representative of the cross-section of the entire flow thus obtaining a well-mixed sample. The standard sampling method used was a grab sampling technique from anaerobic digestion influent streams. The samples collected were stored in a cold room inside a 4°C laboratory fridge before analysis. Samples were set aside for physicochemical tests & to conduct a metagenomics analysis on the AD feedstock.

3.1.2. Chemicals

The chemicals used for ADs tests were hydrochloric acid (HCl, 99%), sodium hydroxide (NaOH, solid pellets) and sodium bicarbonate ($NaHCO_3$, 99%), Zinc Chloride ($ZnCl_2$, solid), and Potassium Hydroxide (KOH, solid pellets). All chemicals were of analytical grade and purchased from Merck, Qatar.

3.1.3. Organic co-substrates Sources

The co-substrates were collected randomly from the following source;

- Soft drink waste, sourced from Coca-Cola Beverage SA (CCBSA)
- Brewery-spent grains were provided by SAB Miller (InBev) Rosslyn Pretoria.
- The sugar cane molasses was collected from Northern works provided by Durban Sugar Mill.
- Animal manure mixture was collected from Cavalier Abattoir, Pretoria
- Fresh produce Waste was provided by JHB Fresh Produce market, City Deep Johannesburg.
- Food waste was collected from the CSIR cafeteria, Knowledge Commons, and CSIR Pretoria.

Since there was no prior knowledge of each form of co-substrates produced daily, the random sampling method was used. It was also difficult to collect all of the different types of co-substrates generated at the source. During the tests, however, attempts were made to capture the percentage of waste produced at the market using weekly sales data from the company's website. While this method did not account for the specific form of waste produced, it did provide a fair foundation for a portion of waste in the substrate mix. Before being transported to the laboratory, the collected waste was placed in a sample holding container.

3.2. Preparation of substrates

The fresh produce and food wastes were cut into small pieces in the laboratory macerated and homogenized with an industrial food grinder to produce small pieces (1 mm in size). The maceration was carried out without the use of water. Before the samples were packed into labeled plastic containers and kept at -18 °C when not immediately used, a homogenized sample was taken for characterization. The frozen substrates were thawed to room temperature before use and stored at 1 °C in a cold room. To minimize the seasonal effect on substrate content, AD tests were performed within one month of substrate preparation (Vítěz et al., 2011).

Sludge & co-substrate characterization was carried out before the BMP test to understand the composition of the feedstock to assist in designing the experiment. These physical and chemical compositions include volatile solids (VS), and total solids (TS) according to the standard method (APHA 1995).

3.3. Proximate and Ultimate Analysis of Organic Waste

After homogenization, proximate analysis was performed in triplicate for each substrate, and digestate was collected to determine the TS, VS, and ash content of the substrate. Emptied crucibles were filled to 2/3 of their volume with the substrate using a spatula or by pouring for digestate to assess the proximate characteristics. The crucible with the substrate was placed in a preheated Thermo Scientific Flash 6000 Oven. The substrate is dried in the oven for 24 hours at 105°C. This is how the drying procedure works. The dried sample was placed in a muffle furnace set to 550°C and heated for three hours (Eaton et al, 2015). This is how the ashing procedure works. The TS was calculated using Equation (3.1), and the VS was calculated on a dry basis using Equations (3.2) based on the TS of the substrate.

$$\%TS = \frac{M_3 - M_1}{W_2 - W_1} \quad (3.1)$$

$$\%VS = \frac{M_3 - M_4}{M_3 - M_1} \quad (3.2)$$

where M_1 is the weight of the empty crucible; M_2 is the weight of the crucible with wet substrate or digestate; M_3 is the weight of the crucible after drying at 105 ℃, and M_4 is the weight of the crucible after ashing at 550 ℃. Using a Thermo Scientific Flash 2000 Organic Element Analyzer, the final analysis for each substrate was performed after homogenization to determine the amount of CHN present in the dry sample. Both of the procedures were carried out according to the manufacturer's instructions (Krotz, 2020). For CHNS/O determination, three dried sewage sludge samples were analyzed. For CHNS analysis, the instrument was calibrated with 2 – 3 mg BBOT (2,5-Bis (5-tert-butyl-benzoxazol-2-yl) thiophene) using the K factor as a calibration method. Samples were weighed at 3 – 4 mg.

3.4. Inoculum

For continuous AD process, efficiency can be reduced due to operational difficulties and instability problems associated with poor start-up and lack of adapted inoculum. Hence the seeding process has to be conducted using biologically active sludge. Inoculum supplies the microorganism to the anaerobic digestion process and is one of the most important factors since it has the ability to significantly influence methane yield results

(Gonzalez-Fernandez et al., 2015). The standard method to prepare inoculum was followed in the order adapted from Gonzalez-Fernandez et al., (2015). A quality check to indicate whether the operational parameters of the digester are of good quality. The most common recommendation is to pre-incubate the inoculum for 1 to 5 days at 35 ◦C to degas and reduce the impact of its methane production. The inoculum used for both the batch and starting the semi-continuous AD processes was provided by IBERT, inside Cavalier Abattoir in Cullinan Pretoria. IBERT Pty provided the inoculum sourced from a plant treating abattoir waste.

IBERT Ptys supplied the inoculum that was used in both the batch and semi-continuous AD processes. IBERT Ptys is a Johannesburg-based biogas manufacturing, procurement, design, and management firm. The inoculum came from a facility that processed abattoir waste. The plant runs at 37 °C, and the inoculum had a pH of 7.75. Since sludge will be digested, inoculum from AD plants that handle such waste would have been the best choice. However, the majority of biogas plants in the City of Johannesburg (CoJ) use non-food as a substrate. As a result, only inoculum from such plants can be used.

According to Morales-Polo et al., (2019) there was no substantial difference in BMP findings for the same substrate using different inoculum sources. They concluded that the degradation would continue if the inoculum had enough diverse microbial communities to cope with the substrate's disintegration. Al-Addous et al., (2018) also found that the effect of inoculum sources on the degree of biodegradation was negligible. The source of inoculum, on the other hand, may influence the kinetic rate of degradation.

3.5. Theoretical Biogas Potential

The importance of the theoretical yield of anaerobic digestion is to predict the biogas amount of the biowaste that have proposed in this study. The theoretical biogas potential for the substrates analyzed was calculated from the stoichiometric equation based on the atomic composition of the waste material according to Symons and Buswell (2004) as shown in Equation (3.3). Equation (3.3) assumes the total conversion of the organic matter into CO_2, CH_4, NH_3, and H_2S. The specific theoretical biomethane potential was calculated by Equation (3.4). element present and are calculated by

dividing the wet weight fraction of each element by its molar mass. The BMP theoretical is expressed as NmL CH_4/kgVS.

$$CcH\hbar OoNnSs + \mathrm{h}H_2O \rightarrow yCH_4 + zCO_2 + nNH_3 + sH_2S \quad (3.3)$$

$$BMPtheoretical = 22.4y \,/\, (12c + \hbar + 16o + 14n + 32s) \quad (3.4)$$

Where C carbon, H hydrogen, O Oxygen, H nitrogen, and y,c,x,c,o,n,s are the stoichiometric coefficients as shown in Equation 3.3.

3.6. Surface Characterization techniques

3.6.1. Fourier Transform Infrared (FTIR)

The presence or absence of functional groups with distinct vibration frequencies, such as C=O, NH_2, OH, CH, C-O, etc., was observed using the FTIR spectrometer to analyze and interpret the structural changes of the sample material (Bodîrlău et al., 2009). Infrared spectroscopy involves passing IR radiation through a sample. The sample absorbs some of the infrared radiation and passes some of it around (transmitted). The resulting spectrum depicts the sample's molecular absorption and transmission, resulting in a molecular fingerprint. No two unique molecular structures emit the same infrared spectrum, just like fingerprints. As a result, infrared spectroscopy can be used for a variety of purposes (Ferrasse et al., 2015).

3.6.2. Scanning Electron Microscope (SEM)

The SEM was used for the examination and analysis of the microstructure morphology and chemical composition characterizations of the synthesized adsorbents (Anup, 2018; Liu et al., 2020). The SEM images with Energy Dispersive X-ray analysis (EDX) presented in this work were obtained on a new generation Philips XL30 SEM, (Foster City, CA, United States) with a maximum voltage of 15-20 kV, to obtain preliminary images

3.6.3. Thermogravimetric Analysis (TGA)

A typical approach for measuring the thermal degradation of a small sample is thermogravimetric analysis (TGA). In a regulated setting, the sample is heated at a particular rate while the weight loss or gain, time, and temperature are all recorded. The TGA method allows for a quantitative assessment of weight changes caused by thermally induced transformations over time or at different temperatures. Physical details about

second-order phase transitions including vaporization, sublimation, adsorption, absorption, and desorption can be captured using TGA. Chemical data such as chemisorption, devolatilization, decomposition, and solid-gas reagents are also available. The derivate of the thermogravimetry (DTG) is the weight loss rate of the biomass concerning time or temperature (Pan et al., 2005).

Using a pulverizer and a collection of sieves, the biomass samples were ground into particles of up to 50 g. To extract moisture, the collected particles were heated to 105 °C for 24 hours. In an alumina crucible, 100 mg of the dehydrated sample was inserted. To extract any moisture trapped during the sample preparation for TGA, the sample was heated from room temperature to 105 °C and held for 10 minutes (Ferrasse et al., 2015). Following that, it was heated to 900 °C in an inert atmosphere at a rate of 10 °C/min using nitrogen at a flow rate of 100 ml/min as recommended by (Williams & Besler, 1993). To assess combustion parameters, the weight loss (TG) and weight loss rate (DTG) data were normalized and analyzed.

3.6.4. Surface area analysis

Brunauer Emmett and Teller were the first to propose the BET idea. The BET theory is based on the phenomenon of physical adsorption of gases on the external and internal surfaces of a porous material to determine the exact surface (Brame & Griggs, 2016). A substance surrounded by and in equilibrium with a specific gas with a specific temperature, T, and relative vapour pressure, p/po, adsorbs a specific amount of gas physically. The volume of adsorbed gas is proportional to the total external and internal surface area of the substance and is determined by its relative vapour pressure (Yao et al., 2018).

The connection between relative vapour pressure and the amount of adsorbed gas at a constant temperature is called an adsorption isotherm (Fagerlund, 1973). Meanwhile, the BET surface area was measured using the Nova 1000e surface and pore size analyzer at a degas temperature of 80 °C for 1 h with a nitrogen coolant.

3.6.5. Ultraviolet-visible spectroscopy (UV-Vis)

The residual Cr (VI) concentration after adsorption was determined using a Perkin Elmer Lambda UV-Vis spectrometer set to 540 nm and an indicator reagent such as 1,5 diphenyl carbazide reagents. UV-Visible spectroscopy (wavelengths between 10 and 1000

nm) provides details on the transition of the atoms' most external electrons. Since various wavelengths of UV-visible radiation are absorbed by different atoms or molecules, spectroscopy/spectrometry is often used in physical and analytical chemistry to identify substances based on the spectrum emitted from or absorbed by them. The Lambert-Beer-law method is often used to determine the concentration or volume of a given species. (Lee et al., 2013).

This law relates the absorption of radiation to the properties of the material through which is passing through. States that there is a logarithmic dependence between the transmission (and transmissivity), T, of light through a substance and the product of the absorption coefficient of the substance, α, and the distance the beam travels through the material (i.e., the path length), l. The absorption coefficient can, in turn, be written as a product of either the Molar absorptivity of the absorber or the concentration (C) of absorbing species in the material. For liquids, these relations are usually written as

$$\mathrm{Log\ (T)} = \log(\mathrm{I})_{\mathrm{Io}}\ \epsilon \mathrm{lC} \qquad (3.5)$$

where I and I0 are the intensity of the incident and the transmitted beams, respectively. The transmission also can be expressed in terms of absorbance (A):

$$A = -logT \qquad (3.6)$$

And so, the Lambert-Beer equation can be written finally as $A = \epsilon lC$ (3.7)

Either transmittance or absorbance can be measured experimentally with the spectrometer. The concentration of the material (or the number density of absorbers) can be calculated if the path length and molar absorptivity are known and the absorbance is measured. For a given set of experiments, all parameters are usually constant, so a plot of the sample absorbance against the concentration of the absorbing material should be a straight line. A calibration curve is created by plotting the measured absorbance of a series of standard samples as a function of their concentration in practice. The concentration of the absorbing component can be calculated from this graph if the absorbance of an unknown sample is measured.

3.7. Physicochemical Characterization techniques

The different characterizations of the collected sludge such as total chemical oxygen demand (COD), volatile solid (VS), total solid (TS), Chemical Oxygen Demand (COD), Total Kjeldahl Nitrogen, (TKN), Total Alkalinity (TA), Total Organic Carbon (TOC), Ammonium Nitrogen (NH_4-N), Total Phosphorus (TP) & Volatile Acids (VA). The measure of pH, temperature, TS & VS parameters were performed according to standard methods procedures (Eaton et al., 2015) using a pH & temp meter, laboratory oven, and furnace. The analysis was carried out as soon as the sludge was conveyed to the university's laboratory. The COD, TKN, TA, TOC, NH_4-N, TP & VA were determined spectrophotometrically by use of standard test kits (Hach-DR3900, USA), See Figure 3.1. The COD was used to estimate potential methane instead of volatile suspended solids (VSS) as usual for organic matter reduction. The COD of methane was calculated using 1 g COD = 0.35 L CH_4 as explained in (Filer et al., 2019).

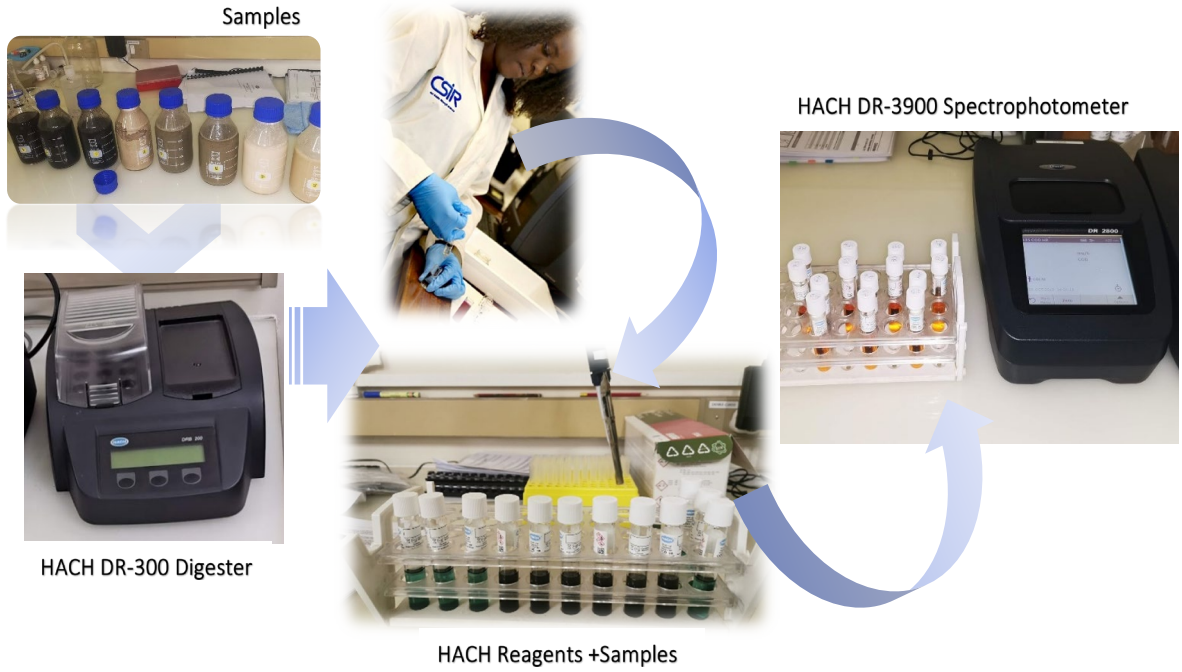


Figure 3.1: Spectrophotometric analysis method using standard Hach test kits

The amount of biogas produced in a given time from any substrate through anaerobic digestion is dependent on several factors which include digester temperature, digester pH, organic loading rate (OLR), hydraulic retention time (HRT), solid retention time (SRT),

digester shape and type. The above-mentioned factors are variables that are at the operator/designer's disposal to manipulate to increase the biogas production from any given substrate, however, the feed composition determines the limit of the amount of biogas that can be produced. Therefore, understanding the feed composition is crucial when one is considering optimizing biogas production from any substrate. Their feed composition can be described by numerous determinants but the key parameters for anaerobic digestion include chemical oxygen demand (COD), total solids (TS), volatile solids (VS), total organic carbon (TOC), Total Kjeldahl nitrogen (TKN) and volatile fatty acid (VFA) (Eaton et al., 2015).

The parameters describe certain characteristics of the feed. The VFA, COD, TS, and VS quantify the organic matter that is available for biodegradation and ash content contained in the feedstock. The COD determines the limit of biogas that can be produced from a given substrate. TOC and TKN determine the Carbon-to-Nitrogen (C/N) ratio which is the measure of the nutritional balance of the feed. The ratio does not have any effect on a limit of the biogas that can be produced from a substrate, however, maintaining the ratio within the optimum range ensures optimum biogas production. The total alkalinity (TA), orthophosphates (PO_4^{3-}), and ammonium nitrogen (NH_4^+-N) are responsible for buffering capacity of the digester, and their composition together with VFA is important in determining the pH of the digester. Total phosphorus (TP) is important in determining the organically bound phosphorus. This is important in determining how much phosphorus will be contained in the digestate liquor.

3.8. Microbiological Characterization techniques

This part of the research aims to characterize microbial community diversity and structure of the sewage sludges from Driefontein and the Northern Works WWTP as well as to access their contribution toward anaerobic digestion. To characterize the composite microbial consortium that may develop in the biogas digester, a microbiological analysis was conducted. All the samples used for microbiological analysis were collected on the 28th of February 2019 from the Driefontein and the Northern Works WWTP and were in a cold room while awaiting the analysis. The microbial community structures, functional profiles, and metabolic pathways of the anaerobic digestion sludge can be revealed. In

particular, key microorganisms involved in hydrolysis, acidogenesis, acetogenesis, and methane production can be comprehensively analyzed based on the obtained metagenomics data (Mandal et al., 2017; Ramdani et al., 2015). Furthermore, this report highlights possible genes associated with methanogenesis pathways.

The microbiological analysis was conducted by a PacBio microbial analytical method, see Figure 3.2. This technique generates new insights into how microbial communities function in a new improved approach. It provides long-read sequencing enables species-level resolution and drives functional insights. DNA extraction of the microorganisms was performed using a DNA extraction kit. The DNA sequencing was carried out by an application of the full-length 16S rDNA and shotgun sequencing for metagenomic profiling and assembling. The sequencing library was prepared by random fragmentation of genomic DNA samples and adapters ligating on both fragments' ends. The library was then loaded into a flow cell and the fragments were hybridized to the flow cell surface. Each bound fragment was amplified into clonal clusters, which are ready for sequencing. The sequencing reagent was added to the clusters and the first base was then incorporated (Gerardi, 2003; PacBio, 2015). The flow cell was imaged and the emission from each cluster is recorded.

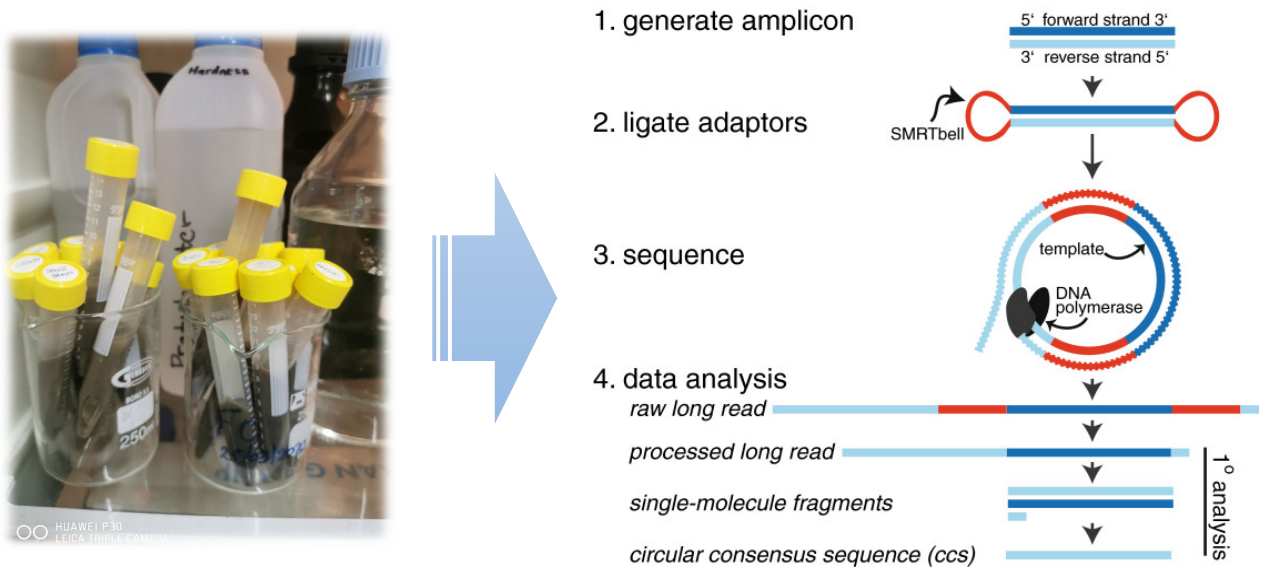


Figure 3.2: Illustration of Sample & PacBio sequence generation procedure, adapted from (PacBio, 2015)

For every sample, data were trimmed, every read was BLASTED, and the result file is then saved. The top hit for every BLAST result (genes and species name) is counted and a record is kept of how many times each species appeared as a hit. The "read count" is the number of reads that matched the corresponding organism. If no BLAST result is found for a particular read, that read count would be recorded under 'No Hits'. Taxa information for every BLAST hit is recorded and the data is saved on the CSV file.

To have a better understanding of microbial dynamics in the digester feed, the bacterial community was characterized. The samples from the digestion reactors were collected and saved for DNA extraction. First, the biomass samples were filtered through 0.22 μm membrane filters (Millipore Laboratories, Billerica, MA) and then stored at −80 °C. DNA in these samples was extracted using UltraClean® Soil DNA Isolation Kits (MoBIO Laboratories, Carlsbad, CA) and subsequently purified via ethanol precipitation. A detailed description of the detection procedure of the archaeal and bacterial community-related DNA can be found in Doloman et al., (2017) & Regueiro et al., (2014) respectively.

The ZymoBIOMICS DNA extraction was used to extract gDNA from the samples as per the manufacturer's protocol. Organic material from the sample was analyzed in separately following the method developed by (Ahmadi et al., 2013). The water content of the sewage sludge was adjusted to 97.0% first and then centrifuged (4000 × g) for 30 min. The solid residue collected after centrifugation was slowly mixed with 200 mL of 25% (v/v) NH_4OH for 24 h and filtered through a 0.45 μm membrane filter. The collected organics-containing filtrate was diluted (50 times) and acidified to a pH level of 2. The diluted and acidified organics were fractionated into five fractions using XAD-8/XAD-4 resins: a hydrophobic acid (HPO-A), a hydrophobic neutral (HPO-N), a transphilic acid (TPI-A), a transphilic neutral (TPI-N), and a hydrophilic (HPI) fraction. A complete description of the fractionation methods is given in (Lu et al., 2017).

Universal 16S primers (27F and 1492R) tagged with universal PacBio adaptor sequences were used to generate a full-length 16S amplicon for sequencing on the PacBio Sequel system. For alignment, raw subreads were processed through the SMRTlink (v6.0) Circular Consensus Sequences (CCS) algorithm to produce highly accurate reads (>QV40). For data analysis, these highly accurate reads were then processed through Usearch

(https://drive5.com/usearch) and taxonomic information was determined based on the Ribosomal Database Project's 16s database v16 (http://rdp.cme.msu.edu/index.jsp).

3.9. Anaerobic Digestion & Co-digestion with Biochemical Methane Potential

The batch BMP experimental design was created to investigate the effect of co-digestion on the AD process and to find the best semi-continuous process parameters. Under laboratory-controlled conditions, it was set up to calculate the derivable CH_4 per unit mass of substrate, yield efficiency, and in-situ upgrading capacity of biogas with biochar amended substrate. The study aimed to see how a combination of process parameters, such as the mix ratio between sewage sludge and other biowastes affected the output of an AD.

The performance characteristics are specific biomethane (NmL/gVS), CH_4 concentration, lag phase, maximum daily specific biomethane (NmL/gVS.d), electrical conductivity, and pH. The base substrate & co-substrate was 1:1 while the combined waste concerning sewage sludge was investigated at different ratio. All substrates used in the BMP experiment were from a single prepared substrate batch. This allows for the comparison of results without the effect of substrate variability on obtained results.

Biogas production laboratory tests can be carried out as both continuous and batch experimental setup. Continuous experiments are carried out in benchtop laboratory bioreactors, where the substrate is continuously added and residual digestate is continuously withdrawn, simulating full-scale processes. These types of experiments are useful because they provide information about long-term effects such as microbial adaptation to new substrates/conditions and whether certain metabolites accumulate slowly. They are, however, time-consuming and slow because long experiments that are difficult to restart or reproduce.

Regardless, batch experiments are used to determine the BMP of different substrates. In theory, a batch experiment can run indefinitely to determine the maximum biogas yield from a substrate. In practice, however, BMP tests are terminated once biogas production has ceased and reached a plateau. Furthermore, batch experiments can be used to compare the relative effects of substrate pre-treatments on biogas production kinetics (Figure 3.3A) to an untreated reference, or to determine the effects of a specific pre-

treatment on BMP (Figure 3.3B). That is, to determine whether or not a more microbially accessible substrate is released during the pre-treatment stage (Odnell, 2018).

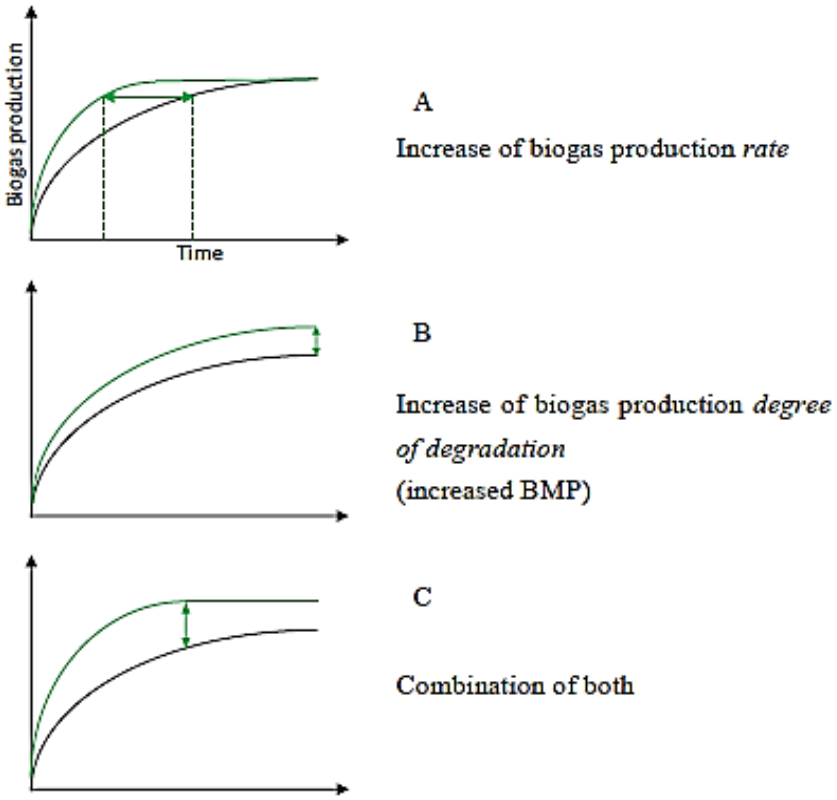


Figure 3.3: Accumulation of biogas production in BMP (A) increased kinetic rate to an untreated reference (B) shows an increase due to degree of degradation and (C) is an increase due to rate and degree of degradation (Odnell, 2018).

3.9.1. Batch Experimental Set-up

The co-digestion-only tests were conducted in triplicates, to create a reference for the comparison of the co-digestion; and to study the interaction among the process parameters during the batch BMP test. In addition, the inoculum-only test was conducted to account for the biogas contribution of the inoculum in all the batch samples. The hybrid experimental design was implemented by using the Automatic Methane Potential Test System II (AMPTS II), which was specifically designed for BMP analysis. Under laboratory conditions, the sludge was mixed at the recommended volume ratio of 50:50 (sludge: spent grain). It was then homogenized, screened through a 3 mm sieve, and portioned. The setup consists of a temperature-controlled water bath for

fifteen 500 ml bottle reactors. It was equipped with an automatic motorized mixer capable of clockwise and anti-clockwise continuous or intermittent rotation. Biogas produced from the digesters was passed through an 80 ml alkaline reagent for absorption of CO_2 and other non-methane gas.

The alkaline reagent was made from 3.0 M NaOH (reagent grade 97%, pellets). A 0.4% Thymolphthalein pH-indicator was prepared by dissolving the dye powder (2',2"-Dimethyl-5,5"-di-iso-propylphenolphthalein, dye content 95%) in a mixture containing 10% water and 90% ethanol. Procedures for the alkaline solution preparation are presented in detail in the AMPTS II manual from Bioprocess Control. The mixed alkaline solution appears bluish when unsaturated with CO_2 and colorless once saturated with CO_2, thereby indicating that the spent solution needs to be replaced. The cleaned biogas, now biomethane, leaving the alkaline reagent unit goes into a water displacement measuring unit with 15 parallel operating tipping bucket cells. Following the law of buoyancy, each cell will open and release the trapped gas when approximately 10 ml of biomethane has been accumulated. For each cell response, the time, the temperature, and the pressure are logged automatically; and they are used to normalize the volume of biogas at 0 ℃, 1 atm, and dry gas conditions. The experimental result is downloaded as a. csv file for further analysis.

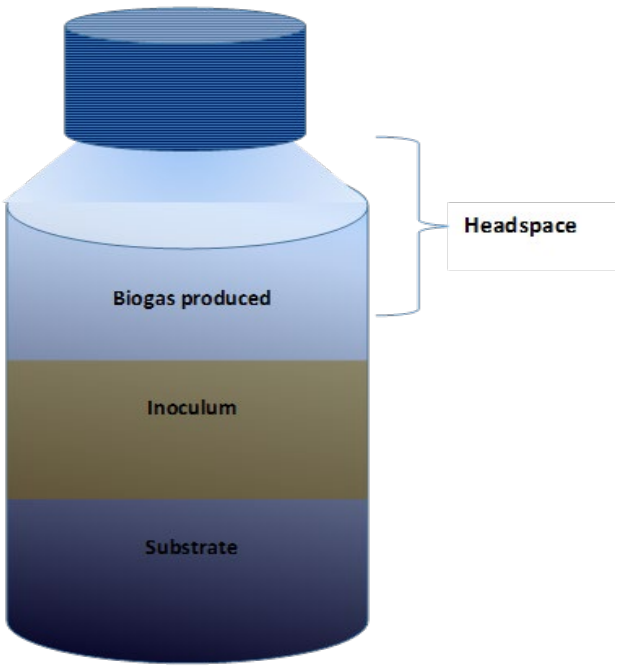


Figure 3.4: The Digester setup in the BMP setup Substrates & inoculum measurements

The Eudiometer-based BMP was equipped with 500ml & 1L Schotts bottle operating as an anaerobic digester, refer to Figure 3.4. These small digesters are fed with a calculated volume of substrates & inoculum. Inoculum is mixed with the substrate to provide a consistent & controlled bacterial supply to the system. Figure 3.5 indicates the anaerobic digester setup used in the system. Nitrogen gas is pumped into the system to flush the headspace of the reactor and the biogas pipelines. This is done to ensure that anaerobic condition is achieved before the experiment was started, this also helps in ensuring that the system is airtight and there are no leaks.

To measure the volumetric production of biogas, Eudiometer volumetric method is used. This method uses liquid displacement to measure the biogas produced. The method allows measuring the CH_4 produced after removing CO_2 from biogas by bubbling it through a barrier solution, which in this case is a NaCl 6.0 M solution. The BMP tests were carried out under mesophilic conditions mimicking the procedure & conditions at the WWTP. The results of biogas accumulation and composition were collected daily, using the Geotech Biogas 5000 instrument by Goodspeed SA. Biogas quality (CH_4, CO_2, & balance) was analyzed 10 times in course of the digestion. Each variant was replicated two to four times. Biogas production from inoculum alone was measured as well and subtracted from the biogas production that was measured in the digesters that contained inoculum and biomass.

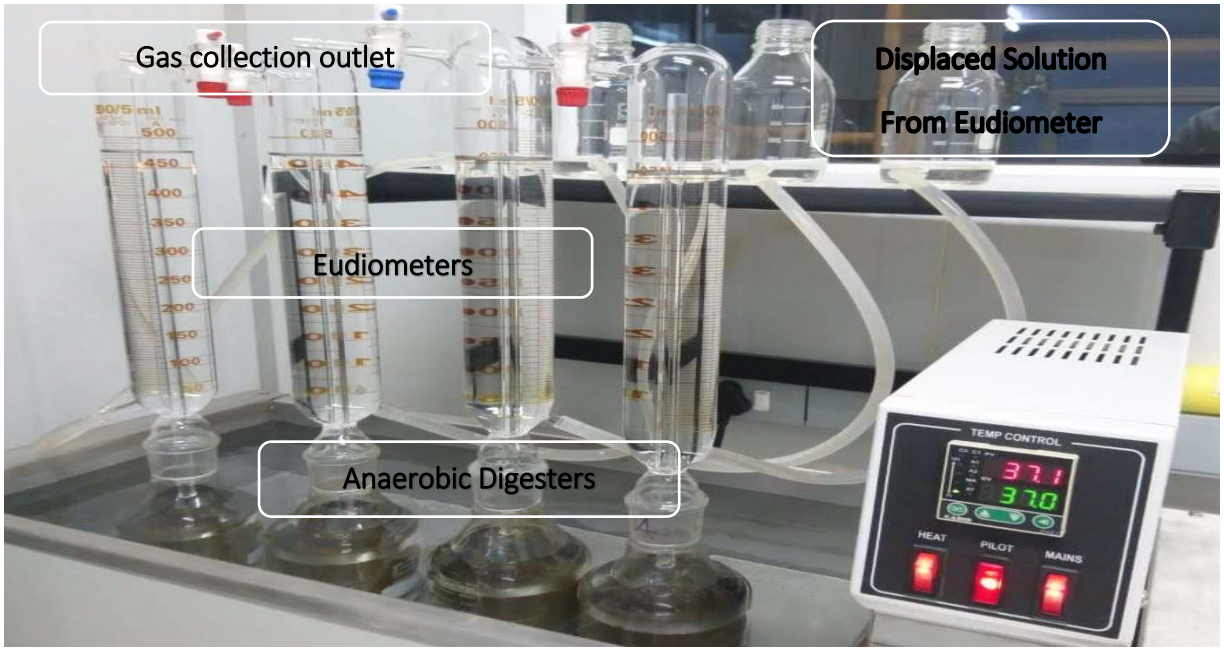


Figure 3.5: Eudiometer setup for estimating biogas from substrates

For validation purposes, a few other experiments were then carried out using the AMPTS II designed specifically for BMP analysis, see Figure 3.6. The inoculum-only test was used to account for the inoculum's biogas contribution in all batch samples. The AMPTS II instrument has an (A) temperature-controlled water bath for fifteen 500 mL bottle reactors, as well as (B) an automatic motorized mixer with continuous or intermittent clockwise and anti-clockwise spinning. The digester biogas is routed through (C) an 80 mL alkaline reagent to absorb CO_2 and other non-methane gases present in the biogas that is produced. The purified biogas leaves the alkaline reagent unit as pure methane and goes into (D) a water displacement measuring unit with 15 parallel operating tipping bucket cells. Periodical monitoring analyses were performed for both methane productions.

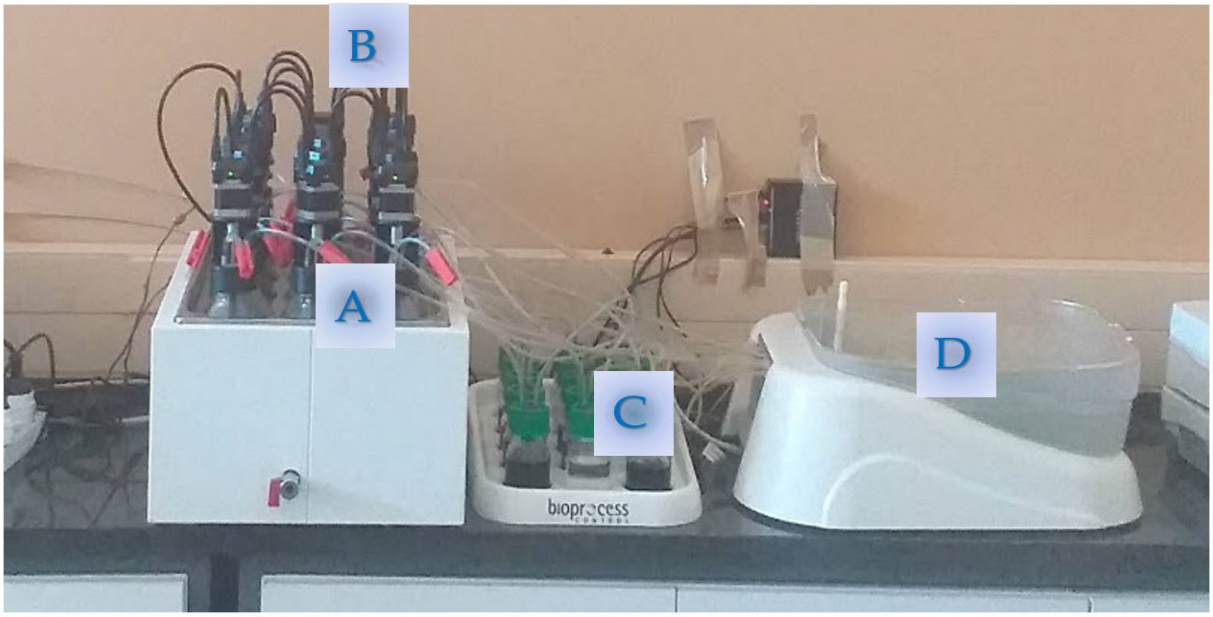


Figure 3.6: The biochemical methane potential test using the automatic methane potential test system (AMPTS II).

The duration of the experiments depends on the kind of substrate and subject of their productivity, where production of less than 1% would indicate the end of the experiment. Once the assays were finished, the main parameters were analyzed in order to evaluate the effectiveness of the process, considering the removal results. The chemical oxygen demand (COD), VFA, alkalinity, pH level, and ammonia nitrogen and orthophosphate phosphorus were determined in the supernatant. The supernatant samples were obtained by centrifuging the sample at 4000 r min−1 for 30 min.

3.10. Anaerobic Digestion: Semi-continuous process

3.10.1. Benchtop study

To investigate a nearly practical performance of the AD process, 5 L reactors were used as shown in Figure 3.7. This setup was designed and fabricated for the semi-continuous digestion experiment. One of the digesters treated substrate. Each cycle of the semi-continuous operation was for 24 hrs including the following steps: feeding (~1 hr); anaerobic digestion (23 hrs); and digestate partial draining (~1 hr simultaneously with feeding). Both digesters were filled with only inoculum and sealed at the beginning of the experiment. The experimental set-up was operating at 35-40±1 ℃, as well as a biogas flow rate meter. The temperature of the digester was supplied by a 75 W submersible heating element, and this was connected to a temperature controller. The operating volume of the digester unit was 3 L. The reactor was fitted with an IKA overhead stirrer that operates at 100 RPM over 10 mins/hr. The stirrer was programmed to switch on and off periodically as it is communicated by the automatic timer. The semi-continuous test was conducted for 150 days. The experimental samples were collected daily in triplicate in a cycle of 24 h using a Geotech Biogas 5000 instrument. For the co-digestion of sewage sludge and spent grain, a 1:1 ratio was used, and the results of co-digestion were compared with those from the control experiment, where the experiment contained only inoculum as a reference for methane production.

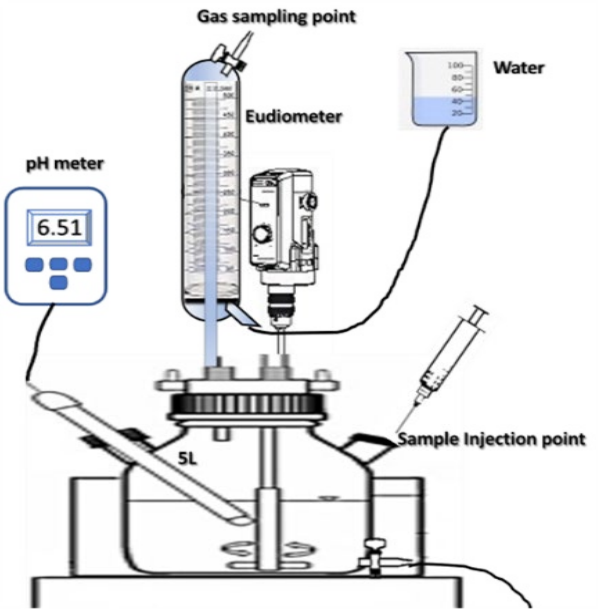


Figure 3.7: The semi-continuous test was conducted for 150 days.

3.10.2. Pilot trials

The semi-continuous pilot trials were carried out in 200 L digesters equipped with 50 L hydrolysis or feeder reactors, as shown in Figure 3.8. The idea behind the planning and fabrication of this digestor was to upscale and investigate a nearly industrial realistic output of the AD process. In a mono-digestion test, the digesters only handled substrate and then ran with co-substrate,) and their output was compared to each other, AD (mono-digestion) & ACD (Anaerobic Co-digestion). To prevent nutrient or metabolite fouling, Al bkoor Alrawashdeh et al., (2017) suggested mixing co-substrate with substrate before AD. The tendency of co-substrate adsorption of both nutrients and inhibitors poses no threat to the system since they can still be degraded by the introduced micro-organisms.

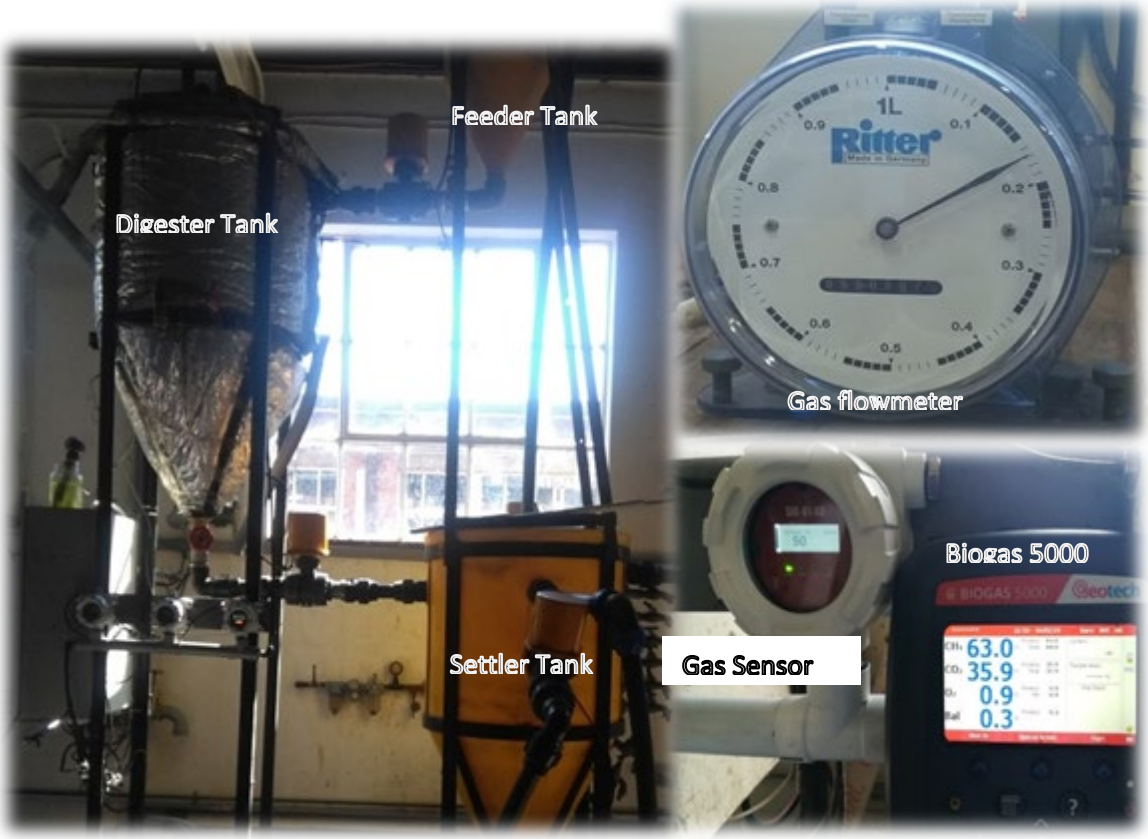


Figure 3.8: CSIR Semi-continuous Digester, Ritter gas flowmeter, and Geotech Biogas5000

Each cycle of the semi-continuous operation was for 24 hrs including the following steps: feeding (~1 hr); anaerobic digestion (23 hrs); and digestate draining (~1 hr simultaneously with feeding). Both digesters were filled with only inoculum and sealed at the beginning of the trial. The set-up includes; a 50 L hydrolysis unit operating at 37±1

℃, a vertical continuously stirred 200 L digester operating at 37±1 ℃, as well as a biogas flowrate meter. The temperature of the digester was supplied by a 75 W submersible heating element, and this was connected to a temperature controller. The operating volume of the digester hydrolysis unit was 42.5 L and the digester was 179.0 L. The hydrolysis tank was manually agitated by shaking twice a day; while the main digester was fitted with an IKA agitator that operates at 100 RPM.

The agitator was connected to an automatic timer switch that controls it's on and off behavior. The semi-continuous test was conducted for 200 days. The experimental investigation involves a start-up phase and 3 other major phases: digestion of solely sewage sludge phase; co-digestion of sludge with biowastes phase. The start-up phase requires gradually bringing up the digester to its full loading capacity and then adapting the microbial community to its daily dosage of a substrate. To adapt the microbial community to the new substrate as against its source, a low OLR was used as the initial feeding; the OLR was gradually increased until the starting inoculum was completely replaced, and the microbial population had been acclimated. To collect the biogas analysis, the sample was taken from the gas chamber/ eudiometer connected to the digester, the eudiometer reports the gas flow rate per day. The biogas composition data were collected on a daily basis using the Geotech Biogas 5000, UK as shown in figure 3.8. The instrument report on methane, carbon dioxide, and the percentage balance of the gas, other gases such as H_2S, H_2, and siloxanes.

For the first week, the OLR was set to 0.5 gVS/L.d and then increased iteratively according to Masebinu, (2018) procedure, as shown in Figure 3.9. The OLR was guided by volatile fatty acids to a total alkalinity ratio (VFA/TA). If the VFA/TA ratio was below 0.2 after a week, the OLR needed to be increased by 0.5 g VS/L.d for another week. However, if the VFA/TA ratio range was between the range of 0.2 and 0.4, the OLR needed to be maintained at 0.5 g VS/L.d. There are cases where the VFA/TA was above 0.4; in this scenario, pH was used as a guidance for OLR. When the pH of the material was between 6.5–7.0, the OLR was reduced by 0.5 g VS/L.d; for a pH below 6.5 but above 6.0, OLR was reduced by 1.0 g VS/L.d. If the pH was lower than 6.0, the feeding was stopped and the material was neutralized with an alkaline substrate until the pH was between 6.5 and 7.0.

The first phase following start-up was intended to investigate the yield potential of sludge. The second phase's co-digestion of sludge with biowastes was designed to acclimate the microbial population to the substrate prior to the start of AD loading. The final step, amended codigestion, was planned to see how effective AD is at fostering stability and increasing CH_4 concentration in biogas under conditions close to those found in a full-scale biogas plant. The findings of the amended digester were compared to those of the original digester.

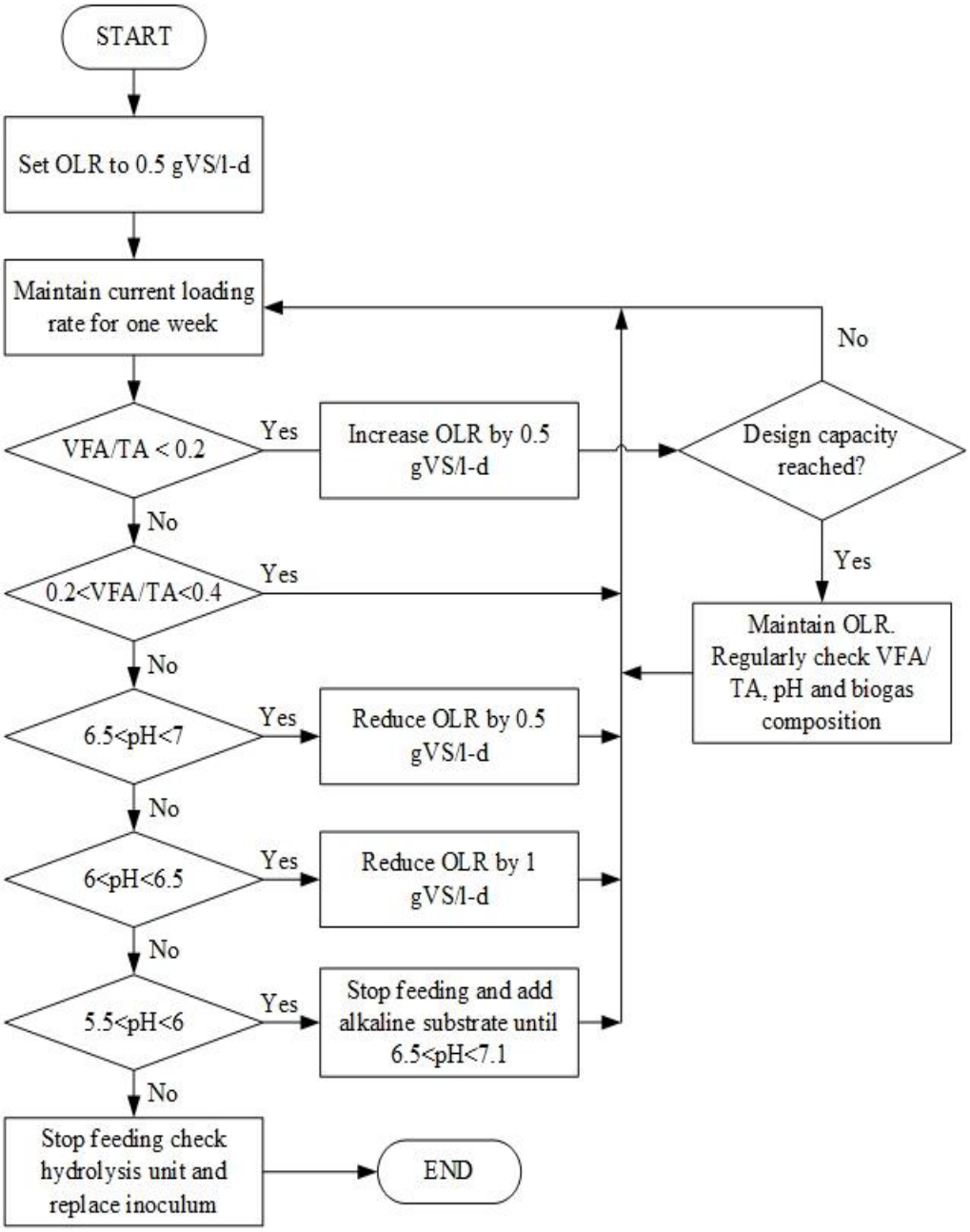


Figure 3.9: Procedure on how to adjust the OLR, adapted from Masebinu, (2018).

3.11. Synthesis of the sewage sludge-based activated carbon

The sludge-based activated carbon was produced using modified methods adapted from Wang et al., (2019). The sample was the non-digested and the digested material from the settling tank in the anaerobic digester system from the nearby municipality. The sample was dried in the atmosphere for at least 2 days until all the sample is moisture free. The portion of the sample was kept in the desiccator for characterization. The surface chemistry of activated carbon can be assessed by detecting specific functional groups using Fourier transform infrared spectroscopy (FTIR) XRF for elemental presence, SEM for morphology & BET for their surface area and porosity. Activated carbon porosity was assessed based on N_2-gas adsorption and desorption in the BET instrument.

Preparation of sludge-based activated carbon (SAC), (Wang et al., 2019)

1. The sample was washed with deionized water and ethanol to remove any dirt or inorganic contamination and dried at 60 °C oven until dry.
2. Crushed and pass through 1000-500 µm screens.
3. 50 grams of the material was introduced into a porcelain crucible, which was heated in a tubular reheating furnace applying a temperature program of pre-carbonized at 550 °C for 1 h under a nitrogen atmosphere.
4. The produced material was mixed with KOH and $ZnCl_2$ at the mass ratio (1:3:0, 1:3:1). Then the mixtures were heated to 800 °C for 2 h
5. The carbon materials were collected through repeated washing with the dilute HCl solution (2.0 M)
6. The adsorbed resulting material was centrifuged from the solution and calcined at 800 °C for 2 h in an N_2 atmosphere to regenerate the adsorbent.

And then the products were gathered by repeated washing with a high concentration of potassium hydroxide and distilled water. After drying at 105 °C, the Sludge-based Activated Carbon (SAC) was obtained as shown in Figure 3.10.



Figure 3.10: Sludge-based Activated Carbon (SAC)

3.12. The adsorption performance of the material

For the adsorption studies, a 100 mg/l solution of adsorbate (of Cd^{2+} or Cr^{6+} ion) was prepared by diluting 1000 mg/l stock solution. For this, an amount of 2.036 g of $CdCl_2$ and 2.748 g of $K_2Cr_20_7$ was dissolved in 1000 mL of deionized water, for Cd(II) and Cr(vi) respectively. The working solutions were prepared by diluting the stock solution and the pH was adjusted with HCl (0.1 mol/l) and NaOH (0.1 mol/l) solutions. The pH effect was evaluated by 50.0 mL of the ion solution with an initial concentration of 10 mg/l and pH ranging from 2.0 to 8.0. Aliquots of the prepared solution were placed in contact with SAC material and shaken for 2 hours in a shaker incubator at 25 °C. The remaining ion concentrations were determined by a HACH water quality analyzer (DR2800, U.S.A).

3.12.1. Batch adsorption study

The material was crushed and fractionated by sieving to obtain a 38-90 mm size fraction for the batch adsorption isotherm testing; this was done for all samples, including raw sludge, CGAC, and SAC material. After that, the media were thoroughly cleaned in ultrapure water, dried overnight at 105 °C, and stored in a desiccator until used in the adsorption capacity batch testing. To establish equilibrium isotherms, batch adsorption was performed at various initial concentrations of the adsorbate. Adsorption tests using

20 mg of SAC in 250 mL flasks filled with 200 mL of Cd^{2+} or Cr^{6+} ion solution at a concentration range of 1–5 mg/L at room temperature for 2 hours were carried out for isotherm studies. The solutions were filtered after reaching equilibrium, and the metal solution was examined with an ultraviolet-visible spectrophotometer (UV-vis) instrument. The number of ions adsorbed per mass unit of the SAC (mg/g) was calculated using the calculation given in Equation (6.1) to determine the adsorption capacity, the number of ions adsorbed per mass unit of the SAC (mg/g) was evaluated using the following expression:

$$Qe = \frac{(Ci - Ce)V}{M} \quad (3.8)$$

The removal percentage of the Cd^{2+} or Cr^{6+} ion was calculated as follows:

$$\%\, Removal = \frac{100\,(Ci - Ct)}{Ci} \quad (3.9)$$

Where Qe is the number of ions adsorbed at equilibrium (mg/g), Ci is the initial metal ions concentration (mg/L), Ce is the equilibrium metal ions concentration (mg/L), V is the volume of the aqueous phase (L) and M is the amount of the SAC material used (g).

The initial pH was adjusted to the required pH value (4–12) by using NaOH and HCl solutions. For adsorption kinetics, the mixture of the test solution 200 mL (5 mg/L) and SAC (20 mg) was stirred in a shaker at 25°C continuously for 2 h. Separate standard samples were drawn after 10, 15, 20, 30, 60- and 120-min intervals. The suspension was filtered and then analyzed using UV-Vis.

3.12.2. Batch equilibrium studies

Adsorption experiments were performed to investigate adsorption as a function of adsorbate solution pH (2-9), initial concentration (100-500 mg/L), temperature (25 °C and 35 °C), sorption time, and solution chemistry (i.e., the effect of coexisting ions).

In a typical batch adsorption equilibrium experiment, a specific amount of an adsorbent was contacted with a 50 mL solution contained in a plastic bottle and agitated in a thermostatic shaker operated at 200 rpm for the predetermined time interval, necessary to attain equilibrium. After attainment of equilibrium, the solution was separated from

the adsorbent through a 0.45 µm syringe filter and analyzed for a residual adsorbate concentration.

The adsorption kinetic experiments were evaluated using 1 L of adsorbate solutions at varying concentrations in a stirred reactor. For a given concentration of adsorbate solution, a fixed amount (g) of an adsorbent was added to the reactor and mixed by stirring to enhance adsorbent-adsorbate interactions. Subsequently, 6 mL solutions were collected at specific time intervals and filtered. The filtered solutions were then analyzed for residual adsorbate concentration.

References

Ahmadi, M., Bayati, N., Babaei, A. A., & Teymouri, P. (2013). Sludge Characterization of an Industrial Wastewater Treatment Plant, Iran. Iranian Journal Of Health Sciences, 1(2), 10–18. https://doi.org/10.18869/acadpub.jhs.1.2.10

Al-Addous, M., Saidan, M. N., Bdour, M., & Alnaief, M. (2018). Evaluation of Biogas Production from the Co-Digestion of Municipal Food Waste and Wastewater Sludge at Refugee Camps Using an Automated Methane Potential Test System. Energies, 12(1). https://doi.org/10.3390/en12010032

Al bkoor Alrawashdeh, K., Pugliese, A., Slopiecka, K., Pistolesi, V., Massoli, S., Bartocci, P., Bidini, G., & Fantozzi, F. (2017). Codigestion of Untreated and Treated Sewage Sludge with the Organic Fraction of Municipal Solid Wastes. Fermentation, 3(3), 35. https://doi.org/10.3390/fermentation3030035

Anup, B. N. (2018). Scanning Electron Microscope (SEM). Bioscience Notes.

Bodîrlău, R., Teacă, C. A., & Iuliana, S. (2009). Preparation and Characterization of Composites Comprising Modified Hardwood and Wood Polymers/Poly(Vinyl Chloride). BioResources, 4(4), 1285–1304.

Brame, J. A., & Griggs, C. (2016). Surface Area Analysis Using the Brunauer-Emmett-Teller (BET) Method: Scientific Operation Procedure Series : SOP-C. U.S Army Engineer Research and Development Center, September, 1–23. www.erdc.usace.army.mil.

Chang, V. S., & Holtzapple, M. T. (2000). Fundamental factors affecting biomass enzymatic reactivity. Applied Biochemistry and Biotechnology, 84(1), 5–37. https://doi.org/10.1385/ABAB:84-86:1-9:5

Deng, L. Y., Xu, G. R., & Li, G. B. (2010). Surface properties and adsorption characteristics to methylene blue and iodine of adsorbents from sludge. Water Science and Technology, 62(8), 1705–1712. https://doi.org/10.2166/wst.2010.372

Doloman, A., Soboh, Y., Walters, A. J., Sims, R. C., & Miller, C. D. (2017). Qualitative Analysis of Microbial Dynamics during Anaerobic Digestion of Microalgal Biomass in a UASB Reactor. International Journal of Microbiology, 2017. https://doi.org/10.1155/2017/5291283

Ferrasse, J., Akkache, S., & Roche, N. (2015). Thermochemical Conversion of Sewage Sludge by TGA-FTIR Analysis : Influence of Mineral Matter Added. Drying Technology: An International Journal, 1–9(July), 1–11. https://doi.org/10.1080/07373937.2015.1036283

Filer, J., Ding, H. H., & Chang, S. (2019). Biochemical Methane Potential (BMP) Assay Method for Anaerobic Digestion Research. Water, 11(921), 2–29. https://doi.org/10.3390/w11050921

Gerardi, M. H. (2003). The Microbiology of Anaerobic Digesters. https://doi.org/10.1002/0471468967

Kumar, R., Mago, G., Balan, V., & Wyman, C. E. (2009). Physical and chemical characterizations of corn stover and poplar solids resulting from leading pretreatment technologies. Bioresource Technology, 100(17), 3948–3962. https://doi.org/10.1016/j.biortech.2009.01.075

Lafi, R., Montasser, I., & Hafiane, A. (2019). Adsorption of congo red dye from aqueous solutions by prepared activated carbon with oxygen-containing functional groups and its regeneration. Adsorption Science and Technology, 37(1–2), 160–181. https://doi.org/10.1177/0263617418819227

Lee, R. A., Bedard, C., Berberi, V., Beauchet, R., & Lavoie, J. M. (2013). UV-Vis as a quantification tool for solubilized lignin following a single-shot steam process. Bioresource Technology, 144, 658–663. https://doi.org/10.1016/j.biortech.2013.06.045

Litefti, K., Freire, M. S., Stitou, M., & González-Álvarez, J. (2019). Adsorption of an anionic dye (Congo red) from aqueous solutions by pine bark. Scientific Reports, 9(1), 1–11. https://doi.org/10.1038/s41598-019-53046-z

Liu, Y., Cheng, H., & He, Y. (2020). Application and mechanism of sludge-based activated carbon for phenol and cyanide removal from bio-treated effluent of coking wastewater. Processes, 8(1). https://doi.org/10.3390/pr8010082

Lu, X., Jin, W., Xue, S., & Wang, X. (2017). Effects of waste sources on performance of anaerobic co-digestion of complex organic wastes: Taking food waste as an example. Scientific Reports, 7(1), 1–9. https://doi.org/10.1038/s41598-017-16068-z

Lupoi, J. S., Singh, S., Simmons, B. A., & Henry, R. J. (2014). Assessment of Lignocellulosic Biomass Using Analytical Spectroscopy: An Evolution to High-Throughput Techniques. In Bioenergy Research (Vol. 7, Issue 1). https://doi.org/10.1007/s12155-013-9352-1

Mandal, S. De, Chatterjee, R., & Kumar, N. S. (2017). Dominant bacterial phyla in caves and their predicted functional roles in C and N cycle. 1–9. https://doi.org/10.1186/s12866-017-1002-x

Masebinu, S. O. (2018). Anaerobic Digestion Process Stabilisation and in-situ Upgrading of a Biogas System. University of Johanneburg.

Morales-Polo, C., Cledera-Castro, M. del M., & Soria, B. Y. M. (2019). Biogas production from vegetable and fruit markets waste-compositional and batch characterizations. Sustainability (Switzerland), 11(23). https://doi.org/10.3390/su11236790

Odnell, A. (2018). Influencing anaerobic digestion early stage processes for increased biomethane production from different substrate components (Issue 1807). Linköping University, Sweden.

PacBio. (2015). PacBio Sequel Systems - PacBio. https://www.pacb.com/products-and-services/sequel-system/

Pan, W., Xu, W., & Li, S. (2005). Fundamentals of TGA and SDT. Thermal Analysis. Fundamentals and …, 1–7. http://dialnet.unirioja.es/servlet/articulo?codigo=1986690

Ramdani, N., Hamou, A., Lousdad, A., & Al-Douri., Y. (2015). Physicochemical characterization of sewage sludge and green waste for agricultural utilization N. Environmental Technology, 36(12), 1594–1604. https://doi.org/10.1080/09593330.2014.998716

Regueiro, L., Carballa, M., & Lema, J. M. (2014). Outlining microbial community dynamics during temperature drop and subsequent recovery period in anaerobic co-digestion systems. Journal of Biotechnology, 192(Part A), 179–186. https://doi.org/10.1016/j.jbiotec.2014.10.007

Rozzi, A., & Remigi, E. (2004). Methods of assessing microbial activity and inhibition under anaerobic conditions: A literature review. Reviews in Environmental Science and Biotechnology, 3(2), 93–115. https://doi.org/10.1007/s11157-004-5762-z

Vítěz, T., Haitl, M., Karafiát, Z., Mach, P., Fryč, J., Lošák, T., & Szostková, M. (2011). Use of bio-enzymatic preparations for enhancement biogas production. Acta Universitatis Agriculturae et Silviculturae Mendelianae Brunensis, 59(3), 203–208. https://doi.org/10.11118/actaun201159030203

Wang, Y., Zhao, W., Zheng, W., Chen, S., & Zhao, J. (2019). Preparation of N-doped carbon nanosheets from sewage sludge for adsorption studies of cr(VI) from aqueous solution. Nanomaterials, 9(2). https://doi.org/10.3390/nano9020265

Williams, P. T., & Besler, S. (1993). Thermogravimetric Analysis of the Components of Biomass. Advances in Thermochemical Biomass Conversion, 2, 771–783. https://doi.org/10.1007/978-94-011-1336-6_60

Yao, S., Wang, M., Liu, J., Tang, S., Chen, H., Guo, T., Yang, G., & Chen, Y. (2018). Removal of phosphate from aqueous solution by sewage sludge-based activated carbon loaded with pyrolusite. Journal of Water Reuse and Desalination, 8(2), 192–201. https://doi.org/10.2166/wrd.2017.054

CHAPTER 4

ANAEROBIC CO-DIGESTION OF SEWAGE SLUDGE WITH DIFFERENT BIOWASTES TO ENHANCE BIOGAS PRODUCTION

This chapter provides insights into the physicochemical analysis of the parameters that catalysize and those that can inhibit anaerobic digestion. This chapter also evaluates the impact of co-digestion to enhance methane production when using sewage sludge as primary substrate & biowaste as co-substrate. Should the enhancement be achieved, the research study aims to quantify the enhancement effect and assess the mechanism.

4.1. Introduction

In South Africa, sewage sludge (SS) generated from municipal waste water treatment works (WWTW) remains a challenge. Most urban SS in the country is treated improperly prior to discharge (Mitchell et al., 2014; Van der Merwe-Botha et al., 2016). This is due to the fact that most WWTWs lack trained operators and inadequate wastewater capital and operating funds. There is also a lack of planning to provide for the constant increase in urbanization, as well as a lack of human resources and technical skills (Ntombela et al., 2016). Studies have shown that a substantial number of wastewater treatment works run by municipalities in Gauteng are producing effluent that does not meet DWAF standards. Some of the works produce effluent of low-quality by-products that are released into the environment (Herbig, 2019; Masindi et al., 2018; WRC, 1997). This is mostly the case with underperforming WWTPs, for which some of the reasons are: unplanned treatment loads exceeding treatment capacity, underbudgeting by the municipality for wastewater equipment maintenance, and the use of personnel with insufficient understanding of the technology of wastewater treatment (Herbig, 2019; Ntombela et al., 2016).

Due to various industrial processes, water is contaminated with undesirable compounds. These toxic compounds are harmful to people, animals, and the environment. However, these toxic harmful bacteria can otherwise be utilized in renewable energy production (Wirth et al., 2012). Renewable energy production is currently a major issue worldwide and in South Africa (Department of Energy, 2017). Its usage will relieve countries from non-renewable sources that heavily pollute the environment and compromise their ability

to foster life (Department of Energy, 2019). The current National Development Plan goals are to procure at least 20,000 MW of renewable electricity by 2030 (National Planning Commission, 2010).

These intermediate products are further oxidized to acetate and H_2 by homoacetogenic and obligatory H_2-producing bacteria in the acetogenesis stage, respectively (Doloman et al., 2017). In the final step, methanogenesis, acetate, and H_2 are metabolized into CH_4 by acetolactic and hydrogenotrophic methanogens. The acetolactic methanogen uses only acetic acid in the formation of CH_4, whereas hydrogenotrophic methanogen uses H_2 and CO_2, as shown in Figure 4.1.

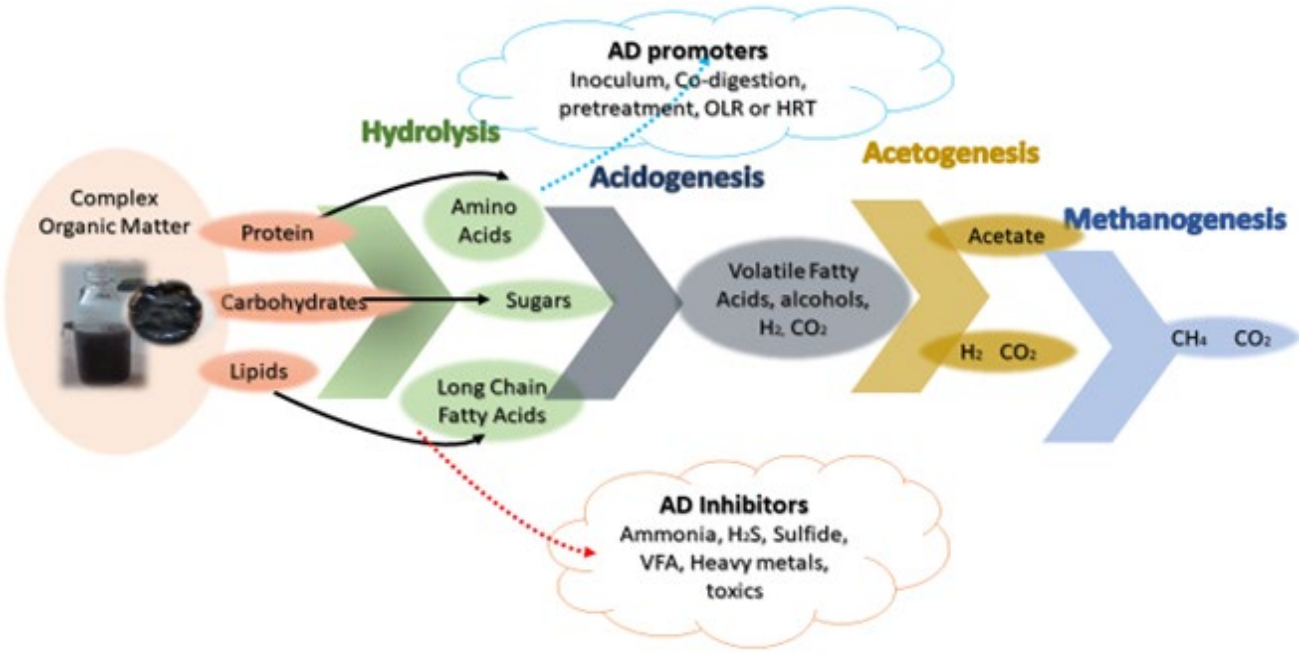


Figure 4.1: A simplified schematic presentation of the anaerobic digestion phases, adapted from (Salihi et al., 2018)

A common problem usually encountered in biogas production is low biogas yield due to the use of single feedstock, i.e., sewage sludge. Too often, sludge is either recalcitrant to digestion or has a low or high C/N ratio. This can be improved by co-digesting the sludge with a co-substrate that increases the conversion of organic solids to biogas, thus increasing the production of methane. This will, in turn, boost energy production, making it possible to offset the required energy in the WWTWs' processes (Martínez et al., 2016; Zahan et al., 2016). Anaerobic co-digestion (ACD) is a practice that includes the mixing of

more than two different feedstocks (Jeung et al., 2019). ACD has recently been proposed as a solution to the limitation of sewage sludge mono-digestion. Low organic load, poor C/N ratio, and low alkalinity are all characteristics of SS. Heavy metals, sulphates, and ammonia are also found in sludge; these act as AD inhibitors (Singh et al., 2019). The addition of a substrate may improve process stability by improving nutrient balance and diluting inhibitory substances in the feedstock (Dido et al., 2014; Oliveira et al., 2018).

Brewery spent grains (BSG) are high in protein, lignocelluloses, and moisture, making them susceptible to microbial degradation. They also have a high C/N ratio and significant alkalinity, as well as a significant amount of easily biodegradable organic matter (Szaja et al., 2020). BSG is a major by-product of the beer-brewing industry and is thus regarded as waste. Therefore, it is not limited by cost or seasonality; it is readily available in large quantities. BSG can be produced from a variety of sources, including breweries, the ethanol industry, and households. The chemical composition of different sources of BSG varies depending on the chemical content of the parent feedstock. Due to the limited biodegradability of lignin, which results in low biogas yields and requires an extended hydraulic retention time (HRT), the mono-digestion of BSG is ineffective (Szaja et al., 2020). However, SS contains inorganic compounds that can disrupt the naturally ordered structure of BSG and remove lignin to make it less recalcitrant to biodegradability (Jojima et al., 2014; Lijó et al., 2015).

The objective of this study is to evaluate the impact of anaerobic co-digestion on methane production from sewage sludge and brewery spent grain blend. This paper focuses on a physicochemical and metagenomics synergy analysis, especially in relation to the microbial communities that influence or inhibit the production of biogas.

4.2. Materials and Method

Please refer to Section 3.1-3.5 and Section 3.7-3.10 for information on materials and methods

4.3. Results and Discussion

4.3.1. SEM Imaging

A scanning electron micrograph (SEM) was carried out to evaluate the morphology of the materials from a microbiological point of view. The micrographs were obtained from native sewage sludge and digested sewage sludge, according to the methodology described earlier in Section 3.6. These micrographs were selected in order to show a representative image of the observed structures; the magnification may differ in order to highlight certain areas of interest. Since organic samples are sensitive and could easily react to the effect of the electron beam, the SEM used is a new generation microscope equipped with analytical techniques sufficient for the complete characterization of a wide range of materials. It is made to reduce the sample vacuum, avoid surface damage, be electrically conductive, void of free particles, and be volatile matter-free. Additionally, the reduced electron beam was used, and it was optimized so that image resolution did not suffer as a result.

As shown in Figure 4.2a microscopic observations showed that the raw sewage sludge exhibited a structure with a rough and granular texture, with a large amount of open porosity. This is similar to the images reported by Han et al. (2011) and Yan et al. (2009). Figure 4.2a shows that large amounts of hydration products cover the surface of sludge particles. Figure 4.2b shows an excessive growth of filamentous microorganisms after anaerobic digestion. Different groups of filamentous bacteria were present, but no dominant type of morphology was observed. As a result, floccs are present in a skeleton form of structure which promotes the attachment of other microorganisms by their extracellular polymeric substances, according to the mechanism which was suggested by Alemahdi et al. (2012). Similar SEM images of wastewater sludge were described by the same source. It is well known that a large filamentous population causes detrimental effects on liquid waste treatment systems due mainly to the loss of sludge settling (bulking) and foam generation. However, relatively little is known regarding the factors that affect the growth of these filaments.

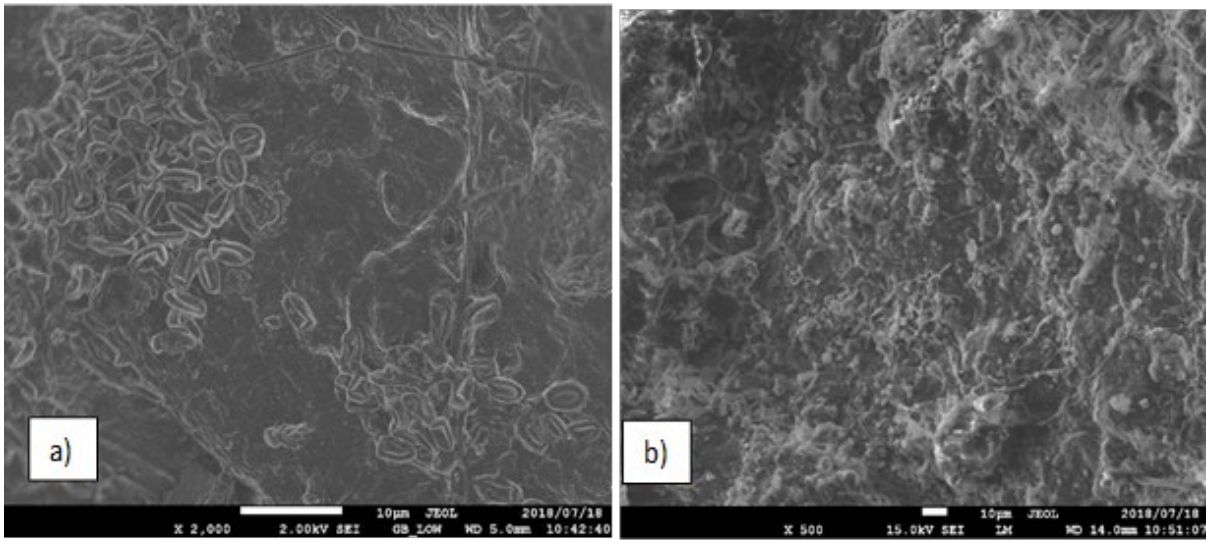


Figure 4.2: SEM micrographs of sewage sludge a) Raw sludge before anaerobic digestion b) Digested sewage sludge.

4.3.2. Taxonomic Profile of the Microbial Community

The taxonomic distribution of the microbial community indicated that the most abundant domain was the Bacteria (Figure 4.3), followed by the Archaea (Figure 4.5). This analysis reveals that 94 of the amplicons were of bacterial origin, whereas only one amplicon could be assigned to the kingdom of *Archaea*. *Proteobacteria* was most abundant followed by the group of *Bacteroides, Firmicutes, and Actinobacteria*. Among the *Proteobacteria* subclass, *Alpha-* and *Delta-* were more dominant than *Gamma-* and *Beta-proteobacteria*. The genera that dominated were *Dechloromonas Propionivibrio*, and *Nitrospirathere*. There is an acceptable count of methanogens and other species. Some of the sequences belong to the phylum *Spirochaetae*, with the most abundant class being *Anaerolineae*. This class contributed to the majority of the Bacteria domain in the sludge sample. In the Archaeal domain, the most abundant family was the *Methanomicrobiales*. These species have been identified frequently in the anaerobic digestion of sewage sludge and food waste (Cuetos et al., 2017; Siddique & Wahid, 2018; Wirth et al., 2012).

Besides the appearance of *Proteobacteria,* there was an appearance of *Nitrospirae*, which uses urea as a source nutrient and converts it to carbon dioxide (CO_2), which then reacts with hydrogen (H_2) to form methane (Derilus et al., 2019). As indicated in Figure 4.4, about 5.61% of *Firmicutes* are unclassified; these are Gram-positive bacteria known for carbohydrate metabolism (Campanaro et al., 2016). Further sequences were assigned to the class *Bacteroidetes*, which is similar to *Firmicutes*; these are known for breaking down

carbohydrates into simple sugars. Additionally, *Bacteroidetes* are good energy converters and amino acids metabolizers; hence, they appear frequently during AD and biogas production (Treu et al., 2016). The phylum *Chloroflexi* and the class *Actinobacteria* were identified as non-abundant taxa. Only a few sequences could be allocated to lower taxonomic ranks such as 'family' or 'genus' (W. Zhang et al., 2015).

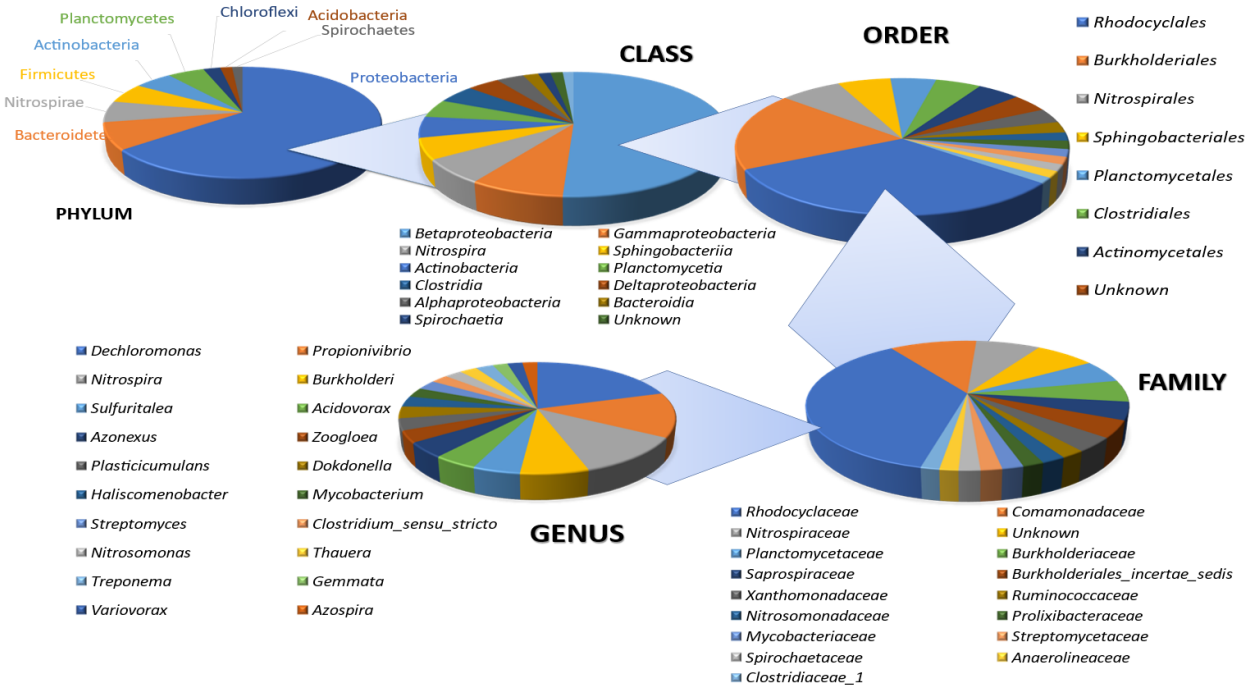


Figure 4.3: The Bacterial community composition classified as phylum, class, order, family, and genus; the taxonomic distribution of the microbial community in the sewage sludge sample

4.3.3. Microbial Community in Anaerobic Digestion

Anaerobic degradation requires the participation of various bacterial species, and each step is driven by a group of microorganisms such as hydrolytic, acid-forming, acetogenic, and methanogenic archaea that produce carbon dioxide (CO_2) and methane (CH_4) as end products (Ghosh et al., 2020). The first step in anaerobic degradation is the hydrolysis of complex organic substrates, which involves the breakdown of large molecules (Jingura & Kamusoko, 2017; Oladejo et al., 2019). The communities of bacteria that are involved in this step are identified by efficient hydrolysis of plant biomass that is rich in lignocellulose. Most of these bacteria belong to the classes of *Clostridia* and *Bacilli*. As expected, the overwhelming majority of the identified abundant species in the AD system are members of the *Betaproteobacteria* (36.61%), *Clostridia* (14.81%), and *Bacilli* (6.18%) classes, together with members of the *Mollicutes* (1.75%), *Gammaproteobacteria* (3%),

and *Actinobacteria* (5.09%) classes (Figure 4.4). Among the *Clostridia, Clostridium thermocellum* occurred most frequently and, in the *Bacilli* family, *Bifidobacterium* dominated. This species can hydrolyze cellulose efficiently by means of its extracellular cellulases, which are organized into cellulosomes (Mandal et al., 2017).

Literature reports that the predominant species are likely to change significantly during the initial 15 days of digestion, Chow et al., (2020) reports that there is a significant percentage increase of *Firmicutes* and *Chloroflexi* (from 15.65% to 22.6% and 9.34% to 20.27%, respectively). Ziganshin *et al*. 2017 and Regueiro *et al*. 2006 reported that *Firmicutes* and *Chloroflexi* efficiently hydrolyze refractory cellulose and carbohydrates into soluble acidic during anaerobic digestion which might be the main reason for the significant decomposition of those polymer organics during the first days of digestion.

The second stage is acidogenesis, in which the acid-forming bacteria ferment the hydrolytic products into volatile fatty acids, acetate, and hydrogen (Ghosh et al., 2020; Wirth et al., 2012). In this study, the phyla that contain many known species of acidogens are *Proteobacteria* (61.93%), *Firmicutes* (5.61%), *Bacteroidetes* (5.54%), and *Chloroflexi* (2.28%) were identified. Under the phylum *Proteobacteria, Betaproteobacteria* dominated the most, in *Firmicutes Lactobacillus* gave the highest read count and *Anaerolinaceae* in the phylum *Chloroflexi. Acidovorax* dominated the phylum *Actinobacteria* and a few thermophilic bacteria.

The fermentation pathways yield organic acids such as acetate and butyrate or acetone, butanol, and ethanol (Wirth et al., 2012). The phylum *Firmicutes* and *Proteobacteria* belong to the genera *Syntrophomonas* and *Syntrophobacter* which generates lactate, acetate, and butyrate from sugars, and through its hydrogenase process, which also produces H_2. Similarly, to *C. thermocellum, C. cellulolyticum* is a well-known strain that degrades cellulose to acetate and evolves CO_2 and H_2. *C. saccharolyticum* additionally possesses cellulolytic activity. The fermentation products include acetate, ethanol, H_2, and CO_2. The last stage is methanogenesis in which the most commonly observed methanogenic genera such as *Methanolinea, Methansaeta,* and *Methanospirillum* produce methane (Cuetos et al., 2017; Siddique & Wahid, 2018). The archaea community hydrogenotrophic methanogen genus enrichment of methanogens such as *Methanobacterium, thermoautotrophicum, Methanosarcina barkeri*, and *Methanobacterium wolfei*.

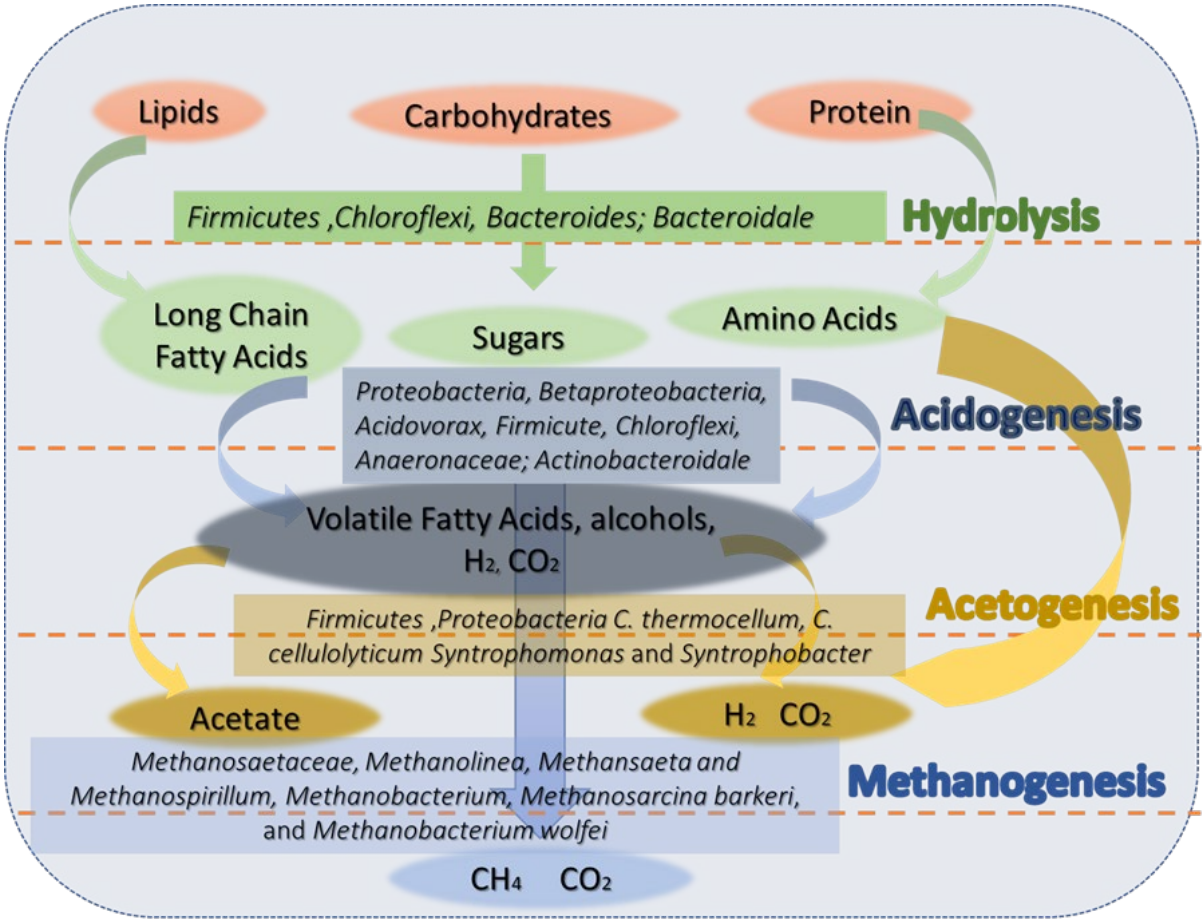


Figure 4.4: The microbial metabolic pathway during anaerobic digestion constructed using the most abundant AD species.

4.3.4. Archaeal community composition.

As shown in Figure 4.5, *Methanosaetaceae*, producing CH_4 utilizing acetic acid, H_2, and CO_2, was the dominant species in the anaerobic digester. The percent abundance of acetoclastic *Methanosaetaceae* increased is 49.75% in the sewage sludge digestion sample, almost reaching the required maximum methane productivity, 60%. In comparison, the abundance of hydrogenotrophic methanogens of *Methanobacteria* and *Methanomicrobiales* was reported to be 23.54% and 43.41%, respectively, demonstrating that hydrogenotrophic methanogenesis has a great potential to play a great role during the conversion of those hydrolyzed organics into CH_4. In addition, the percentage of *Methanocellaceae* (the dominant acetoclastic group) is 3.24%.

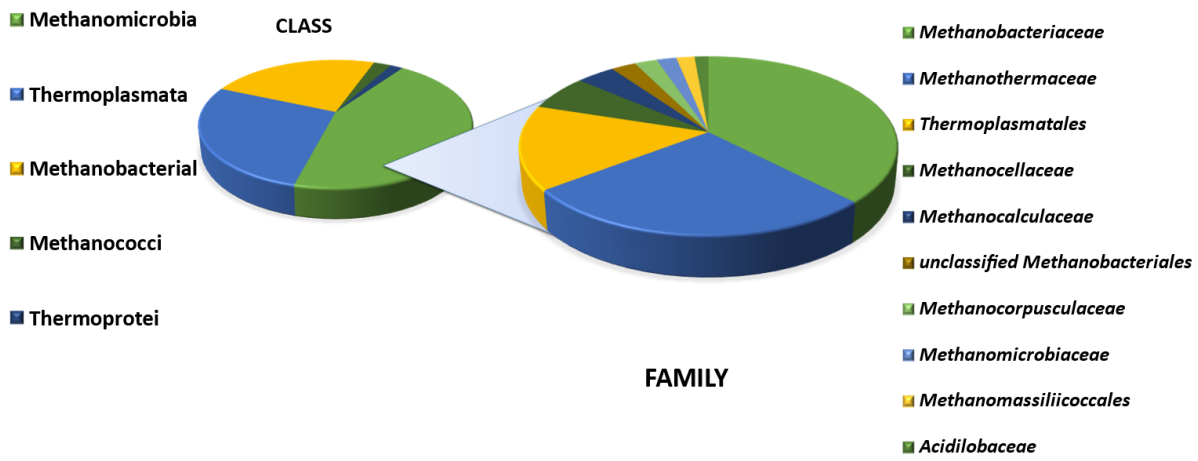


Figure 4.5: Kingdom Archaeal community composition in the classification of class and significant family.

4.4. Anaerobic Co-digestion experiments

4.4.1. Physicochemical characteristics of co-substrates

The importance of feedstock analysis in the AD phase cannot be overstated. The amount and composition of biogas produced, as well as the amount of energy in the biogas, are all calculated using general characteristics or, more specifically, the composition of the substrate (feedstock) (Rabii et al., 2019). The quality of biogas generated, particularly methane, is largely determined by the feedstock characteristics during anaerobic digestion. The primary characteristics of the individual co-substrates are collated in Table 4.1. In this study, the parameters of interest are TS, VS, C/N ratio, COD, TA, and pH.

A clear distinction between each co-substrate is the COD, TS, and VS contents is noticed. Higher TS is noticed from the molasses, spent grain & manure commercial sample, this could be due to the nature of a substrate, manufacturing process, or storage as noted. Molasses is naturally a dense brown liquid or a thick syrup made from boiling down sugar cane. The spent grains are the major by-product of the beer-brewing industry and are collected after beer extraction by the filtration process. Dry stacking manure is the most common and practical method of manure storage for abattoirs and livestock farms. The implication of the higher solids content is a greater propensity to contribute to biogas production, especially in the AD processes where feed requires thickening.

To stabilize the anaerobic digestion process required C/N (carbon to nitrogen) ratio should be between 15 and 30 (B. Wang, 2016). The C/N ratio in sewage sludge is less

than ideal. Spent grain, on the other hand, is outside of the ideal range. Brewery spent grains, fresh produce waste, and food waste are lignocellulosic materials that contain a significant amount of carbon and are resistant to degradation, slowing the pace of decomposition (Mudzanani et al., 2019). However, when blended at a 1:3 ratio, the resulting C/N has the potential to favour anaerobic digestion and thus increase methane production. It should be noted that co-substrate selection is also influenced by sourcing considerations. As mentioned before all other co-substrates are essentially waste materials. As a consequence, their properties may be subject to considerable temporal and spatial variation.

Table 4.1: Composition of raw sludge and co-substates

Substrates	Nutrients		Organic matter	Buffering Capacity	C/N Ratio	Physical	
	COD(mg O2/L)	VS (% TS)	Organics (%)	TA (mg/kg)	C/N ratio	TS (%)	pH
Sugar Cane Molasses	362 562	59	25	31634	16.4	42	5
Fresh Produce Waste	56 020	89	9.57	672	46.3	11	5.9
Brewery Spent grains	23 997	91	20.2	8690	25	22	5.12
Animal Manure	89 420	80	23	584	19	23	6.3
Fresh produce Waste	55 400	87	14	467	17	10	7.4
FOG (lipids)	715	68	3.3	787	10.6	4.8	7.1
Ice cream Waste	6 819	62	4	89	18.1	4	7.5
Food Waste	45 900	87	14	467	17	10	7.4
Soft drink waste	42 800	98	21	2.8	14	2.3	4.2
Dairy fermentation residues	34 600	83	17	308	9.6	4.8	4.8
Dairy thick waste	43 300	73	27	1998	23	29	6.8
Slaughter waste (Fats)	4 670	81	12	787	12	4.8	6.3
Slaughter waste (Blood, Content)	6 570	89	6	697	18	11	7.8

Each BMP mix was created differently depending on the inoculum and substrate concentrations to ensure that the BMP was carried out in settings that did not limit or obstruct the anaerobic digestion process. This entails changing the inoculum and test material volumes until the substrate to inoculum ratio, as well as the headspace to total solution volume, are all within the specified parameter limits. Table 4.2 gives the nutrient composition of the samples to assist in the design of the experiment. From the VS results, it can be predicted by now that NW5 will produce the highest methane than the other two raw sewage sludge in mono-digestion experiments. In co-digestion, Driefontein sludge combined with spent grains, fresh produce waste, or molasses is predicted to give a good enhanced methane production.

Table 4.2: Composition of the blends (on 1:3 ratio) sewage sludge & co-substrates for co-digestion experiments.

Raw Samples			CoT co-digestion		NW co-digestion	
Sample ID	TS (%)	VS (%)	TS (%)	VS (%)	TS (%)	VS (%)
(City of Tshwane) CoT	3.1	98.51	3.1	98.51	n/a	n/a
(Northern Works) NW	7.36	88.64	n/a	n/a	7.36	88.64
Inoculum	0.64	5	n/a	n/a	n/a	n/a
Spent Grains	21.71	91.51	16.91	98.51	9.04	93.58
Fresh produce	11.43	89.57	7.27	94.04	9.40	89.11
Food waste	10.24	86.59	4.67	91.76	6.80	86.83
Thick Dairy waste	29	72.81	11.75	97.25	8.7	86.62
Dairy waste 2	4.8	83.58	5.75	98.05	7.88	93.11
Manure	23.43	80.41	5.27	93.61	7.40	88.68
Molasses	41.85	58.71	6.10	95.58	8.23	90.64
Soft drink drain waste	2.28	98.45	2.70	98.48	4.83	93.55

4.4.2. Batch studies, Sludge, and Co-substrates

The assessments for biogas accumulation profiles along with their corresponding profiles for the blank and control assays are presented. The units are normal litres of biogas in a mass of volatile solids content in the substrate per retention time (number of days). In this project, the methane gas is considered normalized to STP (0 ℃ and 101 325 N/m^2) and it is assumed to be a dry gas. From the triplicates, the mean specific biogas (NL biogas/kg VS) was calculated and then plotted. The initial pH of the feedstock was low during the preparation of the feed and thus buffer agent solutions were used to maintain the pH at 6.5-7.5. In this run, the digestion experiment was completed after 31 days.

4.4.2.1. Co-digestion with high solid content wastes

Figure 4.6a shows that as the molasses fraction increased, accumulated methane output increased for both CoT and NW co-digestion. The addition of a co-substrate from 5% to 25% (M-NW) above the optimum point increased the overall methane production. Figure 4.6a, which shows an increase in production and M-NW25% molasses concentration, demonstrates the pattern. Organic loading rate, TS & COD for the anaerobic system assisted this enhancement. This is supported by the study done by Doloman et al., (2017) and Kalemba & Barbusiński, (2017). However, this was not the case for CoT sludge, the same molasses concentration (M-NW25%), achieved lower methane enhancement. This might be due to excessive development and accumulation of volatile fatty acids which resulted from a high carbon/nitrogen stoichiometric ratio. Fatty acid accumulation causes a drop in pH, which inhibits microbiological activity (Babaee et al., 2013; Yue Zhang et al., 2012). Figure 4.6 shows the findings of cumulative biogas production profiles for mono-digestion of sewage sludge and spent grain, as well as co-digestion at a 1:3 ratio. As shown in Table 4.1, the C/N ratio and TS of both feedstocks were beyond the optimal range for AD when used separately, but they were inside the optimal range when combined, the same results have been reported in previous studies (Wei et al., 2019).

The addition of the co-substrate BSG fraction of 25% (BSG-NW and BSG-CoT) did not result in an excessive build-up of volatile fatty acids, and the produced acids had enough time to be digested, See Figure 4.6b. For these co-substrate samples, the removals of TS and VS were found to be about 61 and 47%, respectively. These findings suggest that using BSG as a co-substrate would result in more biosolids development. The co-

substrates had a methane capacity of around 39 & 78 NLCH4/kg VS, respectively. As a result, the biogas production was increased in volume using co-digested samples as compared to sewage sludge alone.

The highest BMP was obtained with co-digestion of NW sludge and 25% BSG, producing approximately 80 NL/kg VS. This is a 3-fold increase when compared to the assay of sludge mono-digestion. The methane production was stabilized from days 1-5, sharp increasing for another 5 days until it stabilizes again, reaching the maximum methane on day 31 (Figure 4.6b). The improvement in methane production could be attributed to the favourable balancing out of the C/N ratio, TS, and the microbial (Ghosh et al., 2020; Wirth et al., 2012). As a result of the following degradation of VFAs by methanogens, co-digestion enhances the organic matter accessible as volatile fatty acids (VFAs) and biogas productivity (Ruan et al., 2019). Furthermore, in the microbiological interpretation co-digestion is the introduction of the hydrolytic-acidogens species which increases the biodegradability of the blend (Xue et al., 2019a). During the steady-state phase, it was also noted that Proteobacteria became the most common phylum, and hydrogenotrophic methanogens dominated over acetoclastic methanogens (Goswami et al., 2016).

Approximately 37.49, 36,45, and 38.5 Nl/kg feed of methane were produced from co-digestion of NW and CoT sewage sludge with different concentrations of animal manure & feeding wastes sourced from an abattoir (AM-NW 5, AN-NW25, and AM-CoT 25) mixed at 5 & 25% respectively. These results are consistent with data from the literature (Dioha et al., 2013; Y. Liu et al., 2014; Nielfa, Cano, Pérez, et al., 2015). It can be observed in Figure 4.6c that methane production was stagnant from day 1 until 5 and started to increase rapidly from day 6 until the production stops on day 16, a slight decrease was observed after day 21. Jung et al., (2019) and Tyagi & Lo, (2011) substantiate that the no production for the first five days could be due to the intra and intermolecular hydrogen bonds that create crystal structure molecules. In addition, the presence of low soluble COD and lignocellulose in the grains increase biodegradability resistance and a slower rate of biodegradation (Yu Zhang et al., 2011).

The methane yield of all organic waste co-substrates was higher than that of merely wastewater sludge. However, when the co-digestion ratio was 5% and 25% (wt/wt), organic overloading was detected for food waste in both test periods (Figure 4.6d).

When the co-digestion ratio was set to 25%, biogas production for FW-NW was significantly lower. At a 25% co-digestion ratio, anaerobic digestion inhibition was also found with manure. Inhibition at high concentrations of food waste co-digestion ratios was related to the build-up of volatile organic acids, as demonstrated by a low pH (less than 5) of the substrate at the end of the experiments of all BMP bottles with poor methane production, similar to the findings published by Rea, (Jia et al., 2019).

All organic waste co-substrates increased the methane yield above that of only wastewater sludge. However, organic overloading was observed for food waste on both sampling occasions when the co-digestion ratio was 5% and 25% (wt/wt) (Figure 4.6d). Indeed, biogas production for FW-NW was substantially lower when the co-digestion ratio was 25%. Anaerobic digestion inhibition was also observed with manure at the co-digestion ratio of 25%. Similar to the results reported by Rea, (2014), it was observed that inhibition at high concentration of food waste co-digestion ratios was attributed to the build-up of volatile organic acids, evidenced by a low pH (less than 5) of the substrate at the end of the experiments of all BMP bottles with poor methane production" (Li et al., 2015)."

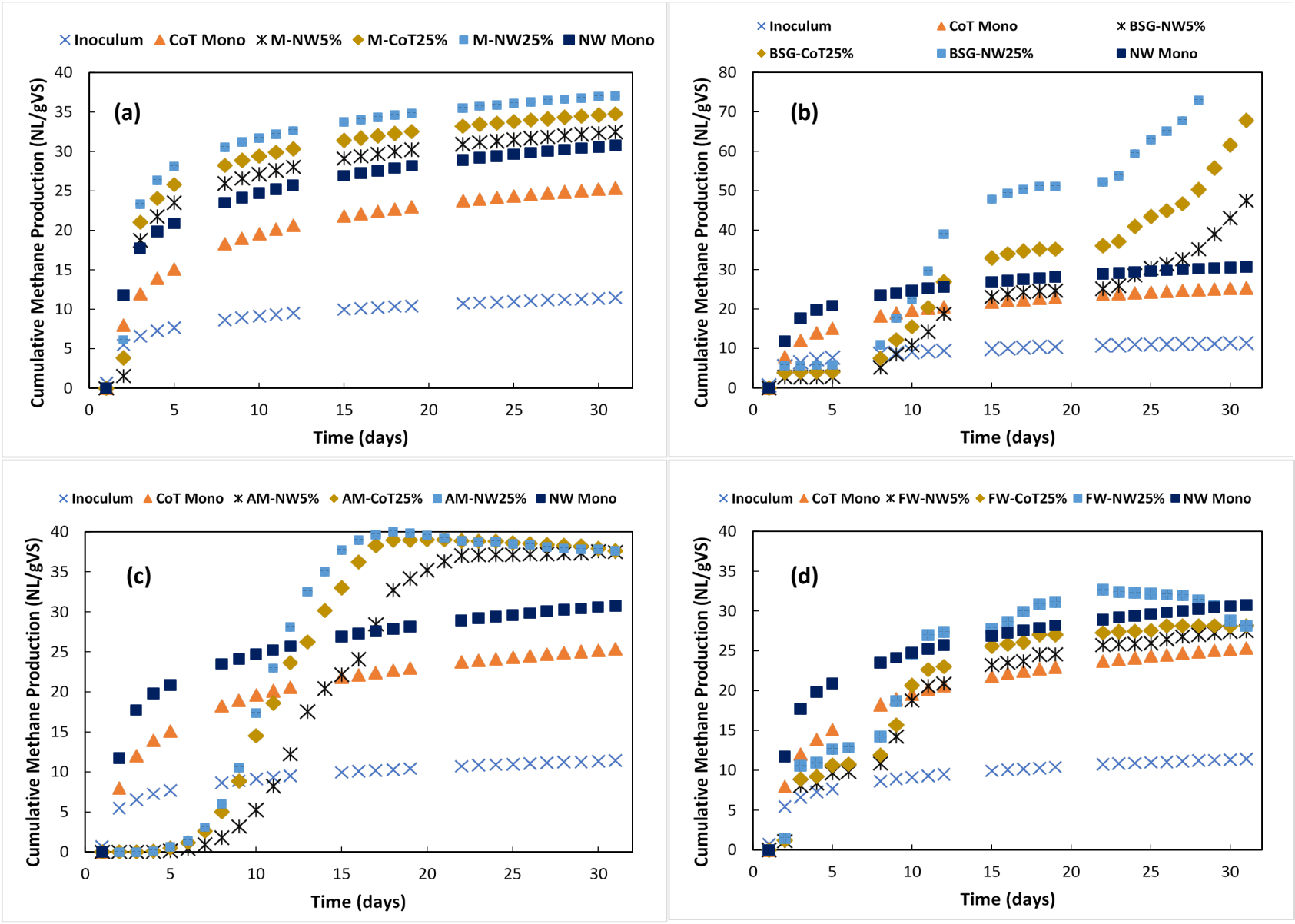


Figure 4.6: Cumulative methane production for co-digestion of sludge and (a) Molasses (b) BSG, spent grains (c) AM, animal manure (d) FW, food waste

Temporal variability of VS and COD of the food waste was observed between the two sampling occasions. Variations in VS and COD values of the two food waste samples were 20 and 65%, respectively. The co-digestion ratio of 5% was suitable for both occasions. Temporal variation in VS and COD content (10 and 90%, respectively) could also be seen with the fresh produce waste samples. Nevertheless, the fresh produce wastes samples did not display any inhibition even at the co-digestion ratio of 25%, see Figure 4.7a.

Whilst the dilution conducted prior to collection proved effective in reducing the inhibition potential, at the same co-digestion ratio the maximum achieved biogas production was lower than that of food waste. Both food & fresh produce waste are food waste materials. In other words, both co-substrates are expected to be similar in composition, and thus should yield similar methane productions. Consequently, a higher co-digestion ratio between co-substrate and sludge would be required to validate the effectiveness of dilution of this co-substrate.

The BMP results from the co-digestion of dairy thick waste (Figure 4.7b) show a continual increase in biogas production as the co-digestion ratio increases. The rate of dairy thick waste hydrolysis may be responsible for the production of volatile fatty acids is faster. Thus, even a low co-digestion ratio of dairy thick waste and sludge did not result in volatile fatty acid accumulation in the system. It is also noteworthy that the benefit of adding additional concentrations beyond 5% was negligible.

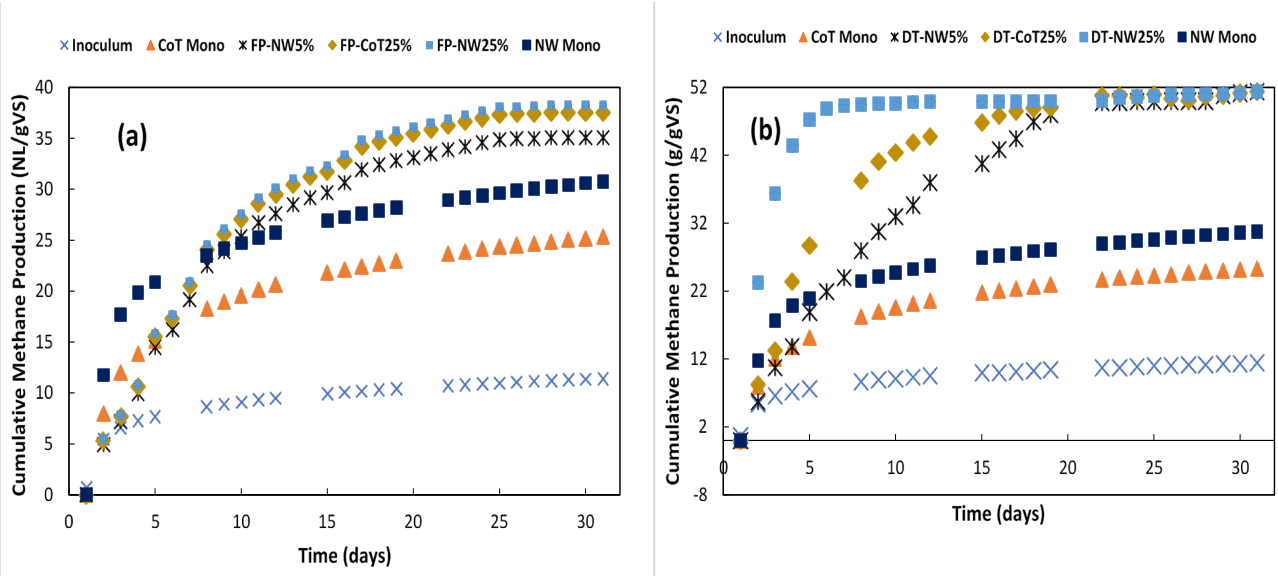


Figure 4.7: Methane cumulative results for co-digestion of sludge with (a) fresh produce and (b) dairy thick waste

The removal efficiencies for TS, VS, and COD were evaluated for all the high TS co-substrates. Brewery spent grain wastes and molasses show a tendency for incomplete removal of these parameters (Table 4.3), indicating that these waste materials may result in additional sludge production and may negatively affect sludge stabilization targets. The food & fresh produce wastes, for which high removal efficiencies for TS and VS were observed. Dairy thick waste also displayed some positive results in terms of the removal of both VS and COD.

Table 4.3: Removal of COD, TS & VS in co-digestion of sewage sludge with high solid content wastes.

Parameters	Molasses	BSG	AM waste	FP waste	FW	DT waste	ST Waste
COD Removal (%)	78	90	55	95	57	89	72
VS Removal (%)	92	47	56	80	87	80	84
TS (%)	45	41	68	62	59	68	44

However, a lower TS removal indicates that dairy waste might also result in additional sludge production. The additional methane yields were calculated based on the best BMP results of these co-substrates. As expected, all high solid content waste materials evaluated in this study produce less methane than BSG and molasses. The BMP results from solid wastes displayed a high reproducibility. Literature confirms this since it is consistent with studies conducted by (Chow et al., 2020; Hallaji et al., 2019; Oliveira et al., 2018; Sandriaty et al., 2018; Wickham, 2019). The results also confirm the validity of BMP as a screening tool for co-substrate evaluation.

4.4.2.2. Co-digestion with low solid content (liquid) wastes

The digestion performance in terms of VS and COD removals when co-digesting with liquid wastes was generally much higher compared to high solid content wastes. In fact, not only did the addition of co-substrate result in no additional VS and COD residual but synergistic removal of COD, VS, and TS was also observed with all liquid co-substrates. In other words, the observed COD, VS, and TS removals were attributed to the synergistic effect of liquid waste co-digestion. The lower digestion performance involving dairy thin waste is likely related to its higher lipid content, similar to FOG wastes. This was also

observed in the study conducted by Awe et al., (2017), Kuang, (2003), and Ohemeng-Ntiamoah & Datta, (2018). Co-digestion of lipid-rich wastes complicates considerations with issues such as lipid floatation, long chain fatty acid accumulation, pre-treatment requirements, and lower degradation rates (Wan et al., 2011, Li et al., 2013). The synergistic removal efficiencies observed in the co-digestion of the other wastes signifies a potential reduction in sludge production and improvement in the final biosolids stability.

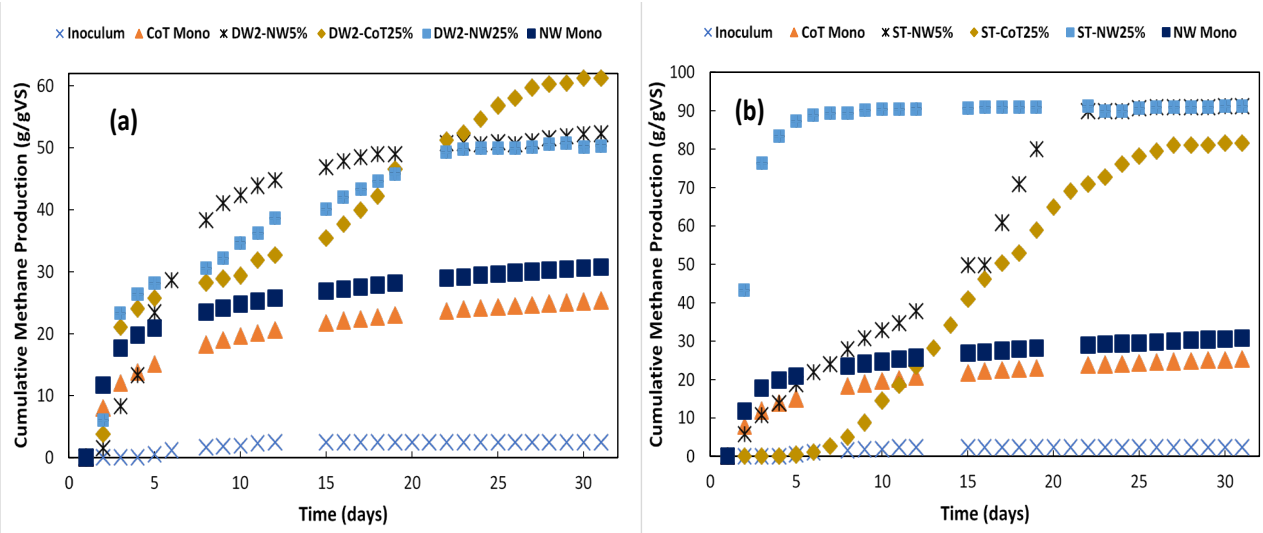


Figure 4.8: Cumulative methane production for co-digestion with liquid wastes as co-substrates

Organic overloading was observed with soft drink waste at a co-digestion ratio of 5 and 25% (wt/wt) (Figure 4.8b). The inhibition of soft drink waste beyond a co-substrate concentration of 10% was attributed to the rapidly degradable organics in the substrate. The sugar content of soft drink waste can be quickly converted into organic acids, which in turn impact the digester's pH. Each of the other co-substrates showed a nearly proportionate increase in biogas production with regards to co-substrate concentration. An added advantage soft drinks only contain sugar and flavours, thus as expected, their co-digestion with sewage sludge does not result in any notable impact on biosolids odour. Similar to the VS and COD removal data, under a stable condition.

4.4.2.3. Collective results for the batch study

To compare the response of raw NW sludge mono-digestion and the response of co-digestion with the co-substrates listed on the x-axis, a bar graph based on the accumulation of methane generation is presented in Figure 4.9. It was observed that the

substrate diversification of substrates improved the AD rate and reduced the inhibitory effect of LCFA. Most of the selected co-substrate achieved an elevated methane yield, however, the highest methane potential was obtained with co-digestion of molasses, spent grain, dairy waste, and fresh produce. The common aspect of this co-substrate is that it is either high in carbohydrates (glucose) or high in protein. These results are in agreement with numerous literature studies that show that the addition of carbohydrate and/or protein to sludge enhance the production of methane (Lima et al., 2016; Tufaner & Avşar, 2016; Xu et al., 2018). The addition decreases LCFA inhibition and improves the growth of methanogenic archaea to enable rapid recovery of digester performance (Gerardi, 2015).

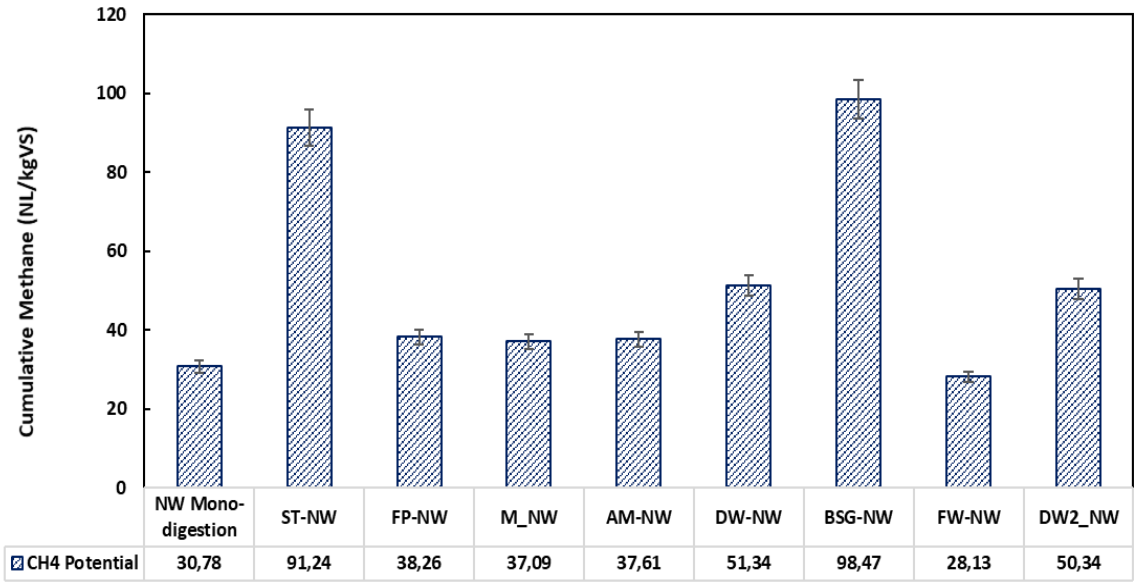


Figure 4.9: Methane production of Driefontein WWTW sludge and the co-substrates

The improvement in methane production can also be due to the favourable balancing out of the C/N ratio, TS, and the microbial community as mentioned previously. The co-digestion increases the organic matter available as volatile fatty acids (VFAs) and the biogas productivity, because of the subsequent degradation of VFAs by methanogens (Ruan et al., 2019). Furthermore, in terms of microbiology, co-digestion is the introduction of the hydrolytic-acidogens species that increase the biodegradability of the blend (Wei et al., 2019; Xue et al., 2019b). It was also noticed that during the steady-state period, a significant shift occurred with Proteobacteria as the most abundant phylum, and hydrogenotrophic methanogens dominated over acetoclastic methanogens (Goswami et al., 2016). From the microbial community richness analysis done in

discussed previously, it was shown that NW sludge presented a higher richness of favourable methanogens. As a rule, a higher community richness reflects better ecological stability and a higher ability in resisting toxicity in the AD process.

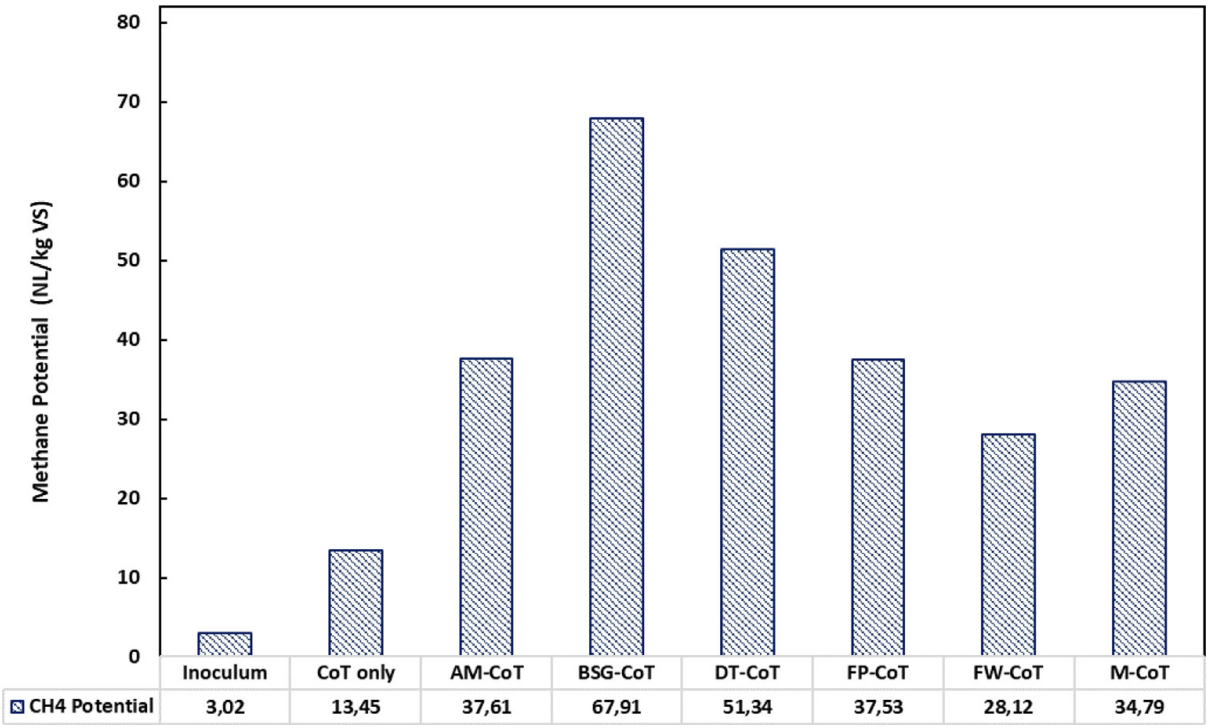


Figure 4.10: Methane production of Driefontein WWTW sludge and the co-substrates

The results of cumulative methane yield of mono-digestion of raw sludge and co-digestion of substrates are shown in Figure 4.10. It can be noticed from the results that there was a significant increase in methane production when adding a co-substrate to sewage sludge. The different co-substrates can change the digestive conditions and thereby affect the microbial diversity, and the methane production performances will be changed. Due to the high fraction of VS on co-substrates, balanced C/N ratio, and favourable TS, temperature, and pH conditions, the activity of the methanogens was promoted resulting in enhanced methane production (Zhao et al., 2019).

The highest specific methane production of 67.91 NL/kg VS was achieved by co-digestion of BSG. This was a significant increase from sewage sludge mono-digestion which produced 13.45 Nl/kg VS. Molasses (M), dairy waste (DT), and animal manure (AM), fresh produce (FP) also resulted in substantially enhanced methane production. This indicates the presence of synergistic effects on biogas production from co-digestion M-NW, AM-NW, DW-NW & FP-NW with both CoT & NW municipal sewage sludge. These findings are in line with those of earlier research that has found a significant

increase in methane generation when sewage sludge is co-digested with carbs and protein-rich co-substrates (Al bkoor Alrawashdeh et al., 2017; Nielfa, Cano, & Pérez, 2015).

Mixing co-substrates with sludge in the AD slightly elevated the carbon-to-nitrogen ratio (C/N) and somewhat shifted it toward the optimal C/N ratios of 20–30 (Yen and Brune, 2007; Calicioglu and Demirer, 2017). The improvement in the C/N ratio may have contributed to the observed synergy in gas production. Additionally, the biodegradable fraction reached a maximum value, indicating that co-digestion improved biomass biodegradation in the mix. These results are explained by the increased diversity and enhanced enzymatic machinery of the AD microbial community. The microbial community functions well in the complex substrates associated with the combination of co-substrates and sludge mixture. Hence, this demonstrates a strong connection between the substrate composition, matrix complexity, C/N ratio, and microbial community structure. However, as opposed to NW5, it was shown that Driefontein sludge presented a low richness of favourable methanogens. Thus, better ecological stability and the ability to resist toxicity in the AD process are not guaranteed.

4.4.3. Biogas Production: Semi-continuous studies

Biogas experiment was carried out as semi-continuous processes in benchtop laboratory bioreactors. The substrate was continuously added and residual digestate was continuously withdrawn, mimicking the WWTP full-scale processes. This was done to provide information about long-term effects such as microbial adaptation to the co-substrates and operating conditions, and whether certain metabolites are slowly accumulating. However, the process was cumbersome and slow (200 days), and because of these effects, the experiments are hard to start over or reproduce is necessary.

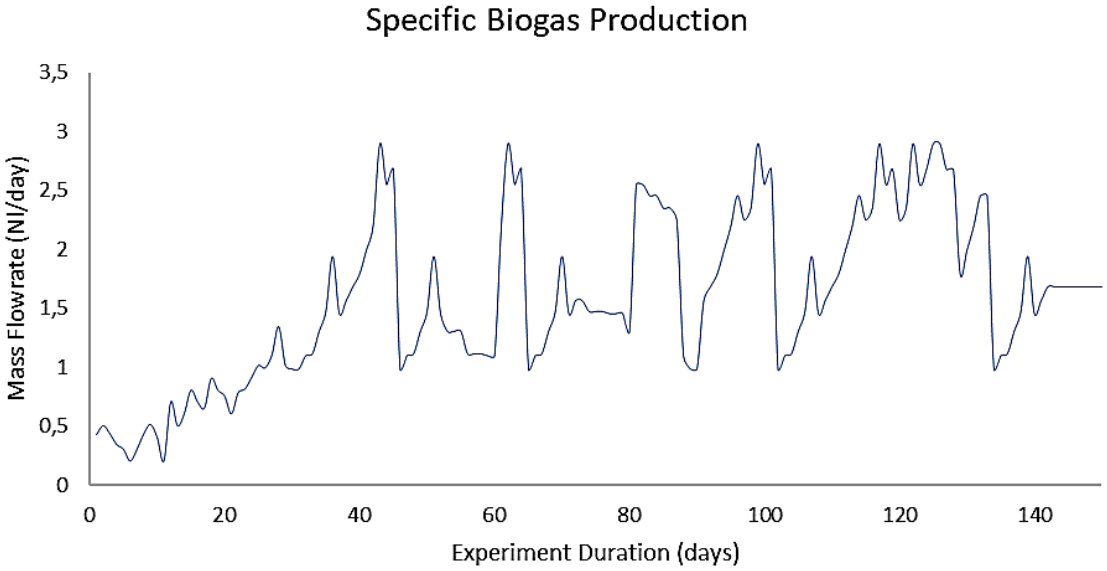


Figure 4.11: Semi-continuous biogas production per day

The result of the semi-continuous experiment revealed that although co-digestion of sewage sludge with spent grain caused an enhancement of the AD process during the BMP study, this was not necessarily the case as can be observed in Figure 4.11. The performance characteristics in the sludge substrate experiment were reduced from the co-digestion in batch studies. Although the target of this research work was to achieve CH_4 concentrations close to that of natural gas under mesophilic conditions (i.e., CH_4 concentration >90%), the highest recorded methane quality was 77.61% (at 0.5 NL/day) first recorded on the second day. The inability to achieve CH_4 concentration >90% can be attributed to the unstable operating conditions especially the temperature, in which this experiment was conducted; that limited the extent of mineralization of the metals and the rate of reaction. A significant reduction in the biogas yield; from 3.03 to 1.02 NL/day was also observed when the OLR reached the level of 2.90 gVS/L.day on day 42.

4.4.4. COD Removal Efficiency in AD Bench Studies

During AD, the bacteria convert COD to methane and carbon dioxide. As such, the COD removal efficiency can be used to assess the accomplishment of the process to produce methane. In this study, all the samples exhibited excellent COD removal above 95%, as it is indicated in Figure 4.12. The effluent COD concentration was below 7.0 g O_2/kg. Similar results of COD removals efficiency were reported elsewhere, the studies conducted by (Bong et al., 2018; Dhinakaran & Navaneethagopalakrishnan, 2015; J.

Zhang et al., 2018) shows that high COD removal efficiency was achieved when the organic loading rate was increased and maintaining constant HRT in the AD system. In addition, the pH of the system was closely monitored on daily basis to avoid a pH drop to below 6.5 which could result in low COD conversion.

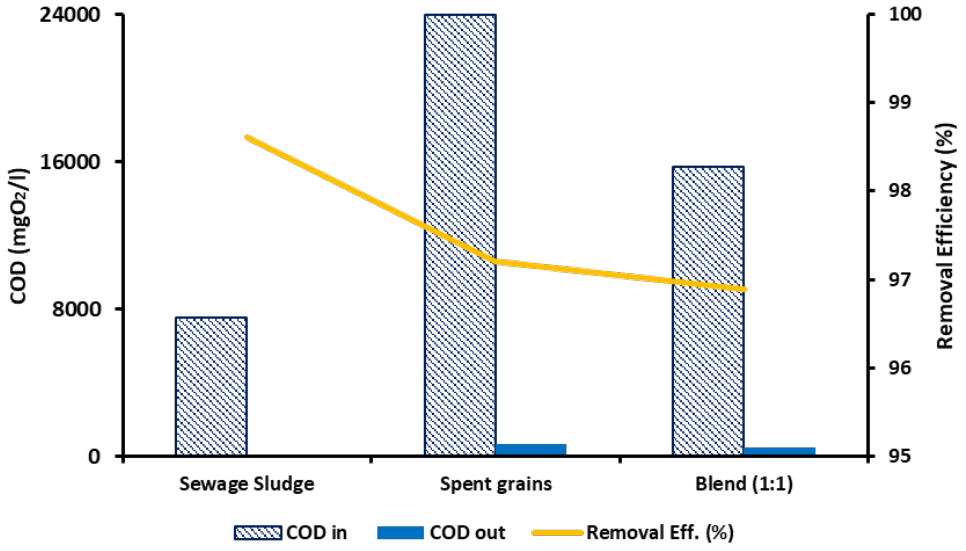


Figure 4.12: The COD of the feed and after the BMP study, and the COD removal efficiency

4.4.5. Pilot plant Trials: CSIR-AD Semi-continuous

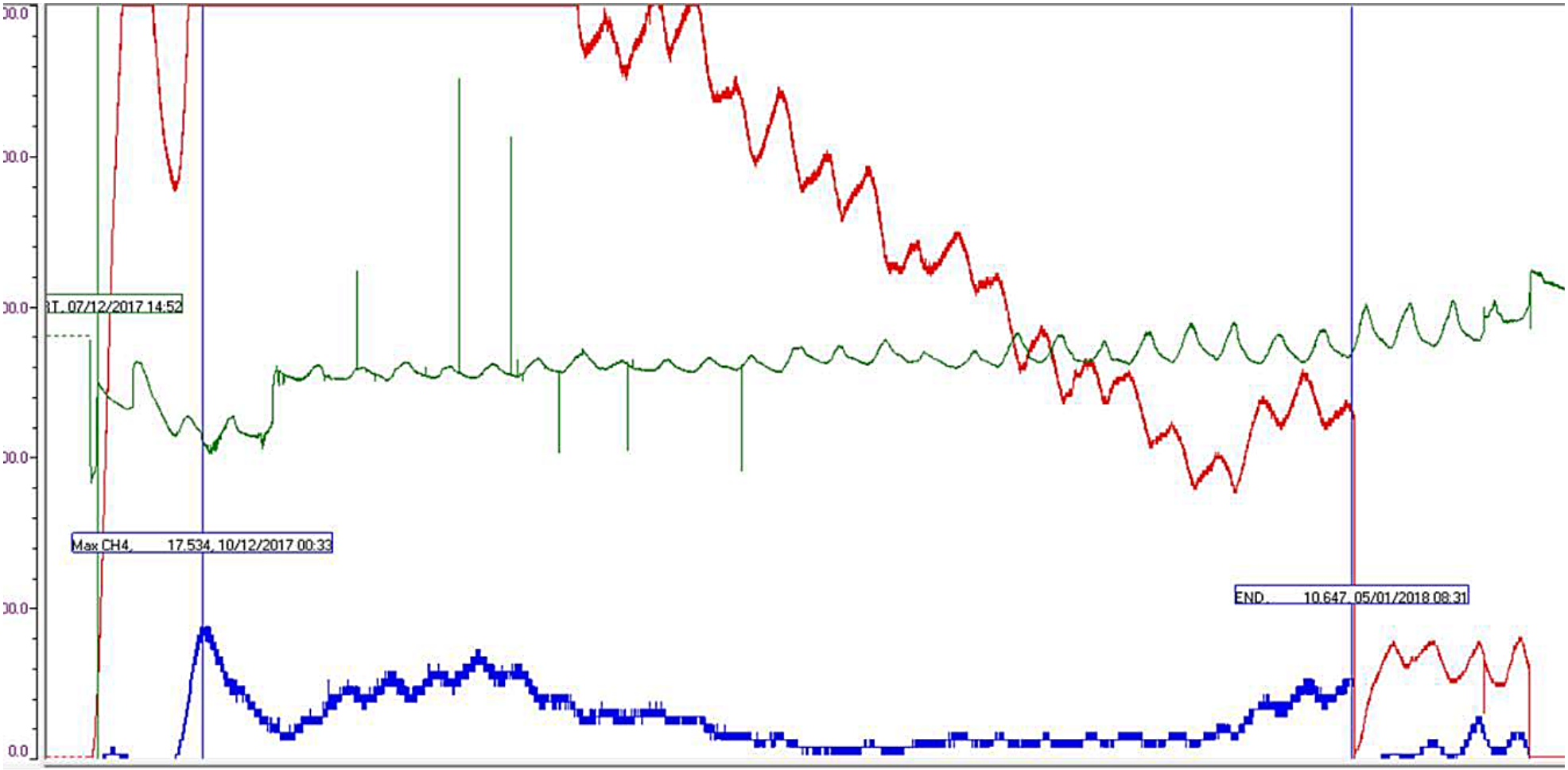
Following the preliminary trial, two experimental trials were performed in this study. Simultaneously with the feedstock characterization, the pilot plant was operated using sewage sludge as a feedstock for mono-digestion and sludge with dairy thick fermentation waste for co-digestion. The trials were carried out for 30 days, with the bioreactors operating at a temperature range of 35 - 45° C. This temperature was sustained by the solar hot water geyser utilized with the use of digital temperature controllers. The sludge was mixed in a feeder tank for homogenization of feedstock and then fed into a 200 L digester. The volumetric flowrate measurements for biogas production were carried out using the Ritter gas flowrate, UK. Biogas produced in the digesters was collected and pumped into the gas sensors and the flowmeter by a natural rubber tubing where it was recorded. Biogas composition measurement was carried by the manifold gas sensors connected to the gas pipelines, the gas volume was determined and recorded. For validation of the results the Geotech biogas 5000, was used and the results were compared with manifold gas sensors.

The data of this operation are presented in Figure 4.13 and Figure 4.14. The information was collected over a 30 days period of operation where the pH, CO_2, and CH_4 data was recorded. In trial 1 it was observed that the maximum obtained methane percentage was 17.5 % which is very low compared to what was previously obtained and what the literature suggests (Akmaliyah, 2014; Chow et al., 2020; Yap et al., 2021). It was then concluded that mono-digestion is not efficient. As outlined previously, problems are emerging in mono-digestion such as imbalanced nutrients, the existence of toxic materials, and recalcitrant compounds in the feedstock. Thus, co-digestion and operational factors, such as SRT, HRT, and digester mixing were optimized as outlined previously since they affect the AD performance.

All the setbacks encountered in Trial 1 were addressed and corrected and thus Trial 2 was started. Trial 2 was carried out as co-digestion of sewage sludge with dairy thick waste and the results are presented in Figure 4.13. It can be observed that the methane composition was improved and it was above 48% after 3 days of start-up and 100 % in 8 days. Literature reports the highest percentage of methane that can be achieved after 16 days is 65% CH_4 (Yue Zhang et al., 2012).

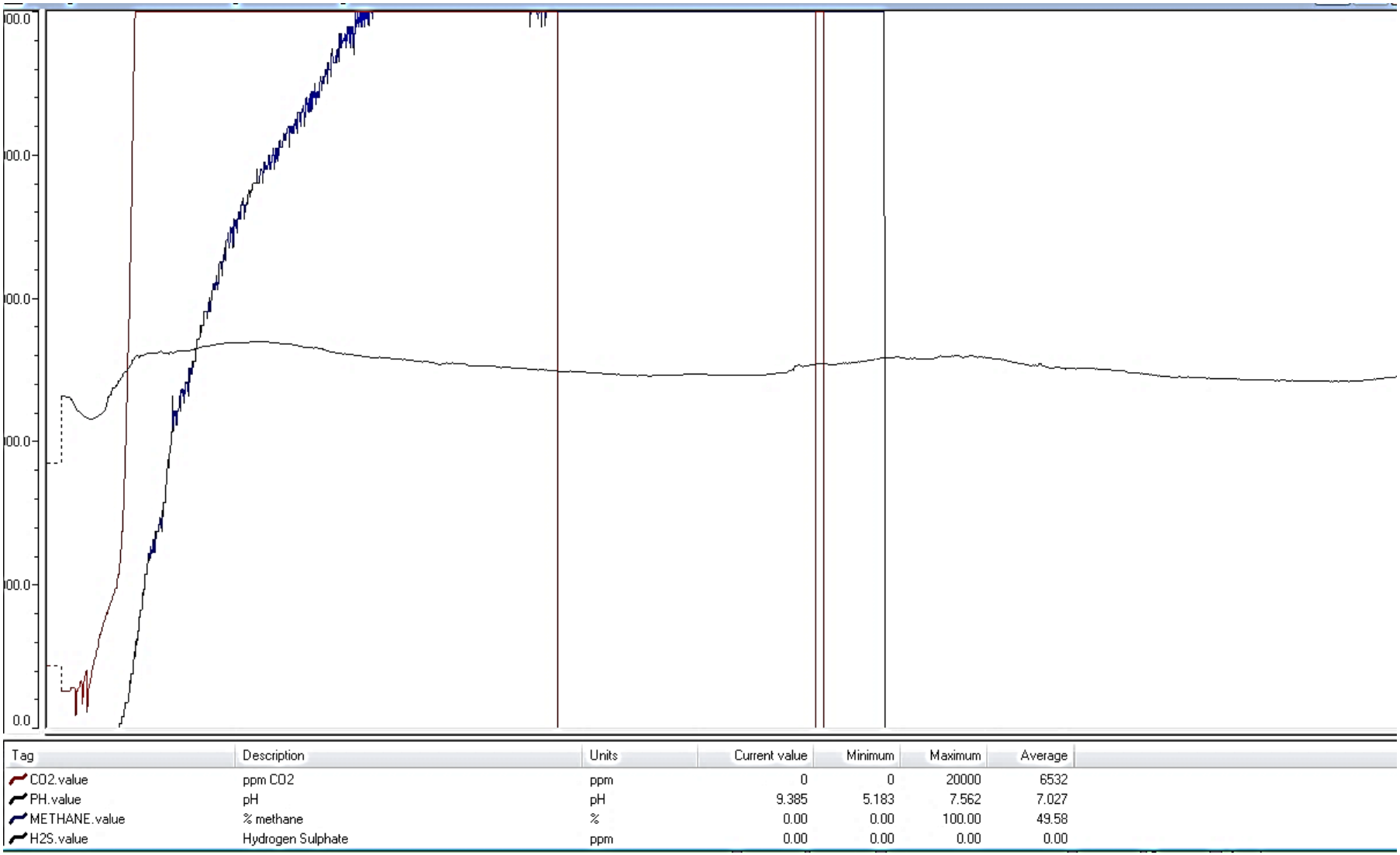
The influence of adding co-substrate in the anaerobic digestion of sewage sludge showed improved biogas production. Primarily anaerobic co-digestion has some advantages over mono digestion in terms of system stability, bioenergy production, and solids reduction (Rabii et al., 2019). This is due to the influence of adding co-substrates on microbial consortia diversity and their synergistic impact on biogas improvement (Derilus et al., 2019).

The results obtained under operational conditions of; pH of 7, the temperature of 35 °C, HRT was 35 days, and organic loading rate of 20 L/day is shown in Figure 4.14. The gas quality or composition was CH_4 of 63 % & CO_2 is 33 %. The flow rate recorded was 84 L/day and the biogas yield was 4.2 L biogas/L influent. The biogas composition was similar to the literature study conducted by (Rathnasiri, 2016). The HRT and OLR confirm their reproducibility due to the consistency of flow rate & yield recorded as per studies conducted by (Akmaliyah, 2014; Al-Addous et al., 2018; Yap et al., 2021).



Tag	Description	Units	Current value	Minimum	Maximum	Average
CO2.value	ppm CO2	ppm	68	59	20000	13044
PH.value	pH	pH	9.426	5.125	12.653	7.407
METHANE.value	% methane	%	0.00	0.00	17.53	4.50
H2S.value	Hydrogen Sulphate	ppm	0.00	0.00	0.00	0.00

Figure 4.13: Pilot plant Trial 1, methane & carbon dioxide concentration and pH profile



Tag	Description	Units	Current value	Minimum	Maximum	Average
CO2.value	ppm CO2	ppm	0	0	20000	6532
PH.value	pH	pH	9.385	5.183	7.562	7.027
METHANE.value	% methane	%	0.00	0.00	100.00	49.58
H2S.value	Hydrogen Sulphate	ppm	0.00	0.00	0.00	0.00

Figure 4.14: Pilot plant Trial 2 methane and carbon dioxide concentration and pH profile

4.4.6. COD Removal Efficiency in AD Pilot Plant trial

The removal efficiencies for TS, VS, and COD were evaluated for all the pilot trials. Similar to batch studies, sludge & dairy thick waste blend showed an incomplete removal of the TS parameter (Table 4.4), indicating that the clover waste materials may result in additional sludge production and may negatively affect sludge stabilization targets. However, dairy thick waste also displayed some positive results in terms of the removal of both VS and COD. However, a lower TS removal indicates that dairy waste might also result in additional sludge production (Goswami et al., 2016).

Table 4.4: Removal of COD, TS & VS in co-digestion of sewage sludge with dairy thick wastes.

Parameters	Sewage Sludge Mono-digestion	Sludge & Dairy Thick waste
COD Removal (%)	63	72
VS Removal (%)	84	85
TS Removal (%)	59	71

4.5. Conclusion

The comprehensive objective of this study was to evaluate the composition of the feed sludge source from CoT and JW, in South Africa and their possible effect on methane production. To do this, the physicochemical and microbiological characterization to obtain the composition of the anaerobic digestion feedstock was carried out before anaerobic digestion. The physicochemical characterization was performed on the wastewater treatment plant sewage sludge, along with the microbial community composition to reveal functional traits in a typical full-scale anaerobic digester.

The results presented showed that WWTW sewage sludge contains a high potential methane production, 28.6 & 27.8 gCH_4/kg feed in COT2 PS and JW1 NW sewage sludge, respectively. However, it should be noted that extremely high COD may lead to the accumulation of volatile fatty acids, making a delay in biogas production or reducing the pH of bioreactors. Thus, a well-balanced high COD with C/N ratio and VS concentration in the ranges of 10-100 gCH_4/kg feed, C/N of 17–36, and VS 80–98% TS is recommended. The characterization of sewage sludge as a feedstock for biogas production showed that most sludges shortlisted contain reasonable COD, organic matter, total solids (TS), volatile solid (VS) along with the inhibitory parameters which show potential for high yield of methane in biogas production, as long as the stability of AD is maintained at throughout the process. The microbiology data showed that the

high-throughput sequencing analysis showed clear differences in microbial communities available in the sewage sludge along with the AD inhibiting microbes. From the present study, it was demonstrated that sewage sludge from COT and JW WWTP can be a suitable substrate for efficient anaerobic digestion. However, depending on the operating conditions such as pH, temperature, and organic loading rate, the process can be improved or deteriorated in terms of the methane yield. Different operational strategies can be put into practice to find the most stable environment and avoid inhibitory effects.

This study examined the anaerobic co-digestion of sewage sludge and six organic waste materials as possible co-substrates for enhancement of bio-methane potential and possible impact on digested sludge content in terms of TS, VS, and COD. When compared to conventional anaerobic digestion of sewage sludge, both co-substrates increased bio-methane yield by three to six times. Although high solid content co-substrates generated significantly more methane gas, they also increased the risk of organic overloading. Co-substrates such as molasses, food waste, animal manure, and fresh produce waste performed well at maximum co-digestion ratios. The maximum co-digestions ratio of soft drink waste and sewage sludge was 25%. Furthermore, except for manure, all other solid co-substrates co-digestion resulted in additional VS and COD residuals in digested sludge. By contrast, most liquid co-substrates evaluated here showed a notable synergistic effect, which enhanced the removals of TS, VS, and COD during anaerobic digestion.

Therefore, the anaerobic co-digestion might be considered a cost-effective solution that could contribute to the energy self-efficiency of WWTPs and sustainable waste management. However, the operating conditions should be optimized and monitored at all times. Based on the experimental results, it is recommended to upscale the co-digestion of the feed for the pilot biogas plant. The feed should comprise sludge from the WWTP sludge and the brewery spent grains. However, a significant reduction in the biogas yield; from 10.23 to 2.02 NL/day was also observed in a semi-continuous setup, when the OLR reached the level of 2.90 gVS/L.day

References

Achinas, S., & Euverink, G. J. W. (2019). Effect of combined inoculation on biogas production from a hardly degradable material. *Energies*, *12*(2). https://doi.org/10.3390/en12020217

Akmaliyah, M. (2014). *Anaerobic Digestion from the Laboratory to The Field: An Experimental Study into the Scalability of Bench to Pilot-Scale Anaerobic Digestion*. Graduate School Appalachian State University.

Al-Addous, M., Saidan, M. N., Bdour, M., & Alnaief, M. (2018). Evaluation of Biogas Production from the Co-Digestion of Municipal Food Waste and Wastewater Sludge at Refugee Camps Using an Automated Methane Potential Test System. *Energies*, *12*(1). https://doi.org/10.3390/en12010032

Al bkoor Alrawashdeh, K., Pugliese, A., Slopiecka, K., Pistolesi, V., Massoli, S., Bartocci, P., Bidini, G., & Fantozzi, F. (2017). Codigestion of Untreated and Treated Sewage Sludge with the Organic Fraction of Municipal Solid Wastes. *Fermentation*, *3*(3), 35. https://doi.org/10.3390/fermentation3030035

Awe, O., Lu, J., Wu, S., Zhao, Y., Nzihou, A., Lyczko, N., & Doan, P. (2017). *Effect of oil content on biogas production and performance stability of anaerobic digestion of food waste* (pp. 1–11).

Babaee, A., Shayegan, J., & Roshani, A. (2013). Anaerobic slurry co-digestion of poultry manure and straw: effect of organic loading and temperature. *Journal of Environmental Health Science and Engineering*. https://doi.org/10.1186/2052-336X-11-15

Bohutskyi, P., Keller, T. A., Phan, D., Parris, M. L., Li, M., Richardson, L., & Kopachevsky, A. M. (2019). Co-digestion of wastewater-grown filamentous algae with sewage sludge improves biomethane production and energy balance compared to thermal, chemical, or thermochemical pretreatments. *Frontiers in Energy Research*, *7*(JUN), 1–19. https://doi.org/10.3389/fenrg.2019.00047

Bong, C. P. C., Lim, L. Y., Lee, C. T., Klemeš, J. J., Ho, C. S., & Ho, W. S. (2018). The characterization and treatment of food waste for improvement of biogas production during anaerobic digestion – A review. *Journal of Cleaner Production*, *172*. https://doi.org/10.1016/j.jclepro.2017.10.199

Campanaro, S., Treu, L., Kougias, P. G., De Francisci, D., Valle, G., & Angelidaki, I. (2016). Metagenomic analysis and functional characterization of the biogas microbiome using high throughput shotgun sequencing and a novel binning strategy. *Biotechnology for Biofuels*, *9*(1), 1–17. https://doi.org/10.1186/s13068-016-0441-1

Cavinato, C. (2011). *Anaerobic Digestion Fundamentals I* (Issue August, pp. 1–47). University of Jyvaskyla. http://www.biogas-info.co.uk/

Chen, S., Gao, J., & Dong, B. (2021). Bottlenecks of anaerobic degradation of proteins in sewage sludge and the potential targeted enhancing strategies. *Science of the Total Environment*, *759*. https://doi.org/10.1016/j.scitotenv.2020.143573

Chow, W. L., Chong, S., Lim, J. W., Chan, Y. J., & Chong, M. F. (2020). Anaerobic Co-Digestion of Wastewater Sludge : A Review of Potential Co-Substrates and Operating. *Processes*, *8(1)*(39), 1–21.

Cuetos, M. J., Martinez, E. J., Moreno, R., Gonzalez, R., Otero, M., & Gomez, X. (2017). Enhancing anaerobic digestion of poultry blood using activated carbon Enhancing anaerobic digestion of poultry blood. *Journal of Advanced Research*, *8*(3), 297–307. https://doi.org/10.1016/j.jare.2016.12.004

Department of Energy. (2017). *State of Renewable Energy in South Africa*. www.energy.gov.za

Department of Energy. (2019). The South African Energy Sector Report 2019. In *Department of Energy*. http://www.energy.gov.za

Derilus, D., Forestil, A., Fortuné, J., Polyanska, O., Louime, C., Gervais, G., & Massey, S. E. (2019). Functional Metagenomics Characterization of an Anaerobic Saltwater Bioreactor. *Journal of Renewable Energy*, *2019*, 1–15. https://doi.org/10.1155/2019/4527628

Dhinakaran, S., & Navaneethagopalakrishnan, A. (2015). Feasibility studies on performance improvement for tannery effluent through chemical oxidation- biological treatment. *Journal of Chemical and Pharmaceutical Sciences*, *2015-April*, 439–442.

Dido, M. S., Rieker, C., Bursche, J., Lopez Velarde Santos, M., & Hamhaber, J. (2014). Anaerobic Digestion of spent grains: Potential use in small-scale Biogas Digesters in Jos, Nigeria. *Köln Bibliothek Der Technischen Hochschule Köln*, 19–25.

Dioha, I. J., Ikeme, C., Nafi, T., Soba, N. I., & Mbs, Y. (2013). Effect of Carbon To Nitrogen Ratio on Biogas Production. *International Research Journal of Natural Sciences*, *1*(3), 1–10.

Doloman, A., Soboh, Y., Walters, A. J., Sims, R. C., & Miller, C. D. (2017). Qualitative Analysis of Microbial Dynamics during Anaerobic Digestion of Microalgal Biomass in a UASB Reactor. *International Journal of Microbiology*, *2017*. https://doi.org/10.1155/2017/5291283

Franks, L., Euston-Brown, M., Ferry, A., & Giljova, S. (2013). *Municipal wastewater treatment works - biogas to energy*. http://www.cityenergy.org.za/uploads/resource_336.pdf

Gerardi, M. H. (2015). The Microbiology of Anaerobic Digesters. In *Environmental Technology (United Kingdom)* (Vol. 14, Issue 1). The Author(s). https://doi.org/10.1080/09593330.2014.998716

Ghosh, P., Kumar, M., Kapoor, R., Kumar, S. S., Singh, L., Vijay, V., Vijay, V. K., Kumar, V., & Thakur, I. S. (2020). Enhanced biogas production from municipal solid waste via co-digestion with

sewage sludge and metabolic pathway analysis. *Bioresource Technology*, *296*(122275).

Gonzalez-Fernandez, C., Sialve, B., & Molinuevo-Salces, B. (2015). Anaerobic digestion of microalgal biomass: Challenges, opportunities and research needs. In *Bioresource Technology* (Vol. 198). https://doi.org/10.1016/j.biortech.2015.09.095

Goswami, R., Chattopadhyay, P., Shome, A., Banerjee, S. N., Chakraborty, A. K., Mathew, A. K., & Chaudhury, S. (2016). An overview of physico-chemical mechanisms of biogas production by microbial communities: A step towards sustainable waste management. In *3 Biotech*. https://doi.org/10.1007/s13205-016-0395-9

Guo, J., Peng, Y., Ni, B. J., Han, X., Fan, L., & Yuan, Z. (2015). Dissecting microbial community structure and methane-producing pathways of a full-scale anaerobic reactor digesting activated sludge from wastewater treatment by metagenomic sequencing. *Microbial Cell Factories*. https://doi.org/10.1186/s12934-015-0218-4

Hallaji, S. M., Kuroshkarim, M., & Moussavi, S. P. (2019). Enhancing methane production using anaerobic co-digestion of waste activated sludge with combined fruit waste and cheese whey. *BMC Biotechnology*, *19*(1), 1–10. https://doi.org/10.1186/s12896-019-0513-y

Herbig, F. J. W. (2019). Talking dirty - effluent and sewage irreverence in South Africa: A conservation crime perspective. *Cogent Social Sciences*, *5*(1), 1–18. https://doi.org/10.1080/23311886.2019.1701359

Jeung, J. H., Chung, W. J., & Chang, S. W. (2019). Evaluation of anaerobic co-digestion to enhance the efficiency of livestock manure anaerobic digestion. *Sustainability (Switzerland)*, *11*(24), 1–12. https://doi.org/10.3390/su11247170

Jia, X., Li, M., Zhu, J., Jiang, Y., Wang, Y., & Wang, Y. (2019). Enhancement split-phase hydrogen production from food waste during dark fermentation: Protein substances degradation and transformation during hydrothermal pre-treatments. *International Journal of Hydrogen Energy*, *44*(32), 17334–17345. https://doi.org/10.1016/j.ijhydene.2018.12.199

Jingura, R. M., & Kamusoko, R. (2017). Methods for determination of biomethane potential of feedstocks: A review. In *Biofuel Research Journal* (Vol. 4, Issue 2). https://doi.org/10.18331/BRJ2017.4.2.3

Jojima, T., Noburyu, R., Suda, M., Okino, S., Yukawa, H., Inui, M., Lu, J. J., Chen, W. H., Peleteiro, S., Rivas, S., Alonso, J. L., Santos, V., Parajó, J. C., Sahoo, P., Sluiter, A., Hames, B., Ruiz, R., Scarlata, C., Sluiter, J., … Sakthivel, M. (2014). Utilization of Ionic Liquids in Lignocellulose Biorefineries as Agents for Separation, Derivatization, Fractionation, or Pretreatment. *Fermentation*, *2*(1), 5. https://doi.org/10.3390/en7010013

Jung, K. W., Lee, S. Y., & Lee, Y. J. (2019). Optimized preparation of activated carbon from municipal sewage sludge and application to the adsorption of azo dye from aqueous

solutions. *Environmental Progress and Sustainable Energy*, *38*(s1), S267–S276. https://doi.org/10.1002/ep.13008

Kalemba, K., & Barbusiński, K. (2017). Anaerobic co-digestion of sewage sludge and molasses. *E3S Web of Conferences*, *22*, 00075. https://doi.org/10.1051/e3sconf/20172200075

Kuang, Y. (2003). *Enhancing anaerobic digestion of lipids in wastewater by addition of co-substrates*.

Lijó, L., González-García, S., Bacenetti, J., Negri, M., Fiala, M., Feijoo, G., & Moreira, M. T. (2015). Environmental assessment of farm-scaled anaerobic co-digestion for bioenergy production. *Waste Management*, *41*. https://doi.org/10.1016/j.wasman.2015.03.043

Lima, D. M. F., Rodrigues, J. A. D., Boe, K., Alvarado-Morales, M., Ellegaard, L., & Angelidaki, I. (2016). Anaerobic modeling for improving synergy and robustness of a manure co-digestion process. *Brazilian Journal of Chemical Engineering*, *33*(4), 871–883. https://doi.org/10.1590/0104-6632.20160334s20150314

Liu, X., Wang, M., Hu, X., & Song, Y. (2014). Effect of Total Solids Content on the Biogas Production and Phosphorus Release from Excess Sludge. *Advanced Materials Research*, *1010–1012*(August 2014), 1006–1009. https://doi.org/10.4028/www.scientific.net/AMR.1010-1012.1006

Liu, Y., Luo, P., Xu, Q., Wang, E., & Yin, J. (2014). *Cellulose Chemistry and Technology Investigation of the Effect of Supercritical Carbon Dioxide Pretreatment on Reducing Sugar Yield of Lignocellulose Hydrolysis. 48*, 89–95.

Mandal, S. De, Chatterjee, R., & Kumar, N. S. (2017). *Dominant bacterial phyla in caves and their predicted functional roles in C and N cycle*. 1–9. https://doi.org/10.1186/s12866-017-1002-x

Martin Vincent, N., Wei, Y., Zhang, J., Yu, D., & Tong, J. (2018). Characterization and Dynamic Shift of Microbial Communities during Start-Up, Overloading and Steady-State in an Anaerobic Membrane Bioreactor. *International Journal of Environmental Research and Public Health*, *15*(7). https://doi.org/10.3390/ijerph15071399

Martínez, E. J., Gil, M. V, Fernandez, C., Rosas, J. G., & Gómez, X. (2016). Anaerobic Codigestion of Sludge : Addition of Butcher ' s Fat Waste as a Cosubstrate for Increasing Biogas Production. *PLoS ONE*, *11*(4), 1–13. https://doi.org/10.1371/journal.pone.0153139

Masebinu, S. O. (2018). *Anaerobic Digestion Process Stabilisation and in-situ Upgrading of a Biogas System*. University of Johanneburg.

Masindi, V., Chatzisymeon, E., Kortidis, I., & Foteinis, S. (2018). Assessing the sustainability of acid mine drainage (AMD) treatment in South Africa. *Science of the Total Environment*. https://doi.org/10.1016/j.scitotenv.2018.04.108

Mitchell, S. A., de Wit, M. P., Blignaut, J. N., & Crookes, D. (2014). *Waste Water Treatment Plants : The Financing Mechanisms Associated with Achieving Green Drop Rating* (Issue 2085). http://www.wrc.org.za/wp-content/uploads/mdocs/2085-1-14.pdf

Mudzanani, K., Ejekwu, O., Ayeni, A. O., & Daramola, M. O. (2019). Dissolution kinetics of corncob in lithium perchlorate solvent system. *European Biomass Conference and Exhibition Proceedings*, 307–311.

National Planning Commission. (2010). National Development Plan (2030). In *Department: The Presedency Republic of South Africa*. https://doi.org/ISBN: 978-0-621-41180-5

Nielfa, A., Cano, R., & Pérez, A. (2015). *Co-digestion of municipal sewage sludge and solid waste : Modelling of carbohydrate , lipid and protein content influence*. https://doi.org/10.1177/0734242X15572181

Nielfa, A., Cano, R., Pérez, A., & Fdez-Polanco, M. (2015). Co-digestion of municipal sewage sludge and solid waste: Modelling of carbohydrate, lipid and protein content influence. *Waste Management & Research*, *33*(3), 241–249. https://doi.org/10.1177/0734242X15572181

Ntombela, C., Funke, N., Meissner, R., Steyn, M., & Masangane, W. (2016). A critical look at South Africa's green drop programme. *Water SA*, *42*(4), 703–710. https://doi.org/10.4314/wsa.v42i4.21

Ohemeng-Ntiamoah, J., & Datta, T. (2018). Evaluating analytical methods for the characterization of lipids, proteins and carbohydrates in organic substrates for anaerobic co-digestion. *Bioresource Technology*, *247*. https://doi.org/10.1016/j.biortech.2017.09.154

Oke, M. A., Suffian, M., Annuar, M., & Simarani, K. (2016). Mixed Feedstock Approach to Lignocellulosic Ethanol Production — Prospects and Limitations. *BioEnergy Research*. https://doi.org/10.1007/s12155-016-9765-8

Oladejo, J., Shi, K., Luo, X., Yang, G., & Wu, T. (2019). A review of sludge-to-energy recovery methods. *Energies*, *12*(1), 1–38. https://doi.org/10.3390/en12010060

Oliveira, J. V, Alves, M. M., & Costa, J. C. (2018). Biochemical methane potential of brewery by-products. *Clean Technologies and Environmental Policy*, *20*(2), 435–440. https://doi.org/10.1007/s10098-017-1482-2

Rabii, A., Aldin, S., Dahman, Y., & Elbeshbishy, E. (2019). A Review on Anaerobic Co-Digestion with a Focus on the Microbial Populations and the Effect of Multi-Stage Digester Configuration. *Energies*, *12*(1106), 1–25. https://doi.org/10.3390/en12061106

Rathnasiri, P. G. (2016). Dynamic Modelling and Simulation of Pilot Scale Anaerobic Digestion Plant Treating Source Separated Food Waste and Effect of Recycling Sludge. *Procedia Environmental Sciences*, *35*, 740–748. https://doi.org/10.1016/j.proenv.2016.07.082

Rea, J. (2014). Kinetic Modeling and Experimentation of Anaerobic Digestion. In *Massachusetts Institute of Technology*.

Ruan, D., Zhou, Z., Pang, H., Yao, J., Chen, G., & Qiu, Z. (2019). Enhancing methane production of anaerobic sludge digestion by microaeration: Enzyme activity stimulation, semi-continuous reactor validation and microbial community analysis. *Bioresource Technology*, *289*, 121643. https://doi.org/https://doi.org/10.1016/j.biortech.2019.121643

Salihi, I. U., Kutty, S. R. M., & Ismail, H. H. M. (2018). Copper Metal Removal using Sludge Activated Carbon Derived from Wastewater Treatment Sludge. *MATEC Web of Conferences*, *203*. https://doi.org/10.1051/matecconf/201820303009

Sandriaty, R., Priadi, C., Kurnianingsih, S., & Abdillah, A. (2018). *Potential of biogas production from anaerobic co-digestion of fat , oil and grease waste and food waste*. *02047*, 1–5.

Siddique, M. N. I., & Wahid, Z. B. A. (2018). Enhanced Methane Yield by Codigestion of Sewage Sludge with Microalgae and Catering Waste Leachate. *Water Environment Research*, *90*(9), 835–839. https://doi.org/10.2175/106143017x15131012153031

Singh, A., Kamble, S., Kazmi, A., & Starklhors, M. (2019). Environmental and economic performance evaluation of municipal wastewater treatment plants in India : a life cycle approach. *Water Science & Technology*, *79*(6), 1102. https://doi.org/10.2166/wst.2019.110

Szaja, A., Montusiewicz, A., Lebiocka, M., & Bis, M. (2020). The effect of brewery spent grain application on biogas yields and kinetics in co-digestion with sewage sludge. *PeerJ*, *8*. https://doi.org/10.7717/peerj.10590

Treu, L., Kougias, P. G., Campanaro, S., Bassani, I., & Angelidaki, I. (2016). Deeper insight into the structure of the anaerobic digestion microbial community; The biogas microbiome database is expanded with 157 new genomes. *Bioresource Technology*, *216*, 260–266. https://doi.org/10.1016/j.biortech.2016.05.081

Tufaner, F., & Avşar, Y. (2016). Effects of co-substrate on biogas production from cattle manure: a review. *International Journal of Environmental Science and Technology*, *13*(9), 2303–2312. https://doi.org/10.1007/s13762-016-1069-1

Tyagi, V. K., & Lo, S.-L. (2011). Application of physico-chemical pretreatment methods to enhance the sludge disintegration and subsequent anaerobic digestion: An up to date review. *Reviews in Environmental Science and Biotechnology*, *10*(3), 215–242. https://doi.org/10.1007/s11157-011-9244-9

Van der Merwe-Botha, M., Juncker, K., Visser, A., & Boyd, R. (2016). *Guiding principles in the design and operation of a wastewater sludge digestion plant with biogas and power generation : report to the Water Research Commission*.

Wang, B. (2016). Factors that influence the biochemical methane potential (BMP) test. In *Lund University*.

Wang, Q., Liang, Y., Zhao, P., Li, Q. X., Guo, S., & Chen, C. (2016). Potential and optimization of two-phase anaerobic digestion of oil refinery waste activated sludge and microbial community study. *Scientific Reports*, *6*(August), 1–10. https://doi.org/10.1038/srep38245

Wei, L., Qin, K., Ding, J., Xue, M., Yang, C., Jiang, J., & Zhao, Q. (2019). Optimization of the co-digestion of sewage sludge, maize straw and cow manure: microbial responses and effect of fractional organic characteristics. *Scientific Reports*, *9*(1), 1–10. https://doi.org/10.1038/s41598-019-38829-8

Wickham, R. J. (2019). *Anaerobic co-digestion of municipal wastewater sludge with organic wastes*. University of Wollongong.

Wirth, R., Kovács, E., Maráti, G., Bagi, Z., Rákhely, G., & Kovács, K. L. (2012). Characterization of a biogas-producing microbial community by short-read next generation DNA sequencing. *Biotechnology for Biofuels*. https://doi.org/10.1186/1754-6834-5-41

WRC. (1997). *Permissible Utilisation and Disposal of Sewage Sludge Edition 1* (Issue August, p. 83). Water Research Commission.

Xu, R., Zhang, K., Liu, P., Khan, A., Xiong, J., Tian, F., & Li, X. (2018). A critical review on the interaction of substrate nutrient balance and microbial community structure and function in anaerobic co-digestion. In *Bioresource Technology* (Vol. 247). https://doi.org/10.1016/j.biortech.2017.09.095

Xue, S., Zhao, N., Song, J., & Wang, X. (2019a). Interactive Effects of Chemical Composition of Food Waste during Anaerobic Co-Digestion under Thermophilic Temperature. *Sustainability*, *11*(2933), 1–15.

Xue, S., Zhao, N., Song, J., & Wang, X. (2019b). *sustainability Interactive E ff ects of Chemical Composition of Food Waste during Anaerobic Co-Digestion under Thermophilic Temperature*. 1–15.

Yap, C. C., Chan, Y. J., Loh, S. K., Supramaniam, C. V., Soh, A. C., Chong, M. F., & Lim, L. K. (2021). Pilot-scale investigation of the integrated anaerobic−aerobic bioreactor (IAAB) treating palm oil mill effluent (POME): Startup and performance evaluation. *Industrial and Engineering Chemistry Research*, *60*(10), 3839–3859. https://doi.org/10.1021/acs.iecr.0c05878

Zahan, Z., Othman, M. Z., & Rajendram, W. (2016). Anaerobic Codigestion of Municipal Wastewater Treatment Plant Sludge with Food Waste: A Case Study. *BioMed Research International*, *2016*. https://doi.org/10.1155/2016/8462928

Zhang, J., Zhao, W., Zhang, H., Wang, Z., Fan, C., & Zang, L. (2018). Recent achievements in

enhancing anaerobic digestion with carbon- based functional materials. *Bioresource Technology*, *266*, 555–567.

Zhang, W., Zhang, L., & Li, A. (2015). Enhanced anaerobic digestion of food waste by trace metal elements supplementation and reduced metals dosage by green chelating agent [S , S] - EDDS via improving metals bioavailabili ... Water Research Enhanced anaerobic digestion of food waste by trac. *Water Research*, *84*(December 2017), 266–277. https://doi.org/10.1016/j.watres.2015.07.010

Zhang, Yu, Culhaoglu, T., Pollet, B., Melin, C., Denoue, D., Barriere, Y., Baumberger, S., & Mechin, V. (2011). Impact of lignin structure and cell wall reticulation on maize cell wall degradability. *Journal of Agricultural and Food Chemistry*, *59*(18), 10129–10135. https://doi.org/10.1021/jf2028279

Zhang, Yue, Banks, C. J., & Heaven, S. (2012). Anaerobic digestion of two biodegradable municipal waste streams. *Journal of Environmental Management*, *104*, 166–174. https://doi.org/10.1016/j.jenvman.2012.03.043

Zhao, T., Chen, Y., Yu, Q., Shi, D., Chai, H., Li, L., Ai, H., Gu, L., & He, Q. (2019). Enhancement of performance and stability of anaerobic co-digestion of waste activated sludge and kitchen waste by using bentonite. *PLoS ONE*, *14*(7), 1–20. https://doi.org/10.1371/journal.pone.0218856

CHAPTER 5

APPLICATION OF THE MODIFIED ADM1 MODEL TO STUDY KINETICS OF THE ANAEROBIC DIGESTION OF SEWAGE SLUDGE FOR THE METHANE PRODUCTION PROCESS

The process model described in this chapter simulates the dynamic behavior of a pilot-scale anaerobic sewage sludge digestion process. The model was created to help with experimental research into the anaerobic stage digestion process. The International Water Association's (IWA) established Anaerobic Digestion Model No.1 (ADM1) was created to serve as a backup for experimental findings regarding the actual anaerobic digestion process. In this chapter, the derivative of the model concept is implemented in the simulation software package MATLAB/Simulink™. The previous model idea was adjusted and used to simulate an anaerobic digestion process in this study. Testing procedures such as benchmark tests & balance checks were performed in order to verify the accuracy of the implementation. These measures worked in tandem to ensure that the model was implemented flawlessly and without inconsistencies. The primary objective of this chapter is to construct a method that is based on the ADM1 for evaluating co-digestion and predicting the performance of the digestion process or methane yield based on the analyzed substrate's physicochemical properties. Additional equations and simulations have been added to the standard model to create tools for evaluating the feasibility of anaerobic co-digestion. The study's two most important aspects are the optimal mixture and parameter dependence. The adjusted ADM1 is accurate in predicting the measured values of effluent COD, pH, methane, and produced biogas flows with a reasonable degree of accuracy, according to the validation results. This research shows how to use the ADM1 in a wastewater treatment plant and other settings where anaerobic digestion is of interest.

5.1. Introduction

As previously stated, anaerobic digestion is a well-known biological treatment process that results in the production of valuable methane gas through the degradation and stabilization of municipal sewage sludge (Barrera et al., 2015; Blumensaat & Keller, 2005; Ramdani et al., 2015). The need to reduce operating costs, as well as changing standards for the use and disposal of sewage sludge, has sparked interest in more effective sewage

sludge treatment processes (Mudzanani et al., 2021). One method for increasing efficiency is to physically divide the single-stage anaerobic digestion process into two process stages: a thermophilic pre-treatment stage followed by a mesophilic main treatment stage (Wickham, 2019; Xu, 2019).

The advancement of different mathematical models for various substrates has resulted from the growing interest in anaerobic digestion modeling in recent years. The Anaerobic Digestion Model 1 (ADM 1) was published in the IWA's Scientific and Technical Report No. 9 and has since become the most relevant model developed for the simulation of anaerobic treatment (Batstone, 2013; Rosen & Jeppsson, 2006). The ADM1 was designed in such a way that a standard parameter, Chemical Oxygen Demand (COD), and the process configuration of a continuously stirred tank reactor were used to determine the composition of various wastes (Astals et al., 2014).

A model approach was evaluated and updated for both thermophilic & mesophilic digestion processes. It was then implemented in MATLAB/Simulink to better understand this specific process configuration. The system was experimented with, adjusted with laboratory scale and pilot-scale studies, and thus validated with data from the literature (P. Li et al., 2021). This model was designed to assist with an easy translation of lab-scale data to pilot scale study of anaerobic digestion using municipal sewage sludge as a feedstock (Blumensaat & Keller, 2005; Mendes et al., 2015). The proposed model used in this study is based on the ADM1, a structured mathematical model for wastewater characterization that uses COD as it is a widely accepted measured parameter to describe the efficiency of the anaerobic digestion process (Blumensaat & Keller, 2005). It was created to concentrate on sewage sludge, which is most suited for anaerobic digestion in a CSTR reactor (Fezzani & Cheikh, 2009).

The biochemical activities covered in the ADM1 are classified as composite disintegration, substrate degradation mechanisms, hydrolysis of particulate COD, and particular biomass growth and decay processes (see Figure 5.1). In complex particulate waste, carbohydrate, protein, and lipid particle substrates, as well as particulate and soluble inert material, dissolve first. The disintegration step was largely implemented to facilitate the modeling of activated sludge digestion. This allows for the lysis of biological sludge and complicated organic matter, with the composites acting as a pre-lysis store for degrading biomass (Kainthola et al., 2019).

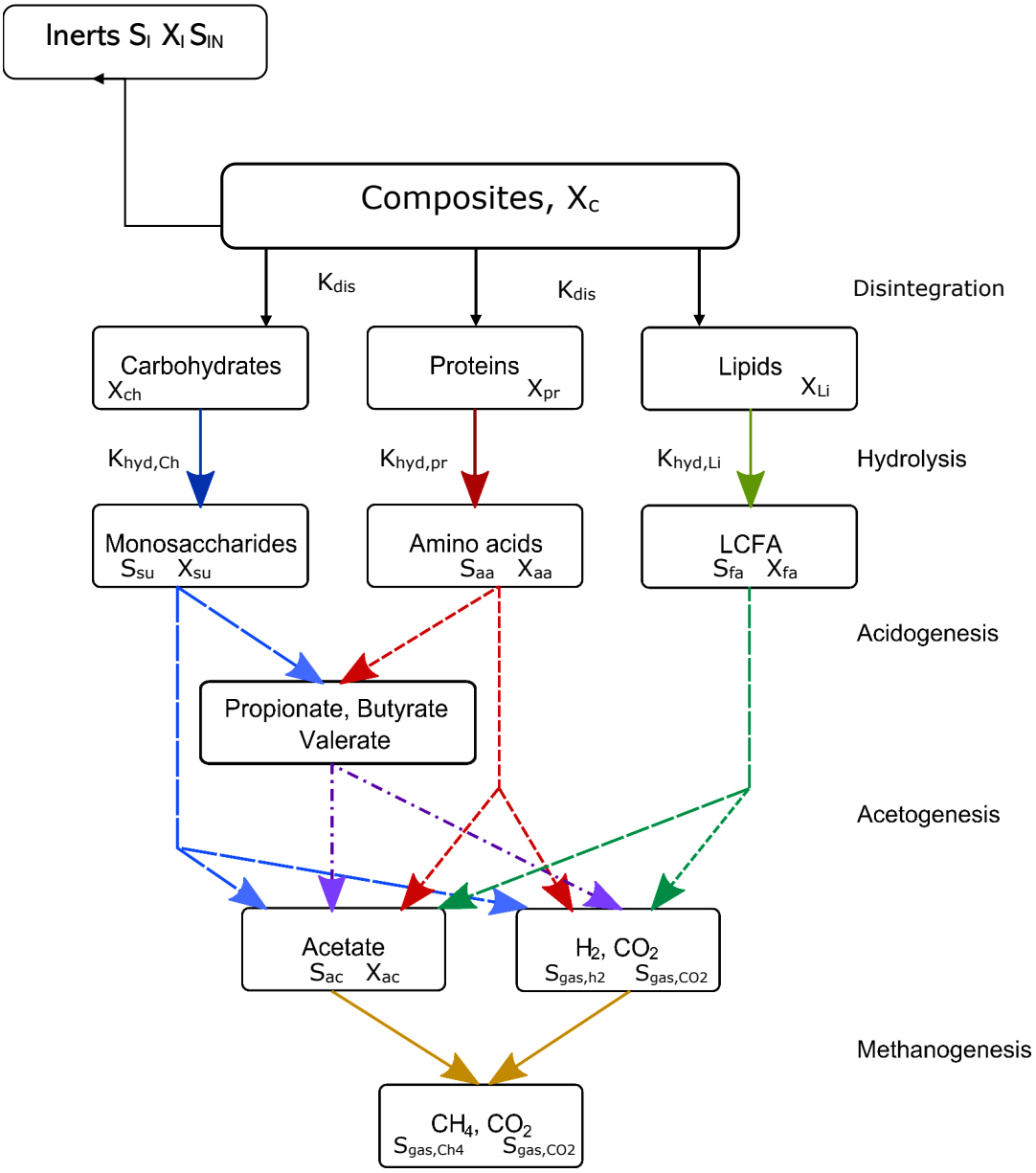


Figure 5.1: Anaerobic digestion process, composites degradation to inerts and hydrolysis reactants, through a disintegration step.

The model uses state variables to describe the behavior of particulate and soluble components to address these mechanisms. Chemical oxygen demand (COD) is used to describe molecular hydrogen and all organic compounds. The molar concentrations of nitrogenous and inorganic carbon species are used to describe them (Biernacki, et al., 2013; Xu, 2019). Soluble components that can flow through microbial cellular walls include monomers of complex polymers such as LCFA, sugars, and amino acids; volatile organic acids such as propionate, valerate, butyrate, and acetate; hydrogen and methane (D. Li et al., 2021). The model considers inorganic carbon, such as bicarbonate and

carbon dioxide, and nitrogenous species in addition to organic species (ammonia and ammonium). All species that dissociate have variables defined for protonated and non-protonated species as a function of pH, VFAs, and ammonia. For all of these compounds, a dissociation equilibrium has been assumed.

The application of ADM1 has attracted a lot of attention globally, Batstone et al., (2002); Biernacki, et al (2013), Blumensaat & Keller, (2005); P. Li et al., (2021); Rivera-Salvador et al., (2014) successfully applied ADM1 to simulate the anaerobic mono-digestion of sewage sludge using MATLAB and other software. Dereli et al., (2010) conducted a lab-scale study simulation of the ADM1, with AQUASIM software using industrial effluents in Turkey as a feed. Mendes et al. (2015) used the same software to investigate the influence of organic shock loads on the system of an anaerobic digester, and it was discovered that an organic loading rate can cause AD instability and even failure when fermentation reactions exceed methanogenesis, resulting in a drop in pH, the accumulation of VFAs and a reduction in methane gas production. The majority of articles in the literature report on anaerobic mono-digestion, with a few findings on co-digestion, such as Catenacci et al., (2021). Because the use of ADM1 in anaerobic co-digestion is limited, this article will focus on the co-digestion of sewage and dairy waste.

It was discovered that South Africa and the African continent lack comprehensive research on to use of the ADM1 to improve and optimize the AD process. Ngila et al., (2020) and Ndeba-Nganongo et al., (2018) conducted a study on the mathematical modeling of AD. This model was created to guide in identifying important design characteristics and quantifying system parameters that assured optimal performance. The data gave insight into wastewater characteristics such as biodegradability, flow distribution, pollutants, and the possibilities for source management. Few researchers use MATLAB as a simulation tool for the mathematical modeling of AD and simulation due to its complexity. The method outlined here clearly demonstrates the usage of MATLAB Simulink software to simulate mathematical modeling that will describe, forecast, and control the complicated interaction of wastewater treatment processes.

In this study, the purpose is to construct an ADM1 simulation approach to estimate the performance of anaerobic digestion of sewage sludge from wastewater and define the biodegradation kinetics. This will be accomplished by first detailing all of the important biochemical and physicochemical processes involved in COD and VFAs complexation, as well as precipitation, dissolution, and substrate absorption in the AD system. The simulation will be carried out to mimic the AD process on important parameters with

MATLAB Simulink. The developed model will be validated and calibrated and sensitivity will be examined. Once validated the optimization will be done to ensure a maximum gas output with the PSO approach.

5.2. Material and Methodology

Please refer to section 3.1: substrate and inoculum and Sections 3.7-3.10 for batch and semi-continuous tests.

5.2.1. Analytical Method

The VS, TS (VSS, TSS), TA, TKN, and concentrations of N—NH_3, N—NO_2, and N—NO_3 were determined using Standard Methods (APHA, 2012); COD was determined using Cell Tests on samples centrifuged (10 min at 4000 rpm) and filtered at 0.45 m. (MERCK-referring to EPA 410.4 method). Based on the total COD of the sewage sludge, organic matter was fractionated into 40% inert particulate COD, 30% hydrolysis products, and 30% particulate degradable COD. These were further divided into 9% amino acids, 6% sugars, 13.5% LCFA, and 1.5% p inert soluble COD (Eaton et al., 2005). The inputs that were applied to the different factors of the constructed model are listed in Table 5.1.

Table 5.1: Measured parameters as inputs for ADM1

Component	Description	Min	Max	Average
Flow [m^3/day]	Influent Flow	165	170	167,5
pH		5,1	7	6,05
Temperature [°C]		31	37	34
TCOD [mg/l]	Total COD	7940	10500	9220
SCOD [mg/l]	Soluble COD	5342	8500	6921
PCOD [mg/l)	Particulate COD	2598	1000	1799
TSS [mg/l]	Total Suspended Solids	603,44	750,03	676,735
VSS [mg/l]	Volatile Suspended Solids	573,268	609,23	591,249
VFA [meq/l]	Volatile Fatty Acids	721,3	821,56	771,43
Total Alkalinity	as $CaCO_3$	584	589	586,5
TOC	Total Organic Carbon	25	31	28
TKN [mg N/l]	Total Kjeldahl Nitrogen	925	946,3	935,65
NH_4-N [mg N/l]	Ammonium Nitrogen	127	129	128
NO_2-N [mg N/l]	Nitrate	54	54,3	54,15

NO_3-N [mg N/l]	Nitrite	190	197	193,5
Total-P [mg P/l]	Total Phosphorus	3,69	6	4,845
PO_4-P [mg P/l]	Orthophosphates	0,1	0,12	0,11
Ca [mg/l]	Calcium	5,4	5,4	5,4
Mg [mg/l]	Magnesium	0,87	0,87	0,87
SO_4 [mg/l]	Sulphates	0,32	0,45	0,385
	Outputs			
CH_4 content [%]	Methane %	65	71	68
CO_2 content [%]	Carbon dioxide	31	32	31,5

5.2.2. Mathematical Model Development

Mathematically, ADM1 is described as a non-linear structured ODE model that depicts the anaerobic digestion reaction in a CSTR by incorporating several biological and physicochemical phenomena (Vega De Lille, 2015). In this process, biodegradable organic compounds are transformed into carbon dioxide and methane with a trace of inert by-products. The key biochemical processes evaluated starts with the disintegration stage followed by the hydrolysis step, acidogenesis, and acetogenesis until methanogenesis, refer to Figure 5.2.

5.2.2.1. Model structure philosophy

ADM1 has biochemical and physical mechanisms that are widely accepted in Alzheimer's research (Asadi & McPhedran, 2021; Rosen & Jeppsson, 2006). The Petersen matrix, which describes stoichiometric conversions and kinetic rates, has the same format. ADM1's general framework allows for the uniform representation of precipitation, complexation, and adsorption models. To introduce the basic methodology of modeling conceptualized ADM1, a simple representation of the soluble component, I (S_i), particulates (X_i), and gas component (S_{GAS}) has been presented. The model is built by first defining the various reactions that will be considered. As shown in Figure 5.2, substrates are taken up by cells in a particulates-containing liquid influent stream (Batstone, 2013). The AD reaction takes place, converting the substrate to products (gas phase) and various biomass constituents (liquid and particulates phase).

Mass balance equations govern the particulate and soluble components concentrations' in the liquid phase. According to Batstone et al. (2002), a description of each component

is required to implement the model and complete mass balances for all model components. As a result, ADM1 grouped these particulates into state variables termed composite particulates (Xc) (Hassam et al., 2015). Carbohydrates (X_{Ch}), lipids (X_L), proteins (X_{pr}), soluble inerts (S_1), and particulate inerts (X_I) are also defined as disintegration particulates as shown in Figure 5.2.

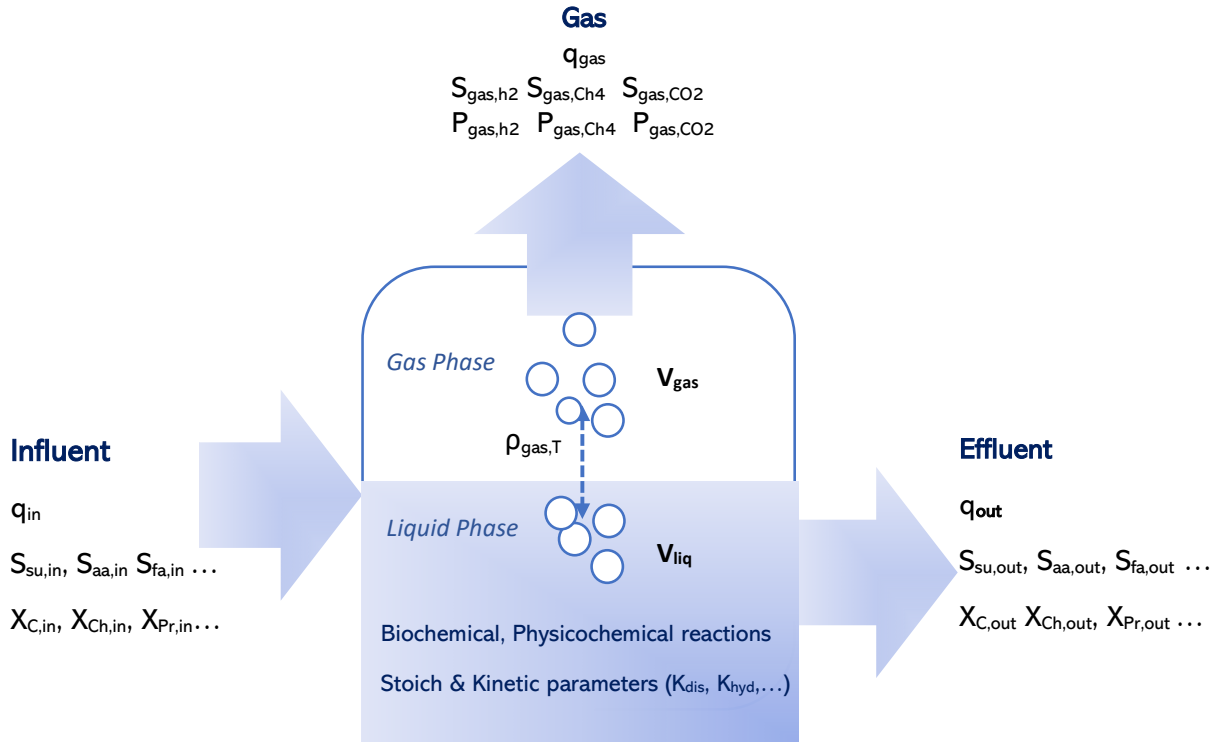


Figure 5.2: Mass balance boundary around CSTR in the anaerobic digestion system, adapted from Batstone et al (2002).

Provided that one COD mass unit of X_C disintegrates completely, the following results will be obtained:

$$f_{S_I\ X_C} S_I + f_{X_I\ X_C} X_I + f_{ch\ X_C} X_{ch} + f_{pr\ X_C} X_{pr} + f_{li\ X_C} X_{li} = 0.1S_I + 0.25X_I + 0.2X_{ch} + 0.2X_{pr} + 0.25X_{li} \quad (5.1)$$

The COD balance matters as much as the sum of all $f_{i;XC}$=1. However, it is proposed that the nitrogen concentration of X_C(N_{xc}) be 0.002 kmol N/kg COD. Instead, the nitrogen concentration is 0.0021(kmol N) based on the disintegration output and parameter values from Batstone et al. (2002). Thus, it indicates that 0.1 mol of nitrogen is produced for every kilogram of COD that degrades, 5% more than the original. Although the "default" parameter values should automatically close the mass balances, the nitrogen

content and production from composites are likely to vary and may need to be adjusted for each specific case study (Rosen & Jeppsson, 2006).

5.2.2.2. Mathematical Equations

For each component considered in the liquid phase and particulates, the mass balance equations can be written in the general form of Equations (5.2) & (5.3).

$$\frac{d}{dt}\left(S_{liq,i}\right) = \frac{Q}{V_{liq}}\left(S_{in,i} - S_{liq,i}\right) + \sum_{j=1}^{19} \rho_j v_{i,j} \tag{5.2}$$

$$\frac{d}{dt}\left(X_{liq,i}\right) = \frac{Q}{V_{liq}}\left(X_{in,i} - X_{liq,i}\right) + \sum_{j=1}^{11} \rho_j v_{i,j} \tag{5.3}$$

Where:

$S_{liq,i}$ = Soluble state variables no. 1 to 12, 25 and 26 (Please see Appendix A)

$X_{liq,i}$ = Particulate state variables no. 13-24 (Please see Appendix A for state variable)

Q = Influent or feed volumetric flow, equal to outflow (assuming no accumulation)

V_{liq} = Volume of the digester

$S_{in,i}$ = Soluble components concentration, influent stream

$X_{in,i}$ = Concentration of influent stream, particulate components

ρ_j = Specific kinetic rate are calculated; $\rho_j = K_m \left(\frac{S}{Ks+S}\right) X$ (5.4)

K_M = Monod kinetic rate

K_S = Substrate concentration

Gas calculations

The rate equations for the gas phase are quite similar to the rate equations for the liquid phase. In ADM1, mass balance for the gas phase components considers methane, hydrogen, and carbon dioxide, with an assumption of no heat transfer in the influent flow. The anaerobic digestion system has continuous gas volume thus Equations (5.5) & (5.6) represent the remaining three state variables, 27 to 29.

$$\frac{d}{dt}\left(S_{gas,i}\right) = \frac{q_{gas}}{V_{gas}}\left(S_{gas,i}\right) + \frac{V_{liq}}{V_{gas}}\rho_{T,i} \tag{5.5}$$

Where:

$S_{gas,i}$ = Gas phase variables no. 27-29

q_{gas} = Total gas outflow

V_{gas} = volume of gas occupying the digester headspace

$\rho_{T,\,i}$ = Specific mass transfer rate of gas, $\rho_{T,i} = K_{La}\left(K_H S_{gas,i} - S_{liq.i}\right)$ (5.6)

k_{La} = Mass transfer coefficient, in gas-liquid volume

K_H = Henry's law coefficient

The gas law can be used to calculate the pressure of each gas, with all gases being interpreted as an ideal gas at the equivalent temperature to the liquid phase components. As a result, each gas component's partial pressure is governed by the ideal gas law, as shown in Equations 5.7, 5.8 & 5.9. The denominators 16 and 24 are COD equivalents for unit conversion.

$$P_{gas,H_2} = S_{gas,H_2} \cdot \frac{RT_{gas}}{16} \tag{5.7}$$

$$P_{gas,CH_4} = S_{gas,CH_4} \cdot \frac{RT_{gas}}{64} \tag{5.8}$$

$$P_{gas,CO_2} = S_{gas,CO_2} \tag{5.9}$$

Assuming that water vapour has saturated the reactor headspace.

Too often the headspace is saturated with water vapour, therefore the maximum headspace pressure is determined by the water vapour (P_{gas}) along with CH_4, CO_2 & H_2. And thus its partial pressure ($P_{gas,\,H2O}$) needs to be subtracted from P_{gas}. Hence the gas production rate, q_{gas} can be calculated using Equation 5.10.

$$q_{gas} = \frac{R \cdot T}{P_{gas} - P_{gas,H_2O}} V_{liq} \left(\frac{\rho_{T,H_2}}{16} + \frac{\rho_{T,CH_4}}{64} + \rho_{CO_2}\right) \tag{5.10}$$

Equation 5.11 is used to modify the benchmark water vapour pressure at 25 °C to the apparent temperature because water vapour pressure is significantly reliant on temperature (T).

$$P_{gas,H_2O} = 0.0313 \cdot e^{\left(5290\left(\frac{1}{298}\right) + \frac{1}{T}\right)} \tag{5.11}$$

pH calculations

H^+ ion calculations are performed using the "pH solver" found in Rosén and Jepsson (2006), this is because Batstone et al (2002) are not particularly precise on how to compute pH for the DE-implementation. As recommended by Rosén et al (2006), acid concentrations were determined by summing up the amount of an acid-base pair and

the negative concentrations of a base in an acid-base pair. The differential equation for determining the amount of negatively charged particles in an acid-base pair is shown in Equation (5.12). According to Rosén et al (2006), the pH inhibitory impact is also taken into account (see Table 5.2).

$$\frac{dS_{acid,i}}{dt} = -K_{A,B\ ;i}\left(S_{acid-,i}(Ka_{acid} + S_{H^+}) - Ka_{acid}S_{acid,total}\right) \quad (5.12)$$

Where

$S_{acid-,i}$ = -ve charged acid pair; acid number I, ion number i

$K_{a,i}$ = Acid-base equilibrium coefficient for acid i,

$k_{A;B;i}$ = Acid-base reaction kinetic parameter for acid i.

S_{H^+} = Concentration of H^+ ions

$S_{acid,total}$ = Acid-base pair sum

$Ka_{,acid}$ = Acid-base equilibrium co-efficient

Inhibition

Toxicity and inhibition may have an impact on the degradation process. The incremental loss effect noticed on the kinetic rates can be explained by using the applicable inhibition factors (I_1, I_2,...I_n) in conjunction with the specific kinetic rates stated in Equation (5.4). The model's inhibition factors are the result of combining one or more of the inhibition equations listed in Table 5.2. Even though the default version of ADM1 only includes four types of inhibition, it is thought to be sufficient for treating common substrates.

Table 5.2: Inhibition factors and equations summarized

Type of Inhibition	Description	Equation	Affected Process
pH Inhibition	pH inhibition at both low & high pH	$I_{pH} = \frac{1 + 2 \times 10^{0.5(pH_{LL} - pH_{UL})}}{1 + 10^{(pH - pH_{UL})} + 10^{(pH_{LL} - pH)}}$	All substrate uptake
	pH inhibition at low pH only	$I_{pH} = \exp\left(-3\left(\frac{pH - pH_{UL}}{pH_{UL} - pH_{LL}}\right)^2\right) \Big\vert_{pH < pH_{LL}}$	
		$I_{pH} = 1 \quad \Big\vert_{pH > pH_{LL}}$	
Competitive Inhibition	Valerate & Butyrate competes for C4	$I_1 = \frac{1}{1 + S_1/S}$	Butyrate, valerate, C4 uptake
Non-competetive Inhibition	Hydrogen and free ammonia inhibition	$I_{h2} = \frac{1}{1 + S_{h2}/K_{I,h2}} \quad I_{Nh3} = \frac{1}{1 + S_{Nh3}/K_{I,Nh3}}$	LCFA, Acetate, Butyrate, valerate, propionate uptake
Secondary substrate	Inhibition due to limited inorganic nitrogen	$I_{IN,lim} = \frac{1}{1 + K_{S,IN}/S_{IN}}$	All substrate uptake

- I_{pH}, I_1 ,I_{H2}, I_{NH2}, $I_{IN,lim}$ – Inhibition factors due to pH, 1 competition, H_2 hydrogen, NH_2 ammonia and IN- inorganic nitrogen, respectively.
- S_1, S_{H2}, S_{NH2}, S_{IN} - Soluble components concentration of 1 competitors, H_2 hydrogen, NH_2 ammonia and IN- inorganic nitrogen, respectively.
- $K_{I,h2}$, $K_{I,Nh2}$, $K_{S,IN}$ - Specific kinetic rate components of H_2 hydrogen, NH_2 ammonia and IN- inorganic nitrogen, respectively.

5.2.2.3. *Model assumptions*

A simplified model based on the scientific and mathematic fundamentals of mass balance was constructed in this work. For the anaerobic treatment unit's kinetic model, assumptions were made with caution, and system observations were reported for mass balance calculations around the digester.

- The first assumption was that sewage sludge from municipal wastewater treatment comprises organic matter in a soluble state and thus does not comprise organic and inorganic suspended particles.
- The digester is entirely homogenized, and the wastewater is heated to 37±2°C, with consistent substrate concentration throughout the digestion (Altinay Perendeci et al., 2012; Danielsson, 2014).
- Only acidogenic microbes are thought to be present in the hydrolysis process, whereas both methanogenic and acidogenic microorganisms are present in the remaining AD reactions (Rosen & Jeppsson, 2006).
- Acidogenic bacteria decompose dissolved organic material into volatile fatty acids and CO_2 during hydrolysis. Volatile fatty acids (VFA) are transformed into acetic acid,

hydrogen, and carbon dioxide in the second stage, which are the key substrates for methanogenesis, resulting in CH_4.

- The hydrolysis process is primarily responsible for the formation of VFA from sugar monomers. However, it is anticipated that unhydrolyzed glucose is transformed into VFA and methane in the anaerobic digester at the same time (Mendes et al., 2015).
- The microbiology of anaerobic digestion focuses on the entire conversion of organic matter to methane by primarily two bacteria populations. Acetogenic and methanogenic microorganisms are inhibited by unionized acetic acid, which results in methane generation.
- As a result of the high VFA concentration expressed as HAc, unionized acetic acid (HAc) inhibits the hydrolysis process. Above 200 g Nm^{-3}, the major source of nitrogen, ammonium (NH_4), also has an inhibitory effect. Because the average influent NH_4–N concentration was measured to be 11.9 g Nm^{-3}, there should be no ammonium inhibitory impact (Rozzi & Remigi, 2004).
- Because of the high ion concentration and rising temperature in the digester, it's safe to infer that CH_4 solubility is nearly nil.
- The pollutant level of wastewater was measured in terms of glucose and, VFA & volatile organic compounds (VOCs).
- The total COD concentration in the influent was subtracted from the VFA, which is a measured system variable equivalent to COD (1 g HAc l^{-1}), and the residual COD in the wastewater was converted to glucose equivalent using the formula 1 g glucose equivalent to 1.066 g COD).

5.2.3. Sensitivity analysis

The model is comprised of a complex set of variables and parameters. It is critical to understand how parameters affect the reliability of results when applying simulation results to real-world implementation in a real plant. The topic that is frequently raised is whether any parameters define the space in which calculations are performed that have a bigger impact on findings than others. If this is the case, studying certain parameters in order to choose them appropriately is more significant than studying parameters that do not have the same impact on results.

Generated methane gas was selected as an important model result outcome to investigate the model's parameter dependence. The effect of methane production was studied by keeping all parameters constant and gradually increasing them one percent at a time. The definition of the derivative can be used to investigate parameter dependency

from those recorded effects in gas production; the parameter is denoted by x in Equation (5.13).

$$\frac{dF}{dx} = \frac{f(x+\Delta h)-f(x)}{\Delta h} \tag{5.13}$$

However, in order to make calculations simple and feasible, the steps of h as the limit is approaching zero, are chosen to be 0.01. By choosing all parameters as they were supposed to be and then increasing them 1% at a time, the effect of methane production was investigated. Thus Equation (5.13) is converted to Equation (5.14) instead of utilizing the usual derivative definition:

$$\frac{dF}{dx} = \frac{F(1.01x)-F(x)}{0.01} \tag{5.14}$$

Using this method for measuring sensitivity (using ×1.01 instead of Δh), the design for parameter dependence can be thought of as a simplified Jacobian matrix comprising numerically calculated gas production partial derivatives as a function of each parameter is studied. This can be written for the parameter p1;p2;.....; pn as;

$$J = \left[\frac{\partial q_{gas,CH_4}}{\partial P_1}, \frac{\partial q_{gas,CH_4}}{\partial P_2} \dots \dots \frac{\partial q_{gas,CH_4}}{\partial P_1}\right] \tag{5.15}$$

While this is a straightforward and considered an easily justified method of determining variable reliance, there can be complexities when comparing different parameter dependencies. Because the denominator of the derivative definition is dimensionally dependent, all sensitivity has different components, making the comparison of various parameters impractical. A similar approach is used in the definition, but only the numerator is used. The finite difference is a term used to describe this procedure, and it has the following equation;

$$\text{Change in gas production} = |f(1.01 \cdot x) - f(x)| \tag{5.16}$$

The parameters examined will influence the outcome of methane gas generation using this method. An important feature of this numerical approach to determining parameter dependency is that it is only valid in a single parameter space position; altering any of the parameters renders the result invalid and needs a new analysis. This holds even if the input variables specifying how the model works are modified. These will affect the parameter space in which the calculations are performed. As a result, comparing the outcomes of dependent simulations for different sections of the parameter space is intriguing. If a parameter dependency evaluation is carried out prior to the enhancement of biogas production, the dependence evaluation must be carried out after the optimization to see if any changes in parameter dependency have occurred. The

parameter sensitivity changes when the input variables are modified dynamically. Sensitivity was calculated to determine how much a change in input variables affects outflow, and methods for changing input variables dynamically were developed.

5.2.4. Flow chart for code running ADM1 model.

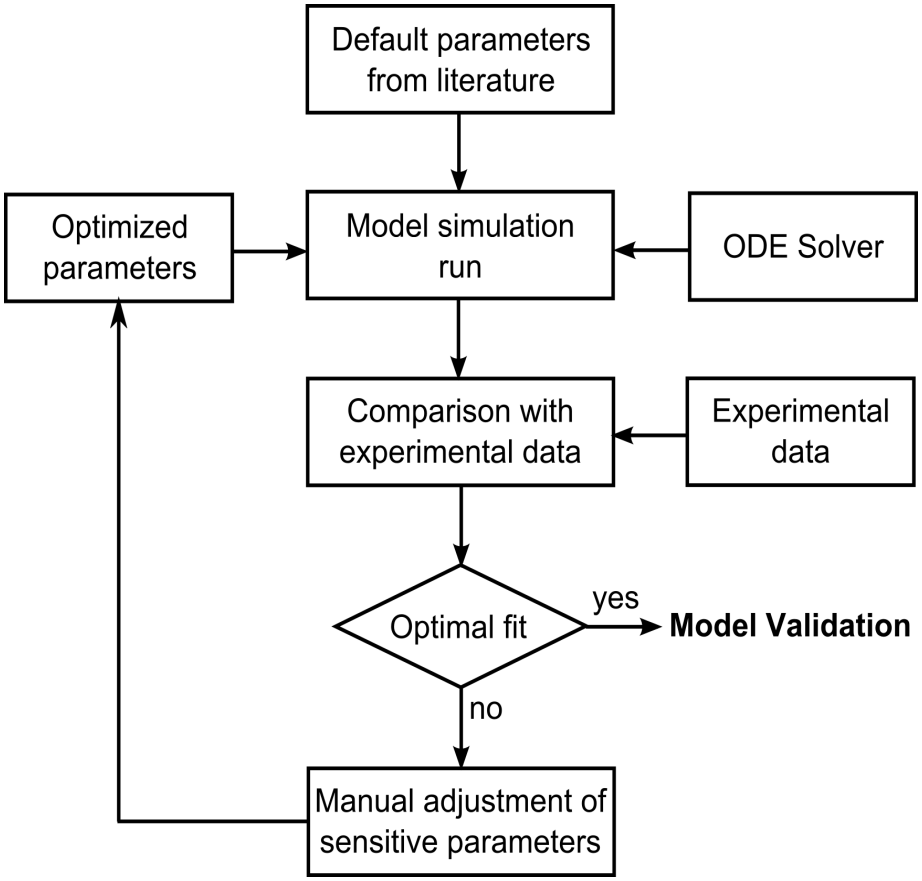


Figure 5.3: Flow chart for running the ADM1 model using Matlab/Simulink™

5.2.4.1. Sensitivity analysis & variable dependence of parameters

Calculated parameter dependence, as previously stated, is valid in a single section of parameter space only. Nevertheless, there are sporadic inflows that change over time. The fluxes entering the digester influence the point in parameter space where computations are done. To establish the effects on system sensitivity, multiple analyses, one for each location investigated, are necessary. By gradually changing the inflow while computing the sensitivity of significant parameters, the generalized reliance of sensitivity connected to one variable is investigated. This type of simulation is thus performed using the following method where p is the parameter value and v is the variable value, f(v,p) is the quantity of CH_4 gas created as a function of v;p (measured in [m^3/d]) (Danielsson, 2014).

5.3. Results and Discussion

A series of simulation tests are performed to evaluate the model implementations offered in this study. These tests include 1) steady-state simulations for comparing transient behaviour in detail, 2) two variable simulations for comparing total simulation times, and 3) dynamic simulations for comparing overall simulation times (Rosen & Jeppsson, 2006). The ODE model is a differential equation model that has been used in this work. The simulations have been performed on a modern PC with Windows 10 and MATLAB/Simulink R2020a. It is necessary to be familiar with the systems on which the created methods are meant to be used in order to use them. This requires some lab analysis as well as conversion to conventional ADM1 units, which are not always the same as those employed in lab scale investigations. As a result, the model can be used to assess and test the compatibility of different raw materials for digestion methods. Please refer to Appendix A, Table A1 to A.5 for supplementary information used.

A simplified kinetic model based on unstable material balances was used to predict mass balance, VFA, and COD equivalent glucose concentration in a hydrolysis tank, as well as mass balance, VFA, and gas output in a lab-scale anaerobic digester. The algorithm of the kinetic model simulated factors other than COD in the anaerobic tank. Because the internal states of anaerobic digestion cannot be measured using ordinary measurement equipment, the data needed to train and evaluate the pattern recognition systems under review must be generated synthetically. As a result, in order to create the synthetic dataset, a full-scale biogas plant simulation model data is created, and a simulation model is created and calibrated for this biogas plant. Anaerobic digestion modeling using the complex ADM1 has proven to be an effective all-around technique. The ADM1 is often implemented as a nonlinear differential equation system (Tassew et al., 2019).

The model that has been implemented can be utilized as a stand-alone model for evaluating a specific system or as the foundation for future applications. This article's framework is meant to be simple to understand and adaptable to new applications. As closely as possible, it follows Rosen and Jeppsson's proposed implementation. When you run the model with typical values that lead to steady state solutions, you get the plots shown in Figures 5.3 to 5.8, and when you compile the result to get more information out of the data, you get the plots shown in Figures 5.9 and 5.10 for produced gas and pH, respectively. Gas production is shown as gas flow Figure 5.11.

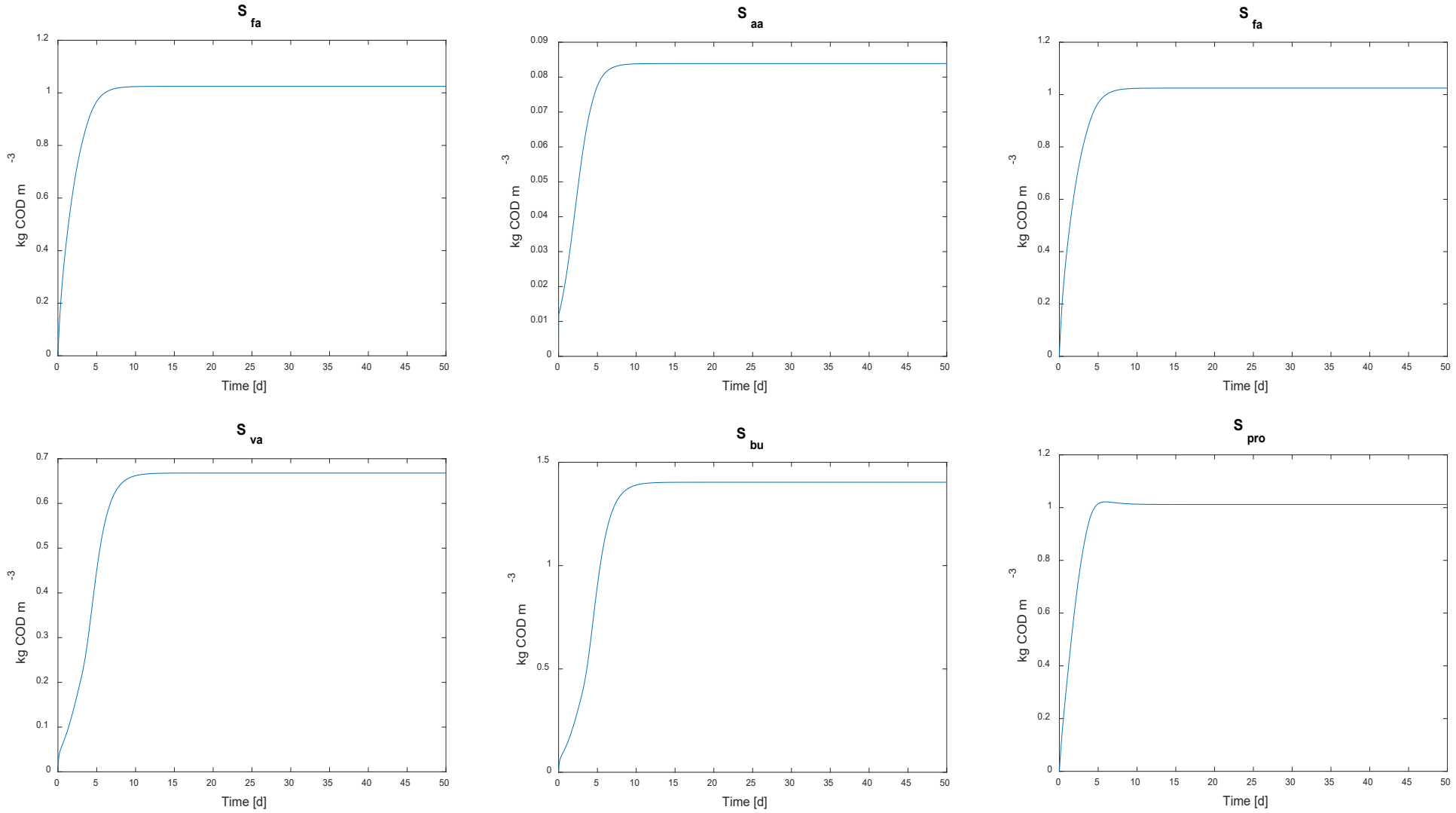


Figure 5.4: Model simulation component output, Substrate number output 1-6

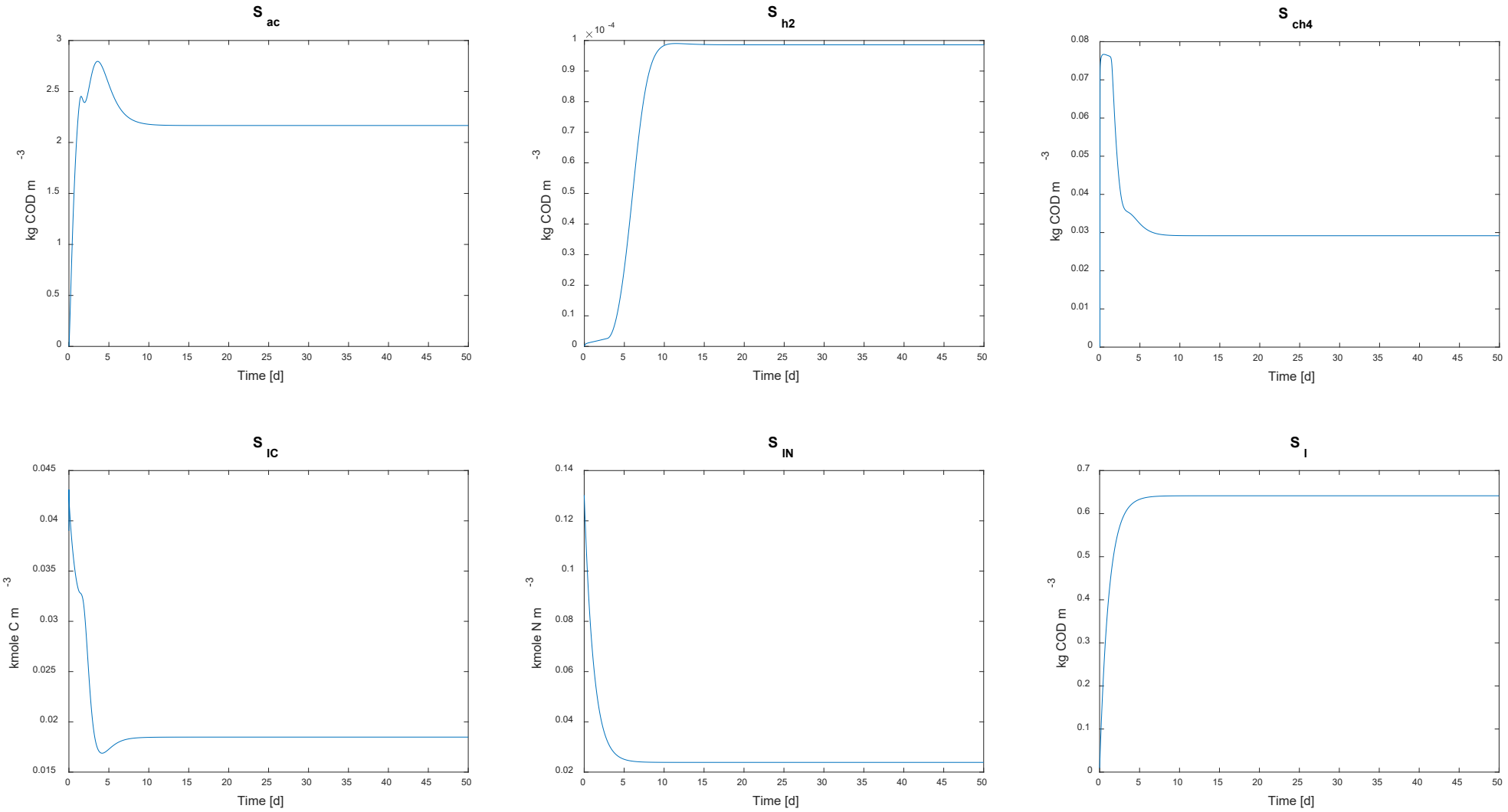


Figure 5.5: Model simulation component output, Substrate number output 7-12

5.3.1. ADM1 Simulation using Measure Parameters

Figure 5.4 illustrates the models of the six output predictions when multiple independent variables are utilized. This result represents the uncalibrated model. With the exception of Ammonia (S_{IN}), graphic inspection showed that all simulated outputs closely tracked the pattern of the industrial plant measurements. Because inconsistent responses were reported across various geographical locations and different timescales, the anticipated ammonia trend is considered irregular (Danielsson, 2014). This observation could be attributed to the use of ADM1 on an influent with a highly fluctuating substrate composition. Because particulate COD concentration is translated into ADM1 state variables that represent proteins, carbohydrates, and lipids using a constant compositional ratio, disagreement is inherent when the substrate's composition ratio varies (Danielsson, 2014). In actuality, as in this instance, the substrate composition can be changed dynamically.

The effect of VSS concentration was greatly understated. Given the projection's close similarity in trend, the lack of correlation is most likely owing to inconsistent kinetic parameters relating to organic particle biodegradation such as biomass decay, hydrolysis, or biomass growth (Shi et al., 2019). As a result, sensitivity analysis, calibration, and cross-validation are likely to improve on these discrepancies. Despite the fact that some parameters were uncalibrated, the pH, methane gas flow (qCH_4), and VFA fit well. A good pH match is expected since Parra-Orobio et al., (2020) pointed out that pH in a well-buffered digester will remain stable. Because the digester has a long hydraulic retention time, (HRT) of ± 2 days, the majority of the alkalinity created during methane production is kept.

A stable alkalinity buffer is also ensured by the predominantly alkaline substrate. A stoichiometric process converts the three components i.e. carbon dioxide, acetate, and hydrogen to methane. As a result, the production rate is proportional to the concentration range of these constituents, which are determined by the kinetics and composition of the influent. To put it another way, COD fractionation into ADM1 system parameters that are calibrated, along with state variables, have a big influence. Because, irrespective of how COD is partitioned, when no inhibition is present, all biodegradability COD will play an active role in methanogenesis activities unrestrictedly, it is possible to derive a relatively accurate estimate of methane gas generation even with uncalibrated parameters. Although the trend was similar, the simulated carbon dioxide flow (q_{CO2}) was continuously higher than the plant data. This is similar to the results obtained in Danielsson, (2014) in which it was explained that it could be owing to a pH prediction that is lower than the real pH and/or an overestimation of inorganic carbon (S_{IC}).

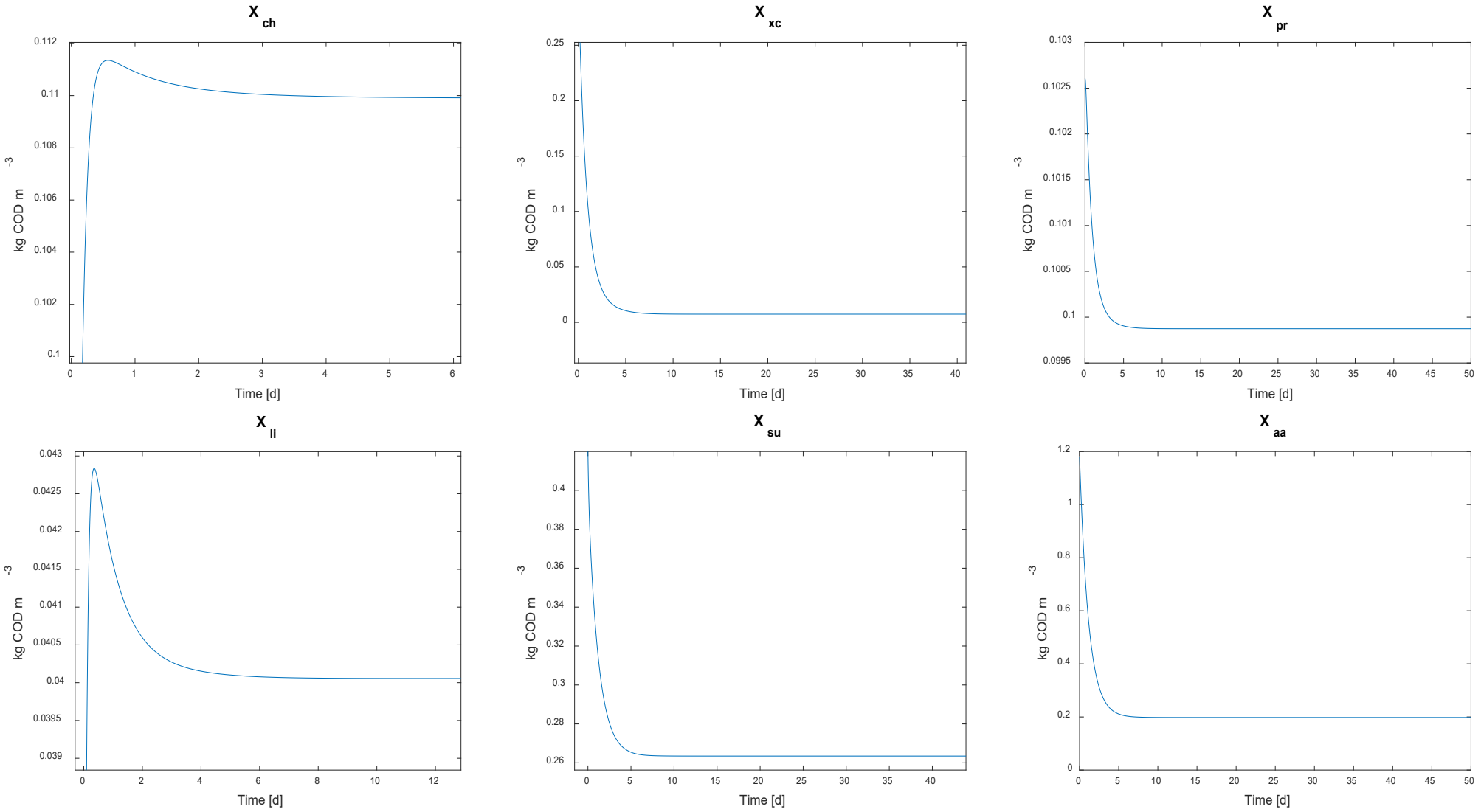


Figure 5.6: Model simulation component output, Substrate number output 13-19

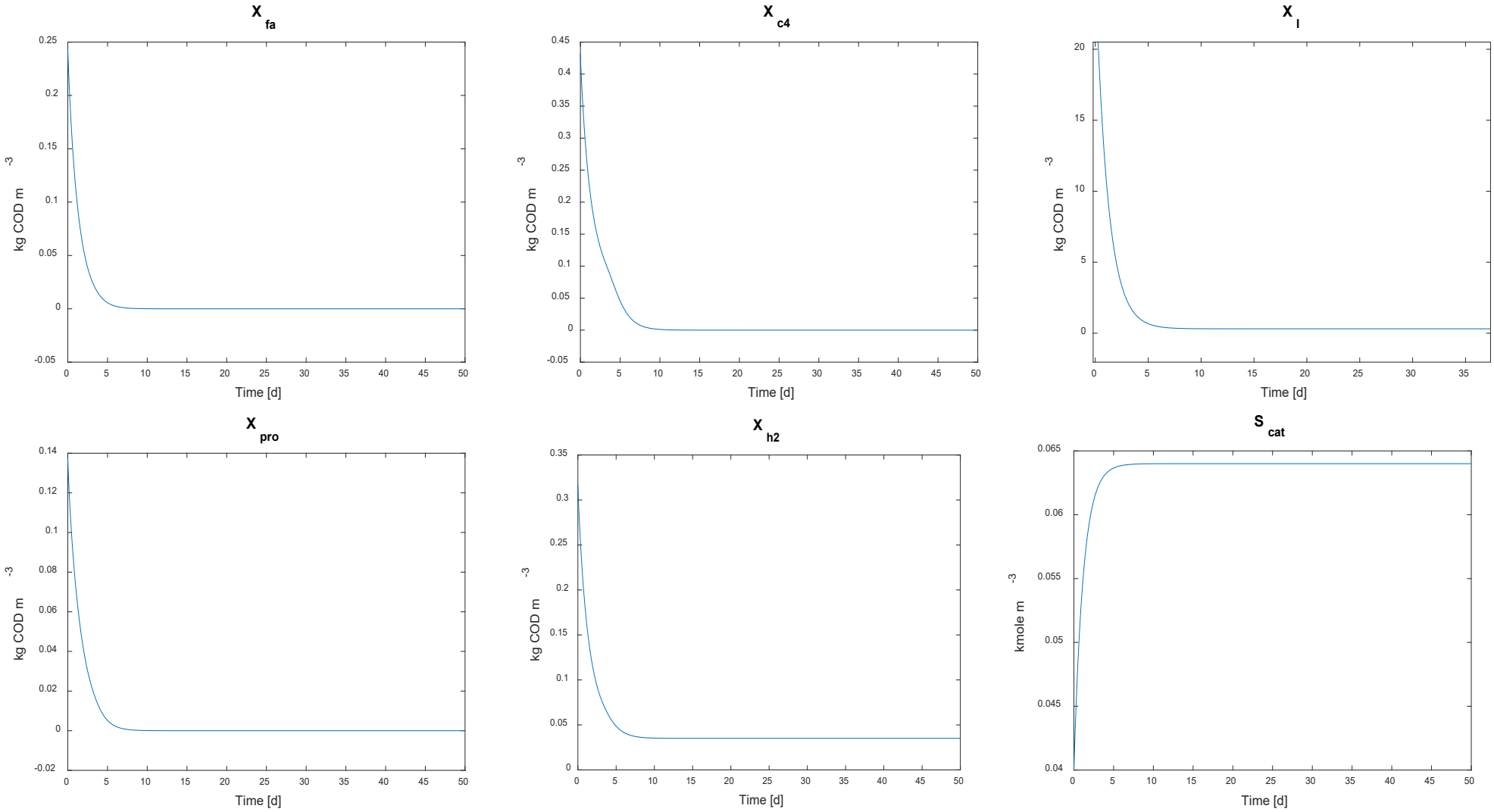


Figure 5.7: Model simulation component output, Substrate number output 20-25

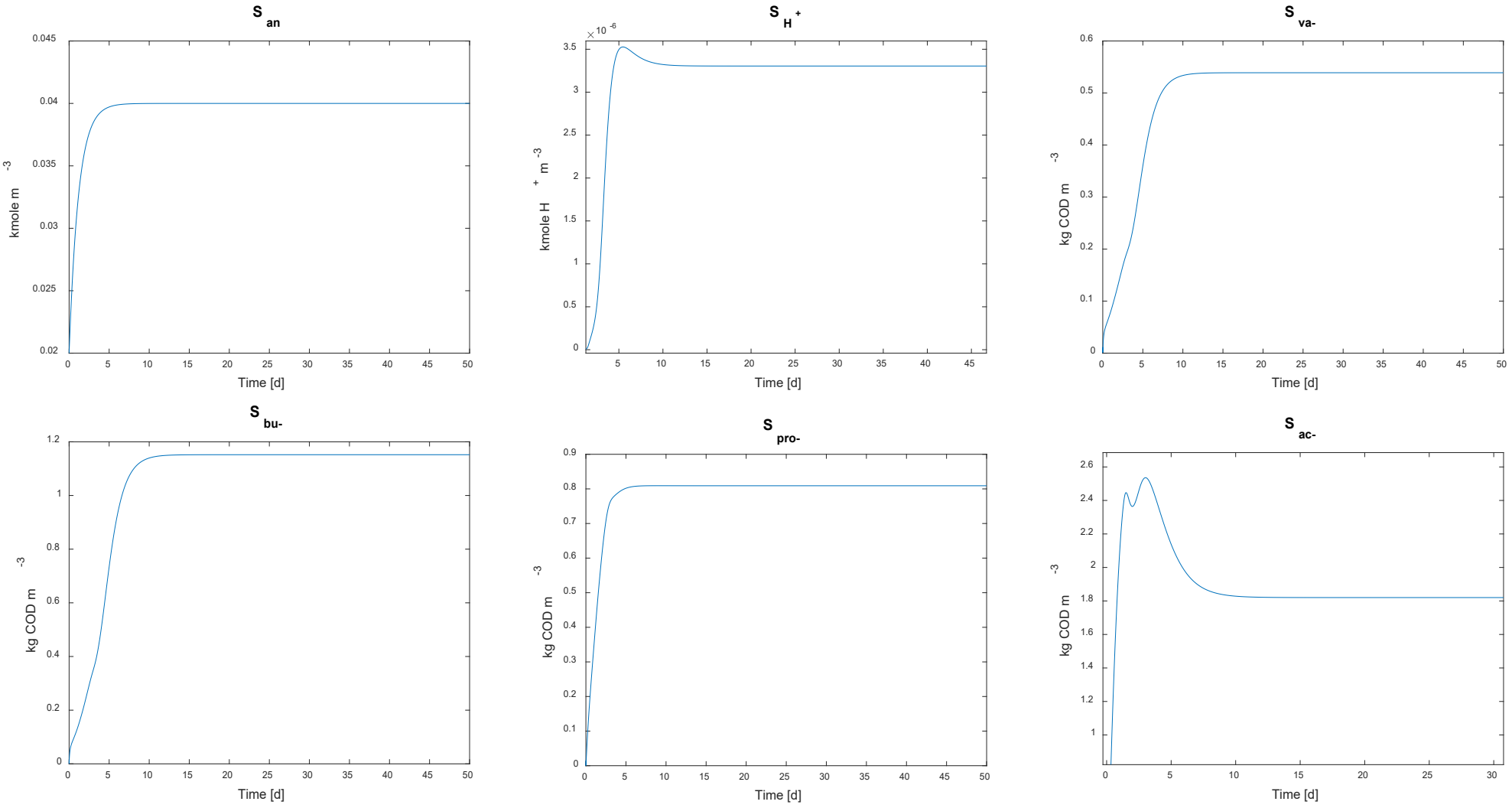


Figure 5.8: Model simulation component output, Substrate number output 20-25

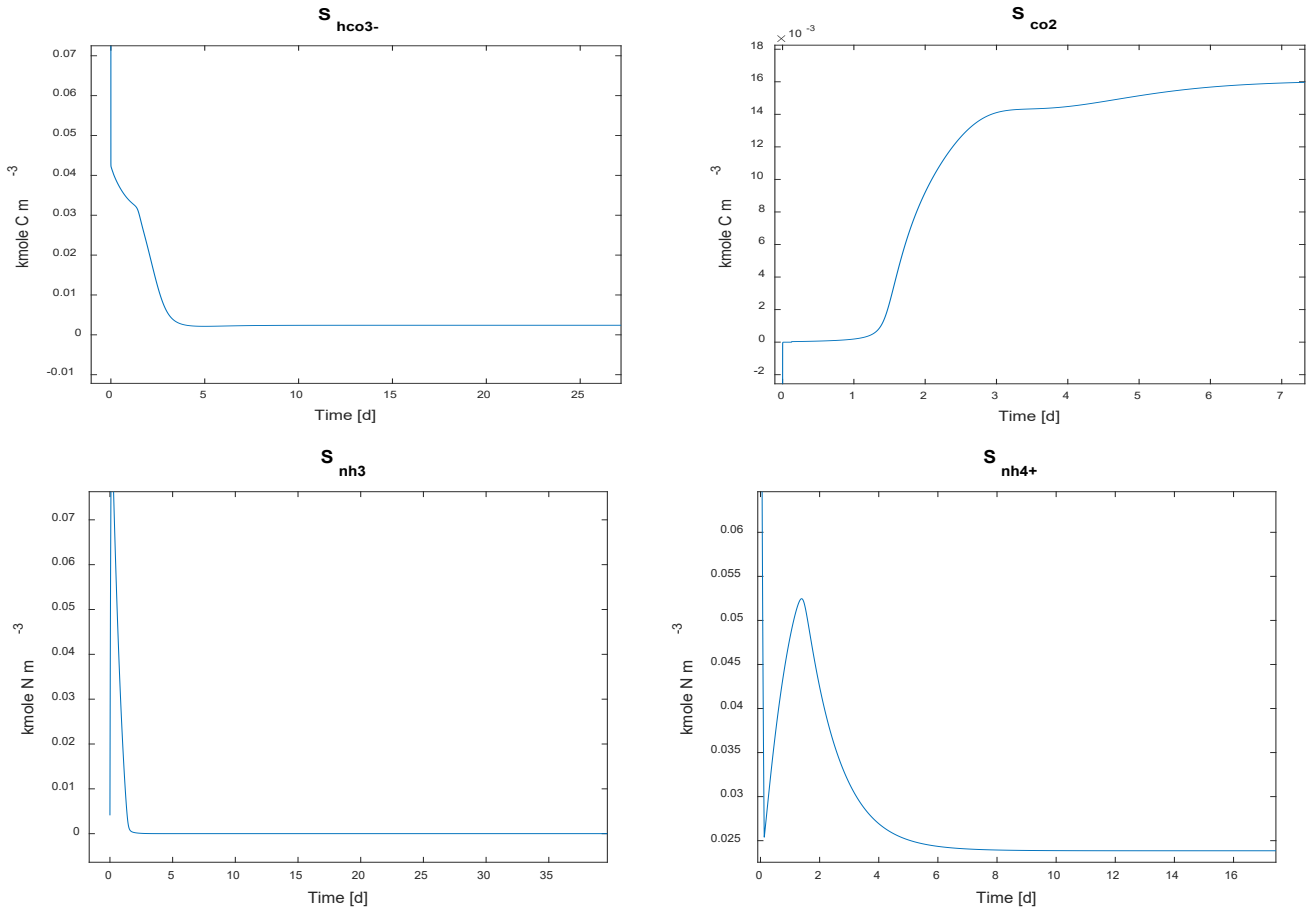


Figure 5.9: Model simulation component output, Substrate number output 26-30

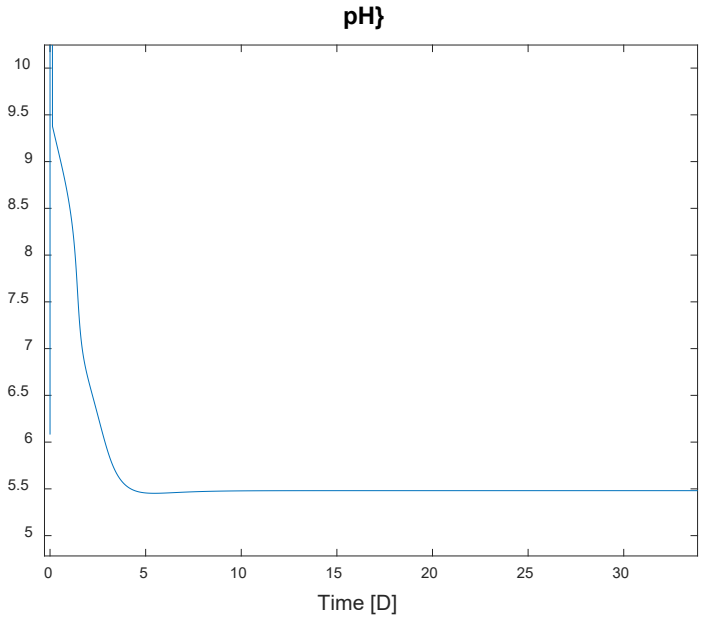


Figure 5.10: Component pH output from model simulation

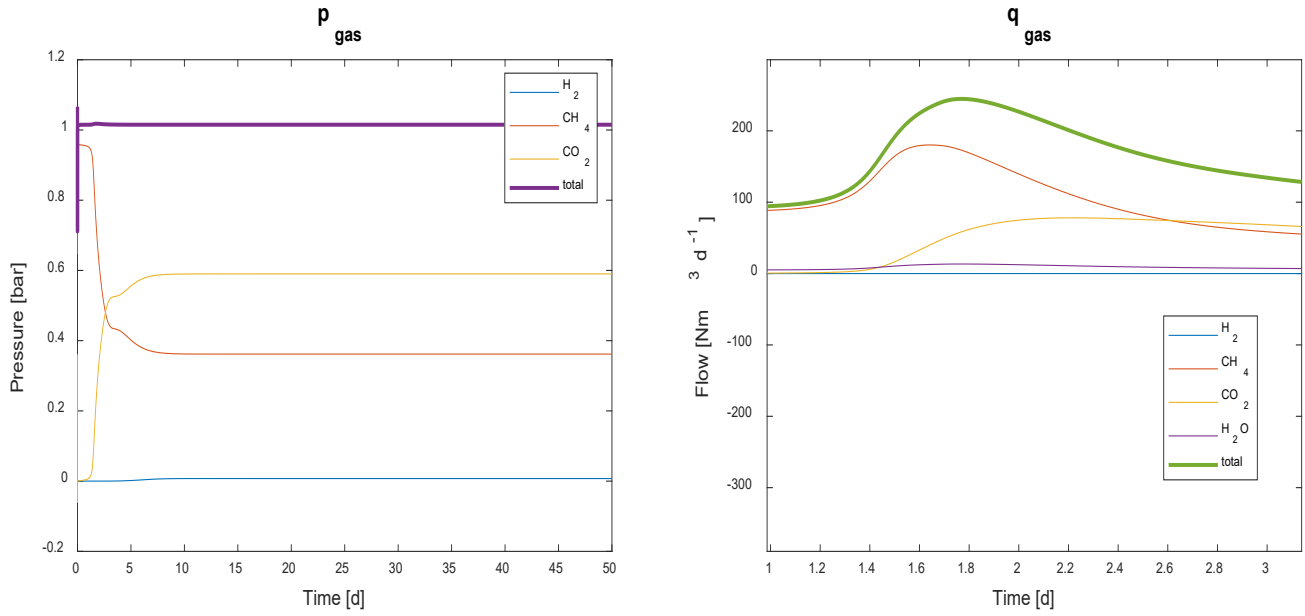


Figure 5.11: Component output for gas production, pressure, and flow rate.

pH is the output that has been most precisely modeled. Across a wide range of periods, all approaches, including the uncalibrated model, produced modest residuals. As seen in Figure 5.10, the used method overstated pH forecasts. Because pH is linked to soluble carbon dioxide concentration, in the model created by the approach, reduced carbon dioxide production explains why pH is higher (Fezzani & Cheikh, 2008). The breakdown of monosaccharides, amino acids, and propionate produces carbon dioxide. Nevertheless, as previously stated, the settings were adjusted so that monosaccharide and amino acid metabolism was considerably slowed. The amount of carbon dioxide and propionate produced as a result is lowered (Mendes et al., 2015).

5.3.2. Model calibration and Validation

5.3.2.1. Sensitivity Analysis Results

When the model is applied to an existing plant, the sensitivity analysis reveals which components are critical in an actual scenario. The technique advises on which factors are crucial to appropriately select based on their impact on the ultimate result. The sensitivity analysis is carried out using the finite difference approach. The more mathematically rational technique of determining the derivative requires dimensionless units, and because the model is established with dimensional qualities, working with dimensions is easier, hence the method is dimensional dependant.

The results are produced by modifying each parameter 1% at a time and then calculating the impact on methane gas generation with the newly obtained parameter set. A bar graph is constructed to visualize the data, as shown in Figure 5.12. If any of the standard parameter set's parameters are comparable to zero, they are retained 0 during comparison, showing no observable change. Large bars for measured sensitivity are associated with key implementation factors. (Morales et al., 2017).

The sensitivity of three groups of biochemical parameters was evaluated, this included the kinetic parameters, such as maximum specific uptake rates, the second group was constituted by stoichiometric parameters, and the third group included hydrolysis or disintegration-related parameters as presented by the x-axis in Figure 5.12, see Appendix A. However, the non-biochemical parameters, e.g. limiting/inhibiting constants, and equilibrium constants for gas-transfer and acid–base reactions were not included. The specific reaction constants ammonia & inorganic, $k_{l,NH3}$, $K_{S,IN}$ and the disintegration, hydrolysis constant had different effects on biogas production simulations for BMP tests, as shown in Figure 5.12 parameter 19, 30-32 which represents k_{dis}, k_{hydch}, k_{hydpr} and k_{hydli} all showed asymmetric characteristics and great sensitivity when these parameters were varied at low ranges. This is due to the fact that those are the first steps of AD and, at low hydrolysis constant rates, the whole process can be limited by the unavailability of the substrate (Silva et al., 2009; Zhao et al., 2019). Low concentrations and quantities were used in this study hence the sensitivity is very high.

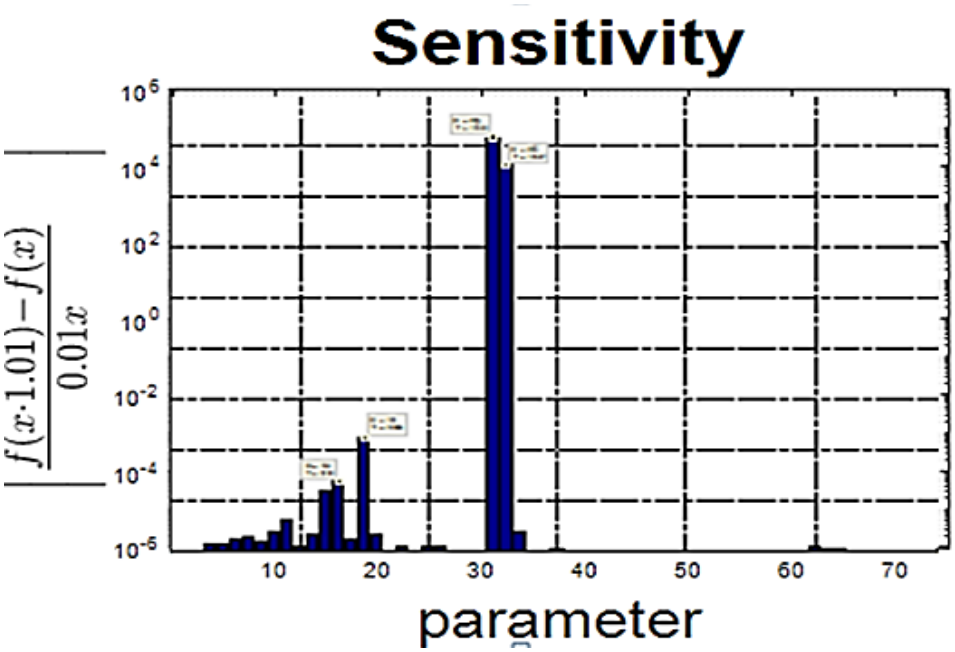


Figure 5.12: Sensitivity analysis plot for the simulated ADM1 based on the biochemical parameters

Based on the sensitivity results, it is reasonable to consider that hydrolysis should be focused on parameter calibration. The sensitivity of all four hydrolysis parameters showed a sharp rise at low ranges, and this is in accordance with the literature regarding the importance of the hydrolysis step in AD (Vavilin et al., 2008; Bordeleau and Droste, 2011).

Figure 5.13 depicts a graph depicting standardized regression, partial correlations, and correlations based on the results obtained for the evaluation of sensitivity analysis. This shows how the sensitivity of two parameters, $k_{l,NH3}$, $K_{S,IN}$ changes as the amount of inorganic nitrogen, S_{IN} in the input changes. This is based on what was shown previously that the most effective inhibition factor is the introduction of inorganic nitrogen into the system. A high correlation between k_{l_nh3} and K_{S_iN} . Similar results were presented by Chen et al., (2016). Despite this, high correlations still have the potential to produce the problem of poor identifiability. Thus, the threshold range of K_{S_IN} and $K_{l,Nh3}$ are 0.015 & 0.002 ± 100%, respectively were artificially based on the optimized values reported by Batstone et al., 2002, Rathnasiri, 2016, and Shi et al., (2014), in order to ensure that the estimation value of KS, IN is within a reasonable range.

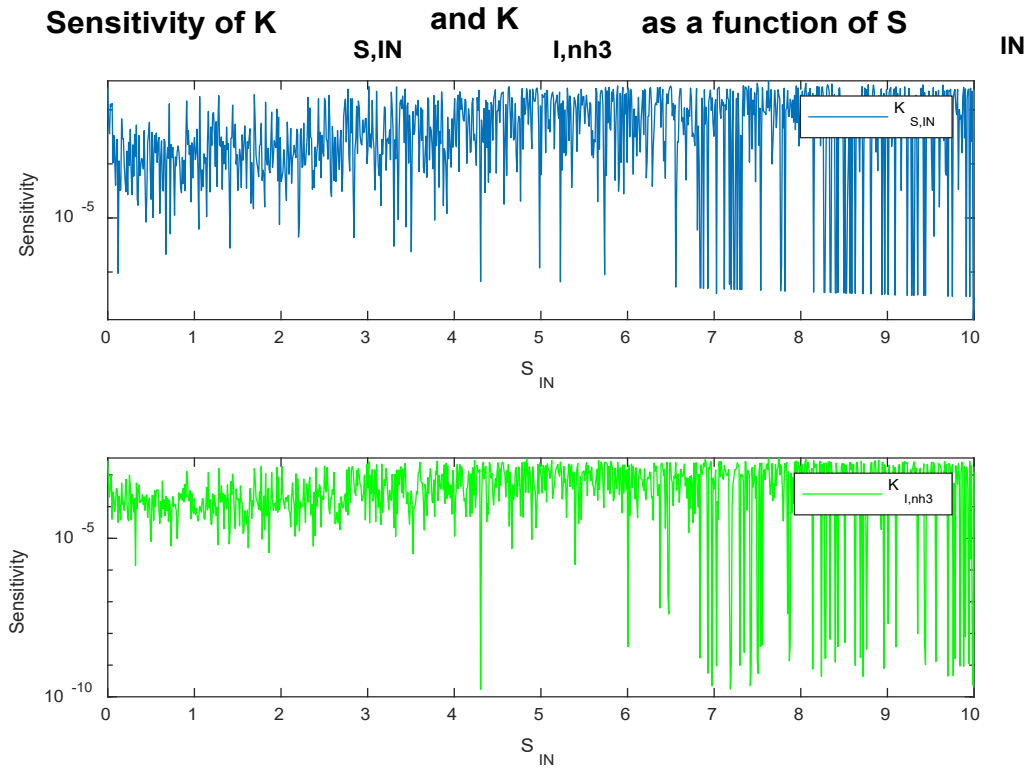


Figure 5.13: Variable dependence of sensitivity for two parameters. Sensitivity is constantly tested meanwhile a variable is changed. $K_{S,IN}$ and $K_{i,nh3}$ are investigated as function of S_{IN}

5.3.2.2. Model Cross Validation: Comparison of simulation results with experimental results

For calibration, the least square cost-function measuring the differences between experimental and simulated values was minimized using the fminsearch function from the MATLAB® toolset. Cross-validation was performed using semi-continuous operation data and the BMP test, to compare with the calibrated parameters for the corresponding type of feeding (raw sludge and dairy waste). Substrate concentrations and flow rates were input as temporal vectors to represent the variability of the substrate and time along the operation, according to operational data. Before variations on substrate and time were input, though, simulations were started with a constant concentration and flow rate for 31 days batch and 200 days semi-continuous, similar to those corresponding to the first operational condition. This was performed to assure steady-state conditions both for substrates and microbial populations, which is a good approach to define initial conditions in both batch and semi-continuous systems.

In order to further evaluate the ability of the modified ADM1 to simulate the results of the calibration experiments, the results are shown in Figures 5.14 and 5.15. This illustrates a clear deviation between the methane production curve simulated by the original ADM1 and the experimental results. This inconsistency is due to the fact that the kinetic parameters of the original ADM1 can sometimes result in inaccurate results when parameter optimization was not used before to predict the biogas production model of additional co-substrates (Chen et al. 2016). Similar results were reported by Razaviarani and Buchanan (2015), who found that the modified ADM1 model applied to lab-scale ADs predicted biogas production levels that were highly consistent with experimental data.

Figure 5.14 shows the fit of the simulation results using the modified ADM1 to the experimental data for cumulative methane production. The R^2 value for the simulation results was 0.9928, which is similar to the R^2 values for the calibration experiments. This indicates that the modified ADM1 predicted the experimental results of the batch experiments with high accuracy. In order to further analyze the subtle differences between the simulation results and the experimental results, this study also converted the simulated methane production to daily methane production, which was then

compared with the daily methane production of the experimental AD. This is similar to the findings of other studies (Chen et al., 2016, Poggio et al., 2016).

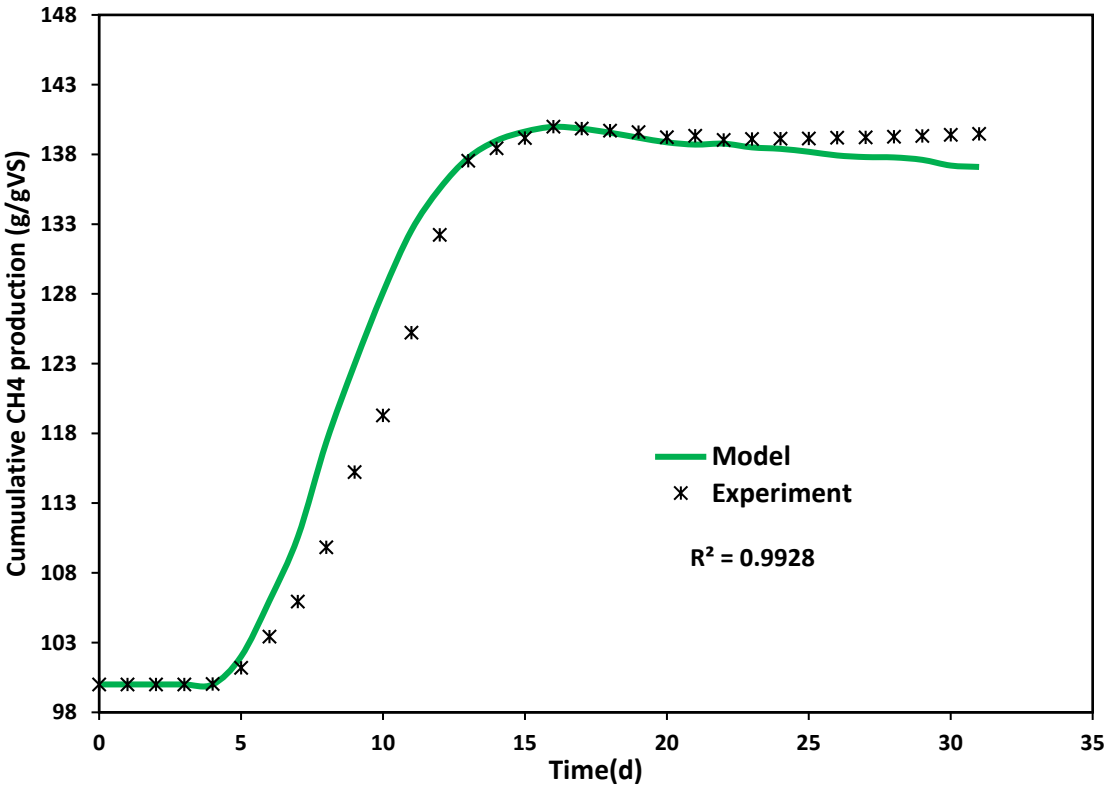


Figure 5.14: Comparison of the batch experimental and simulated methane production results.

The gap mainly manifests during three stages: 0–5 days, 5–16 days, and 16–30 days. This intermittent fluctuation is a manifestation of the adaptation of microorganisms to the environment. At the beginning of the fermentation, the reactor contains a certain amount of dissolved organic matter and background alkalinity, which can provide microorganisms with sufficient substrates and a suitable methanogenic environment (Zhao et al, 2019). The rapid hydrolysis of the substrate subsequently generates large amounts of volatile organic acids (VFA), which inhibit the activity of methanogens and reduces methane production. As organic matter content gradually decreases during the AD, VFAs production decreases due to substrate limitation. As a result, the inhibition of methane production is weakened and gas production gradually increases. However, the responses of microorganisms to environmental changes were not included in the modified ADM1, which resulted in simulations of purely mechanical local phases (Zhao et al, 2019).

Although the modified ADM1 achieved very good results in batch experiments, full-scale reactors are primarily operated in semi-continuous or continuous mode. Therefore, it is important to verify the simulation ability of the modified ADM1 in similar semi-continuous reactors. Figure 5.15 shows the fit between the simulated and experimental results for methane production. Overall, methane production predicted by the modified ADM1 agreed well with methane production. The R^2 value for fit was 0.9792, higher than the 0.900 reported by Poggio et al. (2016) for AD of FW, indicating that the modified ADM1 has a better predictive ability for methane production during the steady operating period.

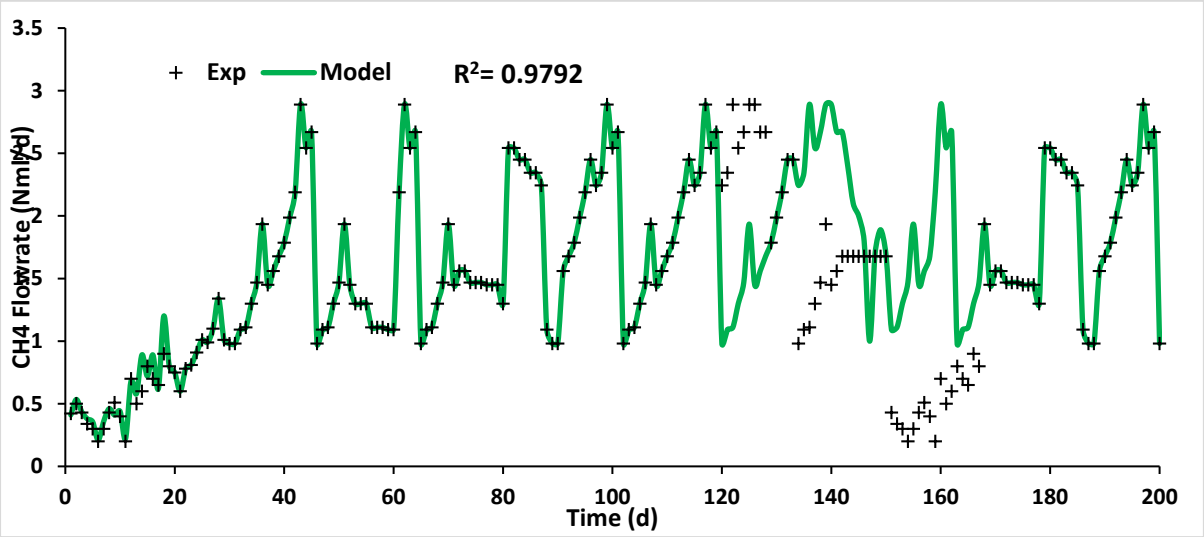


Figure 5:15: Comparison of the semi-continuous experimental and simulated methane production results.

However, Figure 5.15 shows that the model poorly predicted methane production when the OLR was suddenly increased. For example, during the first few days, days 120–125 and 135–168, the predicted values did not show the same fluctuations as the experimental values. The reason may be that the ADM1 model considers the adaptation of microorganisms to a changing environment. OLR affects the activity of microorganisms, and excessive OLR can even inhibit this activity (Li et al., 2018b). AD reactors often experience fluctuations in methane production, or may even become unstable, under fluctuating load conditions.

5.3.3. Model Optimization

Real-world samples from a wastewater treatment plant were used to calibrate and validate the suggested anaerobic simulation model. To test the model, a 50-day operation period was chosen, with samples from the first 30 days used to optimize sensitive parameters and calibrate the model, and samples from the next 20 days used to validate the model's effectiveness. According to Rosen and Jeppsson, the set of differential and algebraic equations in ADM1 was implemented using MATLAB 2019b/Simulink with ODE45s solvers.

Using the optimization technique, new biochemical and physicochemical parameters were uncovered. The discovery of ideal sets of disintegration and hydrolysis parameters for complex substances such as wastewater treatment sludge enabled a more precise description of anaerobic degradation. For comparison, the ADM1 default values for disintegration were used, as well as ADM1 values for high rate and ADM1 values for solids. After upgrading the approach and leaving most of the parameters and fractions in ADM1 alone, the results show very impressive simulation results. Furthermore, the results of the methane content simulation show a significant correlation with previously reported data in the literature reported in Asadi & McPhedran, (2021).

Anaerobic digestion process improvement can result in increased biogas production and, as a result, more practical and cost-effective beneficial utilization in municipal WWTPs. The graphical analysis, data-driven modeling, and uncertainty analysis were used to determine the optimal operating parameter values for anaerobic digestion at a WWTP.

5.3.3.1. Maximizing biogas production

One of the goals with the co-digestion together with getting rid of the produced manure is to obtain as much biogas as possible. To test and verify this the standard way is to do a trial and error search for optimal settings for the digesting process. This is not optimal
and hence there needs to be a better and more effective way of optimizing the problem. In this project simulation is used and around the implemented ADM1 model a Particle Swarm Optimization (PSO) framework is built, which can be used to investigate optimal settings for obtaining as much methane as possible (Danielsson, 2014). All variables in the PSO algorithm's output are limited to a present range, which may be readily modified to different dimensions.

Changing the parameters necessitates rerunning the optimization process because the optimal combination determined by this technique is only valid in a small fraction of the parameter space. A method that permits changes to be done in any dimension was devised in order to create the most beneficial way possible. This approach can be used to define distinct ranges for all substrates specified in the model. The ranges can be adjusted to a finite value if no optimization is desired in any of the dimensions offered. The best combination of two separate input variables identified was for S_{IN}, $S_{IC,}$ and q, based on the trial and error observation this propagates during a simulation. The results of S_{IN}, S_{IC} are shown in Figure 5.16, the intake q, and how the consequent gas production fluctuates during the simulation are shown in Figure 5.17.

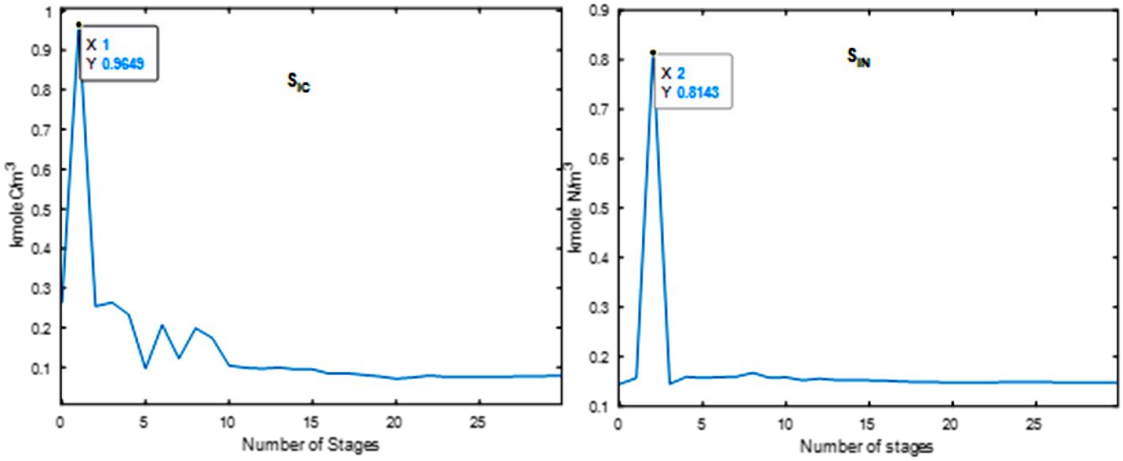


Figure 5.16: Optimal combination of S_{IC} and S_{IN} input variables propagates during a simulation

The simulation was run until the box's boundaries were reached, which were [0;1] kmole/m^3 for N, C, and [100;200] m^3/d for flow. As illustrated in the graph, the ideal position does not reside inside the chosen interval, hence the particles were not successful in finding a place within the limits., but were instead relocated to the boundaries. The interval must be stretched to the point where a theoretical best position may be discovered within the interval to determine the optimal position, theoretically.

The general goal of the research is to lower the amount of AD feedstock used and the amount of energy required while enhancing gas output in digestive chambers. To do so, it is vital to establish which mixture should be fed in order to capture as much gas as possible from the digester. It takes a lot of trial and error to figure out what the standard operating procedure is. On top of the ADM1 model, an optimization framework is constructed to improve the effectiveness of the search. The optimization framework was

chosen to be Particle Swarm Optimization (PSO). The advantage of using PSO over other methods is that it requires relatively little information about the situation.

The chosen algorithm is not the fastest and may never reach the optimal solution, causing it to become locked in a local maximum, but it is a sophisticated approach that allows for simultaneous optimization of a huge number of variables. This is a considerably superior alternative to optimizing each dimension one at a time because various quantities affect each other. As a result, PSO can be used to find the optimum global combination. The result shown in Figure 5.17 illustrates how the answer propagates to the best possible result. One noticeable peak each was discovered in both S_{IC} and S_{IN} , stages 1 and 2 respectively See Figure 5.17.

The picture was computed in three distinct dimensions, and the solution was shown to show how the process works. It was noticed that when conducting an actual simulation, the results show the best-identified position, this is thus an excellent way to demonstrate the simulation technique. Meanwhile, the real optimum determined numbers mixing is more important, hence the plots are only used to get a sense of the process and its dissemination. The flow and the number of feasible steps to optimize are all input variables as written. The algorithm was not changed to account for varied sets of variables to optimize. The only changes required are to set the concentration intervals to fixed values for items that aren't worth optimizing or to a limited interval for those that are interested to optimize. The PSO approach consumes time differently depending on what is optimized and how many steps are required for convergence, but the simulation time is also affected by randomly picked start positions in the search space.

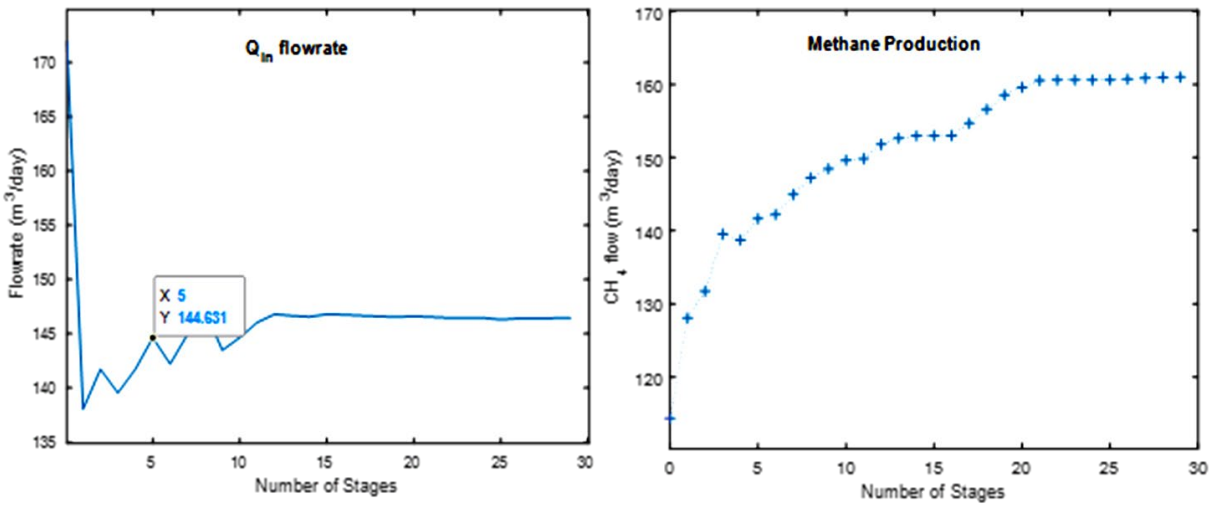


Figure 5.17: Flowrate in, q and how the resulting gas production changes during the simulation.

Each simulation takes around three seconds, and it appears that using about 20 particles in the optimization is sufficient, suggesting that the initialization procedure will take around one minute, and the actual process will take much longer. Even though the flow rate shows a poor fitment to the PSO, the increase in gas production is noticed until the maximum of 161 m^3/day is noticed at stage 20. This corresponds to the operating conditions that were mentioned previously.

5.4. Conclusion

This chapter discusses some elements of the ADM1 MATLAB/Simulink implementation used in this study. The goal of this research was to develop methods for evaluating the co-digestion of dairy thick waste and sewage sludge to produce biogas.

- A model based on the Anaerobic Digestion Model No. 1 (ADM1) was constructed with the purpose to implement this simulation approach to estimate the performance of anaerobic digestion, validate the model and optimize the process.
- This was achieved by first detailing all of the important biochemical and physicochemical processes involved in COD and VFAs complexation, as well as precipitation, dissolution, and substrate absorption in the AD system. The simulation was carried out to mimic the AD process on important parameters with MATLAB Simulink.
- The sensitivity analysis was conducted on biochemical parameters i.e. kinetic parameters, stoichiometric parameters, and hydrolysis or disintegration-related parameters.
- To calibrate the model, the least square cost function was used and comparison of simulation results with experimental results for cross-validation.
- Once validated, the optimization was done to ensure maximum gas output and was achieved using the PSO approach.
- Several practical implementation challenges are highlighted, the optimal combination discovered by this technique is only valid in a small portion of the parameter space, and changing the parameters demands that the optimization process should be re-run.

Reference

Altinay Perendeci, N., Tanyolaç, A., & Serdar Çelebi, S. (2012). A simplified kinetic model for a full scale anaerobic wastewater treatment plant of a sugar factory under unsteady conditions. *Desalination and Water Treatment*, *40*(1–6), 118–128. https://doi.org/10.1080/19443994.2012.671155

Asadi, M., & McPhedran, K. (2021). Biogas maximization using data-driven modelling with uncertainty analysis and genetic algorithm for municipal wastewater anaerobic digestion. *Journal of Environmental Management*, *293*(March), 112875. https://doi.org/10.1016/j.jenvman.2021.112875

Astals, S., Batstone, D. J., Mata-Alvarez, J., & Jensen, P. D. (2014). Identification of synergistic impacts during anaerobic co-digestion of organic wastes. *Bioresource Technology*, *169*, 421–427. https://doi.org/10.1016/j.biortech.2014.07.024

Barrera, E. L., Spanjers, H., Solon, K., Amerlinck, Y., Nopens, I., & Dewulf, J. (2015). Modeling the anaerobic digestion of cane-molasses vinasse: Extension of the Anaerobic Digestion Model No. 1 (ADM1) with sulfate reduction for a very high strength and sulfate rich wastewater. *Water Research*, *71*, 42–54. https://doi.org/10.1016/j.watres.2014.12.026

Batstone, D. J. (2013). Modelling and control in anaerobic digestion: achievements and challenges. *13th World Congress on Anaerobic Digestion*.

Biernacki, P., Steinigeweg, S., Borchert, A., & Uhlenhut, F. (2013). Application of Anaerobic Digestion Model No. 1 for describing anaerobic digestion of grass, maize, green weed silage, and industrial glycerine. *Bioresource Technology*, *127*(1), 188–194. https://doi.org/10.1016/j.biortech.2012.09.128

Biernacki, P., Steinigeweg, S., Borchert, A., Uhlenhut, F., & Brehm, A. (2013). Application of anaerobic digestion model no. 1 for describing an existing biogas power plant. *Biomass and Bioenergy*, *59*(1), 441–447. https://doi.org/10.1016/j.biombioe.2013.08.034

Blumensaat, F., & Keller, J. (2005). Modelling of two-stage anaerobic digestion using the IWA Anaerobic Digestion Model No. 1 (ADM1). *Water Research*, *39*(1), 171–183. https://doi.org/10.1016/j.watres.2004.07.024

Catenacci, A., Grana, M., Malpei, F., & Ficara, E. (2021). Optimizing ADM1 calibration and input characterization for effective co-digestion modelling. *Water (Switzerland)*,

13(21), 1–16. https://doi.org/10.3390/w13213100

Danielsson, O. (2014). Modeling and simulation of anaerobic manure digestion into biogas. In *Master Thesis*. http://publications.lib.chalmers.se/records/fulltext/211706/211706.pdf

Dereli, R. K., Ersahin, M. E., Ozgun, H., Ozturk, I., & Aydin, A. F. (2010). Applicability of Anaerobic Digestion Model No. 1 (ADM1) for a specific industrial wastewater: Opium alkaloid effluents. *Chemical Engineering Journal*, *165*(1), 89–94. https://doi.org/10.1016/j.cej.2010.08.069

Eaton, A. D., Clesceri, L. S., Franson, M. A. H., Association, A. P. H., Rice, E. W., Greenberg, A. E., Association, A. W. W., & Federation, W. E. (2005). *Standard Methods for the Examination of Water #& Wastewater* (Issue v. 21). American Public Health Association. https://books.google.co.za/books?id=buTn1rmfSI4C

Fezzani, B., & Cheikh, R. Ben. (2008). Implementation of IWA anaerobic digestion model No. 1 (ADM1) for simulating the thermophilic anaerobic co-digestion of olive mill wastewater with olive mill solid waste in a semi-continuous tubular digester. *Chemical Engineering Journal*, *141*(1–3), 75–88. https://doi.org/10.1016/j.cej.2007.10.024

Fezzani, B., & Cheikh, R. Ben. (2009). Extension of the anaerobic digestion model No. 1 (ADM1) to include phenolic compounds biodegradation processes for the simulation of anaerobic co-digestion of olive mill wastes at thermophilic temperature. *Journal of Hazardous Materials*, *162*(2–3), 1563–1570. https://doi.org/10.1016/j.jhazmat.2008.06.127

Goswami, R., Chattopadhyay, P., Shome, A., Banerjee, S. N., Chakraborty, A. K., Mathew, A. K., & Chaudhury, S. (2016). An overview of physico-chemical mechanisms of biogas production by microbial communities: A step towards sustainable waste management. In *3 Biotech*. https://doi.org/10.1007/s13205-016-0395-9

Hassam, S., Ficara, E., Leva, A., & Harmand, J. (2015). A generic and systematic procedure to derive a simplified model from the anaerobic digestion model No. 1 (ADM1). *Biochemical Engineering Journal*, *99*, 193–203. https://doi.org/10.1016/j.bej.2015.03.007

Jimenez, J., Latrille, E., Harmand, J., Robles, A., Ferrer, J., Gaida, D., Wolf, C., Mairet, F., Bernard, O., Alcaraz-Gonzalez, V., Mendez-Acosta, H., Zitomer, D., Totzke, D.,

Spanjers, H., Jacobi, F., Guwy, A., Dinsdale, R., Premier, G., Mazhegrane, S., … Steyer, J. P. (2015). Instrumentation and control of anaerobic digestion processes: a review and some research challenges. *Reviews in Environmental Science and Biotechnology*, *14*(4), 615–648. https://doi.org/10.1007/s11157-015-9382-6

Kainthola, J., Kalamdhad, A. S., & Goud, V. V. (2019). A review on enhanced biogas production from anaerobic digestion of lignocellulosic biomass by different enhancement techniques. *Process Biochemistry*, *84*, 81–90. https://doi.org/10.1016/j.procbio.2019.05.023

Li, D., Lee, I., & Kim, H. (2021). Application of the linearized ADM1 (LADM) to lab-scale anaerobic digestion system. *Journal of Environmental Chemical Engineering*, *9*(3), 105193. https://doi.org/10.1016/j.jece.2021.105193

Li, P., Pei, Z., Liu, D., Shi, F., Wang, S., Li, W., Sun, Y., Liu, J., Gao, Y., & Yu, Q. (2021). Application of Anaerobic Digestion Model No. 1 for modeling anaerobic digestion of vegetable crop residues: Fractionation of crystalline cellulose. *Journal of Cleaner Production*, *285*(1), 124865. https://doi.org/10.1016/j.jclepro.2020.124865

Mendes, C., Esquerre, K., & Matos Queiroz, L. (2015). Application of Anaerobic Digestion Model No. 1 for simulating anaerobic mesophilic sludge digestion. *Waste Management*, *35*(1), 89–95. https://doi.org/10.1016/j.wasman.2014.10.013

Morales, L. A., Rodriguez, A. D., & Rojas, H. E. (2017). Assessment of the Input Substrate Characteristics Included in the Anaerobic Digestion Model No. 1 (ADM1). *Ingenieria*, *22*(2), 269–282.

Mudzanani, K., Van Heerden, E., Mbhele, R., & Daramola, M. O. (2021). Enhancement of biogas production via co-digestion of wastewater treatment sewage sludge and brewery spent grain: Physicochemical characterization and microbial community. *Sustainability (Switzerland)*, *13*(15). https://doi.org/10.3390/su13158225

Ndeba-Nganongo, L. A. N., Ntwampe, S., O, S. K., Szabolcs, S., & Itomba-Tombo, E. F. (2018). The Application of ADM/ASM Interface in Sumo Wide Plant Model. *10th Int'l Conference on Advances in Science, Engineering, Technology & Healthcare (ASETH-18)*, 237–242. https://doi.org/10.17758/eares4.eap1118257

Ngila, J., Matheri, A., Muckoya, V., Ngigi, E., Ntuli, F., Seodigeng, T., & Zvinowanda C. (2020). *Mathematical Modelling for Biological Wastewater Treatment Plants Gauteng, South Africa* (Issue 2563/1/19).

Parra-Orobio, B. A., Donoso-Bravo, A., & Torres-Lozada, P. (2020). Energy balance and carbon dioxide emissions comparison through modified anaerobic digestion model No 1 for single-stage and two-stage anaerobic digestion of food waste. *Biomass and Bioenergy*, *142*(October). https://doi.org/10.1016/j.biombioe.2020.105814

Ramdani, N., Hamou, A., Lousdad, A., & Al-Douri., Y. (2015). Physicochemical characterization of sewage sludge and green waste for agricultural utilization N. *Environmental Technology*, *36*(12), 1594–1604. https://doi.org/10.1080/09593330.2014.998716

Rivera-Salvador, V., López-Cruz, I. L., Espinosa-Solares, T., Aranda-Barradas, J. S., Huber, D. H., Sharma, D., & Toledo, J. U. (2014). Application of Anaerobic Digestion Model No. 1 to describe the syntrophic acetate oxidation of poultry litter in thermophilic anaerobic digestion. *Bioresource Technology*, *167*(1), 495–502. https://doi.org/10.1016/j.biortech.2014.06.008

Rosen, C., & Jeppsson, U. (2006). Aspects on ADM1 implementation within the BSM2 framework. In *Technical report*.

Rozzi, A., & Remigi, E. (2004). Methods of assessing microbial activity and inhibition under anaerobic conditions: A literature review. *Reviews in Environmental Science and Biotechnology*, *3*(2), 93–115. https://doi.org/10.1007/s11157-004-5762-z

Shi, E., Li, J., & Zhang, M. (2019). Application of IWA Anaerobic Digestion Model No. 1 to simulate butyric acid, propionic acid, mixed acid, and ethanol type fermentative systems using a variable acidogenic stoichiometric approach. *Water Research*, *161*(1), 242–250. https://doi.org/10.1016/j.watres.2019.05.094

Silva, F., Nadais, H., Prates, A., Arroja, L., & Capela, I. (2009). Modelling of anaerobic treatment of evaporator condensate (EC) from a sulphite pulp mill using the IWA anaerobic digestion model no. 1 (ADM1). *Chemical Engineering Journal*, *148*(2–3), 319–326. https://doi.org/10.1016/j.cej.2008.09.002

Tassew, Bergland, Dinamarca, & Bakke. (2019). Effect of Particulate Disintegration on Biomethane Potential of Particle-Rich Substrates in Batch Anaerobic Reactor. *Applied Sciences*, *9*(14), 2880. https://doi.org/10.3390/app9142880

Vega De Lille, M. I. (2015). Modeling, Simulation and Control of Biotechnological Processes in Decentralized Anaerobic Treatment of Domestic Wastewater. Friedrich-Alexander-Universität

Wickham, R. J. (2019). Anaerobic co-digestion of municipal wastewater sludge with organic wastes. University of Wollongong.

Xu, Z. (2019). ADM1 Parameter Calibration Method based on Partial Least Squares Regression Framework for Industrial-scale Anaerobic Digestion Modelling. Stellenbosch University. https://scholar.sun.ac.za

Zhao, X., Li, L., Wu, D., Xiao, T., Ma, Y., & Peng, X. (2019). Modified Anaerobic Digestion Model No. 1 for modeling methane production from food waste in batch and semi-continuous anaerobic digestions. *Bioresource Technology*, *271*(1), 109–117. https://doi.org/10.1016/j.biortech.2018.09.091

CHAPTER 6

FEASIBILITY STUDY ON SYNTHESIS OF SEWAGE SLUDGE-BASED ACTIVATED CARBON: PROSPECTS OF MUNICIPAL WASTEWATER REMEDIATION

Due to waste management challenges faced by the municipality and industrial wastewater treatment works, it is essential to turn the waste generated into value-added products such as granular activated carbon (GAC). This study evaluates the potential to synthesize an adsorbent for wastewater remediation application, from an anaerobic digestion by-product via a non-toxic and less energy-intensive process. The performance of the synthesized sludge-based Activated Carbon (SAC) was tested on target pollutants chromium vi (Cr(VI)) and cadmium (Cd(II)) in a batch reactor stirred for 24 hours at 25°C. This study focuses on treatment Cr(VI) and Cd(ii) motivated by the in-house laboratory analytical method. It was identified that these pollutants are the most challenging heavy metals to remove in the JW municipal wastewater. Furthermore, humans are more likely to be exposed to these heavy metals through water consumption. They are very toxic elements in which rapid bioaccumulation occurs in the human body and thus it must be treated prior to human exposure. The surface chemistry of the material was assessed porosity with BET, SEM for morphology, ED-XRF for elemental analysis, and functional groups on these materials using FTIR and TGA for the thermal profile. SBET of the SAC was discovered to be 481.370 m^2/g with a V_T of 0.337 cm^3/g, 9.02 and 2.23 times greater than raw sludge, respectively. The modification to SAC shows a dramatic increase in performance from 40% to 98.9 % equilibrium adsorption rate. Thus, it can be concluded that activation of sewage sludge was effective in enhancing the surface area and pore volume which made it suitable for AMD remediation application.

6.1. Introduction

The physical and chemical interactions between the metal and the activated carbon surface constitute the basis for surface adsorption mechanisms. In a fluid phase, atoms or ions (adsorbate) flow to the surface of a solid (adsorbent), where they bind or are retained by weak intermolecular interactions (Lafi et al., 2019; Seo et al., 2019). These pollutants are absorbed into the pores of the material during operation, which gradually becomes saturated over time. The adsorbent material reaches an exhaustion point at saturation point, where it can no longer continue the adsorption process. An appropriate choice of adsorbent material is required for the total efficient functioning of adsorption systems (Seo et al., 2019) GAC is a renowned adsorbent for a wide range of contaminants during water treatment (Bian et al., 2018; Setshedi, 2014; Setshedi et al., 2013).

GAC is now the most cost-effective and frequently utilized material for removing organic micropollutants from wastewater treatment. This is because of its large surface area, affinity for a wide range of organic compounds, and cost-effectiveness. Activated carbon is a carbonaceous adsorbent with a porous structure that is highly developed (Rashed, 2018). The GAC adsorption mechanism is one of the most widely used and cost-effective technologies. This is due to its resilience, simplicity, environmental friendliness, restriction to low sludge production, ability to recover valuable metals at low concentrations, selectivity, and social acceptance. Because of the high quality of the effluent obtained, simplicity of design, convenience of operation, and insensitivity to harmful compounds, it has been proven to be superior to many other ways of removing pollutants through the adsorption concept process (Lafi et al., 2019; Rashed, 2018). Due to a dramatic increase in the price of commercial pure GAC, municipal and other wastewater treatment industries are looking for a more cost-effective material to substitute GAC.

Thus, the implementation of SAC adsorption material for the removal of toxic heavy metals from wastewater has been deemed a solution. This is because it is synthesized from waste sludge, low cost of the modification process, highly efficient, and has low installation, operations, and maintenance costs. This study looks at the feasibility of using SAC for the removal of heavy metals, Cr(VI) and Cd(II)) in terms of its preparation or synthesis, characterization, and its performance evaluation using an adsorbent synthetized from waste municipal sludge. The specific aim of the present research is to

investigate the adsorption characteristics of heavy metal ions by SAC material. The effects of contact time and SAC dosage on the adsorption isotherm and kinetics of adsorption of heavy metal ions are reported.

6.2. Materials and Methods

Please refer to Section 3.6 and Section 3.11-3.12 for information on materials and methods.

6.3. Results and Discussion

6.3.1. SAC Characterization

6.3.1.1. The textural properties

The most significant attribute of any adsorbent is its adsorption capacity, which is directly proportional to its specific surface area and pore volume (Agrafioti et al., 2013). Table 6.1 shows the textural properties of raw sludge, SAC, and commercial granular activated carbon (CGAC). The textural parameters of the material were determined using N_2 adsorption/desorption isotherms and the Brunauer-Emmett-Teller equation (BET). The total pore volume (VT) of the dry medium was derived using BET theory as the adsorbed volume of N_2 gas approaching the saturation volume (P/P_0 = 0.98) and the surface area, SBET.

Density functional theory (DFT) was used to calculate the distribution for pores (D_P) with diameters ranging from 0.7 to 36 nm. For non-homogeneous liquids over microporous surfaces, the DFT model was used to offer a more precise interpretation of the data. The findings in Table 6.1 reveal fast N_2 adsorption at low relative pressures, which is a feature of a microporous material. The capillary condensation that happens in the mesopores is connected with the adsorption hysteresis loop that appears in the medium relative pressures. (Liu et al., 2020; Setshedi, 2014).

The surface feature for the CGAC adsorbent SBET has been previously reported as being 841 m^2/g and V_T 0.430 cm^3/g respectively (Rashed, 2018). In the current study, the CGAC showed to be higher in strength with many pores, 986 m^2/g, and V_T 0.513 cm^3/g respectively. This is more than double the SBET of SAC with a value of 481.37 m^2/g with a V_T of 0.337 cm^3/g and 53 m^2/g of raw sewage sludge. The D_P of SAC was 4.814 nm,

which was much lower than that of the raw sludge (7.627 nm). The SBET of the CGAC & SAC was found to be 986 m^2/g & 481.370 m^2/g, both of which were almost 18.6 and 9.2 times higher than those of the raw sludge, respectively.

This demonstrates that activating any material increases the surface area and porosity of the material by transforming mesopores or macropores into micropores (Liu et al., 2020). As previously reported the continuous increase in temperature to activate the material result in the breaking down of the hemicellulose/cellulose and conversion into pyrolytic gas which result in the formation of pores. Thus, the increase in the surface area, SBET and pore volume of the material of SAC was due to the activation that improves the carbon content in sludge. Similarly, to SAC the CGAC material is coal heated at a high temperature, above 400 °C to alter the surface structure mainly by adding pores. This is the most likely reason for the significant increase in the surface area and pore volume of the material.

Table 6.1: Characteristics of the porous structure of the raw sludge and SAC.

Sample	S_{BET}(m2/g)	V_T (cm3/g)	V_{MIC} (cm3/g)	V_{MES} (cm3/g)	D_P (nm)
Raw sludge	53.389	0.148	0.019	0.010	7.627
SAC	481.370	0.337	0.341	0.21	4.814
CGAC	986.601	0.513	0.155	0.120	16.1

As outlined in the methodology, the raw materials were washed with KOH solution and were sufficiently dosed with a low concentration of $ZnCl_2$. The impregnation of SAC material with $ZnCl_2$ results in Cl resting on the outer layer or the surface of the material. This causes a localized breakdown, which extends the pore size. As a result of this process, mesopore production is enhanced, and the resultant SACs have relatively large surface areas (Ait Ahsaine et al., 2017). When compared to ordinary activated carbons, the SACs generated had a comparatively large micropore volume (V_{MIC}) (Jung et al., 2019). The addition of $ZnCl_2$ is involved in two conflicting mechanisms: micropore formation and pore widening (Faisal et al., 2018)

6.3.1.2. SEM: Morphology Analysis

The morphology of the materials was evaluated using SEM. According to the approach outlined earlier in the experimental section, micrographs were obtained from CGAC, raw sludge, and carbonized sewage sludge, SAC. These micrographs were chosen to provide a typical representation of the observed structures; the magnification may vary to emphasize certain regions of interest. As shown in Figure 6.1(A), the raw sewage sludge has a compact structure with no cavities. After activation, the SAC shown in Figure 6.1B has a loose structure in which the surface of the carbon is decorated with macropores 8. The CGAC surface structure looks compact, it's similar to that of a raw sludge, see Figure 1C. However, when it's zoomed closer at 1000x magnification, the structure in Figure 6.1D is more porous and appears to have spherical uniformity that can serve as adsorption sites for adsorbates.

As can be seen in Figure 6.1, the raw sludge material (A) does not differ structurally from the SAC itself (B). However, on the surface of the particles even at a magnification of 5000x, carbon spheres are visible (Figure 6.1B). The polymer's regular spherical form is well kept after activation, which can be attributed to the chloromethylated spherical polymer's additional post-crosslinking during activation. This boosts the sphere's strength and thermos stability. The micrograph (x5000) reveals a dense network of interspaces on the scale of a nanometre, indicating a highly developed disordered porosity (De Mes et al., 1972).

These findings were consistent with the textural features shown in Table 6.1, which demonstrated that the surface area increased after modification owing to the activation and release of volatile chemicals during the carbonization process. BET results show the attack on the surface and the lignocellulosic structure of the raw sewage sludge resulting in the more porous structure of SAC. Figure 6.1A presents a dense surface whereas SAC & CGAC in Figures 6.1B and 6.1D depict a rougher surface with voids of varying sizes, suggesting a well-developed porous structure. The pores on the surface of SAC provide ideal routes for adsorbate ions to penetrate into the carbon structure, enabling access to its mesopores and micropores where they can interact with the surface functional groups (Bodîrlău et al., 2009; Y. Wang et al., 2019)

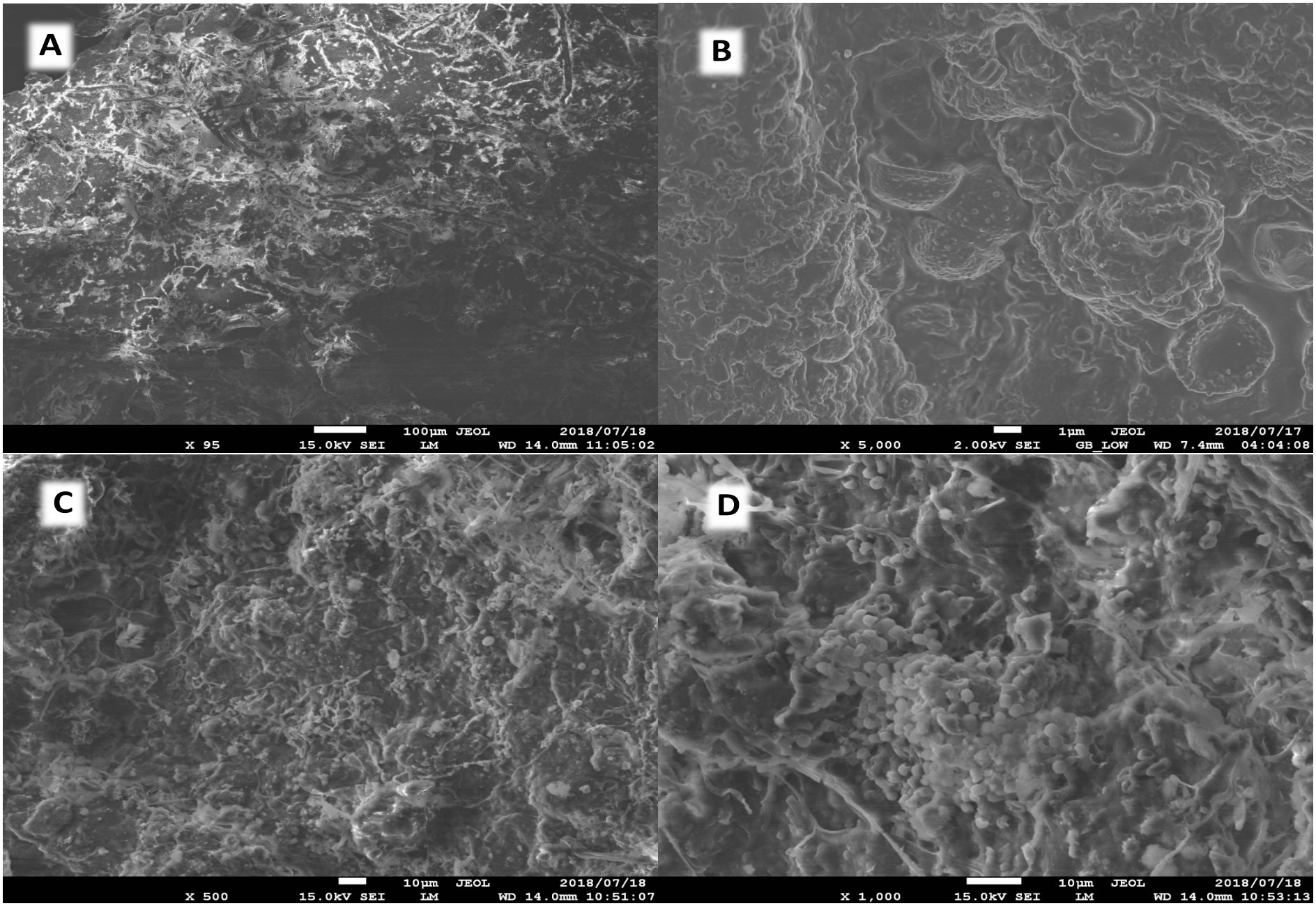


Figure 6.1: SEM micrographs, (A): Raw sludge; (B): SAC shows spherical carbon particles on the surface of carbonized.

6.3.1.3. TGA: Thermogravimetric Analysis

The thermogravimetric analysis of sewage sludge, CGAC, and SAC represented in Figure 6.2 shows the mass loss percentage versus temperature. As shown in the figure, the weight loss in phase 1, range of 50°C–200°C corresponds to the dehydration of the materials meaning the elimination of both surface and lattice water. The pyrolytic reactions take place mainly from 200°C to about 500°C, this is when the material is converted into the pyrolytic gas which results in pores, as mentioned previously. The weight loss in phase 2, between 200 and 550 °C can be attributed to the elimination of different vapors such as NH_3, NO_2, and O_2. The mass loss was lower but non-negligible in the range between 500°C and 1000°C. The plateau at higher temperatures (phase 3, above 550°C) corresponds to the existence of some oxide minerals in the samples (SiO_2, MgO, and Al_2O_3) which do not breakdown or decompose (Salihi et al., 2018). Figure 6.2 shows that remarkable weight losses of ~30.64% and ~64% were observed for raw sludge and SAC material, respectively.

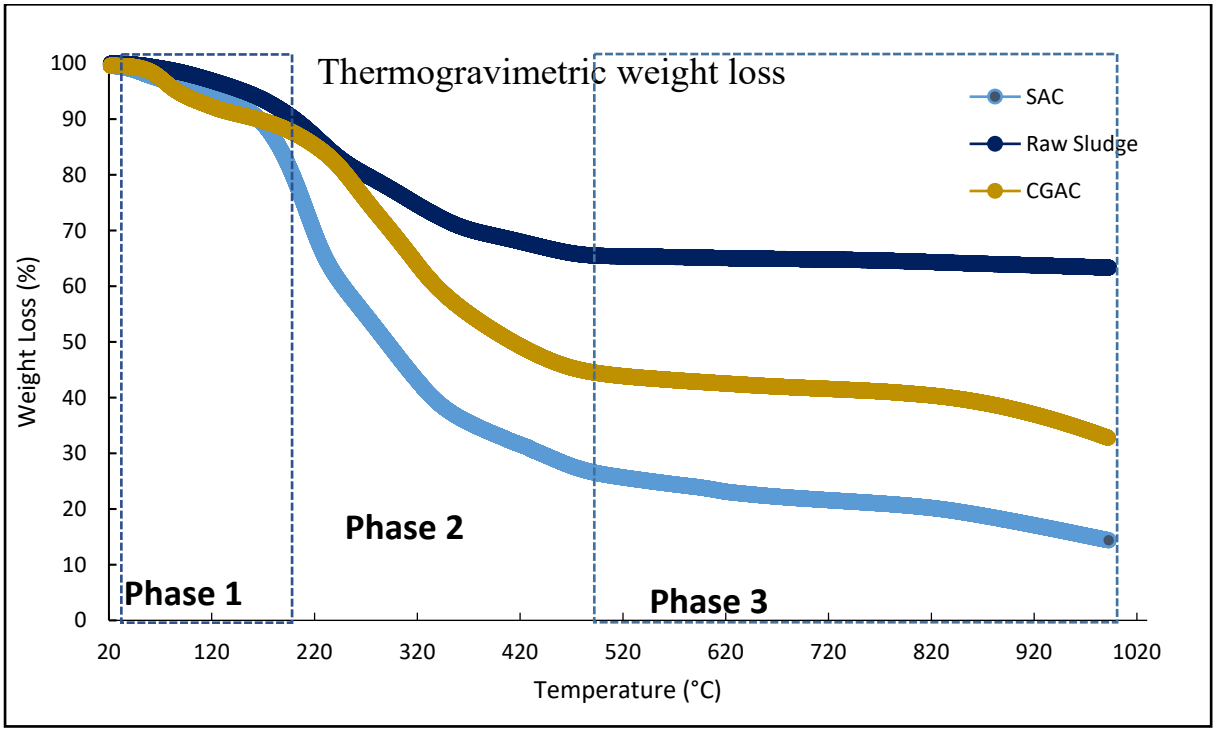


Figure 6.2: Thermal decomposition of raw sewage sludge and SAC

6.3.1.4. FT-IR analysis

To analyze and compare the chemical bonding in the CGAC, raw sludge, and SAC material, Fourier transforms infrared (FT-IR) spectra were obtained. Figure 6.3 (a), (b), and (c) show the FTIR spectra of the CGAC raw sludge and SAC samples, respectively. Figure (3a) shows that CGAC exhibits four primary absorption bands in the wavelength range of 4000–400 cm^{-1}. The O-H stretching vibrations cause the absorption maxima at 3400 cm^{-1} and 1600 cm^{-1}. The absorption peak at 1726 cm^{-1} is caused by skeletal stretching vibrations, whereas the absorption peak at 1060 cm^{-1} is caused by C=O stretching vibrations.

Figure 6.3 (b) shows that raw sludge has limited stability, as evidenced by the noise below 600 cm^{-1}, whereas Figure 3 (c) shows that SAC material exhibits the characteristic of C=O and C-O stretching vibrations at 1650 cm^{-1} and 1425 cm^{-1}, respectively. However, the additional peaks at 966 cm^{-1} confirm the development of an N-H bond, indicating that nitrogen was successfully doped in the carbon framework. Meanwhile, the rise at 1020–1360 cm^{-1} can be explained by the stretching and bending vibrations of nitrogen-containing functional groups such as C=N and C-N and the bending vibration of nitrogen-containing functional groups (Bodîrlău et al., 2009).

It is widely known that functional groups on the surface of AC, such as carboxyl, carbonyl, phenolic hydroxyl, and lactones, have a considerable influence on its adsorption ability (Y. Wang et al., 2019). The O-H stretching vibrations, which correspond to related peaks of hydroxyl groups from phenols and alcohols, are responsible for the wide absorption band in the 3300–3600 cm^{-1} range (Y. Wang et al., 2019). The characteristic peak at 1624 cm^{-1} can be ascribed to carbonyl's C=O and C=C vibration in carboxylic or ester groups (Betsholtz et al., 2018). The lactone groups appear to be responsible for the absorption peak at 1383 cm^{-1}. Alcohol groups are responsible for the rather strong band at 1042 cm^{-1} (C-OH). In addition, the peaks at 665-200 cm^{-1} represent the C-H stretching vibration. In this study, the activation led to an increase of oxygen-containing functional groups (C-OH, O-H and C=O), which might be attributed to the use of KOH and $ZnCl_2$ during synthesis.

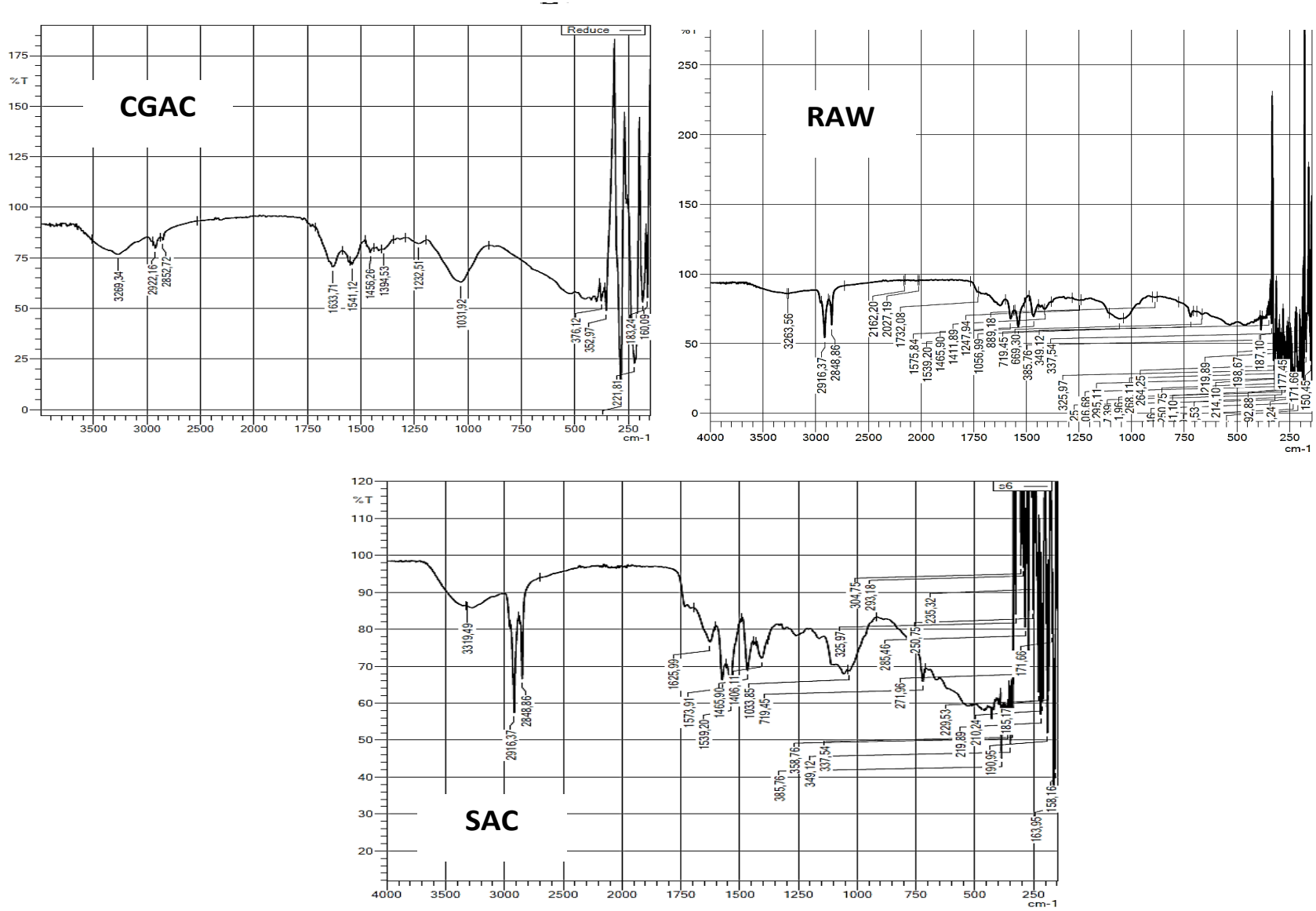


Figure 6.3: FTIR spectra of CGAC (a) raw sewage (b) and SAC (c) samples.

6.3.1.5. ED-XRF analysis

In elemental form, sewage sludge is a mixture of nitrogen- and Sulphur-containing organic materials, microorganisms, and minerals, mainly C, O, N, P, Na, K, Fe, Si, Al, and Ca (Park et al, 2010). It also contains trace elements like Ti, Ba, Bi, and Co. Figure 6.4 depicts an element screening analysis of GAC, dry raw sludge sample, and SAC using an energy dispersion X-ray fluorescence spectrometer (ED-XRF) (Epsilon 3 XL, PANalytical). Semi-quantitative elemental analyses of finely ground solids for elements heavier than oxygen are possible with this (Mu & Wang, 2016). Sludge contains fertilizing nutrients such as phosphorus, potassium, magnesium, sodium, calcium, and sulfur (Wang et al, 2016). The high potassium and chlorine concentration results from the use of zinc chloride for dosing during synthesis and washing of the SAC material with KOH. The SAC material was washed numerous times, hence the increase in low concentrations of most elements as compared with raw sewage sludge (Park et al., 2010; Rio et al., 2005). The presence of carbon was due to the heating activation that result in carbonization, similarly to the CGAC. The material was centrifuged from solution and calcined for 2 h in an N_2 atmosphere hence the presence of trace N in the SAC material.

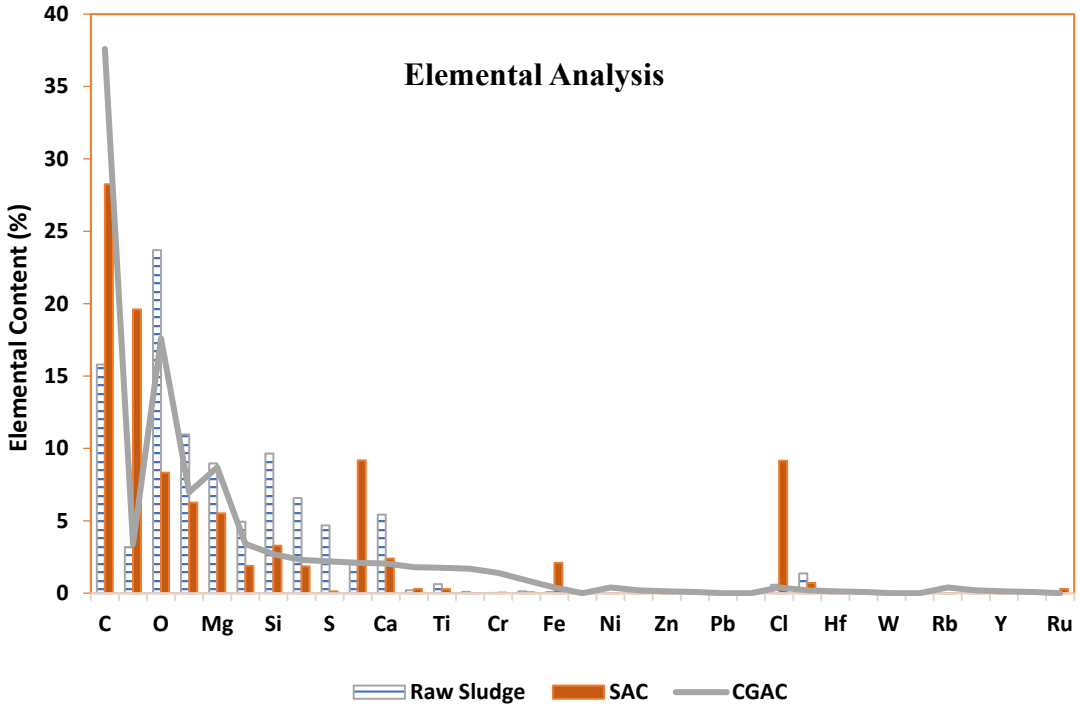


Figure 6.4: EDX spectra or Semi-quantitative XRF analysis of the raw sludge SAC and raw sludge samples

6.3.2. Material Performance: Comparison

6.3.2.1. Comparison of SAC against CGAC and raw sludge

According to the literature, an assessment of the mechanisms of activated carbon adsorption can be performed in batch shake-flask experiments using an equilibrium approach, from which adsorption isotherms can be developed in order to obtain the material's maximum uptake capacity. In order to investigate the performance of sludge-based activated carbon for adsorption of hexavalent chromium (Cr (VI)) ions from an aqueous solution, Cr (VI) solution was used. To compare the performance of SAC material against what is already on the market, commercial GAC (CGAC) was used. Furthermore, to see the effect of modifying the raw sludge into SAC, dried municipal sewage was tested under the same conditions. Figure 6.5 shows the adsorption removal efficiency of Cr(VI) when using SAC, CGAC & raw sludge as the adsorption materials in different adsorption times ranging from 0 to 24 hours.

As can be observed in Figure 6.5, the adsorption time has a significant impact on Cr(VI) adsorption (González et al., 2018). In batch tests, the concentration in the solution of each of the compounds considered decreased continuously over time until an equilibrium point was reached for all adsorbents. This equilibrium point is a property of both the material and the adsorbate. The results show that when comparing SAC and raw sludge, the SAC achieved the highest Cr(VI) removal efficiency of 99.99 %, while the raw sludge achieved only 40.71 % removal efficiency. The increased surface area of the sludge material results in an increase in SAC removal efficiency. From these findings, the SAC can be regarded as a highly effective adsorbent as compared to raw sludge (C. Wang et al., 2021).

As indicated in Figure 6.5, the removal efficiency of Cr(VI) with CGAC and SAC went up to adsorption equilibria of 99.98, and 60,50%, respectively. The SAC adsorbent reached equilibrium sooner than raw sludge and also exhibited a higher removal capacity for Cr(VI) followed by CGAC which is due to the availability of the adsorption sites in the material leading to the longer equilibrium time as observed in Figure 6.5. As a result, these compound molecules took longer to initiate adsorption, but once started, they achieved a higher level of adsorption (González et al., 2018; Ragheb, 2018).

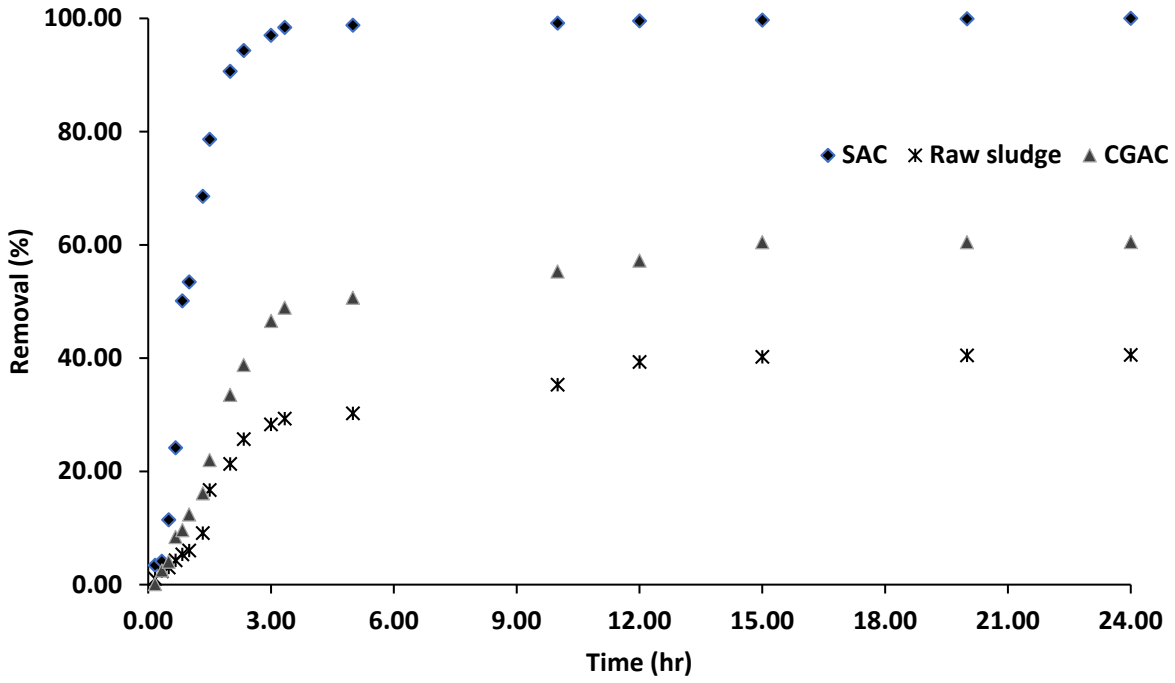


Figure 6.5: Adsorption of Cr(VI) by the sewage sludge-based activated carbon with time

6.3.3. SAC Performance: Effect of the operation conditions

6.3.3.1. Effect of the initial pH

Figure 6.6 depicts the results of an investigation into the sorption efficiency of adsorbate onto SAC material as a function of pH (1-11). The pH of the solution has a significant impact on the adsorption of metal ions and dyes. This is due to the fact that the adsorbent's surface charge density and metallic speciation are pH-dependent (Tocharoen et al., 2019). The results show that the removal efficiency of Cr (VI) and red dye decreases as pH increases. At low pH (pH 1- 3), the removal efficiency of 99.99 % was achieved with the SAC whereas only 1% removal efficiency was achieved for Cd (II) and methylene blue. However, at higher pH (e.g., at pH of 10) high adsorption was achieved.

It became necessary to investigate the electrostatic attraction/repulsion, chemical interaction, and ion exchange within the system to explain the observed adsorption behavior with varying pH. The adsorption capacity of Cd (II) increases with an increase in the initial pH in the solution, regardless of adsorbent type, according to the literature (Litefti et al., 2019). Because of the high concentration of hydronium ions (H^+) on the material surface at low pH, the affinity for positively charged Cd^{2+} anions decreases

because they compete for the same adsorption sites (Hu & Hu, 2014). Conversely, at higher pH values, the presence of H^+ ions is low. Consequently, a greater number of ligands with negative charges (i.e., OH^-) will result in greater Cd (II) adsorption (Wen et al., 2019).

According to Cr(VI) speciation, the monovalent bichromate ($HCrO_4$) and divalent dichromate ($Cr_2O_7^{2}$) ions are the dominant species of Cr(VI) in aqueous solutions in the pH range 2-6, while the chromate (CrO_4^{2-}) ion is the dominant species at pH>6 6. Because of the high concentration of H^+ on the material surface at low pH, the material surface becomes positively charged, increasing the affinity for the negatively charged $HCrO_4$ and $Cr_2O_7^{2}$ anions to bind on the clay without competing for adsorption sites (Kaur et al., 2013; Said et al., 2014). More OH is present in the solution as the pH rises. This competes for adsorbent active sites with the chromate ions (CrO_4^{2}), resulting in low Cr (VI) removal (Wei et al., 2019).

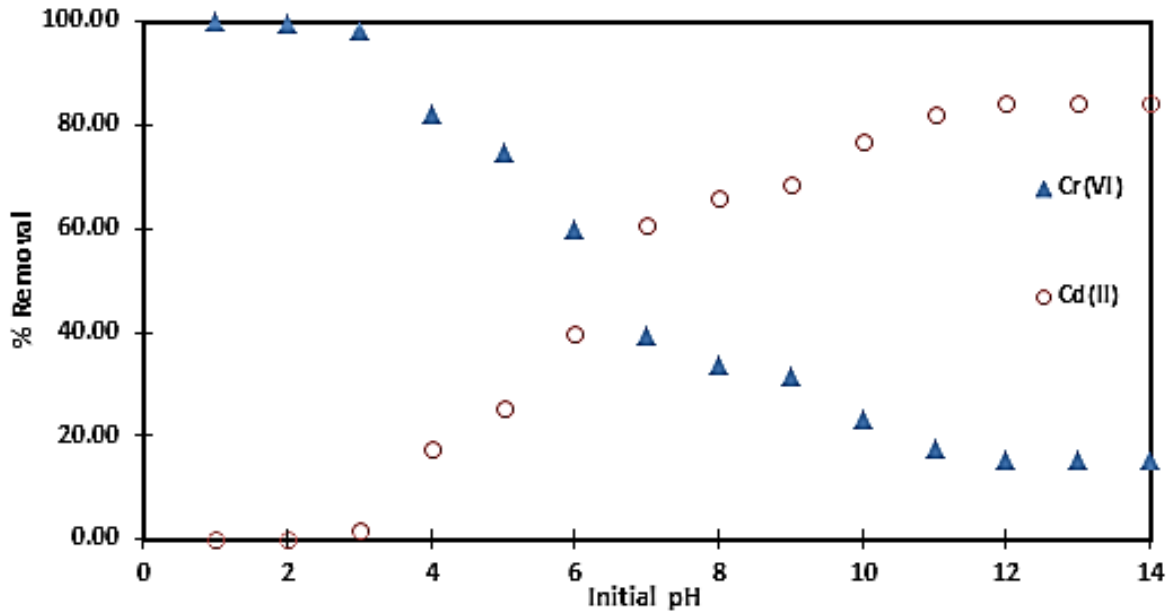


Figure 6.6: Effect of initial pH on adsorption of Cr (VI) and Cd (II)

6.3.3.2. Effect of SAC dosage

The effect of SAC dosage on the removal of Cr (VI) and Cd (II) from aqueous solutions was studied. Figure 6.7 depicts the information. This is a critical parameter because it determines an adsorbent's capacity for a given initial concentration. In a large-scale industrial application of adsorbent in the removal of the desired solute, the quantity or mass of adsorbent is an important factor. A series of adsorption experiments were carried out with different masses of adsorbent at a fixed initial solute concentration to investigate the effect of adsorbent mass on adsorption (Ferrasse et al., 2015; Kaur et al., 2013).

In both cases, the results show that as the mass of the adsorbent increases, solute removal efficiency increases. The contact surface of adsorbent particles increases as the mass of the adsorbent increases, implying that more solute molecules will be adsorbed on the adsorption sites, resulting in an increase in adsorption efficiency. The removal, on the other hand, increases until it reaches a certain point, at which point it becomes constant. This limit refers to the maximum amount of ion that an adsorbate can absorb. The SAC dosage equilibrium removal can be concluded at this point (Reungsang et al., 2012).

The adsorption results show that as the SAC dosage is increased from 0.1 to 1.0 g, the percentage removal of Cr(VI) and Cd(II) increases gradually. At 0.1 g of SAC, exactly 10.8% Cr(VI) and Cd(II) were detected. With 0.8 and 1.4 g SAC dosages, maximum or equilibrium removal (99.99 %) of Cr(VI) and Cd(II) was achieved, respectively. This is due to the fact that as the sorbent dosage is increased, there are more active adsorption sites available for the adsorbate to adhere to, resulting in a high percentage removal. The results show that a minimum of 0.8 and 1.4 g SAC dosage is required for quantitative removal (99.99 %) of respective adsorbate with 250 mg/L concentration in 250 mL solution. As such, this adsorbent dosage was chosen for all subsequent batch experiments where applicable.

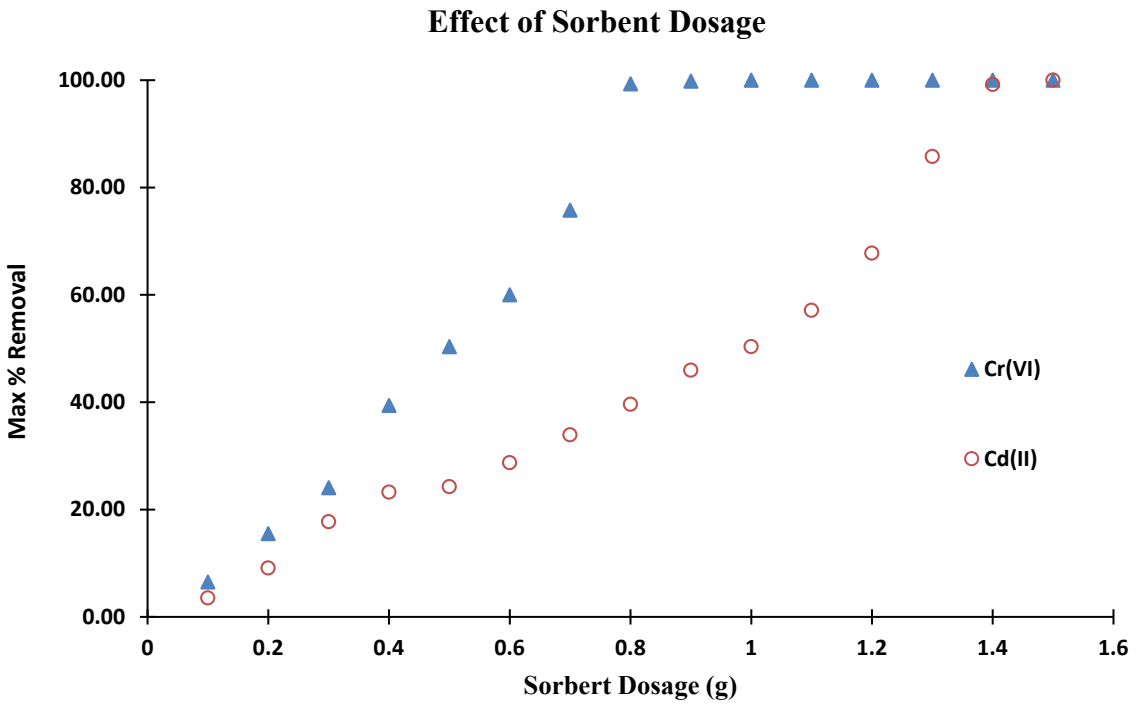


Figure 6.7: Effect of adsorbent dosage on adsorption of Cr (VI), Cd (II. Conditions: pH=10 for Cd (II); pH=2.0 for Cr (VI); 250 mg/L adsorbate concentration; 24 hrs. contact time

6.3.3.3. Effect of initial concentration on adsorption equilibrium

Figure 6.8 shows the adsorption uptake versus the adsorption time at various initial Cr(VI), Cd (II), methylene blue, and red dye concentrations at 30°C. It indicated that the contact time needed for the solutions with initial concentrations of 50 mg/l to reach equilibrium was around 1-2 hours. Such a rapid uptake is indicative of readily available sorption sites in the SAC material. Adsorption normally occurs in three steps and this behavior was observed for all the explored initial concentrations. At an initial concentration of 50 mg/L for instance, the first step (0-1 hr 25 min) was very fast and characterized by the rapid attachment of adsorbates onto the surface of the SAC material (Batool et al., 2018; Jung et al., 2019).

The solutions with initial concentrations of 250 mg/l, required 2.5-3.0 hours to reach equilibrium. The adsorption was slowed down as the reaction approached equilibrium. It is noted that this step (85-180 min) was slower due to the intra-particle diffusion of the

adsorbate to the internal matrix of the adsorbent (Jung et al., 2019). More than 5 hours was required for 500 mg/l initial concentration solutions to reach equilibrium.

It takes longer to attain equilibrium at higher concentrations because molecules have to first encounter the boundary layer effect and then diffuse from the boundary layer film onto the adsorbent surface (Bousba & Meniai, 2013). Then finally, they have to diffuse into the porous structure of the adsorbent. Hence, the solutions of higher initial concentrations will take a relatively long contact time to attain equilibrium due to the higher amount of dye molecules (Okeola et al., 2012).

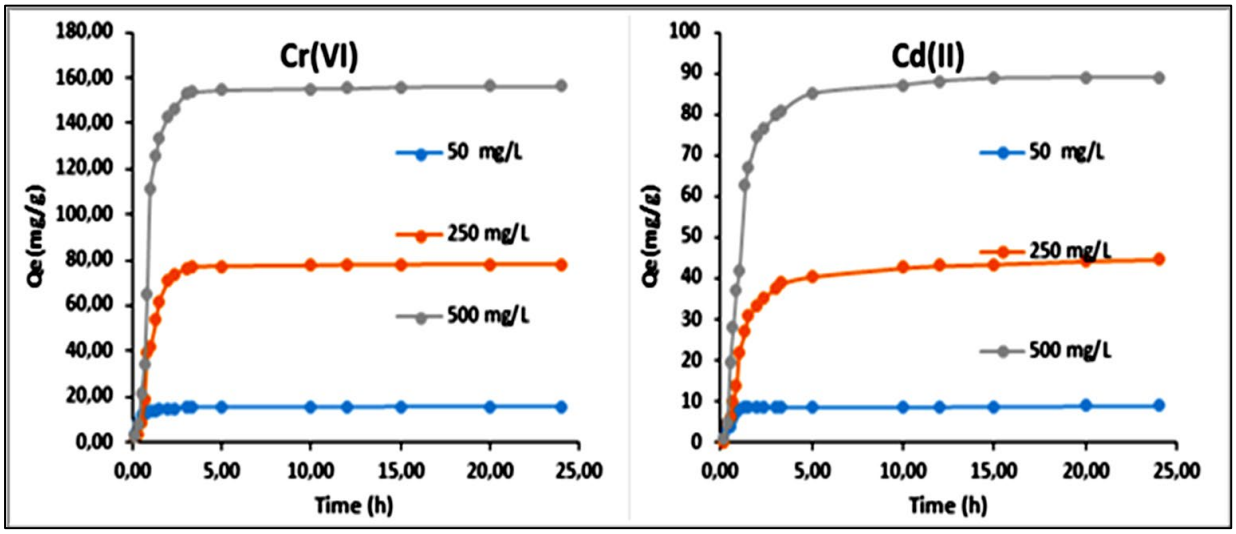


Figure 6.8: The adsorption uptake versus adsorption time at various initial concentrations at 30°C on sludge-based activated carbon.

The amount of dye or ion adsorbed on the SAC increases over time until it reaches a constant value beyond which dye removal from the solution is no longer possible (De Filippis et al., 2013; Lafi et al., 2019). The adsorption reaction will then come to a halt, indicating that the system has reached equilibrium. The maximum adsorption capacity of the adsorbent under those operating conditions is represented by the amount of dye adsorbed at the equilibrium time. With an increase in initial dye concentrations from 50 to 500 mg/L, the adsorption capacity at equilibrium (Qe) was found to increase from 8.91 to 312.50 mg/g in this study. The mass transfer driving force would increase as the initial concentration increased, resulting in higher adsorption (De Filippis et al., 2013; Zha et al., 2018).

6.3.4. Adsorption Isotherm: Effect of Temperature

The adsorption isotherm is useful for describing how solutes interact with adsorbents and for optimizing the adsorbent used. The fitting of adsorption equilibrium data into various isotherm models is also an important step in determining a model that can be used for design purposes (Lafi et al., 2019; Seo et al., 2019). The time series plots and kinetic curves of the adsorption process were also used to develop kinetic parameters. The Langmuir, Freundlich, Temkin, and Dubinin-Radushkevich isotherm models were used to study adsorption isotherms. The isotherm equation's applicability to describe the adsorption process was assessed by the correlation coefficients, and R^2 values.

6.3.4.1. Langmuir isotherm

For the Langmuir isotherm, when Ce/Qe is plotted against Ce, a straight line with a slope of 1/Qo and intercept of (1/Qo) K_L is obtained. The linearized Langmuir isotherm which is based on monolayer sorption on the adsorbent surface with identical sorption sites is represented by Equation (6.3). The date is plotted in Figure 6.9 and the summary is shown in Table 6.2. Langmuir isotherms Equation (6.3):

$$\frac{C_e}{Q_e} = \frac{1}{Q_O} C_e + \frac{1}{Q_O K_L} \tag{6.3}$$

The maximum number of ions per unit mass of adsorbent is presented by Qo (mg/g), this is the ions required to form a complete monolayer on the adsorbent surface. K_L is the rate constant related to the adsorption capacity and intensity of adsorption.

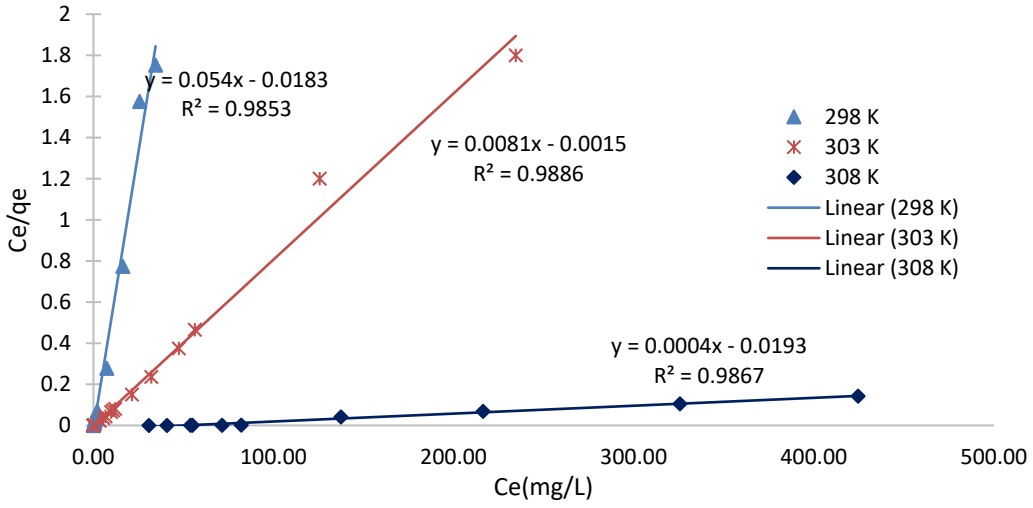


Figure 6.9: The Langmuir linear plots of Ce/Qe versus Ce

Table 6.2: Summary of Langmuir Isotherm model constants and R2 values obtained from the linear plot

Solution T (K)	Equation	R2	1/Qo	Qo	1/QoKL	KL
298	y=0.054x-0.0183	0.985	0.054	18.519	0.018	0.339
303	y=0.081x-0.0015	0.989	0.081	12.346	0.002	0.019
308	y=0.0004x-0.0193	0.987	0.0004	2500.00	0.019	48.250

6.3.4.2. Freundlich isotherm

The plot of log Qe versus log Ce for the Freundlich isotherm yields a straight line with a slope of 1/n and an intercept of log KF. The Freundlich isotherm is an empirical model based on adsorption on a heterogeneous surface, with an equation expressing the linear form in Equation (6.4).

Freundlich isotherms Equation:

$$\log(Q_e) = \log(K_F) + \frac{1}{n}\log(C_e) \qquad (6.4)$$

Where K_F (mg/g) and 1/n constants are related to the adsorption capacity and intensity of adsorption.

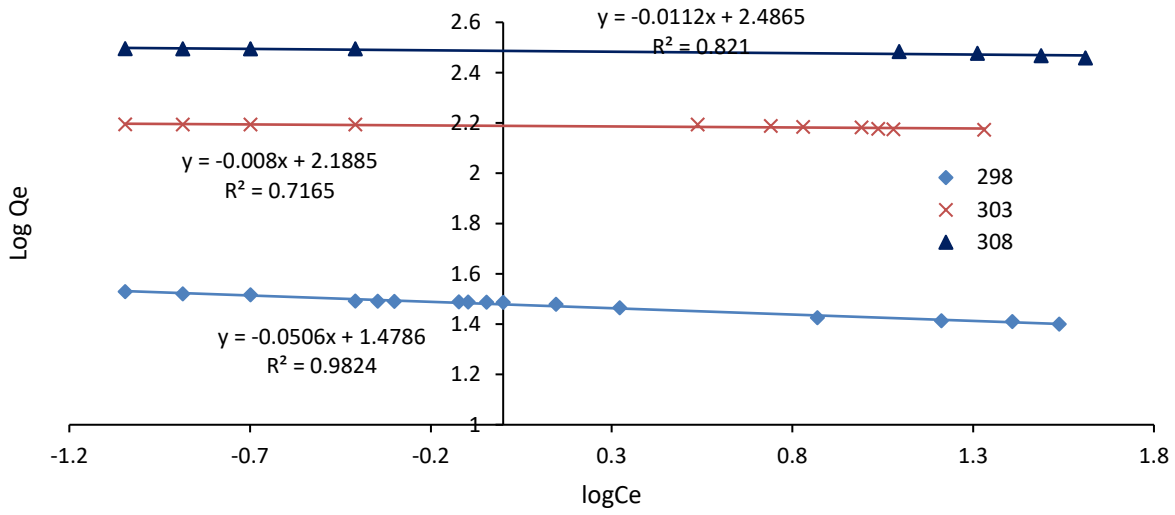


Figure 6.10: Linearized Freundlich isotherm for adsorption

The adsorption capacity and intensity of adsorption are related by the K_F (mg/g) and 1/n constants. The isotherm models used, as well as all the constants and R^2 values obtained from each plot, are shown in Tables 6.2 and 6.3 and Figures 6.9 and 6.10. In comparison to the Freundlich model, the Langmuir model provided the best fit, with an R^2 value of 0.98 or higher.

Table 6.3: Summary of Freundlich Isotherm model constants and R^2 values obtained from the linear plot

Solution T (K)	Equation	R^2	1/n	logK_F	K_F
298	y=-0.0506x+1.4786	0.982	0.051	1.479	30.102
303	y=-0.008x+2.1885	0.717	0.008	2.189	154.348
308	y=-0.0112x+2.4865	0.821	0.011	2.487	306.549

The homogeneous nature of the SAC surface was revealed by fitting the experimental data into the Langmuir isotherm equation. The results also showed the formation of a monolayer of dye molecules on the activated carbon's outer surface. Similar findings have been made elsewhere (de Farias et al., 2018; Han et al., 2020). The adsorption capacity of the activated carbon used in this study was relatively high (312.45 mg/g).

6.4. Conclusions

The study carried out was to evaluate the feasibility to synthesize and develop a sludge-based activated carbon, SAC from municipal sewage sludge and test its performance in the removal of Cr(VI) & Cd(II) heavy metals, from wastewater. The synthesis technique to modify waste sludge into SAC was developed to produce activated carbon from sewage sludge. The main physicochemical findings were:

- The physical activation and the use of $ZnCl_2$ as the chemical activation were successful in increasing the surface area and enhancement of the porous structure.
- The SEM results showed that SAC has a rougher surface with spheres of various dimensions indicating a well-developed porous structure.
- TGA results showed a remarkable weight loss of ~30.64% and ~64.00% observed for raw sludge and SAC material, respectively.

- The activation led to an increase of oxygen-containing functional groups (C-OH, O-H, and C=O) which might increase the adsorption capacity of the material.
- The elements present in the sample based on EDX analyses were mainly P, Na, K, Fe, and Ca

The SAC adsorbent's performance was tested in the removal of Cr(VI) and Cd(II) ions from an aqueous solution. The test performance carried out revealed that:

- Batch adsorption studies reported that the highest Cr(VI) removal efficiency was achieved with the SAC by 99.99%, whereas 60,50 & 40,71% removal efficiency was achieved from CGAC & raw sludge, respectively.
- The study on the effect of pH revealed that the competitions between H^+ and metal ions at low pH values are the main leading factors that affect the adsorption characteristics of SAC.
- The maximum or equilibrium removal (99.99%) of Cr (VI) and Cd (II) was achieved by 0.8 and 1.4 g SAC dosage, respectively. This behaviour is due to the fact that at increased sorbent dosage, there are more available active adsorption sites for the adsorbate to adhere to, hence, a high percentage removal.
- The adsorption capacity at equilibrium (Qe) was found to increase from 8.91 to 312.50 mg/g with an increase in the initial dye concentrations from 50 to 500 mg/L.
- It was observed that the Langmuir isotherm model described the adsorption process with high coefficient of determination R^2, better than the Freundlich isotherm model and for low initial concentration of heavy metal.
- When the values of amount of heavy metal removal from solution are predicted by the Langmuir isotherm model, it showed best fits the batch study.
- It is clear from the results that heavy metal, Cr(VI) removal with the SAC adsorbent appears to be technically feasible and with high efficiency.

References

Agrafioti, E., Bouras, G., Dimitrios, K., & Diamadopoulos, E. (2013). Biochar production by sewage sludge pyrolysis. *Journal of Analytical and Applied Pyrolysis*, *101*(0165–2370), 72–78.

Ait Ahsaine, H., Zbair, M., & El Haouti, R. (2017). Mesoporous treated sewage sludge as outstanding low-cost adsorbent for cadmium removal. *Desalination and Water Treatment*, *85*, 330–338. https://doi.org/10.5004/dwt.2017.21310

Batool, F., Akbar, J., Iqbal, S., Noreen, S., & Bukhari, S. N. A. (2018). Study of Isothermal, Kinetic, and Thermodynamic Parameters for Adsorption of Cadmium: An Overview of Linear and Nonlinear Approach and Error Analysis. *Bioinorganic Chemistry and Applications*, *2018*. https://doi.org/10.1155/2018/3463724

Betsholtz, A., Jacobsson, S., & Haghighatafshar, S. (2018). *Sewage sludge-based activated carbon: Production and potential in wastewater and stormwater treatment Alexander* (Issue 12).

Bian, Y., Yuan, Q., Zhu, G., Ren, B., Hursthouse, A., & Zhang, P. (2018). Recycling of waste sludge: Preparation and application of sludge-based activated carbon. *International Journal of Polymer Science*, *2018*. https://doi.org/10.1155/2018/8320609

Bodîrlău, R., Teacă, C. A., & Iuliana, S. (2009). Preparation and Characterization of Composites Comprising Modified Hardwood and Wood Polymers/Poly(Vinyl Chloride). *BioResources*, *4*(4), 1285–1304.

Bousba, S., & Meniai, A. H. (2013). Adsorption of 2-chlorophenol onto sewage sludge based adsorbent: Equilibrium and kinetic study. *Chemical Engineering Transactions*, *35*(January), 859–864. https://doi.org/10.3303/CET1335143

Charlou, C., Milhé, M., Sauceau, M., & Arlabosse, P. (2015). A new methodology for measurement of sludge residence time distribution in a paddle dryer using X-ray fluorescence analysis. *Water Research*, *69*, 1–18.

de Farias, R. S., Buarque, H. L. de B., da Cruz, M. R., Cardoso, L. M. F., Gondim, T. de A., & de Paulo, V. R. (2018). Adsorption of congo red dye from aqueous solution onto amino-functionalized silica gel. *Engenharia Sanitaria e Ambiental*, *23*(6), 1053–1060.

https://doi.org/10.1590/s1413-41522018172982

De Filippis, P., Di Palma, L., Petrucci, E., Scarsella, M., & Verdone, N. (2013). Production and characterization of adsorbent materials from sewage sludge by pyrolysis. *Chemical Engineering Transactions*, *32*, 205–210. https://doi.org/10.3303/CET1332035

De Mes, T. Z. D., Stams, A. J. M., Reith, J. H., & Zeeman, G. (1972). Methane Production by Anaerobic Digestion of Wastewater and Solid Waste. In *New England Journal of Medicine* (Vol. 286, pp. 1035–1042). https://doi.org/10.1016/j.biortech.2010.08.032

Faisal, S., Hafeez, F. Y., Zafar, Y., Majeed, S., & Leng, X. (2018). A Review on Nanoparticles as Boon for Biogas Producers — Nano Fuels and Biosensing Monitoring. *Applied Sciences*, *9*(59), 1–19. https://doi.org/10.3390/app9010059

Ferrasse, J., Akkache, S., Marseille, E. C. De, Roche, N., & Analysis, T. (2015). *Thermochemical Conversion of Sewage Sludge by TGA-FTIR Analysis : Influence of Mineral Matter Added Drying Technology : An International Journal Thermochemical Conversion of Sewage Sludge by TGA- FTIR Analysis : Influence of Mineral Matter Added*. *July*. https://doi.org/10.1080/07373937.2015.1036283

González, J., Sánchez, M., & Gómez, X. (2018). Enhancing Anaerobic Digestion: The Effect of Carbon Conductive Materials. *C*, *4*(4), 59. https://doi.org/10.3390/c4040059

Han, M., Zhang, J., Chu, W., Zhou, G., & Chen, J. (2020). Surface-modified sewage sludge-derived carbonaceous catalyst as a persulfate activator for phenol degradation. *International Journal of Environmental Research and Public Health*, *17*(9). https://doi.org/10.3390/ijerph17093286

Hu, S. H., & Hu, S. C. (2014). Application of magnetically modified sewage sludge ash (SSA) in ionic dye adsorption. *Journal of the Air and Waste Management Association*, *64*(2), 141–149. https://doi.org/10.1080/10962247.2013.842947

Jung, K. W., Lee, S. Y., & Lee, Y. J. (2019). Optimized preparation of activated carbon from municipal sewage sludge and application to the adsorption of azo dye from aqueous solutions. *Environmental Progress and Sustainable Energy*, *38*(s1), S267–S276. https://doi.org/10.1002/ep.13008

Kaur, S., Rani, S., & Mahajan, K. R. (2013). Adsorption Kinetics for the Removal of Hazardous Dye Congo Red by Biowaste Materials as Adsorbents. *Journal of*

Chemistry, *2013*(628582), 12.

Lafi, R., Montasser, I., & Hafiane, A. (2019). Adsorption of congo red dye from aqueous solutions by prepared activated carbon with oxygen-containing functional groups and its regeneration. *Adsorption Science and Technology*, *37*(1–2), 160–181. https://doi.org/10.1177/0263617418819227

Litefti, K., Freire, M. S., Stitou, M., & González-Álvarez, J. (2019). Adsorption of an anionic dye (Congo red) from aqueous solutions by pine bark. *Scientific Reports*, *9*(1), 1–11. https://doi.org/10.1038/s41598-019-53046-z

Liu, Y., Cheng, H., & He, Y. (2020). Application and mechanism of sludge-based activated carbon for phenol and cyanide removal from bio-treated effluent of coking wastewater. *Processes*, *8*(1). https://doi.org/10.3390/pr8010082

Masindi, V., Chatzisymeon, E., Kortidis, I., & Foteinis, S. (2018). Assessing the sustainability of acid mine drainage (AMD) treatment in South Africa. *Science of the Total Environment*. https://doi.org/10.1016/j.scitotenv.2018.04.108

Mu, B., & Wang, A. (2016). Adsorption of dyes onto palygorskite and its composites: A review. *Journal of Environmental Chemical Engineering*, *4*(1), 1274–1294. https://doi.org/10.1016/j.jece.2016.01.036

Okeola, O. F., Odebunmi, E. O., & Ameen, O. M. (2012). Comparison of sorption capacity and surface area of activated carbon prepared from jatropha curcas fruit pericarp and seed coat. *Bulletin of the Chemical Society of Ethiopia*, *26*(2), 171–180. https://doi.org/10.4314/bcse.v26i2.2

Park, S., Baker, J. O., Himmel, M. E., Parilla, P. A., & Johnson, D. K. (2010). *Cellulose crystallinity index : measurement techniques and their impact on interpreting cellulase performance*. 1–10.

Ragheb, S. (2018). Removal of Heavy Metals from Wastewater Using Sewage Sludge Ash (SSA) as Adsorbent. *SSRN Electronic Journal*, *Iv*, 1–11. https://doi.org/10.2139/ssrn.3164094

Rashed, M. N. (2018). Heavy Metals Removal from Wastewater by Adsorption on Modified Physically Activated Sewage Sludge. *Archives of Organic and Inorganic Chemical Sciences*, *1*(1), 18–25. https://doi.org/10.32474/aoics.2018.01.000102

Reungsang, A., Pattra, S., & Sittijunda, S. (2012). Optimization of key factors affecting methane production from acidic effluent coming from the sugarcane juice hydrogen fermentation process. *Energies*, *5*(11), 4746–4757. https://doi.org/10.3390/en5114746

Rio, S., Faur-Brasquet, C., Le Coq, L., & Le Cloirec, P. (2005). Structure characterization and adsorption properties of pyrolyzed sewage sludge. *Environmental Science and Technology*, *39*(11), 4249–4257. https://doi.org/10.1021/es0497532

Said, A., Hakim, M. S., & Rohyami, Y. (2014). The Effect of Contact Time and pH on Methylene Blue Removal by Volcanic Ash. *International Conference on Chemical, Biological and Environmental Sciences*, *May*, 12–15. https://doi.org/10.17758/iaast.a0514002

Salihi, I. U., Kutty, S. R. M., & Ismail, H. H. M. (2018). Copper Metal Removal using Sludge Activated Carbon Derived from Wastewater Treatment Sludge. *MATEC Web of Conferences*, *203*. https://doi.org/10.1051/matecconf/201820303009

Seo, J. H., Kim, N., Park, M., Lee, S., Yeon, S., & Park, D. (2019). Evaluation of metal removal performance of rod-type biosorbent prepared from sewage-sludge. *Environmental Engineering Research*, *25*(5), 700–706. https://doi.org/10.4491/eer.2019.201

Setshedi, K. Z. (2014). *Removal of Heavy Metals from Industrial Wastewater Using Polymer-Clay Nanocomposites as Novel Adsorbents* (Vol. 153) [TSHWANE UNIVERSITY OF TECHNOLOGY]. https://doi.org/10.1017/CBO9781107415324.004

Setshedi, K. Z., Bhaumik, M., Songwane, S., Onyango, M. S., & Maity, A. (2013). Exfoliated polypyrrole-organically modified montmorillonite clay nanocomposite as a potential adsorbent for Cr(VI) removal. *Chemical Engineering Journal*, *222*(Vi), 186–197. https://doi.org/10.1016/j.cej.2013.02.061

Tocharoen, S., Atong, D., & Sricharoenchaikul, V. (2019). Utilization of Sewage Sludge from Beverage Industry as Dye Adsorption Materials. *IOP Conference Series: Earth and Environmental Science*, *219*(1). https://doi.org/10.1088/1755-1315/219/1/012015

Wang, C., Wu, L., Zhang, Y. T., Wei, W., & Ni, B. J. (2021). Unravelling the impacts of perfluorooctanoic acid on anaerobic sludge digestion process. *Science of the Total Environment*, *796*, 149057. https://doi.org/10.1016/j.scitotenv.2021.149057

Wang, Y., Zhao, W., Zheng, W., Chen, S., & Zhao, J. (2019). Preparation of N-doped carbon nanosheets from sewage sludge for adsorption studies of cr(VI) from aqueous solution. *Nanomaterials*, *9*(2). https://doi.org/10.3390/nano9020265

Wei, L., Qin, K., Ding, J., Xue, M., Yang, C., Jiang, J., & Zhao, Q. (2019). Optimization of the co-digestion of sewage sludge, maize straw and cow manure: microbial responses and effect of fractional organic characteristics. *Scientific Reports*, *9*(1), 1–10. https://doi.org/10.1038/s41598-019-38829-8

Wen, H., Zhang, D., Gu, L., Yu, H., Pan, M., & Huang, Y. (2019). Preparation of sludge-derived activated carbon by fenton activation and the adsorption of Eriochrome Black T. *Materials*, *16*(6). https://doi.org/10.3390/ma12060882

Zha, Y., Wang, Y., Liu, S., Liu, S., Yang, Y., Jiang, H., Zhang, Y., Qi, L., & Wang, H. (2018). Adsorption characteristics of organics in the effluent of ultra-short SRT wastewater treatment by single-walled, multi-walled, and graphitized multi-walled carbon nanotubes. *Scientific Reports*, *8*(1), 1–12. https://doi.org/10.1038/s41598-018-35374-8

CHAPTER 7

CONCLUSIONS & RECOMMENDATIONS

7.1. Introduction

The overall study aim was to enhance the biogas production using the AD from the municipal wastewater sludge and evaluate the feasibility of the value-added products from the by-products of the biogas production.

7.1.1. Contribution to knowledge

This study fills in the knowledge gaps in the study by providing details about the use of municipal wastewater treatment effluents from South Africa in anaerobic biogas production. A thorough description of the physicochemical and microbiological properties of the sludge as primary substrates, particularly for CoT and JW, and the co-substrates that industrial wastes are dumped with analysis and are being used as co-substrates. The new and novel BMP technique developed in our lab for this specific research is introduced. a comparison of the co-digestion of sludge with different co-substrates or bio-wastes. The simulation of the modified ADM1 using MATLAB Simulink for a specific substrate and co-substrates blend, with comparison to experimental results. The process of waste beneficiation includes synthesizing the sludge-based Activated Carbon (SAC) from the material that has been digested thus exploring its application in wastewater treatment.

7.2. Conclusions

The study's first objective was to assess the composition of feed sludge sources from CoT and JW in South Africa, as well as their potential impact on methane production. Before anaerobic digestion, physicochemical and microbiological characterization was performed to determine the composition of the anaerobic digestion feedstock. The wastewater treatment plant sewage sludge was physiochemically characterized, as well as the microbial community composition, to reveal functional traits in a typical full-scale anaerobic digester. The study also looked at the anaerobic co-digestion of sewage sludge and six organic waste materials as potential co-substrates for increasing bio-

methane potential and determining the impact on digested sludge content in terms of TS, VS, and COD removal.

The co-substrates interactive mechanism is discussed, and the enhancement effect is quantified. The final goal was to assess the feasibility of synthesizing and developing a sludge-based activated carbon (SAC) from municipal sewage sludge, as well as testing its performance in removing Cr(VI) and Cd(II) heavy metals from wastewater. To produce activated carbon from sewage sludge, a synthesis technique was developed to modify waste sludge into SAC. To increase surface area and enhance the porous structure, this method includes physical activation and the use of $ZnCl_2$ as a chemical activator. Prior batch studies were conducted to assess the textual, physical, and compositional properties of the material.

It was clearly shown that anaerobic digestion is a technology for treating organic waste products under oxygen-free conditions in order to generate biogas, which can then be used for fertilization. The main components of biogas produced by anaerobic digestion are CH_4, CO_2, H_2, and a trace of H_2S. The rate of biogas production is determined by the type of sludge and the digester's operating conditions. Temperature, pH, mixing, retention time, and feedstock composition are all factors to consider. As a result, these parameters must be monitored and controlled in order to improve gas yield and quality.

The temperature in this study was mesophilic (20-45 °C). Bacteria in a mesophilic environment have slower metabolic rates, necessitating longer retention times. As a result, the vast majority of mesophilic anaerobic processes used in practice have a sludge retention time of 20 days. For the overall anaerobic digestion process, pH values should be between 6.4 and 7.2. During the methanogenesis stage, however, the ideal pH is 6.6-7.0. Acid formation during acidogenesis lowers the pH of the medium and inhibits the methanogenesis process if the process is low in alkalinity. Slow mixing is also recommended in the literature to improve microbial consortia's proximity to substrates.

The results show that WWTW sewage sludge has a high potential for methane production, with 28.6 g CH4/kg feed in COT2 PS sewage sludge and 27.8 g CH_4/kg feed in JW1 NW sewage sludge, respectively. Extremely high COD, on the other hand, may result in the accumulation of volatile fatty acids, causing a delay in biogas production or lowering the pH of bioreactors. As a result, a well-balanced high COD with a C/N ratio

and VS concentration of 10-100 g/kg feed, C/N of 17–36, and VS 80–98% TS is recommended.

The characterization of sewage sludge as a feedstock for biogas production revealed that most of the shortlisted sludges contain reasonable levels of COD, organic matter, total solids (TS), volatile solids (VS), and inhibitory parameters, indicating a high yield of methane in biogas production as long as AD stability is maintained throughout the process. The high-throughput sequencing analysis revealed clear differences in microbial communities available in sewage sludge, as well as the AD inhibiting microbes, according to the microbiology data.

The ability of sewage sludge from COT and JW WWTPs to be a suitable substrate for efficient anaerobic digestion has been demonstrated. However, the process can improve or deteriorate in terms of methane yield depending on operating conditions such as pH, temperature, and organic loading rate. To find the most stable environment and avoid inhibitory effects, different operational strategies can be used.

Both co-substrates increased bio-methane yield by three to six times when compared to conventional anaerobic digestion of sewage sludge. Co-substrates with a high solid content produced significantly more methane gas, but they also increased the risk of organic overloading. At maximum co-digestion ratios, co-substrates like molasses, food waste, animal manure, and fresh produce waste performed well. Soft drink waste and sewage sludge had a maximum co-digestion ratio of 25%. Furthermore, all other solid co-substrates co-digestion resulted in additional VS and COD residuals in digested sludge, with the exception of manure. Most of the liquid co-substrates studied here, on the other hand, had a significant synergistic effect, enhancing the removal of TS, VS, and COD during anaerobic digestion.

As a result, anaerobic co-digestion could be viewed as a cost-effective solution that could help WWTPs become more energy self-sufficient and waste management become more sustainable. The operating conditions, on the other hand, should be optimized and monitored at all times. It is recommended to scale up the co-digestion of the feed for the pilot biogas plant based on the experimental results. The feed should be made up of sludge from the WWTP and spent grains from the brewery. However, when the OLR reached 2.90 gVS/L.day, a significant decrease in biogas yield was observed, from 10.23 to 2.02 NL/day in a semi-continuous setup.

The ADM1 Matlab/Simulink implementation used in this study is discussed in Chapter 5. The goal of this study was to devise methods for assessing biogas production from the co-digestion of dairy thick waste and sewage sludge. This project built a model based on Anaerobic Digestion Model No. 1 (ADM1). The goal was to use a simulation approach to estimate anaerobic digestion performance, validate the model, and optimize the process. This was accomplished by outlining all of the key biochemical and physicochemical processes involved in COD and VFAs complexation, as well as precipitation, dissolution, and substrate absorption in the AD system.

The simulation was carried out to mimic the AD process on important parameters with Matlab Simulink. The developed model was validated and calibrated and sensitivity was examined. Once validated, the optimization was done to ensure maximum gas output and was achieved via the PSO approach. Several practical implementation challenges are highlighted, the optimal combination discovered by this technique is only valid in a small portion of the parameter space, and changing the parameters demands that the optimization process should be re-run.

The SEM results showed that SAC material has a rougher surface with spheres of various dimensions indicating a well-developed porous structure compared to what was reported previously in the literature. TGA results showed a remarkable weight loss of ~30.64% and ~64% observed for raw sludge and SAC material, respectively. The activation led to an increase of oxygen-containing functional groups (C-OH, O-H, and C=O) which might increase the adsorption capacity of the material. The elements present in the sample based on EDX analyses were mainly P, Na, K, Fe, and Ca. All these characteristics contributed to a high adsorption capacity of metal ions such as Cr(VI), Cd(II), dyes, and other impurities on SAC.

To evaluate SAC performance, two types of material were tested against SAC i.e. raw sludge & commercial granulated activated carbon, CGAC. For this study, the material performance was carried out by adsorption of Cr(VI) and removal adsorption efficiency was reported. Batch adsorption studies reported that the highest Cr(VI) removal efficiency was achieved with the SAC by 99.99 %, whereas 60, 50 & 40,71 % removal efficiency was achieved from CGAC & raw sludge, respectively. The SAC adsorbent was tested for its performance in the removal of Cr (VI) and Cd (II) ions from an aqueous solution. The study on the effect of pH revealed that the competitions between H+ and

metal ions at low pH values are the main leading factors that affect the adsorption characteristics of SAC.

The maximum or equilibrium removal (99.99 %) of Cr (VI) and Cd (II) was achieved by 0.8 and 1.4 g SAC dosage, respectively. This behaviour is due to the fact that at increased sorbent dosage, there are more available active adsorption sites for the adsorbate to adhere to, hence, a high percentage removal. The adsorption capacity at equilibrium (qe) was found to increase from 8.91 to 312.50 mg/g with an increase in the initial dye concentrations from 50 to 500 mg/L. It was observed that the Langmuir isotherm model described the adsorption process with a high coefficient of determination R^2, better than the Freundlich isotherm model, and for a low initial concentration of heavy metal. When the values of the amount of heavy metal removal from solution are predicted by the Langmuir isotherm model, it showed best fits the batch study. It is clear from the results that heavy metal, Cr(VI) removal with the SAC adsorbent appears to be technically feasible and with high efficiency.

7.3. Recommendations for Future Research

The results of this study point to the possibility of future studies involving various wastewater sludge sources. The co-digestion of organic wastes with primary sludge is the subject of this study, but traditional wastewater treatment requires the anaerobic digestion of a mixture of primary and secondary sludge. The choice of primary sludge as the primary substrate was based on the replicability of its degradation. Because of the durability of primary sludge digestion, more conclusive evidence of synergisms may be gathered. The effects of alternate sources of sewage sludge on the synergistic effect with the demonstrated co-substrates would need to be investigated further.

Continued research into the effects on biosolids quality could boost co-digestion adoption in agricultural sectors, where biosolids are commonly applied to the soil. While this research focused on the effects of co-digestion on biosolids odour, stabilization, and quantity, other factors like dewaterability, residual biological activity, and pathogen destruction need to be investigated further. Negative effects on these parameters will raise operational costs and reduce anaerobic digestion's successful nutrient recovery. Lower dewaterability affects the water content of biosolids and, as a result, the volume and cost of transportation. Furthermore, biosolids classifications necessitate greater

pathogen destruction in order to be suitable for direct land application. Meanwhile, residual biological activity can cause long-term odour formation, which reduces the appeal of using biosolids.

In order to develop robust predictive analytics for digestion performance based on substrate selection, more research is required. Co-substrate pairings and mixing ratios are commonly based on both the organic loading rate and the C/N ratio in the literature. The stoichiometric ratio, on the other hand, ignores considerations like the fraction of readily degradable organics. Indeed, the literature's suggested C/N ratios are diverse and differ between studies. Lipid, protein, and carbohydrate concentrations can represent a more comprehensive predictive ratio.

Experiments to determine the optimal organic ratios using pure sources of proteins, lipids, and carbohydrates have been described, but they are limited in scope and do not recognize the importance of micronutrients. When logistically feasible, determining the characteristics of an ideal anaerobic digestion feed would allow operators to combine different organic wastes to maximize digestion efficiency. Future research may look into the impact of SAC on digestate nutrient bioavailability both before and after it is applied to the soil. Also recommended is a different approach to incorporating biowastes on AD for biomethane processing.

Appendix A

Number	Parameter	Number	Parameter	Number	Parameter
1	$f_{sI,xc}$	26	P_{atm}	51	$K_{S,ac}$
2	$f_{xI,xc}$	27	k_p	52	$K_{I,nh3}$
3	$f_{ch,xc}$	28	$k_{L,a}$	53	$pH_{UL,ac}$
4	$f_{pr,xc}$	29	V_{gas}	54	$pH_{LL,ac}$
5	$f_{li,xc}$	30	k_{dis}	55	$k_{m,h2}$
6	$f_{h2,su}$	31	$k_{hyd,ch}$	56	$K_{S,h2}$
7	$f_{bu,su}$	32	$k_{hyd,pr}$	57	$pH_{UL,h2}$
8	$f_{pro,su}$	33	$k_{hyd,li}$	58	$pH_{LL,h2}$
9	$f_{ac,su}$	34	$K_{S,IN}$	59	$k_{dec,X,su}$
10	Y_{su}	35	$k_{m,su}$	60	$k_{dec,X,aa}$
11	$f_{h2,aa}$	36	$K_{S,su}$	61	$k_{dec,X,fa}$
12	$f_{va,aa}$	37	$pH_{UL,aa}$	62	$k_{dec,X,c4}$
13	$f_{bu,aa}$	38	$pH_{LL,aa}$	63	$k_{dec,X,ac}$
14	$f_{pro,aa}$	39	$k_{m,aa}$	64	$k_{dec,X,h2}$
15	$f_{ac,aa}$	40	$K_{S,aa}$	65	$k_{m,lac,f}$
16	Y_{aa}	41	$k_{m,fa}$	66	$K_{S,lac,f}$
17	Y_{fa}	42	$K_{S,fa}$	67	$k_{m,lac,o}$
18	Y_{c4}	43	$K_{I,h2,fa}$	68	$K_{S,lac,o}$
19	Y_{pro}	44	$k_{m,c4}$	69	$K_{I,h2,lac,o}$
20	Y_{ac}	45	$K_{S,c4}$	70	$K_{I,vfa}$
21	Y_{h2}	46	$K_{I,h2,c4}$	71	$k_{dec,X,lac,f}$
22	$Y_{lac,f}$	47	$k_{m,pro}$	72	$k_{dec,X,lac,o}$
23	$Y_{lac,o}$	48	$K_{S,pro}$	73	$K_{S,p,caco3}$
24	T_{base}	49	$K_{I,h2,pro}$	74	$K_{r,caco3}$
25	T_{op}	50	$k_{m,ac}$		

Table A.1: Parameters denomination in sensitivty analysis plot. The number in the table corresponds to a position on the x-axis.

Appendix A

ADM1 Dynamic State Variables

i	Variable	Unit	Description	*i*	Variable	Unit	Description
1	S_{su}	kgCOD/m³	Monosaccharides	16	X_{li}	kgCOD/m³	Lipids
2	S_{aa}	kgCOD/m³	Amino acids	17	X_{su}	kgCOD/m³	Monosaccharide degraders
3	S_{fa}	kgCOD/m³	Total LCFA	18	X_{aa}	kgCOD/m³	Amino acid degraders
4	S_{va}	kgCOD/m³	Total valerate	19	X_{fa}	kgCOD/m³	LCFA degraders
5	S_{bu}	kgCOD/m³	Total butyrate	20	X_{c4}	kgCOD/m³	C4-degraders
6	S_{pro}	kgCOD/m³	Total propionate	21	X_{pro}	kgCOD/m³	Propionate degraders
7	S_{ac}	kgCOD/m³	Total acetate	22	X_{ac}	kgCOD/m³	Acetate degraders
8	S_{h2}	kgCOD/m³	Hydrogen	23	X_{h2}	kgCOD/m³	Hydrogen degraders
9	S_{ch4}	kgCOD/m³	Methane	24	X_{I}	kgCOD/m³	Particulate inerts
10	S_{IC}	kmol C/m³	Inorganic carbon	25	S_{an}	kmol/m³	Anions
11	S_{IN}	kmol N/m³	Inorganic nitrogen	26	S_{cat}	kmol/m³	Cations
12	S_{I}	kgCOD/m³	Soluble inerts	27	$S_{h2,g}$	kgCOD/m³	Hydrogen (gas)
13	X_{c}	kgCOD/m³	Composites	28	$S_{ch4,g}$	kgCOD/m³	Methane (gas)
14	X_{ch}	kgCOD/m³	Carbohydrates	29	$S_{co2,g}$	kgCOD/m³	Carbon dioxide (gas)
15	X_{pr}	kgCOD/m³	Proteins				

ADM1 Stoichiometric Parameters

Parameter	Description	Parameter	Description
$f_{SI,XC}$	Soluble inerts fraction from composites	$f_{PRO,SU}$	Propionate fraction from monosaccharides
$f_{XI,XC}$	Particulate inerts fraction from composites	$f_{AC,SU}$	Acetate fraction from monosaccharides
$f_{CH,XC}$	Carbohydrates fraction from composites	$f_{H2,AA}$	Hydrogen fraction from amino acids
$f_{PR,XC}$	Proteins fraction from composites	$f_{VA,AA}$	Valerate fraction from amino acids
$f_{LI,XC}$	Lipids fraction from composites	$f_{BU,AA}$	Butyrate fraction from amino acids
$f_{FA,LI}$	Fatty acids fraction from lipids	$f_{PRO,AA}$	Propionate fraction from amino acids
$f_{H2,SU}$	Hydrogen fraction from monosaccharides	$f_{AC,AA}$	Acetate fraction from amino acids
$f_{BU,SU}$	Butyrate fraction from monosaccharides		

ADM1 Kinetic Parameters

Parameter	Unit	Description
k_{dis}	d^{-1}	Disintegration factor
k_{hyd_CH}	d^{-1}	Carbohydrates hydrolysis rate constant
k_{hyd_PR}	d^{-1}	Proteins hydrolysis rate constant
k_{hyd_LI}	d^{-1}	Lipids hydrolysis rate constant
K_{S_IN}	kmol/m³	Inorganic nitrogen concentration threshold; growth ceases when exceeded
pH_{UL_acid}	-	pH threshold; no inhibition when pH is above this level
pH_{LL_acid}	-	pH threshold; full inhibition when pH is below this level
k_{m_su}	$COD.COD^{-1}.d^{-1}$	Monod maximum specific uptake rate for monosaccharide degraders
K_{S_su}	$kgCOD.m^{-3}$	Monod half saturation value for monosaccharide degradation
Y_{su}	$COD.COD^{-1}$	Biomass yield on uptake of monosaccharides
k_{dec_xsu}	d^{-1}	Decay rate constant of monosaccharide degraders
k_{m_aa}	$COD.COD^{-1}.d^{-1}$	Monod maximum specific uptake rate for amino acid degraders
K_{S_aa}	$kgCOD.m^{-3}$	Monod half saturation value for amino acid degradation
Y_{aa}	$COD.COD^{-1}$	Biomass yield on uptake of amino acids
k_{dec_xaa}	d^{-1}	Decay rate constant of amino acid degraders
k_{m_fa}	$COD.COD^{-1}.d^{-1}$	Monod maximum specific uptake rate for LCFA degraders
K_{S_fa}	$kgCOD.m^{-3}$	Monod half saturation value for LCFA degradation
Y_{fa}	$COD.COD^{-1}$	Biomass yield on uptake of LCFA
k_{dec_xfa}	d^{-1}	Decay rate constant of LCFA degraders
KI_{h2_fa}	$kgCOD.m^{-3}$	Hydrogen inhibitory concentration for LCFA degraders
k_{m_c4}	$COD.COD^{-1}.d^{-1}$	Monod maximum specific uptake rate for valerate & butyrate degraders
K_{S_c4}	$kgCOD.m^{-3}$	Monod half saturation value for valerate & butyrate degradation
Y_{c4}	$COD.COD^{-1}$	Biomass yield on uptake of valerate & butyrate
k_{dec_xc4}	d^{-1}	Decay rate constant of valerate & butyrate degraders
k_{m_pro}	$COD.COD^{-1}.d^{-1}$	Monod maximum specific uptake rate for propionate degraders
K_{S_pro}	$kgCOD.m^{-3}$	Monod half saturation value for propionate degradation

Table A.2: Nomenclature for dynamic state variables, stoichiometric and kinetics parameters

Measured Parameters

Component	Description	Min	Max	Avg
Flow [m³/day]	Influent Flow	165	170	167,5
pH		5,1	7	6,05
Temperature [°C]		31	37	34
TCOD [mg/l]	Total COD	7940	10500	9220
SCOD [mg/l]	Soluble COD	5342	8500	6921
PCOD [mg/l)	Particulate COD	2598	1000	1799
TSS [mg/l]	Total Suspended Solids	603,44	750,03	676,735
VSS [mg/l]	Volatile Suspended Solids	573,268	609,23	591,249
VFA [meq/l]	Volatile Fatty Acids	721,3	821,56	771,43
Alkalinity	as CaCO3	584	589	586,5
TOC	Total Organic Carbon	25	31	28
TKN [mg N/l]	Total Kjeldahl Nitrogen	925	946,3	935,65
NH4-N [mg N/l]	Ammonium Nitrogen	127	129	128
NO2-N [mg N/l]	Nitrate	54	54,3	54,15
NO3-N [mg N/l]	Nitrite	190	197	193,5
Total-P [mg P/l]	Total Phosphorus	3,69	6	4,845
PO4-P [mg P/l]	Orthophosphates	0,1	0,12	0,11
Ca [mg/l]	Calcium	5,4	5,4	5,4
Mg [mg/l]	Magnesium	0,87	0,87	0,87
SO4 [mg/l]	Sulphates	0,32	0,45	0,385
CH4 content [%]	Methane %	65	71	68
CO2 content [%]	Carbon dioxide	31	32	31,5

Model Input	Description	Value	Unit
V_digester	Volume of CSTR	175	m^-3
V_head	Volume of headspace	165	m^-3
T (35 °C)	Digester temperature	308	K
Time	Digestion time	50	days
P_atm	Atmospheric pressure	1,013	bar

Literature Parameter

Term	Description	Value	Source
f_d'	Biodegradibility	0,880	Xu
η_{su}	Monosaccharides	0,440	Yang et al., 2003
η_{aa}	Amino acids	0,400	Yang et al., 2003
η_{fa}	Long chain fatty acids	0,160	Yang et al., 2003
$\eta_{va,VFA}$	Valerate fraction	0,090	Yu & Fang, 2002
$\eta_{bu,VFA}$	Butyrate fraction	0,370	Yu & Fang, 2002
$\eta_{pro,VFA}$	Propionate	0,220	Yu & Fang, 2002
$\eta_{ac,VFA}$	Acetate	0,310	Yu & Fang, 2002
Y_va	COD equiv. of valerate	2,039	Grau et al., 2007
Y_bu	COD equiv. of butyrate	1,818	Grau et al., 2007
Y_pro	COD equiv. of propionate	1,514	Grau et al., 2007
Y_ac	COD equiv. of acetate	1,067	Grau et al., 2007
VFA_{COD}	Sum of (va,bu,pro,ac)	1,096	
X_deg	Sum of (su,aa,fa,c4,pro,ac,h2)	-0,899	
η_{ch}	Carbohydrates fraction	0,44	Yang et al., 2003
η_{pr}	Protein fraction	0,4	Yang et al., 2003
η_{li}	Lipids fraction	0,16	Yang et al., 2003
f_acid	Acidification	0,484	Yu & Fang, 2002
Y_acid	Acidogen Yield	0,26	Yu & Fang, 2002
Y_bm	COD equiv. of biomass	1,42	Eastman & Ferguson, 1981
Na	Sodium ion	0,0536	Danalewich et al., 1998
K	Potassium ion	0,00387	Danalewich et al., 1999
H+	Hydrogen ion	3,16E-07	
OH-	Hydroxide concentration	6,58E-08	

Table A3 Biochemical rate coefficients ($\nu_{i,j}$) and kinetic rate equations (ρ_j) for soluble components ($i = 1 - 12$, $j = 1 - 19$)

	Component →	i	1	2	3	4	5	6	7	8	9	10	11	12	Rate (ρ_j, kg COD·m^{-3}·d^{-1})
j	Process ↓		S_{su}	S_{aa}	S_{fa}	S_{va}	S_{bu}	S_{pro}	S_{ac}	S_{h2}	S_{ch4}	S_{IC}	S_{IN}	S_I	
1	Disintegration													$f_{sl,xc}$	$k_{dis} X_c$
2	Hydrolysis carbohydrates		1												$k_{hyd,ch} X_{ch}$
3	Hydrolysis of proteins			1											$k_{hyd,pr} X_{pr}$
4	Hydrolysis of lipids		$1-f_{fa,li}$		$1-f_{fa,li}$										$k_{hyd,li} X_{li}$
5	Uptake of sugars		−1				$(1-Y_{su}) f_{bu,su}$	$(1-Y_{su}) f_{pro,su}$	$(1-Y_{su}) f_{ac,su}$	$(1-Y_{su}) f_{h2,su}$		$-\sum_{i=9,11-24} C_i \nu_{i,5}$	$-(Y_{su}) N_{bac}$		$k_{m,su} \frac{S_{su}}{K_S + S} X_{su} I_1$
6	Uptake of amino acids			−1		$(1-Y_{aa}) f_{va,aa}$	$(1-Y_{aa}) f_{bu,aa}$	$(1-Y_{aa}) f_{pro,aa}$	$(1-Y_{aa}) f_{ac,aa}$	$(1-Y_{aa}) f_{h2,aa}$		$-\sum_{i=1-9,11-24} C_i \nu_{i,6}$	$N_{aa} - (Y_{aa}) N_{bac}$		$k_{m,aa} \frac{S_{aa}}{K_S + S_{aa}} X_{aa} I_1$
7	Uptake of LCFA				−1				$(1-Y_{fa})\,0.7$	$(1-Y_{fa})\,0.3$			$-(Y_{fa}) N_{bac}$		$k_{m,fa} \frac{S_{fa}}{K_S + S_{fa}} X_{fa} I_2$
8	Uptake of valerate					−1		$(1-Y_{c4})\,0.54$	$(1-Y_{c4})\,0.31$	$(1-Y_{c4})\,0.15$			$-(Y_{c4}) N_{bac}$		$k_{m,c4} \frac{S_{va}}{K_S + S_{va}} X_{c4} \frac{1}{1 + S_{bu}/S_{va}} I$
9	Uptake of butyrate						−1		$(1-Y_{c4})\,0.8$	$(1-Y_{c4})\,0.2$			$-(Y_{c4}) N_{bac}$		$k_{m,c4} \frac{S_{bu}}{K_S + S_{bu}} X_{c4} \frac{1}{1 + S_{va}/S_{bu}} I$
10	Uptake of propionate							−1	$(1-Y_{pro})\,0.57$	$(1-Y_{pro})\,0.43$		$-\sum_{i=1-9,11-24} C_i \nu_{i,10}$	$-(Y_{pro}) N_{bac}$		$k_{m,pr} \frac{S_{pro}}{K_S + S_{pro}} X_{pro} I_2$
11	Uptake of acetate								−1		$(1-Y_{ac})$	$-\sum_{i=1-9,11-24} C_i \nu_{i,11}$	$-(Y_{ac}) N_{bac}$		$k_{m,ac} \frac{S_{ac}}{K_S + S_{ac}} X_{ac} I_3$
12	Uptake of hydrogen									−1	$(1-Y_{h2})$	$-\sum_{i=1-9,11-24} C_i \nu_{i,12}$	$-(Y_{h2}) N_{bac}$		$k_{m,h2} \frac{S_{h2}}{K_S + S_{h2}} X_{h2} I_1$
13	Decay of X_{su}														$k_{dec,Xsu} X_{su}$
14	Decay of X_{aa}														$k_{dec,Xaa} X_{aa}$
15	Decay of X_{fa}														$k_{dec,Xfa} X_{fa}$
16	Decay of X_{c4}														$k_{dec,Xc4} X_{c4}$
17	Decay of X_{pro}														$k_{dec,Xpro} X_{pro}$
18	Decay of X_{ac}														$k_{dec,Xac} X_{ac}$
19	Decay of X_{h2}														$k_{dec,Xh2} X_{h2}$
			Monosaccharides (kg COD·m^{-3})	Amino acids (kg COD·m^{-3})	Long chain fatty acids (kg COD·m^{-3})	Total valerate (kg COD·m^{-3})	Total butyrate (kg COD·m^{-3})	Total propionate (kg COD·m^{-3})	Total acetate (kg COD·m^{-3})	Hydrogen gas (kg COD·m^{-3})	Methane gas (kg COD·m^{-3})	Inorganic carbon (kmoleC·m^{-3})	Inorganic nitrogen (kmoleN·m^{-3})	Soluble inerts (kg COD·m^{-3})	Inhibition factors: $I_1 = I_{pH} I_{IN,lim}$ $I_2 = I_{pH} I_{IN,lim} I_{h2}$ $I_3 = I_{pH} I_{IN,lim} I_{NH3,Xac}$

Table A4 Biochemical rate coefficients ($\nu_{i,j}$) and kinetic rate equations (ρ_j) for soluble components ($i = 13-24$, $j = 1-19$)

	Component →	i	13	14	15	16	17	18	19	20	21	22	23	24	Rate (ρ_j, kg COD.m^{-3}.d^{-1})
j	Process ↓		X_c	X_{ch}	X_{pr}	X_{li}	X_{su}	X_{aa}	X_{fa}	X_{c4}	X_{pro}	X_{ac}	X_{h2}	X_I	
1	Disintegration		-1	$f_{ch,xc}$	$f_{pr,xc}$	$f_{li,xc}$								$f_{xI,xc}$	$k_{dis}X_c$
2	Hydrolysis carbohydrates			-1											$k_{hyd,ch}X_{ch}$
3	Hydrolysis of proteins				-1										$k_{hyd,pr}X_{pr}$
4	Hydrolysis of lipids					-1									$k_{hyd,li}X_{li}$
5	Uptake of sugars						Y_{su}								$k_{m,su}\frac{S_{su}}{K_S+S}X_{su}I_1$
6	Uptake of amino acids							Y_{aa}							$k_{m,aa}\frac{S_{aa}}{K_S+S_{aa}}X_{aa}I_1$
7	Uptake of LCFA								Y_{fa}						$k_{m,fa}\frac{S_{fa}}{K_S+S_{fa}}X_{fa}I_2$
8	Uptake of valerate									Y_{c4}					$k_{m,c4}\frac{S_{va}}{K_S+S_{va}}X_{c4}\frac{1}{1+S_{bu}/S_{va}}I$
9	Uptake of butyrate									Y_{c4}					$k_{m,c4}\frac{S_{bu}}{K_S+S_{bu}}X_{c4}\frac{1}{1+S_{va}/S_{bu}}I$
10	Uptake of propionate										Y_{pro}				$k_{m,pr}\frac{S_{pro}}{K_S+S_{pro}}X_{pro}I_2$
11	Uptake of acetate											Y_{ac}			$k_{m,ac}\frac{S_{ac}}{K_S+S_{ac}}X_{ac}I_3$
12	Uptake of hydrogen												Y_{h2}		$k_{m,h2}\frac{S_{h2}}{K_S+S_{h2}}X_{h2}I_1$
13	Decay of X_{su}		1				-1								$k_{dec,Xsu}X_{su}$
14	Decay of X_{aa}		1					-1							$k_{dec,Xaa}X_{aa}$
15	Decay of X_{fa}		1						-1						$k_{dec,Xfa}X_{fa}$
16	Decay of X_{c4}		1							-1					$k_{dec,Xc4}X_{c4}$
17	Decay of X_{pro}		1								-1				$k_{dec,Xpro}X_{pro}$
18	Decay of X_{ac}		1									-1			$k_{dec,Xac}X_{ac}$
19	Decay of X_{h2}		1										-1		$k_{dec,Xh2}X_{h2}$
			Composites (kg COD·m^{-3})	Carbohydrates (kg COD·m^{-3})	Proteins (kg COD·m^{-3})	Lipids (kg COD·m^{-3})	Sugar degraders (kg COD·m^{-3})	Amino acid degraders (kg COD·m^{-3})	LCFA degraders (kg COD·m^{-3})	Valerate and butyrate degraders (kg COD·m^{-3})	Propionate degraders (kg COD·m^{-3})	Acetate degraders (kg COD·m^{-3})	Hydrogen degraders (kg COD·m^{-3})	Particulate inerts (kg COD·m^{-3})	Inhibition factors $I_1 = I_{pH}I_{IN,lim}$ $I_2 = I_{pH}I_{IN,lim}I_{h2}$ $I_3 = I_{pH}I_{IN,lim}I_{NH3,Xac}$